Vol. 51 · No. 2 · May 2026

RDE
Restorative Dentistry & Endodontics

Editorial

e18 Artificial intelligence hallucinations in endodontics: implications for scientific integrity and clinical decision-making
Emmanuel João Nogueira Leal da Silva, Fernanda Nehme Simão Jorge Riche

Review Article

e19 Effectiveness of silver diamine fluoride in managing hypersensitivity of molar-incisor hypomineralization affected molars: a scoping review
Vo Truong Nhu Ngoc, Do Trong Hieu, Tran Anh Tuan, Vo Nhat Minh, Trinh Khanh Linh

Research Articles

e15 The recovery effect of dentin biomodifiers on microtensile bond strength and sealer-penetration depth of coronal and radicular dentin: an *in vitro* experimental study
Mona Rizk Aboelwafa, Yasmin Tawfik Mohamed Sobh

e16 Effect of sugar and sweetener on the bleachability of coffee and tea-induced stains on composites: an *in vitro* experimental study
Nilay Bayraktar, Osman Kerim Arda Karaca, Yunus Ekşılı, Mustafa Furkan Yıldırım, Osman Tolga Harorli

e17 Clinical outcomes of tooth autotransplantation: a systematic review and meta-analysis of survival
Jasmine Wong, Elise Hoi Wan Fok, Kar Yan Li, Chengfei Zhang, Gary Shun Pan Cheung

e20 Initial attachment, viability, proliferation, and migration of osteoblast-like SaOS-2 cells on two resorbable xenogeneic membranes for guided tissue regeneration: *in vitro* experimental study
Rafael Fernández-Grisales, Giovanna García-Suárez, Ximena Guerrero-Rodríguez, Carolina Berruecos-Orozco, Marco Calle-Jaramillo, Wilder Javier Rojas, Vanessa Esmeralda Duque, Daniela Serna-Guisao, Néstor Ríos-Osorio

e21 Fracture resistance of regenerated immature teeth in different simulated stages of root development: an *in vitro* cyclic loading study
Kyveli-Artemis Polydora, Konstantinos Kodonas, Anastasia Fardi, Christos Gogos

e22 Interplay of hypoxia, angiogenesis, and macrophages in pulp and periapical lesions: an immunohistochemical cross-sectional study
Puja Chatterjee, Mala Kamboj, Shweta Mittal, Anjali Narwal, Anju Devi

e23 Effect of high irradiance and short exposure curing time on the fracture toughness of bulk-fill resin-based composite: an *in vitro* study
Beatriz Ometto Sahadi, Tainah Oliveira Rifane, Carolina Bosso André, Vitaliano Gomes Araújo-Neto, Richard Thomas Bengt Price, Marcelo Giannini

e24 Magnitude of pulp space narrowing over time and contributing factors in teeth with vital pulp therapy: a retrospective cohort study
Akarapong Boontankun, Papimon Chompu-inwai, Chanika Manmontri, Nattakan Chaipattanawan, Areerat Nirunsittirat, Phichayut Phinyo, Trasapong Thaiupathump

e25 Comparison of the cyclic fatigue resistance of original and replica-like files: a systematic review and meta-analysis
Mert Unal, Fatih Cakici

e26 *In vitro* assessment of geometric characteristics in canal preparation using nickel-titanium files used for minimal invasiveness: an experimental study
EunJin Jang, Hyeon-Cheol Kim, WooCheol Lee

Case Report

e27 Endodontic treatment of a molar-incisor malformation of the maxillary first molar: a case report
Woo-Lim Kim, Se-Hee Park, Kyung-Mo Cho, Jin-Woo Kim

eISSN 2234-7666
Vol. 51 · No. 2 · May 2026

RDE Restorative Dentistry & Endodontics
Vol. 51 · No. 2 · May 2026
The Korean Academy of Conservative Dentistry

RDE
Restorative Dentistry & Endodontics

RDE Restorative Dentistry & Endodontics

Vol. 51 · No. 2 · May 2026

eISSN 2234-7666

Aims and Scope

The *Restorative Dentistry and Endodontics* (officially abbreviated as Restor Dent Endod; RDE) is a peer-reviewed and open access journal providing up-to-date information regarding the research and developments on new knowledge and innovations pertinent to the field of contemporary clinical operative dentistry, restorative dentistry, and endodontics. In the field of operative and restorative dentistry, the journal deals with diagnosis, treatment planning, treatment concepts and techniques, adhesive dentistry, esthetic dentistry, tooth whitening, dental materials and implant restoration. In the field of endodontics, the journal deals with a variety of topics such as etiology of periapical lesions, outcome of endodontic treatment, surgical endodontics including replantation, transplantation and implantation, dental trauma, intracanal microbiology, endodontic materials (MTA, nickel-titanium instruments, etc), molecular biology techniques, and stem cell biology. RDE publishes original articles, review articles and case reports dealing with aforementioned topics from all over the world.

RDE is indexed/tracked/covered by Web of Science-Emerging Sources Citation Index (ESCI), Scopus, PubMed, PubMed Central, EBSCO, KoreaMed, Synapse, KCI, Crossref, DOAJ, and Google Scholar.

This Journal was supported by the Korean Federation of Science and Technology Societies Grant funded by the Korean Government (MEST).

History

RDE (eISSN 2234-7666) is the official journal of the Korean Academy of Conservative Dentistry and was renamed from the *Journal of Korean Academy of Conservative Dentistry* (pISSN 1225-0864; eISSN 2093-8179), which was first published in 1975. It was initially published once a year but became a biannual journal in 1986, a quarterly journal in 1999, and then a bimonthly journal in 2001. From 2012, the journal name was renamed, the official language of the journal was changed to English, and it is currently published quarterly. This journal is supported in part by a Grant from the Korean Federation of Science and Technology Societies funded by the Korean Government (MEST).

Distribution

Restor Dent Endod is not for sale, but is distributed to members of Korean Academy of Conservative Dentistry and relevant researchers and institutions world-widely on the last day of February, May, August, and November of each year. Full text PDF files are also available at the official website (https://www.rde.ac; http://www.kacd.or.kr), KoreaMed Synapse (https://synapse.koreamed.org), and PubMed Central. To report a change of mailing address or for further information contact the academy office through the editorial office listed below.

Open Access

Official Publication of Korean Academy of Conservative Dentistry

Published on May 31, 2026

Publisher

The Korean Academy of Conservative Dentistry

B163, Seoul National University Dental Hospital, 101 Daehak-ro, Jongno-gu, Seoul, Korea

Tel: +82-2-763-3818

Fax: +82-2-763-3819

Email: kacd@kacd.or.kr

Editorial Office

The Korean Academy of Conservative Dentistry

B163 Seoul National University Dental Hospital, 101 Daehak-ro, Jongno-gu, Seoul 03080, Korea

Tel: +82-2-763-3818

Fax: +82-2-763-3819

Email: editor@rde.ac

Publishing Office

M2PI

#805, 26 Sangwon 1-gil, Seongdong-gu, Seoul 04779, Korea

Tel: +82-2-6966-4930

Fax: +82-2-6966-4945

Email: support@m2-pi.com

RDE Restorative Dentistry & Endodontics

Editorial Board

RDE Restorative Dentistry & Endodontics

Contents

Vol. 51 · No. 2 · May 2026

Editorials

e18 Artificial intelligence hallucinations in endodontics: implications for scientific integrity and clinical decision-making
Emmanuel João Nogueira Leal da Silva, Fernanda Nehme Simão Jorge Riche

Review Article

e19 Effectiveness of silver diamine fluoride in managing hypersensitivity of molar-incisor hypomineralization affected molars: a scoping review
Vo Truong Nhu Ngoc, Do Trong Hieu, Tran Anh Tuan, Vo Nhat Minh, Trinh Khanh Linh

Research Articles

e15 The recovery effect of dentin biomodifiers on microtensile bond strength and sealer-penetration depth of coronal and radicular dentin: an *in vitro* experimental study
Mona Rizk Aboelwafa, Yasmin Tawfik Mohamed Sobh

e16 Effect of sugar and sweetener on the bleachability of coffee and tea-induced stains on composites: an *in vitro* experimental study
Nilay Bayraktar, Osman Kerim Arda Karaca, Yunus Ekşılı, Mustafa Furkan Yıldırım, Osman Tolga Harorli

e17 Clinical outcomes of tooth autotransplantation: a systematic review and meta-analysis of survival
Jasmine Wong, Elise Hoi Wan Fok, Kar Yan Li, Chengfei Zhang, Gary Shun Pan Cheung

e20 Initial attachment, viability, proliferation, and migration of osteoblast-like SaOS-2 cells on two resorbable xenogeneic membranes for guided tissue regeneration: an *in vitro* experimental study
Rafael Fernández-Grisales, Giovanna García-Suárez, Ximena Guerrero-Rodríguez, Carolina Berruecos-Orozco, Marco Calle-Jaramillo, Wilder Javier Rojas, Vanessa Esmeralda Duque, Daniela Serna-Guisao, Néstor Ríos-Osorio

e21 Fracture resistance of regenerated immature teeth in different simulated stages of root development: an *in vitro* cyclic loading study
Kyveli-Artemis Polydora, Konstantinos Kodonas, Anastasia Fardi, Christos Gogos

e22 Interplay of hypoxia, angiogenesis, and macrophages in pulp and periapical lesions: an immunohistochemical cross-sectional study
Puja Chatterjee, Mala Kamboj, Shweta Mittal, Anjali Narwal, Anju Devi

e23 Effect of high irradiance and short exposure curing time on the fracture toughness of bulk-fill resin-based composite: an *in vitro* study
Beatriz Ometto Sahadi, Tainah Oliveira Rifane, Carolina Bosso André, Vitaliano Gomes Araújo-Neto, Richard Thomas Bengt Price, Marcelo Giannini

e24 Magnitude of pulp space narrowing over time and contributing factors in teeth with vital pulp therapy: a retrospective cohort study
Akarapong Boontankun, Papimon Chompu-inwai, Chanika Manmontri, Nattakan Chaipattanawan, Areerat Nirunsittirat, Phichayut Phinyo, Trasapong Thaiupathump

e25 Comparison of the cyclic fatigue resistance of original and replica-like files: a systematic review and meta-analysis
Mert Unal, Fatih Cakici

e26 *In vitro* assessment of geometric characteristics in canal preparation using nickel-titanium files used for minimal invasiveness: an experimental study
EunJin Jang, Hyeon-Cheol Kim, WooCheol Lee

Case Report

e27 Endodontic treatment of a molar-incisor malformation of the maxillary first molar: a case report
Woo-Lim Kim, Se-Hee Park, Kyung-Mo Cho, Jin-Woo Kim

RDE Restorative Dentistry & Endodontics

Editorial

eISSN 2234-7666
Restor Dent Endod. 2026 May;51(2):e18
https://doi.org/10.5395/rde.2026.51.e18

Artificial intelligence hallucinations in endodontics: implications for scientific integrity and clinical decision-making

Emmanuel João Nogueira Leal da Silva[1,2,*], **Fernanda Nehme Simão Jorge Riche**[2]

[1]Postgraduate Program in Translational Biomedicine (BIOTRANS), Grande Rio University (UNIGRANRIO), Rio de Janeiro, RJ, Brazil
[2]Department of Endodontics, Rio de Janeiro State University (UERJ), Rio de Janeiro, RJ, Brazil

Artificial intelligence (AI) is rapidly transforming how knowledge is generated, accessed, and communicated. As with previous technological shifts, AI should not be viewed as a replacement for human expertise, but as a tool that can expand creativity, support problem-solving, and facilitate learning. However, its integration into scientific and clinical practice requires careful scrutiny to preserve ethical standards, originality, and critical thinking. At the same time, the rapid incorporation of AI tools into scientific writing has begun to raise important concerns for journals, editors, and reviewers regarding the reliability of submitted manuscripts and the integrity of the scientific record.

Unlike human intelligence, which arises from complex biological processes, large language models operate through statistical pattern recognition. These systems are probabilistic models trained to predict the most likely sequence of words based on vast datasets. Consequently, they do not truly "understand" concepts; instead, they simulate knowledge by reproducing linguistic patterns. Their outputs are therefore constrained by the quality of training data, algorithmic design, and even commercial or institutional influences that may shape which information is emphasized or omitted. These limitations raise important concerns about intellectual autonomy and the preservation of analytical reasoning in scientific environments.

One of the most widely discussed limitations of large language models is the phenomenon known as "hallucination". Originally described in research on neural machine translation and later adopted to characterize generative AI systems, hallucination refers to the confident production of factually incorrect or unsupported information [1,2]. Because these models prioritize linguistic plausibility rather than factual verification, they may generate coherent yet erroneous responses instead of acknowledging uncertainty. As a result, outputs may appear convincing and well-structured while containing fabricated details, inaccurate claims, or nonexistent references. In healthcare, such hallucinations extend beyond technical inaccuracies; they can reinforce misinformation, create misplaced confidence in algorithmic authority, and ultimately influence professional judgment, potentially affecting diagnostic reasoning and treatment decisions.

In endodontics, the implications of hallucinated information can be particularly concerning. In the scientific domain, increasing reliance on AI for drafting manuscripts, summarizing literature, or assisting in the development of research protocols introduces the

Received: March 4, 2026 **Accepted:** March 10, 2026

Citation
Silva EJNL, Riche FNSJ. Artificial intelligence hallucinations in endodontics: implications for scientific integrity and clinical decision-making. Restor Dent Endod 2026;51(2):e18.

***Correspondence to**
Emmanuel João Nogueira Leal da Silva, PhD
Department of Endodontics, Rio de Janeiro State University (UERJ), Rua Herotides de Oliveira, Blvd. 28 de Setembro, 157, Vila Isabel, RJ 20551-030, Brazil
Email: nogueiraemmanuel@hotmail.com

risk of fabricated references, distorted interpretations, or oversimplified representations of complex findings. In this context, manipulated citations generated by AI in endodontic research can distort literature reviews, mislead readers, and compromise the integrity of scientific discussion. Moreover, literature is beginning to witness the emergence of highly speculative conceptual publications proposing novel terminologies, theoretical constructions, or mechanistic explanations that remain entirely unvalidated. When such frameworks are generated or amplified through AI-assisted writing, they may create an illusion of scientific novelty while lacking biological plausibility or empirical support. Without rigorous verification, these ideas may introduce misleading concepts into literature. Once inaccurate information enters the scientific record, it may propagate through secondary citations, gradually contaminating the evidence base and conferring unwarranted legitimacy to incorrect claims. Because academic publications form the foundation for guidelines, education, and clinical decision-making, the introduction of hallucinated content threatens not only individual studies but also the reliability of the broader knowledge framework that supports the discipline. Editors and reviewers must therefore remain particularly vigilant when evaluating manuscripts that may involve AI-assisted writing or AI-generated content.

The potential consequences extend to clinical practice. Endodontic diagnosis relies on the careful integration of clinical findings, radiographic interpretation, and patient history. AI-generated responses that present confident but oversimplified conclusions risk masking uncertainty and discouraging differential diagnosis. Similarly, treatment suggestions generated without appropriate contextual understanding may promote generalized protocols that overlook anatomical variability and patient-specific conditions. When such outputs are accepted without verification, clinical reasoning and ultimately patient care may be compromised.

Addressing these challenges requires more than technological refinement; it demands a culture of critical appraisal. AI-generated information must be interpreted through the lens of professional expertise and verified against primary scientific evidence. Cross-checking claims, maintaining rigorous peer review, and restricting AI to supportive roles—such as information retrieval or hypothesis generation—are essential safeguards.

AI undoubtedly offers important opportunities to enhance access to information, accelerate knowledge exchange, and support education. Yet its limitations, including hallucinations, bias, and the risk of misinformation, require sustained vigilance. Dentistry must therefore engage with AI in a balanced and reflective manner: embracing its benefits while preserving the methodological rigor and critical reasoning that underpin evidence-based practice. Safeguarding the reliability of the scientific record must remain a shared responsibility among authors, reviewers, and editors as AI tools become increasingly integrated into the research ecosystem. Only through such collective vigilance can AI strengthen—rather than undermine—the scientific and clinical foundations of endodontic practice.

CONFLICT OF INTEREST

Emmanuel João Nogueira Leal da Silva is an Associate Editor of *Restorative Dentistry and Endodontics* and was not involved in the review process of this article. The authors declare no other conflicts of interest.

FUNDING/SUPPORT

None.

AUTHOR CONTRIBUTIONS

Conceptualization: Silva EJNL. Project administration: Silva EJNL, Riche FNSJ. Writing - original draft: Silva EJNL, Riche FNSJ. Writing - review & editing: Silva EJNL, Riche FNSJ. All authors read and approved the final manuscript.

REFERENCES

1. Koehn P, Knowles R. Six challenges for neural machine translation. In: Luong T, Birch A, Neubig G, Finch A, eds. Proceedings of the First Workshop on Neural Machine Translation. Vancouver, Canada: Association for Computational Linguistics; 2017. p. 28-39.
2. Dziri N, Milton S, Yu M, Zaiane O, Reddy S. On the origin of hallucinations in conversational models: is it the datasets or the models? [Preprint]. arXiv; 2022 [cited 2026 Mar 6]. Available from: https://arxiv.org/abs/2204.07931

https://doi.org/10.5395/rde.2026.51.e18

RDE Restorative Dentistry & Endodontics

Review Article

eISSN 2234-7666
Restor Dent Endod. 2026 May;51(2):e19
https://doi.org/10.5395/rde.2026.51.e19

Effectiveness of silver diamine fluoride in managing hypersensitivity of molar-incisor hypomineralization affected molars: a scoping review

Vo Truong Nhu Ngoc[1], **Do Trong Hieu**[2], **Tran Anh Tuan**[1,*], **Vo Nhat Minh**[1], **Trinh Khanh Linh**[1]

[1]School of Dentistry, Hanoi Medical University, Hanoi, Vietnam
[2]Faculty of Dentistry, University of Medicine and Pharmacy, Vietnam National University, Hanoi, Vietnam

ABSTRACT

This study aimed to evaluate the efficacy of dentinal hypersensitivity treatment with silver diamine fluoride (SDF) in molar-incisor hypomineralization (MIH)-affected molars. This scoping review was designed and structured according to the guidelines of the Preferred Reporting Items for Systematic Reviews and Meta-Analyses and its extension for scoping reviews. A search strategy was conducted across PubMed, The Cochrane Library, ScienceDirect, and Google Scholar to identify articles related to the topic. Two authors screened titles, abstracts, and full texts for review. Five studies met the eligibility criteria, comprising four randomized controlled trials and one case report, with sample sizes ranging from four to 200 participants. All included studies reported improvements in clinical outcomes, including reduced hypersensitivity following SDF application, as indicated by lower Schiff cold air sensitivity scale scores. SDF is a promising treatment strategy for reducing hypersensitivity in MIH-affected molars; however, further research using SDF alone is needed to evaluate its exact effectiveness.

Keywords: Dentin sensitivity; Molar incisor hypomineralization; Noninvasive procedures; Silver fluoride; Tooth demineralization

INTRODUCTION

The first study regarding molar-incisor hypomineralization (MIH) was reported in the late 1970s. However, the first official definition of MIH was established in 2001 by Weerheijm [1] as a systemic-origin syndrome presenting as demarcated, qualitative enamel defects in one to four first permanent molars (FPMs), frequently associated with affected incisors.

Clinically, MIH lesions are demarcated as creamy white to yellow-brown defects, occasionally accompanied by surface enamel breakdown [1–3]. The enamel

Received: August 30, 2025 **Revised:** October 17, 2025 **Accepted:** November 24, 2025

Citation
Ngoc VTN, Hieu DT, Tuan TA, Minh VN, Linh TK. Effectiveness of silver diamine fluoride in managing hypersensitivity of molar-incisor hypomineralization affected molars: a scoping review. Restor Dent Endod 2026;51(2):e19.

***Correspondence to**
Tran Anh Tuan, DDS
School of Dentistry, Hanoi Medical University, No. 1 Ton That Tung Street, Kim Lien Ward, Dong Da District, Hanoi 100000, Vietnam
Email: trananhtuan09302@gmail.com

Vo Truong Nhu Ngoc and Do Trong Hieu contributed equally to this study as co-first authors.

of MIH-affected teeth is often porous like "pollen" with a 15 times higher proportion of amelogenin proteins, reducing mechanical properties, hardness, and elastic modulus compared to normal teeth, which could contribute to its inability to withstand the forces encountered during mastication [4,5], and leading to post-eruptive enamel breakdown (PEB) that could lead to early exposure of porous subsurface enamel or dentine and exacerbate hypersensitivity [6,7]. As a result, the prevalence of patients who experienced frequent hypersensitivity due to MIH-affected molars was relatively high [6], and the need to manage hypersensitivity among this population was rising [8].

The hydrodynamic theory of dentin hypersensitivity, proposed by Brännström [9], posits that "stimuli like cold, heat, or pressure cause fluid movement within exposed dentinal tubules, activating nerve endings and resulting in pain". The often-exposed dentinal tubules, especially in MIH-affected teeth, can lead to pain and prolonged dentin sensitivity when exposed to hot or cold foods or to mechanical stimulation [7,10]. Efforts to overcome dentin hypersensitivity over the decades have agreed on two mechanisms to reduce dentin hypersensitivity, which are (1) disruption of nerve impulse transmission, and (2) occlusion of the exposed dentinal tubules [11,12].

Silver diamine fluoride (SDF) is a colorless preparation of Ag+ ions and fluoride (F^-), forming a complex in ammonia, with a pH of approximately 8 to 9, and a commonly used concentration of 38% [13,14]. The mechanism of managing sensitivity with SDF is that the solution forms a mineral-rich precipitate layer that covers the exposed dentin, partially blocking dentinal tubules and eventually reducing fluid shifts within them, thereby diminishing neural stimulation and pain perception [13]. Moreover, a high fluoride concentration of 44,800 ppm can remineralize tooth enamel. The Ag+ ion is considered to have antibacterial properties, and the addition of diamine groups enhances mineral precipitation [14,15], which could reduce hypersensitivity in MIH-affected teeth [16]. These mechanisms propose a potential role for SDF in reducing hypersensitivity in MIH-affected molar populations [17], whereas the retention rate of restorations or crowns in MIH-affected teeth is low due to their low mineral content and high porosity [7].

Although the efficacy of SDF in treating caries has been widely studied, the evidence that SDF can reduce dentin hypersensitivity, particularly in molars affected by MIH, remains limited and inconclusive. Existing articles varied in their methods, outcome measures, and follow-up durations, leading to inconsistent conclusions across studies. Previous systematic reviews and meta-analyses have primarily focused on the caries-arresting effect of SDF or its general desensitizing efficacy in non-MIH teeth or MIH-affected teeth [16,18]. However, none have specifically examined its role in MIH-affected molars, where structural hypomineralization and hypersensitivity pose unique management challenges.

Therefore, a scoping review is suitable for mapping these gaps in the literature, identifying the proper scope and nature of evidence before conducting focused investigations or systematic reviews and meta-analyses when the scientific data are sufficient. As a result, this scoping review was conducted, regarding the research question as "What is the effectiveness of using SDF alone or in combination with restorative treatment in preventing hypersensitivity of teeth affected by MIH?" and aimed to evaluate current evidence on the effectiveness of SDF in the management of dentin hypersensitivity on MIH-affected molars.

METHODS

This scoping review was designed and structured according to the guidelines of the PRISMA-ScR (Preferred Reporting Items for Systematic Reviews and Meta-Analyses and its extension for scoping reviews) [19].

Research question

A primary research question was formulated for the research: "Evaluate the effectiveness of using SDF alone or in combination with restorative treatment in preventing hypersensitivity of teeth affected by MIH." Also, the PICO (Population, Intervention, Comparison, and Outcomes) strategy was: population: MIH-affected molar undergoing hypersensitive treatment; intervention: SDF alone or in combination with restorative treatment, such as SDF-modified atraumatic restorative technique (SMART); comparison: teeth not undergoing treatment

https://doi.org/10.5395/rde.2026.51.e19

using SDF; outcomes: Schiff cold air sensitivity scale (SCASS).

Search strategy

A comprehensive search strategy was conducted from 14th to 16th October 2025, using Boolean operators (AND, OR, and NOT) to combine phrases with the scientific keywords and related synonyms based on the key concepts: (1) hypersensitivity, (2) SDF, and (3) MIH across four search databases: PubMed, The Cochrane Library, and ScienceDirect as the principal databases and Google Scholar (first 50 to 100 results) as a supplementary database by two authors to determine the eligibility of papers for a full review with the search strings was developed as in Table 1.

Eligibility criteria

For a paper to be considered for review, it must meet the following inclusion criteria and not meet the exclusion criteria in Table 2.

Study selection

The research uses Covidence software [20] to manage and simplify data from four databases. First, the primary author imported all references into the Covidence software, which automatically removed duplicate re-

Table 1. Searching strings

Database	Query
PubMed	((((((sensitivity) OR (hypersensitivity)) OR (sensitive)) OR (dentin hypersensitivity)) OR (dentin sensitivity)) AND ((((((((SDF) OR (silver diamine fluoride)) OR (silver diammine fluoride)) OR (Ag(NH3)2F)) OR (diamine silver fluoride)) OR (conservative management)) OR (preventive approach)) OR (non-invasive strategies))) AND ((((((((((MIH) OR (molar–incisor hypominer-alisation)) OR (molar–incisor hypomineralization)) OR (molar–incisor-hypomineralisation)) OR (molar–incisor-hypomineralization)) OR (hypomineralisation)) OR (hypomineralization)) OR (hypomineralized enamel defect)) OR (hypomineralised enamel defect))
The Cochrane Library	(sensitivity) OR (hypersensitivity) OR (sensitive) OR (dentin hypersensitivity) OR (dentin sensitivity) in Title Abstract Keyword AND (SDF) OR (silver diamine fluoride) OR (silver diammine fluoride) OR (Ag(NH3)2F) OR (diamine silver fluoride) OR (conservative management) OR (preventive approach) OR (non-invasive strategies) in Title Abstract Keyword AND (MIH) OR (molar–incisor hypomineralisation) OR (molar–incisor hypomineralization) OR (molar–incisor-hypomineralisation) OR (molar–incisor-hypomineralization) OR (hypomineralisation) OR (hypomineralization) OR (hypomineralized enamel defect) OR (hypomineralised enamel defect) in Title Abstract Keyword
ScienceDirect	(("sensitivity") OR ("sensitive") OR ("hypersensitivity")) AND (("silver diamine fluoride") OR ("SDF") OR ("non-invasive strategies")) AND (("hypomineralization") OR ("molar–incisor hypomineralization"))
Google Scholar	(("sensitivity") OR ("sensitive") OR ("hypersensitivity")) AND (("silver diamine fluoride") OR ("SDF") OR ("non-invasive strategies")) AND (("hypomineralization") OR ("molar–incisor hypomineralization"))

Table 2. Eligibility criteria of articles used for review

Inclusion criteria	Exclusion criteria
1. Participants: children with at least one permanent molar clinically diagnosed with molar-incisor hypomineralization (MIH), with hypersensitivity symptoms, regardless of gender or geographic location.	1. Non-human research: Studies involving *in vitro*, *ex vivo*, animal, cadaveric, or computational model-based designs.
2. Intervention: application of silver diamine fluoride (SDF), either alone or in combination with other restorative or protective materials (e.g., SDF + potassium iodide, SMART technique, stainless steel crowns).	2. Secondary or non-original literature: Review articles (systematic, scoping, or narrative), editorials, commentaries, letters to the editor, and other non–peer-reviewed or supplementary materials such as conference abstracts, examination documents, indices, tables of contents, book reviews, preview programs, or chart documentation.
3. Outcomes: studies reporting quantitative or qualitative measures of dentin hypersensitivity, such as the Schiff cold air sensitivity scale, visual analog scale, or equivalent clinical sensitivity assessments.	3. Irrelevant study scope: Articles that do not evaluate the effectiveness of SDF in the management of hypersensitivity in MIH-affected molars.
4. Follow-up: any duration of follow-up, but the study must have included at least one post-treatment evaluation of hypersensitivity.	4. Language and accessibility: Non-English publications or studies that are unable to be read in full-text versions.
5. The study design can be observational (case-control, cohort, or other longitudinal) or experimental (randomized controlled trials, non-randomized controlled trials, or quasi-experimental), which published in peer-reviewed journals.	5. Ethical or methodological deficiencies: Studies lacking ethical approval or adequate methodological description to confirm inclusion criteria.

There were no limitations on time, sample size, or study location.

cords. After duplicates were removed, two independent reviewers screened the titles and abstracts against the predefined inclusion and exclusion criteria. In cases of disagreement, a third reviewer was consulted to resolve the conflicts. The same procedure was applied during the full-text review to identify the final set of eligible articles.

Data extraction and analysis

Two independent reviewers (TAT and VNM) conjointly determined which variables to extract, and a standardized data-charting form was automatically built by Covidence software to ensure methodological consistency. Data were retrieved independently by the two reviewers using the software. The extracted data from the selected articles includes: author name, publication year, country, study design, sample characteristics (number of participants and teeth, age, and gender), severity of MIH, intervention and comparison details, follow-up duration, and outcome measures related to dentin hypersensitivity (e.g., SCASS).

In case of disagreement between the reviewers regarding data extraction or study inclusion, the issue was first discussed to reach consensus. If consensus could not be achieved, a third reviewer (DTH) adjudicated the final decision. The process ensured that all included studies met the eligibility criteria. Agreement between the two reviewers during screening and data extraction was continuously monitored within Covidence. The level of agreement was assessed qualitatively through verification of screening logs and consensus discussions.

Due to the heterogeneity of study designs, sample sizes, follow-up durations, and outcome measures, a narrative synthesis was conducted. Extracted data were descriptively summarized in tabular and textual form to map key study characteristics and findings. Quantitative pooling or meta-analysis was not performed, consistent with the exploratory purpose of a scoping review.

As this review aimed to map and summarize the existing evidence rather than to evaluate the methodological quality of studies, no formal risk-of-bias or critical appraisal is required, according to PRISMA-ScR guidelines [19].

Ethical approval

Ethical approval was not required due to the study design. In this review, we conducted a thorough analysis of the current literature on the effectiveness of SDF and/or its combination with restorative treatment in preventing hypersensitivity of MIH-affected molars.

RESULTS

Study selection

After a thorough search, 199 records were identified (Figure 1). Titles and abstracts were used to screen the 171 papers remaining after 28 duplicate studies were removed. Following the exclusion of 155 records, a full-text screening procedure was conducted on the remaining 16 studies. 11 articles were eliminated from consideration for the following reasons: (1) wrong outcomes; (2) wrong intervention; (3) unable to read full-text; (4) not peer-reviewed or published; and (5) non-English articles. This approach produced a final of five articles. From the records that were included for examination, the authors subsequently retrieved both quantitative and qualitative data.

Study characteristics

The characteristics of the included studies and their main findings are summarized in Table 3. In total, five studies were analyzed, with sample sizes ranging from 4 to 200 teeth. 4 out of five were randomized clinical trials (RCTs), while the remaining study was a case report. At the tooth level, the RCTs have sample sizes ranging from 56 to 200 teeth [17,21–23], whereas only four molars were reported in the case report [24]. At the patient level, only one patient was recorded in the case report [24], whereas the RCTs reported sample sizes ranging from 28 to 100 patients across four studies [17,21–23]. Regarding sample severity, the article from Syria focused solely on molars affected by mild MIH [21], while the article from Egypt included a wider range, from moderate to severe, for research [22], and a case report from India reported on four severe-level molars [24]. In contrast, two studies from Türkiye did not mention the severity of the samples [17,23]. Despite variation in sample sizes, which highlights methodological diversity, all studies shared a common inclusion criterion: hypersensitive

https://doi.org/10.5395/rde.2026.51.e19

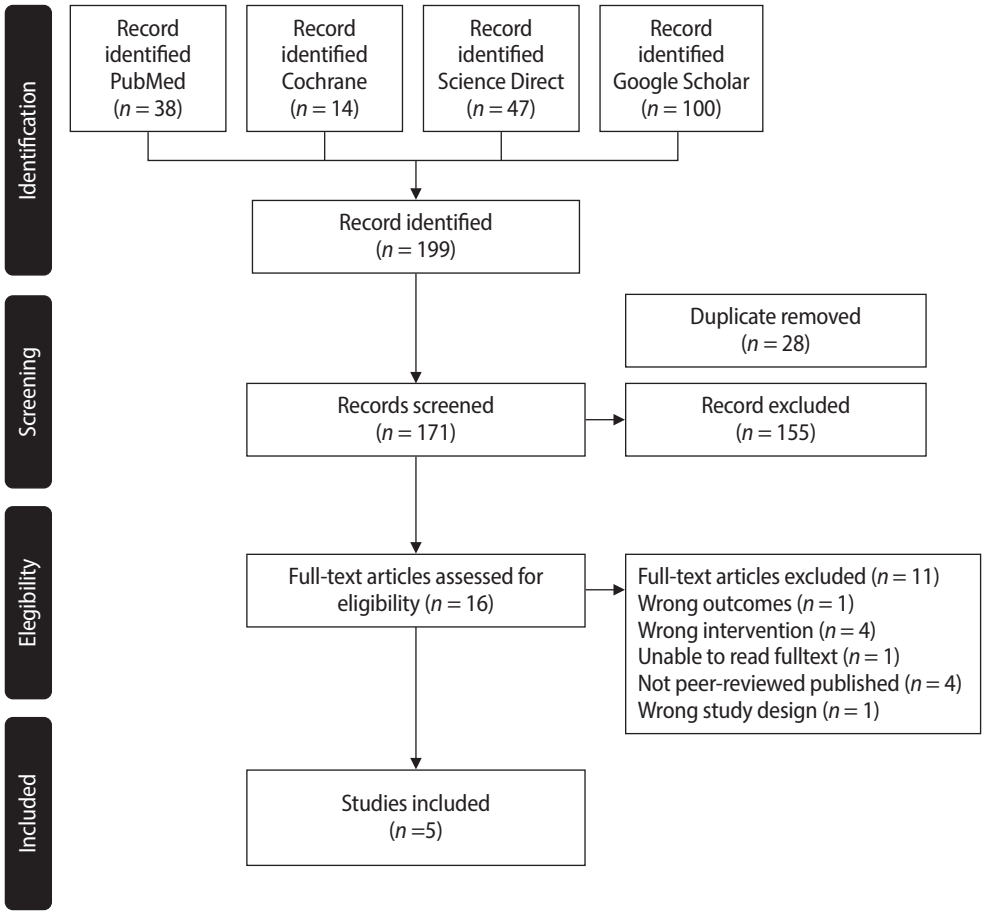

Figure 1. Flow diagram of literature search and study selection.

MIH-affected molars, allowing cross-study comparison.

1. Demographics of participants

The age of participants was relatively similar across the studies, ranging from 6 to 12 years, which corresponds to the mixed dentition period when hypersensitivity symptoms are most prevalent. In research in Türkiye, one original study had a 12-month follow-up [23], while a subsequent study extended the follow-up period to 36 months, with a reported mean age of 8.8 ± 1.58 years [17]. The remaining two studies, conducted in Egypt (6–10 years) and Syria (6–9 years), also included participants within the mixed dentition stage [21,22]. Moreover, a case report from India focused on a single 8-year-old male participant [24]. While the study from Syria did not specify the gender distribution of participants, the studies from Türkiye (30 females and 18 males) and Egypt (20 females and eight males) provided clear details, showing a predominance of female participants.

2. Study locations and treatment methods

The five studies originated from four different countries worldwide. While two of the five studies were conducted in Türkiye [17,23], the remaining studies were conducted in India [24], Egypt [22], and Syria [21]. The treatment methods were different across studies.

Treatment methods were diverse across the five included studies, with all studies utilizing SDF as the primary intervention. Two RCTs investigated the effectiveness of SDF-only in managing hypersensitivity in MIH-affected molars [21,23]. Four out of five studies used a combination of SDF with other materials, such as potassium iodide (KI), glass ionomer cement (GIC),

or stainless steel crowns, in their research [17,22–24]. Additionally, only two studies assessed the efficacy of treatment strategies that did not contain SDF, such as casein phosphopeptide-amorphous calcium phosphate (CPP-ACPFV) fluoride varnish and the combination of conventional restorative treatment with fluoride varnish [21,22].

3. Follow-up periods

The included studies showed variability in follow-up durations. Among the RCTs, follow-up periods ranged from 1 week to 36 months. Two studies from Türkiye assessed outcomes over extended periods, with follow-ups at 12, 18, 24, and 36 months in one study [17] and at 1, 6, and 12 months in another [23]. The trial conducted in Egypt reported follow-ups at 1 week, 6 months, and 12 months [22], whereas the Syrian study evaluated outcomes at 3, 6, 9, and 12 months [21]. In contrast, the case report from India had a shorter follow-up period of 3 months [24].

Results of individual studies

A comprehensive description of the variables related to treatment effectiveness is available in Tables 4 and 5. All five studies reported measurable decreases in dentin hypersensitivity following SDF application. However, the magnitude and duration of improvement varied by intervention type and study design.

A 12-month follow-up study conducted in Türkiye comparing SDF and the SMART technique found no significant difference in hypersensitivity scores between the groups at 1, 6, and 12 months after repeated SDF applications. Both treatments contributed to the reduction of hypersensitivity, as reflected in the SCASS scores, with both studies showing a reduction from 1.77 ± 0.83 at baseline to 0.15 ± 0.38 with SDF alone and to 0.08 ± 0.28 with the SMART technique after a 12-month follow-up period. Moreover, this study, which employed SDF alone, demonstrated immediate symptom relief and a significant reduction in SCASS scores. Moreover, no caries were detected, and the retention rate within the SMART technique group was 88.7% [23].

Another Turkish study with a 36-month follow-up compared the effects of SDF combined with KI (SDF + KI) with those of the SMART technique. There was a significant reduction in SCASS scores at all evaluation periods relative to baseline, with both interventions showing SCASS scores of 0 from the 18-month follow-up onward. The caries-preventive effect was 100%, 67.9%, and 65.4% for SDF + KI-treated teeth; and 100%, 97.6%, and 94.7% for SMART (SDF + KI + GIC)-treated teeth at 12, 24, and 36 months, respectively. The clinical retention rate of SMART sealants at 12, 24, and 36 months was 88.7%, 73.1%, and 66.6%, respectively [17].

A study in Egypt comparing the SMART technique with a combination of conventional restorations and fluoride varnish application found a significant reduction in SCASS scores across four evaluation intervals. In both interventions, the moderate hypomineralized molar severity (MOD) group (with a 1.5-point SCASS score) and the severe hypomineralized molar severity (SEV) group (with a 3-point SCASS score) showed reductions to 0. This result suggests that these approaches are effective in reducing dentin hypersensitivity in molars affected by MIH. There was no difference between 6 and 12 months in each of the four subgroups [22].

In Syria, a study assessing the effectiveness of SDF and CPP-ACPFV found no significant differences in SCASS scores between treatment groups throughout the study. The caries rates were 11%, 15%, 21%, and 23% for SDF-treated teeth, and 33%, 39%, 44%, and 49% for CCP-ACPFV-treated teeth at 3, 6, 9, and 12 months, respectively [21].

A case report from India evaluating the combined effect of SDF and stainless steel crowns showed a reduction in SCASS scores, suggesting decreased hypersensitivity [24].

DISCUSSION

This scoping review is the first article to collect, analyze, and provide a comprehensive evaluation of the effectiveness of SDF treatment in reducing dentin hypersensitivity on molars affected by MIH.

All five included studies reported a reduction in dentin hypersensitivity with each treatment strategy, accompanied by a significant decrease in SCASS scores, particularly with SDF-only or SDF combined with other materials [17,21–24]. Previous studies also suggested that the application of silver ions significantly occludes

https://doi.org/10.5395/rde.2026.51.e19

Table 3. Descriptive characteristics of included articles

No.	Study	Year	Research location	Research type	Sample (people)	Sample (molar)	Sex	Age (yr)	Research strategy	Tooth severity	Follow- up interval
1	Khan [24]	2022	India	Case report	1	4	Male	8	Evaluate the effect of SDF + stainless steel in reducing sensitivity on MIH-affected molars.	Severe	3 mo
2	Ballikaya *et al.* [23]	2022	Türkiye	RCTs	48	112	Female, 30/male, 18	8.8 ± 1.58	Evaluate and compare the effect of SDF and SMART sealants for the treatment of initial carious lesions of permanent molars affected by MIH.	NA	1 mo, 6 mo, and 12 mo
3	Erbas Unverdi *et al.* [17]	2024	Türkiye	RCTs	48	112	Female, 30/male, 18	8.8 ± 1.58	Assess the clinical outcomes of utilizing SDF + KI treatment and SMART/SDF + KI + GIC	NA	12 mo, 18 mo, 24 mo, and 36 mo
4	Saad *et al.* [22]	2024	Egypt	RCTs	28	56	Female, 20/male, 8	6–10	Compare SMART vs the conventional restoration and fluoride varnish application on moderate to severe MIH teeth	Moderate–severe	1 wk, 6 mo, and 12 mo
5	Al-Nerabieah *et al.* [21]	2024	Syria	RCTs	100	200	NA	6–9	Compare the efficacy of SDF and CPP-ACPFV in preventing caries development, enamel breakdown, and sensitivity on molars affected by MIH in children.	Mild	3 mo, 6 mo, 9 mo, and 12 mo

CPP-ACPFV, casein phosphopeptide-amorphous calcium phosphate fluoride varnish; GIC, glass ionomer cement; KI, potassium iodide; MIH, molar incisor hypomineralization; NA, not applicable; RCT, randomized clinical trial; SDF, silver diamine fluoride; SMART, silver-modified atraumatic restorative treatment.

Table 4. Effectiveness of different strategies in reducing the sensitivity of MIH-affected teeth in the included articles

No.	Study	Treatment result					
		SDF	SDF + KI	SMART/SDF + KI + GIC	SDF + stainless steel	CCP-ACPFV	Conventional restoration and fluoride varnish
1	Khan [24]	NA	NA	NA	SCASS scores deduce	NA	NA
2	Ballikaya *et al.* [23]	SCASS scores deduce - Baseline: 1.77 ± 0.83 - 12th month: 0.15 ± 0.38	NA	SCASS scores deduce - Baseline: 1.77 ± 0.83 - 12th month: 0.08 ± 0.28	NA	NA	NA
3	Erbas Unverdi *et al.* [17]	NA	SCASS scores deduce - SCASS scores = 0 (at the 18-month and beyond evaluations)	SCASS scores deduce - SCASS scores = 0 (at the 18-month and beyond evaluations)	NA	NA	NA
4	Saad *et al.* [22]	NA	NA	SCASS scores deduce - Baseline: +MOD: 1.5/+SEV: 3 - 12th month: +MOD: 0/+SEV: 0	NA	NA	SCASS scores deduce - Baseline: +MOD: 1.5/+SEV: 3 - 12th month: +MOD: 0/+SEV: 0
5	Al-Nerabieah *et al.* [21]	SCASS scores deduce	NA	NA	NA	SCASS scores deduce	NA

CPP-ACPFV, casein phosphopeptide-amorphous calcium phosphate fluoride varnish; GIC, glass ionomer cement; KI, potassium iodide; MIH, molar incisor hypomineralization; MOD, moderate hypomineralized molar severity; NA, not applicable; SCASS, Schiff cold air sensitivity scale; SDF, silver diamine fluoride; SEV, severe hypomineralized molar severity; SMART, silver-modified atraumatic restorative treatment.

https://doi.org/10.5395/rde.2026.51.e19

Table 5. Effectiveness of different strategies in caries prevention and retention rate/restoration integrity of MIH-affected teeth in the included articles

No.	Study	Treatment result					
		SDF	SDF + KI	SMART/SDF+KI+GIC	SDF + stainless steel	CCP-ACPFV	Conventional restoration and fluoride varnish
1	Khan [24]	NA	NA	NA	NA	NA	NA
2	Ballikaya *et al.* [23]	- No dental caries presented - Retention rate: NA	NA	- No dental caries presented - Retention rate: 88.7%	NA	NA	NA
3	Erbas Unverdi *et al.* [17]	NA	- The caries preventive effect was 100%, 67.9%, and 65.4% at 12, 24, and 36 months, respectively - Retention rate: NA	- The caries preventive effect was 100%, 97.6%, and 94.7% at 12, 24, and 36 months, respectively - Retention rate: 88.7%, 73.1%, and 66.6% at 12, 24, and 36 months, respectively	NA	NA	NA
4	Saad *et al.* [22]	NA	NA	- Caries prevention: NA - Restoration integrity +6th month: MOD: 1, SEV: 1 +12th month: MOD: 1, SEV: 1	NA	NA	- Caries prevention: NA - Restoration integrity +6th month: MOD: 1, SEV: 1 +12th month: MOD: 1, SEV: 1
5	Al-Nerabieah *et al.* [21]	- Caries rate was 11%, 15%, 21%, and 23% at 3, 6, 9, and 12 months, respectively - Retention rate: NA	NA	NA	NA	- Caries rate was 33%, 39%, 44%, and 49% at 3, 6, 9, and 12 months, respectively - Retention rate: NA	NA

CPP-ACPFV, casein phosphopeptide-amorphous calcium phosphate fluoride varnish; GIC, glass ionomer cement; KI, potassium iodide; MIH, molar incisor hypomineralization; MOD, moderate hypomineralized molar severity; NA, not applicable; SDF, silver diamine fluoride; SEV, severe hypomineralized molar severity; SMART, silver-modified atraumatic restorative treatment.

dentinal tubules and reduces hypersensitivity [25–28]. Silver particles can deposit in the lumens and may form mechanical blockages along the length of the tubules, reducing fluid movement within the dentin tubules and thereby reducing dentin hypersensitivity [13,29]. A series of chemical reactions contributes to tooth desensitization by occluding dentinal tubules, facilitating remineralization of demineralized tooth structure, and inhibiting dentinal collagen degradation. However, these reactions result in a notable side effect—permanent black staining of carious lesions in both enamel and dentin, while sound enamel remains unaffected [30]. Additionally, studies that combined SDF with other treatment strategies, such as KI [17], SMART [17,22,23], or stainless steel crowns [24], also reported reductions in hypersensitivity. The combination of SDF with KI offers both hypersensitivity reduction and mitigates the common detrimental effect of black staining by forming silver iodide precipitates, which enhances patient satisfaction, particularly in aesthetic regions [31]. The SMART technique has been proven to the reduction of hypersensitivity. However, the long-term clinical efficacy of the SMART technique in managing MIH-affected cases remains unclear [32]. Furthermore, stainless steel crown placement offers desensitizing benefits while ensuring long-term mechanical coverage and pulpal protection, making it especially valuable in pediatric dentistry [24]. Ultimately, these findings suggest that SDF, when combined with other restorative or protective strategies, may offer significant benefits in managing hypersensitivity.

Several factors influenced the effectiveness of SDF treatment. The patient age range across the studies was relatively consistent, predominantly covering the mixed dentition period (6–10 years), which corresponds to the phase when enamel porosity and dentin exposure are greatest. This may be because, at the age of 8 years, as recommended by the European Academy of Paediatric Dentistry for MIH prevalence studies, the FPMs typically erupt intact, allowing clear visualization of enamel opacities for diagnosis. In older children, PEB and conservative treatment may obscure MIH characteristics, leading to potential underdiagnosis [33,34]. Younger individuals with MIH may experience greater hypersensitivity, as physiological reparative dentin deposition and

https://doi.org/10.5395/rde.2026.51.e19

exposure to desensitizing agents increase with age. Additionally, older individuals may develop greater awareness and improved ability to manage hypersensitivity symptoms [8]. All five studies demonstrated significant success in reducing dentinal hypersensitivity in MIH-affected molars. Treatment Needs Index or MIH severity scores were inconsistently reported, limiting the ability to stratify the results. However, the severity of MIH lesions still played a crucial role, with mild, moderate, and severe cases responding differently to treatment, with more severe lesions requiring combined restorative approaches (e.g., SMART or SDF + KI), which demonstrated complete hypersensitivity elimination and improved retention rates in the longer term [7].

The follow-up periods also varied significantly, ranging from 1 week to 36 months among the included studies, which may explain the variability in reported long-term effectiveness. Studies with longer observation periods, such as those conducted in Türkiye [17], demonstrated more stable and sustained reductions in hypersensitivity, suggesting that repeated SDF application or the adjunctive use of glass ionomer materials may contribute to prolonged tubule occlusion and mineral deposition. In contrast, shorter-term studies reported rapid symptom relief but lacked evidence of sustained benefit over time [21–24].

Interestingly, studies combining SDF with other agents, such as SDF + KI or SMART, have suggested potential advantages for maintaining long-term hypersensitivity control [17,22–24]. Some findings from the included articles require further discussion. The studies from Türkiye reported complete elimination of hypersensitivity from 18 months onward (SCASS score of 0), showing the potential for prolonged effectiveness of SDF, SDF combined with potassium iodide, and SMART technique in MIH-affected molars [17], similarly to the findings of the previous scientific review by Jayanti and Riyanti [35], which also highlighted the promising role of SDF and its combinations as a minimally invasive treatment option for teeth affected by MIH. However, while Jayanti and Riyanti [35] conducted a broad scoping review summarizing various noninvasive and restorative management strategies for MIH, our review focused specifically on the effectiveness of SDF in reducing dentin hypersensitivity in MIH-affected molars. Consequently, our synthesis provides a more targeted evaluation of SDF alone and its combined protocols (e.g., SDF + KI, SMART), whereas Jayanti and Riyanti's work [35] emphasizes overall treatment modalities, including resin infiltration, GIC, and fluoride varnishes. Additionally, the article from Syria found that there was no difference between using SDF alone and using CPP-ACPFV in reducing hypersensitivity in molars affected by MIH [21]. Moreover, a case report from India also noted a reduction in hypersensitivity when using SDF prior to stainless steel crowns, providing physical protection against external agents [24]. Comparatively, studies using SDF alone generally reported a significant short-term reduction in SCASS scores [21,23], while combination techniques achieved earlier desensitization and longer maintenance of effect [17,22]. These findings support a potential synergistic benefit when SDF is combined with other bioactive restorative materials, though the small number of trials prevents definitive conclusions. These variations highlight the need for further analysis to establish a standardized treatment strategy for molars affected by MIH.

Only a few studies have addressed both caries prevention and hypersensitivity reduction. The 12-month study in Türkiye reported no new caries development, but this study observed a significant reduction in hypersensitivity [23]. Meanwhile, the 36-month Turkish study found that the SMART technique provided superior caries prevention (94.7% after 36 months) compared with SDF + KI (65.4%), although both strategies reduced hypersensitivity [17]. Similarly, the study from Syria showed that SDF was more effective in preventing caries than CPP-ACPFV (23% vs 49% caries incidence after 12 months), but also no significant difference was observed between the two groups in terms of hypersensitivity reduction [21]. This suggests that hypersensitivity in MIH-affected molars is more likely due to MIH itself rather than to dental caries. However, further long-term follow-up research using SDF should be considered to determine the relationship among MIH-affected teeth, hypersensitivity, and dental caries.

The retention rate/integrity of restorations was reported in only a few studies. A 12-month study from Türkiye reported an 88.7% retention rate with the SMART technique [23], whereas a 36-month study from Türkiye

showed a decline to 66.6% at 36 months [17]. Additionally, the study from Egypt evaluated the integrity of restorations and found no significant difference between the SMART technique and conventional restorations combined with fluoride varnish [22]. Despite these variations in restoration retention, all studies consistently reported a significant reduction in hypersensitivity. This suggests that improvements in hypersensitivity may not be directly related to restoration retention. However, further long-term follow-up research is needed to provide conclusive scientific evidence on this matter.

Despite this scoping review achieving its aim of evaluating the effectiveness of SDF in managing hypersensitivity of MIH, some important limitations should be acknowledged to provide proper guidance for future studies.

This scoping review is constrained by the limited number of eligible studies (n = 5), small sample sizes, and heterogeneity in study design, diagnostic criteria, intervention types, and follow-up durations. It is difficult to make direct comparisons, which could limit the accuracy of the evaluation. Moreover, the methodological rigor across studies was inconsistent, and one study included a case report, further limiting generalizability. Furthermore, in almost every study, the researcher's intervention involved combining SDF with other materials to manage dentin hypersensitivity in MIH-affected molars. This could be challenging to determine whether the reduction in dentine hypersensitivity was a direct effect of SDF or of the other materials. These factors reduce the overall certainty of the evidence and underscore the need for larger sample sizes, longer follow-up durations, systematic reporting of severity levels, use of SDF-only, and well-designed RCTs to verify the observed effects. Although a formal risk-of-bias assessment was not conducted, this aligns with the methodological framework of scoping reviews, which aim to provide an overview of available evidence rather than to appraise its quality.

Moreover, some of the exclusion criteria may limit this scoping review, as it included only English-language articles and research from the four mentioned scientific databases, due to language barriers and accessibility issues. The limited search of gray literature, such as conference proceedings, dissertations, or other non-peer-reviewed sources, might also lead to publication bias. Future reviews should adopt a more comprehensive, inclusive search strategy to improve results.

CONCLUSIONS

This scoping review identified a small but growing body of evidence suggesting that SDF, whether used alone or in combination with other restorative strategies, may effectively reduce dentin hypersensitivity in molars affected by MIH. However, the strength of this conclusion is limited due to the small number of available studies, their methodological heterogeneity, and the absence of standardized outcome measures.

Future well-designed randomized controlled trials with standardized diagnostic criteria and follow-up protocols are required to confirm these preliminary observations and determine optimal application. According to current evidence, SDF-based interventions are a promising, minimally invasive approach for managing hypersensitivity in molars affected by MIH.

CONFLICT OF INTEREST

No potential conflict of interest relevant to this article was reported.

FUNDING/SUPPORT

The authors have no financial relationships relevant to this article to disclose.

DISCLOSURE OF GENERATIVE AI IN SCIENTIFIC WRITING

During the preparation of this work, the authors used ChatGPT ver. 5.3 (OpenAI, San Francisco, CA, USA) in order to improve the readability and language of the manuscript during the writing process. After using this tool, the authors reviewed and edited the content as needed and take full responsibility for the content of the published article.

AUTHOR CONTRIBUTIONS

Conceptualization, Methodology: all authors. Data curation, Formal analysis, Investigation: Tuan TA, Minh VN , Linh TK. Writing - original draft: Ngoc VTN, Hieu DT, Tuan TA, Minh VN. Writing - review & editing: all authors. All authors read and approved the final manuscript.

DATA SHARING STATEMENT

The data supporting this article can be made available by the corresponding author upon request.

https://doi.org/10.5395/rde.2026.51.e19

REFERENCES

1. Weerheijm KL. Molar incisor hypomineralisation (MIH). Eur J Paediatr Dent 2003;4:114-120.
2. Kirthiga M, Poornima P, Praveen R, Gayathri P, Manju M, Priya M. Prevalence and severity of molar incisor hypomineralization in children aged 11-16 years of a city in Karnataka, Davangere. J Indian Soc Pedod Prev Dent 2015;33:213-217.
3. Weerheijm KL, Duggal M, Mejàre I, Papagiannoulis L, Koch G, Martens LC, *et al*. Judgement criteria for molar incisor hypomineralisation (MIH) in epidemiologic studies: a summary of the European meeting on MIH held in Athens, 2003. Eur J Paediatr Dent 2003;4:110-113.
4. Almuallem Z, Busuttil-Naudi A. Molar incisor hypomineralisation (MIH): an overview. Br Dent J 2018;225:601-609.
5. Fearne J, Anderson P, Davis GR. 3D X-ray microscopic study of the extent of variations in enamel density in first permanent molars with idiopathic enamel hypomineralisation. Br Dent J 2004;196:634-638.
6. Raposo F, de Carvalho Rodrigues AC, Lia ÉN, Leal SC. Prevalence of hypersensitivity in teeth affected by molar-incisor hypomineralization (MIH). Caries Res 2019;53:424-430.
7. Lygidakis NA, Garot E, Somani C, Taylor GD, Rouas P, Wong FS. Best clinical practice guidance for clinicians dealing with children presenting with molar-incisor-hypomineralisation (MIH): an updated European Academy of Paediatric Dentistry policy document. Eur Arch Paediatr Dent 2022;23:3-21.
8. Shields S, Chen T, Crombie F, Manton DJ, Silva M. The impact of molar incisor hypomineralisation on children and adolescents: a narrative review. Healthcare (Basel) 2024;12:370.
9. Brännström M. Sensitivity of dentine. Oral Surg Oral Med Oral Pathol 1966;21:517-526.
10. Dionysopoulos D, Gerasimidou O, Beltes C. Dentin hypersensitivity: etiology, diagnosis and contemporary therapeutic approaches: a review in literature. Appl Sci 2023;13:11632.
11. Ozen T, Orhan K, Avsever H, Tunca YM, Ulker AE, Akyol M. Dentin hypersensitivity: a randomized clinical comparison of three different agents in a short-term treatment period. Oper Dent 2009;34:392-398.
12. Kim JW, Park JC. Dentin hypersensitivity and emerging concepts for treatments. J Oral Biosci 2017;59:211-217.
13. Greenwall-Cohen J, Greenwall L, Barry S. Silver diamine fluoride: an overview of the literature and current clinical techniques. Br Dent J 2020;228:831-838.
14. Stebbins EA. What value has argenti nitras as a therapeutic agent in dentistry? Int Dent J (Phila) 1891;12:661-671.
15. Peng JJ, Botelho MG, Matinlinna JP. Silver compounds used in dentistry for caries management: a review. J Dent 2012;40:531-541.
16. Cavalcante BG, Mlinkó É, Szabó B, Teutsch B, Hegyi P, Vág J, *et al*. Non-invasive strategies for remineralization and hypersensitivity management in molar-incisor hypomineralization: a systematic review and meta-analysis. J Clin Med 2024;13:7154.
17. Erbas Unverdi G, Ballikaya E, Cehreli ZC. Clinical comparison of silver diamine fluoride (SDF) or silver-modified atraumatic restorative technique (SMART) on hypomineralised permanent molars with initial carious lesions: 3-year results of a prospective, randomised trial. J Dent 2024;147:105098.
18. Piovesan ÉT, Alves JB, Ribeiro CD, Massignan C, Bezerra AC, Leal SC. Is silver diamine fluoride effective in reducing dentin hypersensitivity?: a systematic review. J Dent Res Dent Clin Dent Prospects 2023;17:63-70.
19. Tricco AC, Lillie E, Zarin W, O'Brien KK, Colquhoun H, Levac D, *et al*. PRISMA Extension for Scoping Reviews (PRISMA-ScR): checklist and explanation. Ann Intern Med 2018;169:467-473.
20. Covidence systematic review software [Internet]. Melbourne: Veritas Health Innovation; 2025 [cited 2025 Mar 27]. Available from: https://www.covidence.org/
21. Al-Nerabieah Z, AlKhouli M, Dashash M. Preventive efficacy of 38% silver diamine fluoride and CPP-ACP fluoride varnish on molars affected by molar incisor hypomineralization in children: a randomized controlled trial. F1000Res 2024;12:1052.
22. Saad AE, Alhosainy AY, Abdellatif AM. "Evaluation of Silver Diamine Fluoride Modified Atraumatic Restorative Treatment (SMART) on hypomineralized first permanent molar": a randomized controlled clinical study. BMC Oral Health 2024;24:1182.
23. Ballikaya E, Ünverdi GE, Cehreli ZC. Management of initial carious lesions of hypomineralized molars (MIH) with silver diamine fluoride or silver-modified atraumatic restorative treatment (SMART): 1-year results of a prospective, randomized clinical trial. Clin Oral Investig 2022;26:2197-2205.
24. Khan MK. Comprehensive management of molar-incisor-hypomineralization by preventive, palliative, and restorative treatment modalities in a pediatric patient: a case report and literature review. J Dent Res Rev 2022;9:173-179.

25. Menzel M, Kiesow A, de Souza E Silva JM. Nano-CT characterization of dentinal tubule occlusion in SDF-treated dentin. Sci Rep 2023;13:15895.
26. Kiesow A, Menzel M, Lippert F, Tanzer JM, Milgrom P. Dentin tubule occlusion by a 38% silver diamine fluoride gel: an in vitro investigation. BDJ Open 2022;8:1.
27. Seto J, Horst JA, Parkinson DY, Frachella JC, DeRisi JL. Enhanced tooth structure via silver microwires following treatment with 38 percent silver diamine fluoride. Pediatr Dent 2020;42:226-231.
28. Li Y, Liu Y, Psoter WJ, Nguyen OM, Bromage TG, Walters MA, *et al*. Assessment of the silver penetration and distribution in carious lesions of deciduous teeth treated with silver diamine fluoride. Caries Res 2019;53:431-440.
29. Yoshiyama M, Masada J, Uchida A, Ishida H. Scanning electron microscopic characterization of sensitive vs. insensitive human radicular dentin. J Dent Res 1989;68:1498-1502.
30. Seifo N, Robertson M, MacLean J, Blain K, Grosse S, Milne R, *et al*. The use of silver diamine fluoride (SDF) in dental practice. Br Dent J 2020;228:75-81.
31. Garg S, Sadr A, Chan D. Potassium iodide reversal of silver diamine fluoride staining: a case report. Oper Dent 2019;44:221-226.
32. Bal C, Sozuoz MA, Sari MB, Aksoy M. 1-year results of molar incisor hypomineralization-affected cases treated with silver modified atraumatic restorative treatment: a retrospective study. Int J Clin Pediatr Dent 2024;17:683-689.
33. Ghanim A, Silva MJ, Elfrink ME, Lygidakis NA, Mariño RJ, Weerheijm KL, *et al*. Molar incisor hypomineralisation (MIH) training manual for clinical field surveys and practice. Eur Arch Paediatr Dent 2017;18:225-242.
34. Jälevik B. Prevalence and diagnosis of molar-incisor- hypomineralisation (MIH): a systematic review. Eur Arch Paediatr Dent 2010;11:59-64.
35. Jayanti CN, Riyanti E. Treatment alternative of molar incisor hypomineralisation for young permanent teeth: a scoping review. Clin Cosmet Investig Dent 2024;16:337-348.

https://doi.org/10.5395/rde.2026.51.e19

RDE Restorative Dentistry & Endodontics

Research Article

eISSN 2234-7666
Restor Dent Endod. 2026 May;51(2):e15
https://doi.org/10.5395/rde.2026.51.e15

The recovery effect of dentin biomodifiers on microtensile bond strength and sealer-penetration depth of coronal and radicular dentin: an *in vitro* experimental study

Mona Rizk Aboelwafa[1,*], **Yasmin Tawfik Mohamed Sobh**[2]

[1]Department of Operative Dentistry, Faculty of Dentistry, Sinai University - Kantara branch, Ismailia, Egypt
[2]Department of Endodontics, Faculty of Dentistry, Sinai University - Kantara branch, Ismailia, Egypt

ABSTRACT

Objectives: This study aimed to assess the outcomes of bromelain enzyme and chlorhexidine (CHX) following endodontic irrigation by evaluating coronal dentin microtensile bond strength (μTBS) and radicular dentin sealer penetration depth.

Methods: Fifty-one human molars with flat mid-dentin surfaces were soaked in sodium hypochlorite, then randomly assigned to three groups relying on the biomodification approach (n = 17): group 1, saline; group 2, 8% bromelain; and group 3, 2% CHX. After bonding and resin composite build-ups, the μTBS, failure mode, and bond interface were evaluated. Forty-two root canals of human molars were mechanically prepared and randomly distributed among three groups (n = 14), similar to the coronal-dentin biomodification protocol. The sealer-penetration depth was measured utilizing the scanning electron microscope. One- and two-way analyses of variance and the pairwise t- and chi-square tests were utilized.

Results: The bromelain group showed the highest statistically significant resin-dentin μTBS values, followed by the CHX and control groups. For sealer-penetration assessment, the bromelain group showed the highest penetration at the middle and apical root levels, whereas CHX demonstrated the highest penetration at the coronal level.

Conclusions: Bromelain biomodification positively influenced the resin-dentin bond strength and the sealer-penetration depth in apical and middle levels.

Keywords: Bromelain; Dentin biomodification; Dentin microtensile bond strength; Sealer penetration depth

Received: July 22, 2025 **Revised:** September 18, 2025 **Accepted:** October 30, 2025

Citation
Aboelwafa MR, Sobh YTM. The recovery effect of dentin biomodifiers on microtensile bond strength and sealer-penetration depth of coronal and radicular dentin: an *in vitro* experimental study. Restor Dent Endod 2026;51(2):e15.

***Correspondence to**
Mona Rizk Aboelwafa, PhD
Department of Operative Dentistry, Faculty of Dentistry, Sinai University - Kantara branch, Ismailia 41636, Egypt
Email: monaaboelwafa20@gmail.com

Mona Rizk Aboelwafa's current affiliation: Department of Operative Dentistry, Faculty of Dentistry, Suez University, Egypt.

INTRODUCTION

The root canals are chemomechanically treated to eradicate pulp tissue fragments and related bacteria. Various sodium hypochlorite (NaOCl) concentrations, ranging from 0.5% to 5%, are implemented to eliminate the bacterial burden [1]. Mechanical instrumentation created a thin smear coating that obstructs the dentinal tubules. This layer could be removed using 17% ethylenediaminetetraacetic acid (EDTA), which dissolves inorganic particles, thereby softening dentin [2]. None of these irrigants could be described as optimum. However, from a mechanical standpoint, the gradual breakdown of organic content, particularly type 1 collagen fibrils, and inorganic dentin constituents may contribute to root fracture following treatment [3].

A secure coronal seal, provided by an adhesive restoration, is crucial to prevent bacterial re-entry into fully restored root canals. The chemical effects of endodontic irrigation solutions on the dentin lining the root canals may similarly influence coronal dentin when these substances are infused into it during endodontic therapy. These solutions may impair the bonding of the ultimately inserted adhesive restoration, either by altering the bonding technique or by altering the mechanical and structural properties of the dentin surface [4,5].

In endodontics, collagen cross-linking and dentin biomodifier compounds are used as intraradicular final irrigants to enhance the mechanical, chemical, and physical properties of the dentin substrate; thereby, they may improve sealer penetration depth. These compounds can induce biomodification of dentin, a process traditionally accomplished with artificially manufactured cross-linking agents, such as chlorhexidine (CHX), which produces a stable, long-lasting hybrid layer [6]. Among the limitations of the CHX is its incompatibility with the dentin surface [7]. Additionally, most synthetic cross-linking agents produce a rapid effect, resulting in the formation of a surface barrier over the dentin; hence, they prevent the collagenolytic action at greater dentin depths, in addition to the presence of non-reacted molecules that induce cytotoxicity [8,9]. Therefore, natural dentin biomodifiers could serve as feasible substitutes for synthetic ones, given their biosafety and minimal cytotoxicity. Bromelain is a naturally derived dentin biomodifier that is commercially extracted from the pineapple fruit or stem. Bromelain enzyme is a collection of sulfhydryl proteolytic enzymes that includes a variety of cysteine proteases. It was reported that bromelain promotes the dilation of dentinal tubules on the exposed dentin surface by diminishing collagen on the demineralized surface [10]. However, insufficient data had been documented to investigate the impact of 8% bromelain enzyme as an intraradicular final irrigant on both resin-bond strength to coronal dentin and sealer-penetration following chemo-mechanical root canal debridement, so this research was intended to evaluate the effect of 8% bromelain enzyme and CHX, as intraradicular final irrigant, on the dentin-collagen matrix integrity by assessing the resin-coronal dentin microtensile bond strength (μTBS), dentin-bond interfacial micromorphology, and sealer penetration depth to radicular dentin utilizing scanning electron microscopy (SEM). The null hypotheses are proposed as follows: (i) The different investigated dentin biomodifiers did not have a positive impact on either the resin composite μTBS to coronal dentin or the sealer penetration depth to radicular dentin. (ii) The proposed dentin biomodifiers would not affect the micromorphology of the dentin-bond interface.

METHODS

Sample size calculation

Based on earlier research [11,12], the sample size was quantified adopting G*Power ver. 3.1.9.7 (Heinrich-Heine-Universität Düsseldorf, Düsseldorf, Germany). To assess resin-coronal dentin μTBS and sealer penetration depth, a sample size of (n = 51) and (n = 42) was estimated. This calculation was performed using an alpha level of 0.05, a beta level of 0.10, and effect sizes (d) of 0.53 and 0.58.

Specimens' selection and ethical approval

The research protocol was validated by the Ethical Research Committee of the Faculty of Dentistry, Cairo University, on July 31, 2024 (document number 59/7/24). A total of 51 and 42 anonymous caries-free human mandibular first molars were selected, ultrasonically cleaned, and maintained at 4°C in a saline solution supplemented

https://doi.org/10.5395/rde.2026.51.e15

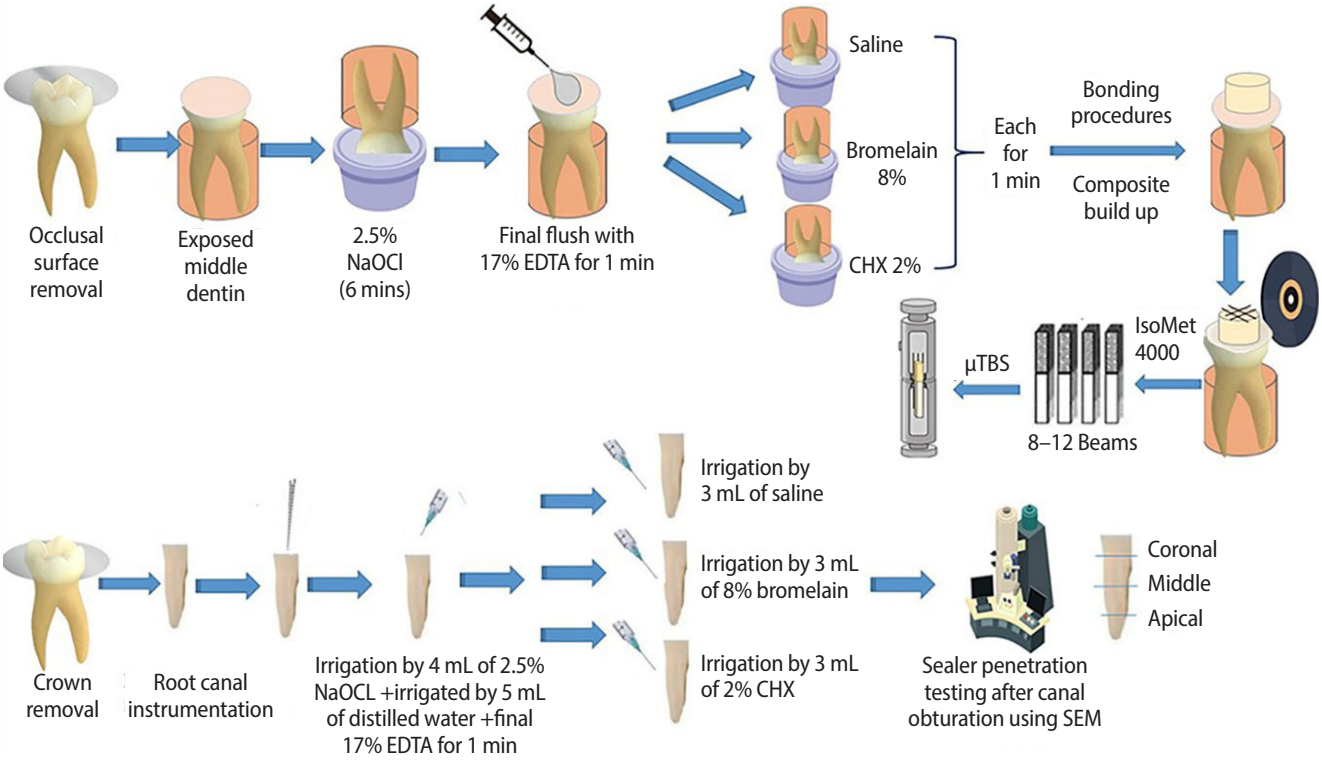

Figure 1. Illustration showing the procedures of the study. CHX, chlorhexidine; EDTA, ethylenediaminetetraacetic acid; NaOCl, sodium hypochlorite; SEM, scanning electron microscopy; µTBS, microtensile bond strength. IsoMet 4000: Buehler, Esslingen am Neckar, Germany.

with 0.02% sodium azide until future use. The entire experimental procedure is illustrated in Figure 1.

Coronal dentin specimens' preparation

Fifty-one lower first molars were embedded in 2 cm diameter cylinder-shaped plastic molds pre-filled with soft acrylic resin. After complete resin polymerization, the occlusal tables of the molars were slit via a diamond saw (Isomet 4000; Buehler, Lake Bluff, IL, USA) along with water stream cooling to produce flat mid-dentin surfaces [13]. Each surface was smoothed using silicon carbide paper (600 grit) for 1 minute with water cooling, and then water flushed to construct a standardized smear layer [14]. For the entire specimens, dentin surfaces were immersed in 20 mL of 2.5% NaOCl (Golden Falcon, Dubai, UAE) for 6 minutes, washed under distilled water (DW) for 15 seconds, and finally flushed with 17% EDTA (3 mL; Root Dental Medical Devices Co., Ltd., Beijing, China) for 1 minute [15].

Bonding procedure and composite build-up

The samples were randomly assigned to three groups (n = 17) according to the dentin biomodification protocol, where each specimen was immersed for 1 minute in a plastic container containing equal amounts (3 mL) of the proposed dentin biomodifier. Group 1: Dentin surfaces biomodified with saline (control group) [12]. Group 2: Dentin surfaces biomodified with 8% bromelain solution, which was prepared by dissolving pure bromelain powder (8 g; Sigma Aldrich, Darmstadt, Germany) in DW (100 mL) [16,17]. Group 3: Dentin surfaces biomodified using 2% CHX (Consepsis; Ultradent Products, South Jordan, UT, USA) [13].

The specimens were subsequently washed out for approximately 15 seconds with DW and gently air-dried. Following the manufacturer's instructions, a universal adhesive (All Bond Universal; BISCO Inc., Schaumburg, IL, USA) was utilized in self-etch mode and was coated on the dentin surfaces and light polymerized for 15 seconds utilizing a light-curing device (Woodpecker, Mini S Curing Light; RTA, Guilin, China) with a 1,000

mW/cm^2 intensity and a 420 to 480 nm wavelength. The resin composite was then incrementally placed to form 4 mm-thick build-ups (Schütz CAPO Composite Universal; Schütz Dental GmbH, Rosbach vor der Höhe, Germany); each composite increment (2 mm) was continuously light polymerized for 40 seconds. The bonded samples were preserved in DW at 37°C for up to 24 hours.

Microtensile bond strength measurements

The bonded samples were cut longitudinally, at right angles to the bonded interfaces, into beams with 1 mm^2 of bonding area. They were obtained by placing the pretreated tooth in the gripping attachment and sequentially sectioned using a cutting machine (IsoMet 4000 Buehler, Esslingen am Neckar, Germany) under copious coolant. Exploiting a digital caliper (Absolute Digimatic; Mitutoyo, Tokyo, Japan), the proportions for all beams were validated. To test μTBS, 8 to 12 beams were chosen from the center of each tooth. Each beam was set up in a universal testing machine (Instron, Model 3345-England) and secured in the testing jig utilizing cyanoacrylate-based adhesive. The beams were stressed in tension at a crosshead rate of 0.5 mm/min till the sample's bonding failure occurred. Finally, bond strength was measured in megapascal (MPa).

Failure mode examination

The failure modes were analyzed using a stereomicroscope (MA 100; Nikon, Tokyo, Japan) at 30× magnification. Three distinct categories of failure patterns were recognized: adhesive failure (in between resin and dentin), cohesive failure (dentin or resin), or mixed failure (both adhesive and cohesive failure).

Scanning electron microscopy

From each group, a randomly selected representative sample was examined using field-emission SEM (Quattro S; Thermo Fisher Scientific, Hillsboro, OR, USA) to investigate the resin-dentin interface. The specimens were prepared, attached to aluminum stubs, and then inspected on the SEM (field emission gun) at a magnification (14× up to 1,000,000), an accelerating voltage (30 kV), and a resolution of 1 nm.

Specimens' selection and preparation for the sealer penetration test

The crowns of 42 lower first molars were cut, and occlusal surfaces were smoothed to establish a point of reference for working length (WL) standardization. The roots were standardized to 17 mm in length. A closed canal system was formed, and the external surface of each root was covered with tray adhesive. The root apex was wrapped in flexible, hot adhesive, which was allowed to set before being embedded in a transparent polyvinyl silicone-filled Plexiglas tube. K-file ISO #10 was placed into the mesiolingual root canal to achieve a 0.1 mm apical diameter with a curvature range of 10°–20°, adhering to the Schneider technique [18]. This was performed to ensure apical clearance till its tip was apparent in the apical foramen. While the file was first observed, its length was reduced by 1 mm to obtain the WL, which was fixed at 16 mm [19].

Root canal instrumentation

The Edge File X5 rotary system (EdgeEndo, Albuquerque, NM, USA) was employed for mechanical root canals' preparation through a crown-down method exploiting an endodontic electric motor (XSmart; Dentsply Maillefer, Ballaigues, Switzerland) rated at a modified torque (2 Ncm) at a rotation rate (300 rpm) following the manufacturer's directions. A pecking motion of the rotary system was performed up to the full WL as follows: 20/6%, 20/4%, 30/6%, followed by 30/4% as the master apical file.

Irrigation protocol

The prepared canals were first washed out with a 2.5% NaOCl solution (2 mL) for 1 minute, followed by the same amount of this solution after the #10 K-file and the #15 K-file, each for 1 minute. During instrumentation, continuous irrigation was performed using 2.5% NaOCl (4 mL) for 1 minute via a plastic single-use syringe (Sung Shim Medical, Bucheon, Korea) with a 30-gauge side-vented needle inserted passively and positioned 2 mm from the WL. Finally, to counteract the NaOCl carryover effect, the canals were washed out with (5 mL) DW for 1 minute and finally washed utilizing 17% EDTA for 1 minute. After that, the root canals were randomly assigned across three groups (n = 14) with

https://doi.org/10.5395/rde.2026.51.e15

regard to the dentin biomodification protocol, which applied intra-radicularly as a final irrigant, whereby the root canals were finally irrigated passively with the same volume and duration of the proposed dentin biomodifiers that were applied in the coronal portion as a final irrigant. The entire quantity of irrigants applied in each canal was NaOCl (20 mL) for 6 minutes and DW (5 mL) for 1 minute. The canal patency was preserved via exploiting a K-file size #10. Each instrument was discarded after being used in five canals. All the prepared canals were rinsed with DW (5 mL) for 1 minute, thoroughly dried using absorbent sterile #30 paper points, and then obturated with a master apical gutta-percha point size 30/4% that was extended to the entire canal length. Using a master apical file, the MTA Bioseal bioceramic sealer (Itena Clinical Products, Paris, France) was blended and applied circumferentially. The lateral compaction technique was then used to plug the canals to ensure a tight, adequate seal [20].

Sealer penetration depth measurement

The specimens were maintained at 37°C with 100% humidity for 2 weeks. Thereafter, sealer penetration was measured using SEM (Quanta FEG 250; FEI Company, Eindhoven, the Netherlands). Each root section was split into four quadrants (mesial, distal, buccal, and lingual). Three measurements were carried out in each quadrant. The sealer penetration values were estimated by a single calibrated investigator as the mean of the measurements' data. Images were taken for each quadrant at 500× magnification. The sealers penetrating the dentinal tubules were identified by energy dispersive X-ray analysis as containing a radiopaque constituent (zirconium oxide). Each quadrant was evaluated for the highest sealer penetration depth [21].

Statistical analysis

Data normality has been assessed by examining the distribution, calculating the mean and median, and using the Kolmogorov-Smirnov and Shapiro-Wilk tests. The data exhibited a parametric distribution; hence, they were displayed as mean and standard deviation values. The effects of the examined factors and their interactions were investigated using one- and two-way analyses of variance (ANOVAs). The main and simple effects were compared using pairwise *t*-tests with Bonferroni correction, and proportions across qualitative parameters were compared using the chi-square test of significance. The significance threshold limit was established at $p \leq 0.05$. Statistical assessment was implemented with IBM SPSS for Windows, ver. 26.0 (IBM Corp, Armonk, NY, USA).

RESULTS

Microtensile bond strength

Table 1 demonstrated that the bromelain biomodified group exhibited the highest statistically significant values (46.38 ± 3.42), followed by CHX (39.26 ± 7.60), and the lowest values were recorded with the control specimens (32.41 ± 7.71) based on the ANOVA test ($p = 0.001$) and Bonferroni *post hoc* test. Regarding failure mode distribution, 41% of the bromelain-treated specimens showed cohesive failure, and 29% revealed adhesive failure. In the CHX-treated group, only 23% of the specimens revealed cohesive failures, and 47% showed adhesive failure. In the control group, 11% of the specimens showed cohesive failure, and 58% showed adhesive failure. The mixed failure pattern was equally distributed among all tested groups (Figure 2).

Scanning electron microscope

Representative SEM micrographs of the resin-dentin bond interface for each group are shown in Figure 3.

Table 1. Coronal dentin μTBS among groups

Variable	Control group	Bromelain group	CHX group
Number of specimens	17	17	17
Mean	32.41^{C}	46.38^{A}	39.26^{B}
Standard deviation	7.71	3.42	7.60
Standard error	1.87	0.83	1.84
95% CI for mean	28.45–36.37	44.62–48.14	35.35–43.17
Range	21.59–44.19	39.92–54.17	18.98–47.68
F-test	19.305	—	—
p-value	0.001*	—	—

CHX, chlorhexidine; CI, confidence interval; μTBS, microtensile bond strength.
Bonferroni *post hoc*: Means sharing the same capital letter are not significantly different. Control group vs. bromelain group ($p = 0.001$); control group vs. CHX group ($p = 0.007$); bromelain group vs. CHX group ($p = 0.011$).
*$p \leq 0.05$, statistically significant.

The control specimens demonstrated a thin hybrid layer exhibiting short extending resin tags. In bromelain-treated specimens, resin tags were more numerous, elongated, and exhibited lateral branching and obvious entanglement. Meanwhile, in the CHX group, resin tags were fewer than in the bromelain-treated specimens.

Sealer penetration

A highly statistically significant difference was identified between the groups and across all canal levels (p = 0.001). At the coronal level, the sealer penetration quantity showed the highest significant values, followed by the middle portion, and the lowest values were recorded apically. According to the *post hoc* test, the amount of sealer penetration for bromelain was greatest at both the middle and apical levels (242.84 ± 36.68 and 192.69 ± 23.76, respectively), followed by CHX (218.66 ± 9.01 and 114.76 ± 38.04, respectively). The control group demonstrated the lowest recorded values (194.24 ± 26.75 and 108.73 ± 4.91). The sealer penetration quantity of the CHX group was significantly the highest value coronally (301.46 ± 51.46), followed by the bromelain and control groups (282.90 ± 31.90 and 240.46 ± 6.44, respectively; p = 0.001) (Table 2, Figure 4).

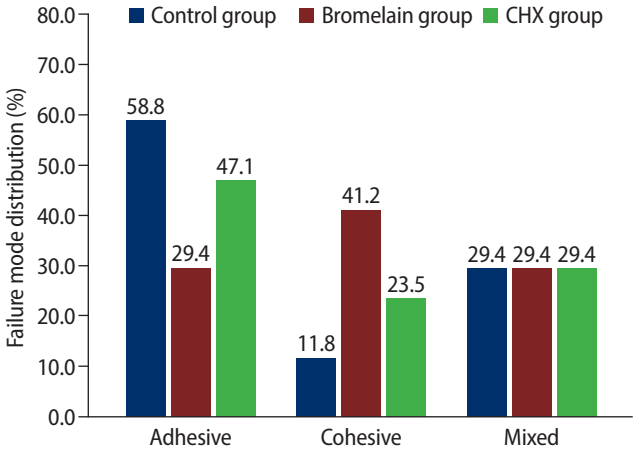

Figure 2. Failure mode distribution (percentage) among the experimental groups. CHX, chlorhexidine.

Table 2. Sealer penetration depth following radicular dentin biomodification

Timeline	Bromelain group	CHX group	Control group	*p*-value
Apical	192.69 ± 23.76^{Ac}	114.76 ± 38.04^{Bc}	108.73 ± 4.91^{Bc}	0.001*
Middle	242.84 ± 36.68^{Ab}	218.66 ± 9.01^{Bb}	194.24 ± 26.75^{Cb}	0.001*
Coronal	282.90 ± 31.90^{Aa}	301.46 ± 51.46^{Aa}	240.46 ± 6.44^{Ba}	0.001*
Mean overall	239.48. ± 30.78^{A}	211.63 ± 32.84^{B}	181.14 ± 12.70^{C}	0.001*
p-value	0.001*	0.001*	0.001*	

Values are presented as mean ± standard deviation.
Different capital letters indicate a significant difference at ($p < 0.05$) among means in the same row. Different small letters indicate a significant difference at ($p < 0.05$) among means in the same column.
*$p < 0.05$, statistically significant.

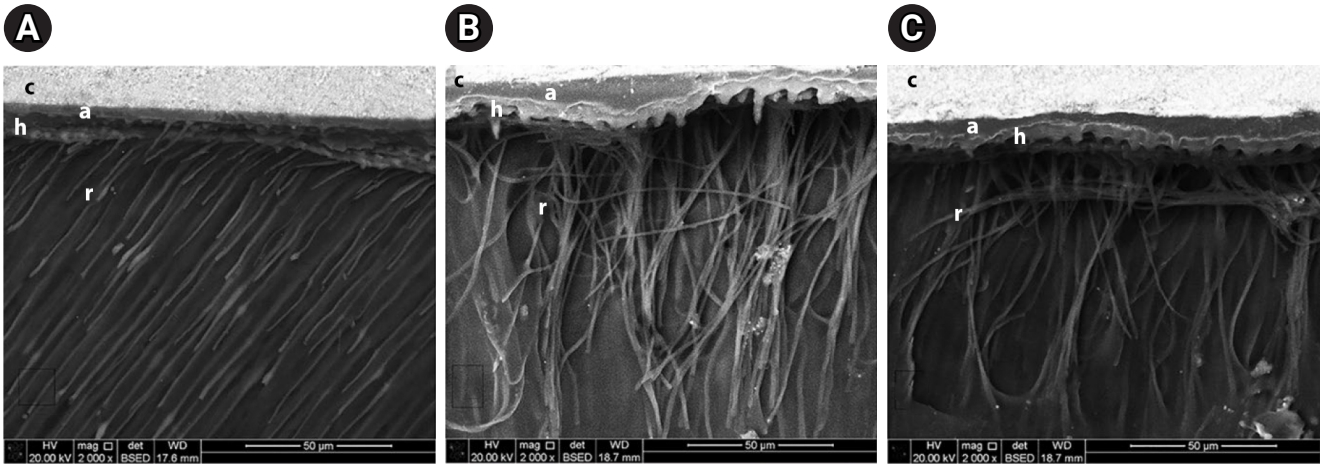

Figure 3. Representative scanning electron microscopy images at magnification 2,000× of the resin-dentin interface of the different groups. (A) Control group, (B) bromelain group, and (C) chlorhexidine group. a, adhesive layer; c, resin composite; h, hybrid layer; r, resin tags.

https://doi.org/10.5395/rde.2026.51.e15

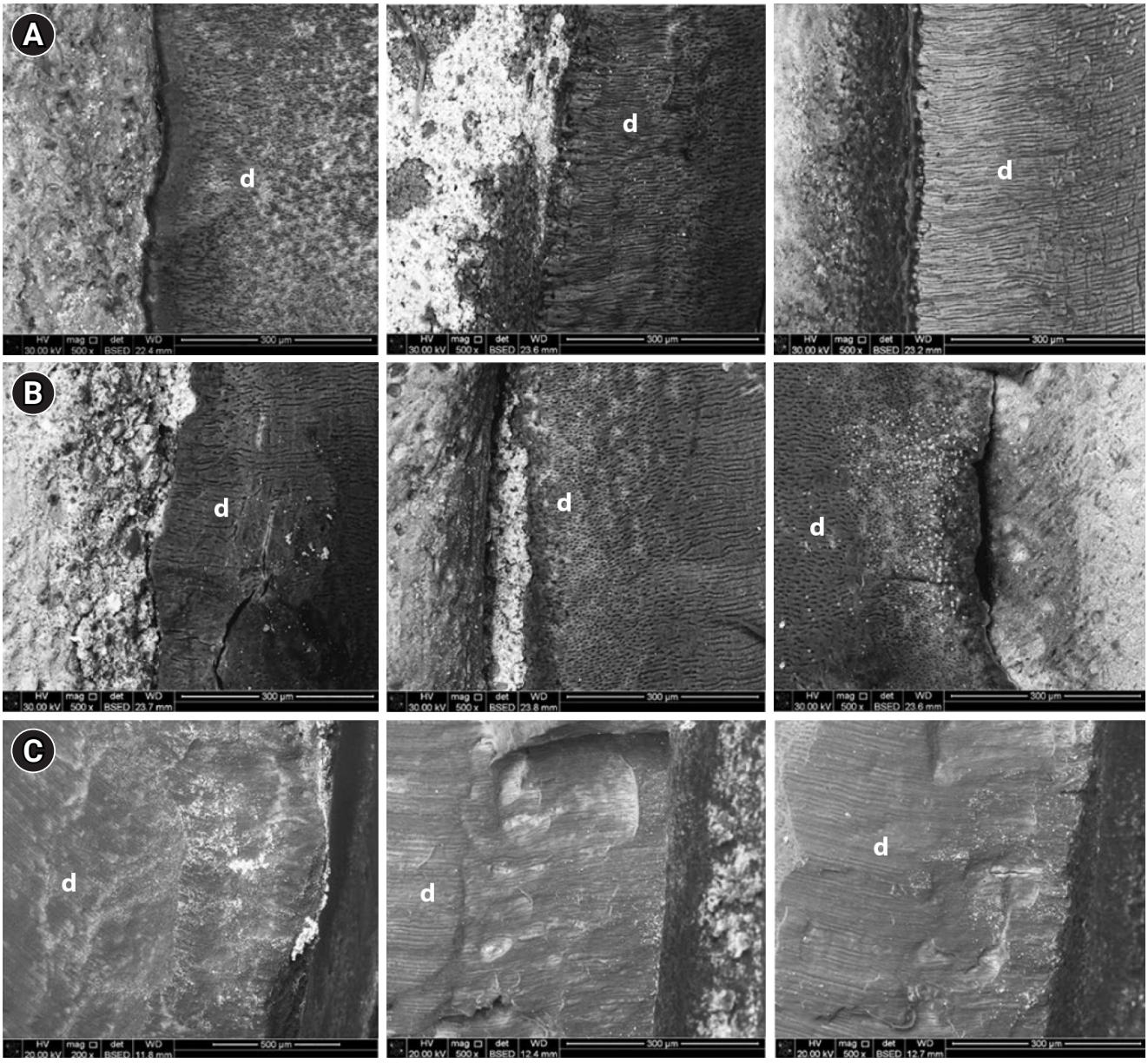

Figure 4. Representative scanning electron microscopy images at 500× magnification showing the sealer penetration depth in the different groups. The images show the coronal third (A.1), middle third (A.2), and apical third (A.3) for the control group; the coronal third (B.1), middle third (B.2), and apical third (B.3) for the bromelain group; and the coronal third (C.1), middle third (C.2), and apical third (C.3) for the chlorhexidine group. d, dentin.

DISCUSSION

Considering the current study's findings, the null hypotheses tested were rejected, as the bromelain enzyme, CHX, influenced both the μTBS in coronal dentin and the sealer penetration depth into radicular dentin, with a remarkable difference compared to the unmodified group.

The primary objectives of endodontic therapy were to effectively clean, shape, and create a fluid-tight seal at both the apical and coronal levels [22]. The irrigants used during biomechanical preparation may influence the bonding of the subsequently applied resinous restorations [5]. Despite the bioceramic sealer's bioactivity, its elevated alkalinity may weaken type I collagen fibrils,

forming nearly all of the radicular dentin [23]. In the current study, an 8% concentration of bromelain enzyme was selected, as it may enhance proteolytic activity, which helps dissolve organic debris without causing dentinal erosion or adverse side effects. So, this research was intended to evaluate the effect of 8% bromelain enzyme, CHX, as an intraradicular final irrigant, on the dentin-collagen matrix integrity by assessing the resin-coronal dentin μTBS, dentin-bond interfacial micromorphology, and sealer penetration depth to radicular dentin utilizing SEM. Regarding the resin-dentin μTBS and sealer penetration results in the middle and apical portions of radicular dentin, bromelain biomodification revealed the highest significant values, followed by CHX. This could be explained by the fact that bromelain deproteinizes dentin by removing the weak, unsupported collagen fibers that may be present following smear layer removal, thereby exposing more dentinal tubules and increasing dentin permeability owing to the elevated surface energy of hydroxyapatite and altered dentin hydrophilic features [10,17]. This result was consistent with previous studies [20,24].

On the other hand, this finding contradicts a previous study that reported that NaOCl, CHX, and Boswellic acid solutions remarkably reduced microbial levels ($p < 0.05$), with no significant differences among them. This controversy might be explained by differences in methodology [25]. CHX dentin biomodification enhanced the resin-dentin bond strength due to its cationic and antibacterial properties. CHX at 0.2% and 2% concentrations inhibited matrix metalloproteinases and cysteine cathepsins, thereby hampering collagen degradation and enhancing bond durability [26,27]. Moreover, its easy binding to phosphate groups and its capacity to raise the dentin's free surface energy would support the notion that using CHX following dentin demineralization could enhance dentin adhesion [28]. These findings were in line with other studies [6]. While inconsistent with a previous study [12], which concluded that lesser collagen degradation was observed in the proanthocyanin-treated group rather than the CHX group. This disparity may be related to the different techniques applied.

At the coronal level, the quantity of sealer penetration for CHX was the highest, followed by bromelain and the control groups. It could be clarified by the substantivity effect of CHX and the enlarged diameter of dentinal tubules coronally [29]. These results were inconsistent with an earlier investigation [30], which found that applying 17% EDTA after CHX gel (2%) for smear film elimination might be recommended, thereby enhancing AH Plus sealer (Dentsply DeTrey GmbH, Konstanz, Germany) penetration. The differences in the results might be related to variations in the evaluation methods or the types of roots used in the study.

The control group showed the least significant values for μTBS and sealer penetration. These findings could be related to the progressive demineralization of the coronal dentin surface [3]. These findings were consistent with another study [31], which found that EDTA, as a final irrigant, could dissolve dentin's inorganic constituents, thereby uncovering the collagen fibrils. Furthermore, it had detrimental impacts on the integrity of the dentin-collagen matrix. Additionally, the chelation of calcium by EDTA could disturb the hydration process of the calcium silicate. The calcium decline at the dentin-sealer interface or degradation of the calcium-silicate sealer's ingredients might hinder the establishment of the mineral-infiltration region, which could finally end in a weaker infiltration of the sealer into the wall of the root canal [32]. These findings were in line with other investigations [33] but conflicted with a previous study that reported that EDTA improved sealer infiltration into dentinal tubules and facilitated the elimination of the smear film [34]. This may be due to the use of a different type of endodontic sealer.

In the current study, sealer penetration depth was greatest coronally, relative to the middle and apical levels. This may be related to reduced tubular density, the presence of sclerotic dentin, and lower apical irrigant efficiency, resulting in less smear layer clearance [35]. The limitations of the current study include the risk of tearing gutta-percha and sealer during SEM specimen preparation of the filled root. Regarding the coronal dentin assessment, bond strength was evaluated only immediately; therefore, bond durability in the pretreated coronal dentin requires further investigation. Further clinical trials are required to investigate the long-term influences of these biomodifiers.

https://doi.org/10.5395/rde.2026.51.e15

CONCLUSIONS

Considering the study's limitations, it can be concluded that bromelain may be promising for clinical use, as its use as a final irrigant may enhance bond strength and sealer infiltration, thereby improving the success rate and prognosis of the entire endodontic treatment.

CONFLICT OF INTEREST

No potential conflict of interest relevant to this article was reported.

FUNDING/SUPPORT

The authors have no financial relationships relevant to this article to disclose.

AUTHOR CONTRIBUTIONS

Conceptualization, Formal analysis, Resources: Aboelwafa MR, Sobh YTM. Data curation, Software, Validation, Visualization: Sobh YTM. Investigation, Methodology, Project administration, Supervision: Aboelwafa MR. Writing - original draft: Aboelwafa MR. Writing - review & editing: Aboelwafa MR. All authors read and approved the final manuscript.

DATA SHARING STATEMENT

The datasets are not publicly available but can be obtained from the corresponding author upon reasonable request.

REFERENCES

1. Wang Z, Shen Y, Haapasalo M. Effectiveness of endodontic disinfecting solutions against young and old enterococcus faecalis biofilms in dentin canals. J Endod 2012;38:1376-1379.
2. Calt S, Serper A. Time-dependent effects of EDTA on dentin structures. J Endod 2002;28:17-19.
3. Omar N, Salem HN, Abdou A, Moharam LM. Effect of various irrigation protocols and antioxidant application on bonding performance of two adhesive systems to coronal dentin. J Clin Exp Dent 2024;16:e406-e415.
4. Nagpal R, Manuja N, Pandit IK. Effect of proanthocyanidin treatment on the bonding effectiveness of adhesive restorations in pulp chamber. J Clin Pediatr Dent 2013;38:49-53.
5. Par M, Steffen T, Dogan S, Walser N, Tauböck TT. Effect of sodium hypochlorite, ethylenediaminetetraacetic acid, and dual-rinse irrigation on dentin adhesion using an etch-and-rinse or self-etch approach. Sci Rep 2024;14:6315.
6. Govindarajan J, Hemasathya BA, Reddy BN, Nathan S, Sankar S, Subramani SK. Comparative assessment of novel collagen cross-linking agents on push-out bond strength of two different sealers: an *in vitro* study. J Contemp Dent Pract 2022;23:1122-1127.
7. Cai J, Palamara JE, Burrow MF. Effects of collagen cross-linkers on dentine: a literature review. Calcif Tissue Int 2018;102:265-279.
8. Nagpal R, Agarwal M, Mehmood N, Singh UP. Dentin biomodifiers to stabilize the bonded interface. Mod Res Dent 2020;5:543-548.
9. Hardan L, Daood U, Bourgi R, Cuevas-Suárez CE, Devoto W, Zarow M, *et al*. Effect of collagen crosslinkers on dentin bond strength of adhesive systems: a systematic review and meta-analysis. Cells 2022;11:2417.
10. Chauhan K, Basavanna RS, Shivanna V. Effect of bromelain enzyme for dentin deproteinization on bond strength of adhesive system. J Conserv Dent 2015;18:360-363.
11. Wang Y, Chen C, Zang HL, Liang YH. The recovery effect of proanthocyanidin on microtensile bond strength to sodium hypochlorite-treated dentine. Int Endod J 2019;52:371-376.
12. Reddy KH, Swetha B, Priya BD, Mohan TM, Malini DL, Sravya MS. Effect of collagen cross-linking agents on the depth of penetration of bioceramic sealer and release of hydroxyproline: an *in vitro* study. J Conserv Dent Endod 2024;27:170-174.
13. Syam AN, Gamal S, Sabra M. Evaluation of micro-tensile bond strength of new composite resins with dentin an in vitro study. Adv Dent J 2019;1:37-43.
14. Costa AR, Garcia-Godoy F, Correr-Sobrinho L, Naves LZ, Raposo LH, Carvalho FG, *et al*. Influence of different dentin substrate (Caries-Affected, Caries-Infected, Sound) on long-term μTBS. Braz Dent J 2017;28:16-23.
15. Elzainy P, Hussein W, Hashem A, Badr M. Post-operative pain after different root canal irrigant activation methods in patients with acute apical periodontitis randomized clinical trial. Open Access Maced J Med Sci 2022;10:331-337.
16. El-Laithy MA, Abdelhakim SH. Effect of bromelain enzyme versus sodium hypochlorite on shear bond strength of resin composite to dentin using two adhesive systems. Egypt Dent J 2024;70:761-767.
17. Sharafeddin F, Safari M. Effect of papain and bromelain enzymes on shear bond strength of composite to superficial dentin in different adhesive systems. J Contemp Dent Pract 2019;20:1077-1081.
18. Schneider SW. A comparison of canal preparations in straight and curved root canals. Oral Surg Oral Med Oral Pathol 1971;32:271-275.

19. Sobh YT, Ragab MH. Residual dentin thickness of root canal transportation by various metallurgical rotary systems: an in vitro study. Saud Endod J 2024;14:69-74.
20. Ali A, Hashem AA, Roshdy NN, Abdelwahed A. The effect of final irrigation agitation techniques on postoperative pain after single visit root canal treatment of symptomatic irreversible pulpitis: a randomised clinical trial. Eur Endod J 2023;8:187-193.
21. Omaia M. SEM evaluation of sealer penetration into dentinal tubules with and without ultrasonic irrigation activation (an in vitro study). Egypt Dent J 2023;69:2447-2454.
22. Santos JN, Carrilho MR, De Goes MF, Zaia AA, Gomes BP, Souza-Filho FJ, *et al*. Effect of chemical irrigants on the bond strength of a self-etching adhesive to pulp chamber dentin. J Endod 2006;32:1088-1090.
23. Yang SY, Liu Y, Mao J, Wu YB, Deng YL, Qi SC, *et al*. The antibiofilm and collagen-stabilizing effects of proanthocyanidin as an auxiliary endodontic irrigant. Int Endod J 2020;53:824-833.
24. Khan R, Sharma N, Garg Y, Kumar G, Garg K, Aleemuddin M. Comparison of different dentin deproteinizing agents on the shear bond strength of resin-bonded dentin. Int J Clin Pediatr Dent 2020;13(Suppl 1):S69-S77.
25. Soliman A, Mohamed M. An alternative therapeutic strategy for root canal disinfection. Egypt Dent J 2022;68:1989-1997.
26. Moon PC, Weaver J, Brooks CN. Review of matrix metalloproteinases' effect on the hybrid dentin bond layer stability and chlorhexidine clinical use to prevent bond failure. Open Dent J 2010;4:147-152.
27. Leitune VC, Collares FM, Werner Samuel SM. Influence of chlorhexidine application at longitudinal push-out bond strength of fiber posts. Oral Surg Oral Med Oral Pathol Oral Radiol Endod 2010;110:e77-e81.
28. de Castro FL, de Andrade MF, Duarte Júnior SL, Vaz LG, Ahid FJ. Effect of 2% chlorhexidine on microtensile bond strength of composite to dentin. J Adhes Dent 2003;5:129-138.
29. Lenzi TL, Guglielmi Cde A, Arana-Chavez VE, Raggio DP. Tubule density and diameter in coronal dentin from primary and permanent human teeth. Microsc Microanal 2013;19:1445-1449.
30. Sabadin N, Hoppe CB, dos Santos RB, Grecca FS. Resin-based sealer penetration into dentinal tubules after the use of 2% chlorhexidine gel and 17% EDTA: in vitro study. Braz J Oral Sci 2014;14:308-313.
31. Qian W, Shen Y, Haapasalo M. Quantitative analysis of the effect of irrigant solution sequences on dentin erosion. J Endod 2011;37:1437-1441.
32. Atmeh AR, Chong EZ, Richard G, Festy F, Watson TF. Dentin-cement interfacial interaction: calcium silicates and polyalkenoates. J Dent Res 2012;91:454-459.
33. Shekhar S, Mallya PL, Ballal V, Shenoy R. To evaluate and compare the effect of 17% EDTA, 10% citric acid, 7% maleic acid on the dentinal tubule penetration depth of bio ceramic root canal sealer using confocal laser scanning microscopy: an *in vitro* study. F1000Res 2022;11:1561.
34. Nunes VH, Silva RG, Alfredo E, Sousa-Neto MD, Silva-Sousa YT. Adhesion of Epiphany and AH Plus sealers to human root dentin treated with different solutions. Braz Dent J 2008;19:46-50.
35. Mokashi P, Shah J, Chandrasekhar P, Kulkarni GP, Podar R, Singh S. Comparison of the penetration depth of five root canal sealers: a confocal laser scanning microscopic study. J Conserv Dent 2021;24:199-203.

https://doi.org/10.5395/rde.2026.51.e15

RDE Restorative Dentistry & Endodontics

Research Article

eISSN 2234-7666
Restor Dent Endod. 2026 May;51(2):e16
https://doi.org/10.5395/rde.2026.51.e16

Effect of sugar and sweetener on the bleachability of coffee and tea-induced stains on composites: an *in vitro* experimental study

Nilay Bayraktar[1,*], Osman Kerim Arda Karaca[2], Yunus Ekşılı[2], Mustafa Furkan Yıldırım[2], Osman Tolga Harorli[1]

[1]Department of Restorative Dentistry, Faculty of Dentistry, Akdeniz University, Antalya, Türkiye
[2]Faculty of Dentistry, Akdeniz University, Antalya, Türkiye

ABSTRACT

Objectives: This *in vitro* study evaluated the effects of various sugary and non-sugary beverages on the color change of a dental composite and the subsequent bleaching efficacy.

Methods: Forty-nine disc-shaped composite samples (Neo Spectra ST, Dentsply Sirona) were split into seven groups at random ($n = 7$). Distilled water was used to hydrate each sample for 24 hours at 37°C. After 24 hours, the first color measurements (T0) were made by using a clinical spectrophotometer (VITA Easyshade Compact; VITA Zahnfabrik). Color measurements were repeated after 7 days (T1) and 14 days (T2) of immersion in distilled water (control), tea, coffee, sugary tea, sugary coffee, tea with sweetener added, and coffee with sweetener added. After staining for 2 weeks, the specimens were bleached for 6 hours a day for a week using 16% carbamide peroxide (Opalescence Ultradent Products). Color measurements were taken again after bleaching (T3). Using CIEDE2000, color differences (ΔE) were computed. Analysis of variance (ANOVA) and repeated measures ANOVA with a Tukey *post hoc* test were used to evaluate the data.

Results: After 1 week, coffee-containing solutions produced significantly greater discoloration than the control ($p < 0.001$). By 2 weeks, tea groups exhibited similar discoloration to coffee groups ($p < 0.001$). The addition of sugar or sweetener had no significant effect ($p > 0.05$). Post-bleaching, coffee groups showed lower Whiteness Index values than the control, without statistical significance ($p > 0.05$).

Conclusions: Coffee and tea markedly stain resin composites, with discoloration persisting post-bleaching, while sugar or sweetener additions exert no significant effect.

Keywords: Color; Composite resins; Tooth bleaching; Sugars

INTRODUCTION

Aesthetics plays a vital role for patients undergoing dental procedures. Resin composite is frequently chosen as a direct restorative material due to its versatility. Achieving an initial and long-term color match with surrounding teeth is crucial for its success. However, continuous exposure of resin composite to beverages can lead to

Received: August 15, 2025 **Revised:** January 5, 2026 **Accepted:** January 6, 2026

Citation
Bayraktar N, Karaca OKA, Ekşılı Y, Yıldırım MF, Harorli OT. Effect of sugar and sweetener on the bleachability of coffee and tea-induced stains on composites: an *in vitro* experimental study. Restor Dent Endod 2026;51(2):e16.

***Correspondence to**
Nilay Bayraktar, DDS
Department of Restorative Dentistry, Faculty of Dentistry, Akdeniz University, Dumlupınar Boulevard, 07070 Antalya, Türkiye
Email: nilay_bayraktar85@hotmail.com

discoloration over time [1]. Intraoral resin composite restorations can undergo discoloration due to either intrinsic or extrinsic factors. Intrinsic factors are linked to the resin composite's composition, such as the type of photo-initiator and resin matrix used. Conversely, extrinsic factors involve the absorption or adsorption of stains from external sources, which are largely influenced by an individual's dietary habits. Common beverages like tea and coffee, for instance, are known to stain both natural teeth and tooth-colored restorations, presenting aesthetic challenges and frustrations for patients [2,3].

Bleaching offers a minimally invasive method to whiten teeth affected by stains, whether they originate from external sources or are embedded within the tooth structure. Techniques for bleaching can be categorized based on whether they target vital or non-vital teeth, as well as whether the procedure is conducted professionally in a dental office or includes a self-administered component for home use [4–6]. These agents, functioning through comparable mechanisms, interact with and dismantle the organic pigment molecules accountable for tooth discoloration [7]. Hydrogen peroxide and carbamide peroxide are the predominant active ingredients in bleaching products. These substances vary in concentration based on the type of bleaching agent used. Home bleaching kits are applied over extended periods with lower concentrations of active ingredients, whereas office-based bleaching procedures involve shorter application times with higher concentrations of active substances [8].

Extraoral spectrophotometers remain the gold standard due to their precision and ability to provide consistent measurements in controlled environments. Conversely, intraoral spectrophotometers offer practical advantages by allowing for on-site color determination, which is particularly valuable during dental procedures [9]. In the context of color measurement, the CIEDE2000 formula provides a more accurate reflection of human color perception compared to older methods such as the original CIELAB system. The perceptibility threshold of ΔE00 = 0.8 indicates the smallest color difference that an average observer can detect, while the acceptability threshold of ΔE00 = 1.8 suggests the limit beyond which color differences are considered unacceptable or noticeable [10].

Stevia has been used as a natural sweetener in many countries for years due to its properties, such as being good for various diseases such as diabetes, being calorie-free, non-toxic, and not participating in browning reactions during food processing. In addition to its features, such as being 300 times sweeter than sucrose, having high heat and pH stability, baking and oven stability, being soluble in alcohol, and not leaving a metallic taste in the mouth, its most important feature is that it can be produced naturally [11].

Although there are many studies in the literature on coloring solutions, there is no study on the addition of sugar or sweetener to these beverages. Considering that tea and coffee in Türkiye are typically consumed with added sugar, this study included sugar and sweeteners in the colored beverages. This *in vitro* study evaluated how these solutions, both with and without sugar or sweetener, impact coloration and the subsequent success of bleaching. The study hypotheses are as follows: (i) Storage in different beverages would not affect the color stability of composite resins. (ii) Adding sugar or a sweetener to beverages would not have any effect on the color change. (iii) The bleaching protocol would not affect the Whiteness Index values of all groups.

METHODS

Sample preparation

An a priori power analysis was conducted using G*Power software (version 3.1.9.6; Heinrich-Heine-Universität Düsseldorf, Düsseldorf, Germany) to determine the minimum sample size required to detect meaningful differences among the experimental groups. The power calculation was based on the main effect of additive (none, sugar, sweetener) in a 2 × 3 two-way analysis of variance (ANOVA) design (beverage × additive), with numerator degrees of freedom = 2. A total of 49 specimens were included; 42 specimens fulfilled the requirements of the 2 × 3 factorial design, while the remaining seven specimens formed an independent control group. A medium-to-large effect size was assumed (f = 0.50), together with a significance level of α = 0.05 and a target statistical power of 0.80. Under these assumptions, the required total sample size was 42 specimens (seven per

https://doi.org/10.5395/rde.2026.51.e16

group), yielding an actual power of 0.80. According to Cohen's classification, the assumed effect size (f = 0.50) corresponds to a medium-to-large effect and was considered appropriate for the present controlled *in vitro* design. Forty-nine composite specimens (Neo Spectra ST; Dentsply Sirona, Konstanz, Germany) were prepared in a Teflon mold (5 mm in diameter and 2 mm in thickness). After applying the composite resin, a Mylar strip was placed and pressed with a glass slide to obtain a flat surface. The specimens were cured for 20 seconds using an LED light-curing unit (VALO; Ultradent Products Inc., South Jordan, UT, USA). The specimens were removed from the mold and assessed visually for voids and structural defects. Defected specimens were excluded from the study. In the next step, the specimen surfaces were polished with Sof-Lex discs (3M ESPE, St. Paul, MN, USA) for 15 seconds. Specimens were randomly divided into seven groups (n = 7). Beverages used in this experiment were the control group (distilled water), instant tea, tea + sugar added, tea + sweetener added, instant coffee, coffee + sugar added, and coffee + sweetener added.

1) Control group: In this group, the composite specimens were kept in distilled water only.
2) Tea group: The tea solution was prepared by means of the following procedure. Two prefabricated doses (2 × 2 g) of tea (Yellow Label Tea; Lipton, Rize, Türkiye) were immersed in 200 mL of boiling water at 100°C for 1 minute. After removing the tea waste, the final solution volume was determined to be 200 mL.
3) Coffee group: The coffee solution was prepared by first pouring 6 g of Nescafé Classic ground coffee powder (Nestlé S.A., Vevey, Switzerland) into a coffee filter. Then, 200 mL of water at 100°C was added. The solution obtained was subsequently subjected to a secondary filtration process, resulting in the attainment of a final volume of 200 mL.
4) Tea + 5 g sugar added group: The tea solution was prepared as described above. After this step, 5 g of sugar was added and mixed until dissolved.
5) Coffee + 5 g sugar added group: The coffee solution was prepared as described above. After this step, 5 g of sugar was added and mixed until dissolved.
6) Tea + sweetener added group: The tea solution was prepared as described above. After this step, two units (0.1 g) of sweetener (Splenda Stevia; Heartland Food Products Group, Indianapolis, IN, USA) were added and mixed until dissolved.
7) Coffee + sweetener added group: The coffee solution was prepared as described above. After this step, two units (0.1 g) of sweetener (Splenda Stevia) was added and mixed until dissolved.

Color measurement

All discoloration solutions were renewed daily, and the specimens were rinsed with distilled water for 10 seconds before measurements. The specimens were stored in these staining solutions at 37°C ± 2°C in a dark environment. The color coordinates of specimens were recorded after 24 hours (T0), 1 week (T1), and 2 weeks (T2) of immersion.

All color measurements were performed by using a clinical spectrophotometer (VITA Easyshade Compact; VITA Zahnfabrik, Bad Säckingen, Germany) according to the CIEDE2000 color coordinates. Prior to each measurement, the spectrophotometer was calibrated following the manufacturer's guidelines [12]. To determine the color differences between groups, the ΔE00 values were calculated by using the following formula [5]:

$$\Delta E_{00} = \sqrt{\left(\frac{\Delta L}{K_L S_L}\right)^2 + \left(\frac{\Delta C}{K_C S_C}\right)^2 + \left(\frac{\Delta H}{K_H S_H}\right)^2 + R_T\left(\frac{\Delta C}{K_C S_C}\right)\left(\frac{\Delta H}{K_H S_H}\right)},$$

With the set of L*, a*, b* values taken with respect to the white background. For this study, each K_L, K_C, and K_H was set to 1.0. It is posited that variations in brightness, chroma, and hue are represented by variables ΔL, ΔC, and ΔH. While S_L, S_C, and S_H are averaging variables for lightness, chroma, and hue, K_L, K_C, and K_H are weighted factors. R_T is a general correction factor that takes into account variations in chroma and hue [13]. The clinically 50:50% acceptable color change threshold level was determined as ΔE00 = 1.8 (10).

Home bleaching procedure

The home bleaching technique, 16% carbamide peroxide (Opalescence 16%; Ultradent Products Inc.) was placed on each sample surface, using a dispenser tip, forming a layer that was up to 1 mm thick. The bleach-

ing agent was left in contact with each tooth sample for a period of 6 hours daily for 1 week and was subsequently removed using a cotton pellet and rinsing [14]. During bleaching intervals, specimens were maintained in the incubator at 37°C. This procedure was repeated on a daily basis for a total of 1 week. After bleaching, color measurements were taken again (T3).

Statistical analysis

Power analysis was conducted using G*Power software (version 3.1.9.6). The analysis of the data was conducted using IBM SPSS ver. 23 (IBM Corp, Armonk, NY, USA). Following a thorough evaluation, it was determined that the distributions exhibited characteristics consistent with normality, as evidenced by the Kolmogorov-Smirnov test. A three-way and two-way ANOVA test was applied in order to ascertain whether there were any significant differences among the groups. The Tukey test was employed as a *post hoc* analysis to evaluate the pairwise comparisons. The significance level was predetermined at $p < 0.05$.

RESULTS

All solutions containing coffee showed significantly more coloration than the control group after 1 week of immersion ($p < 0.001$, $\eta p^2 = 0.72$) (Figure 1). Adding sugar or a sweetener to the tested beverages had no significant effect on coloration ($p > 0.05$). Color change became evident, especially in the tea groups, in the 2nd week (Figure 2).

The results demonstrated that both coffee and tea caused a darkening effect on the samples over time, as indicated by the decrease in L* values in Figure 3. The bleaching treatment was effective in increasing the L* values, indicating a lightening effect. The control group showed a consistent increase in L* values after bleaching, indicating that the treatment works well in the absence of staining agents. Coffee appeared to have a more pronounced darkening effect compared to tea, as evidenced by the larger decrease in L* values over time.

For a* values coffee caused a significant shift towards red on the a* axis over time in Figure 4, while tea had a milder effect. The bleaching treatment was effective in reducing the red shift, bringing the a* values closer to the baseline, especially in the tea group. The control group showed minimal changes in the a* values throughout the experiment, indicating stability in the red-green axis in the absence of staining agents.

When the results were examined in Figure 5, it was seen that coffee caused a significant yellowish tint on the samples over time, as indicated by the increase in b* values. The bleaching treatment was effective in reducing the yellowish tint, bringing the b* values closer to the baseline. The tea group showed a unique behavior at the 2-week mark, where the b* values decreased signifi-

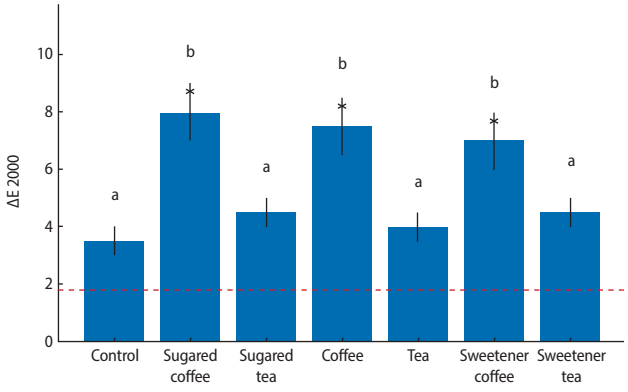

Figure 1. Mean color changes (ΔE_{00}) of composite samples after 1 week of immersion in different beverages. Different letters indicate statistically significant differences among groups. The red dashed line ($\Delta E_{00} = 1.8$) represents the clinical acceptability threshold for perceptible color change.

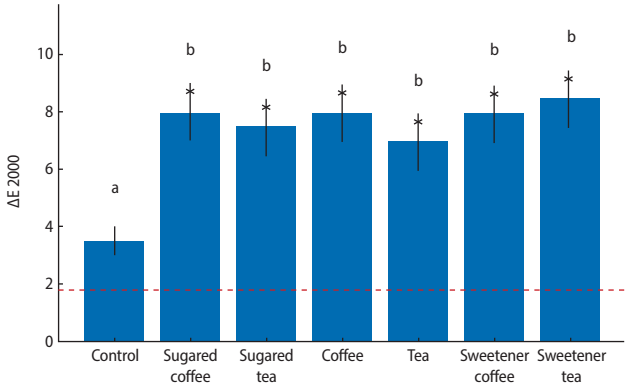

Figure 2. Mean color changes (ΔE_{00}) of composite samples after 2 weeks of immersion in different beverages. Different letters indicate statistically significant differences among groups. The red dashed line ($\Delta E_{00} = 1.8$) denotes the clinical acceptability threshold for perceptible color difference.

https://doi.org/10.5395/rde.2026.51.e16

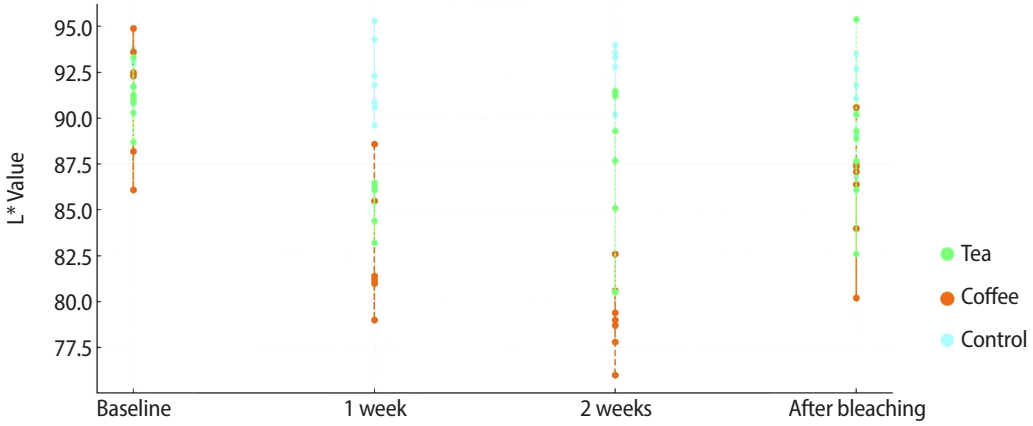

Figure 3. Changes in L* values of composite samples at baseline, after 1 week, 2 weeks of staining, and following bleaching for tea, coffee, and control groups. A decrease in L* indicates darkening, while an increase reflects lightening of the specimens.

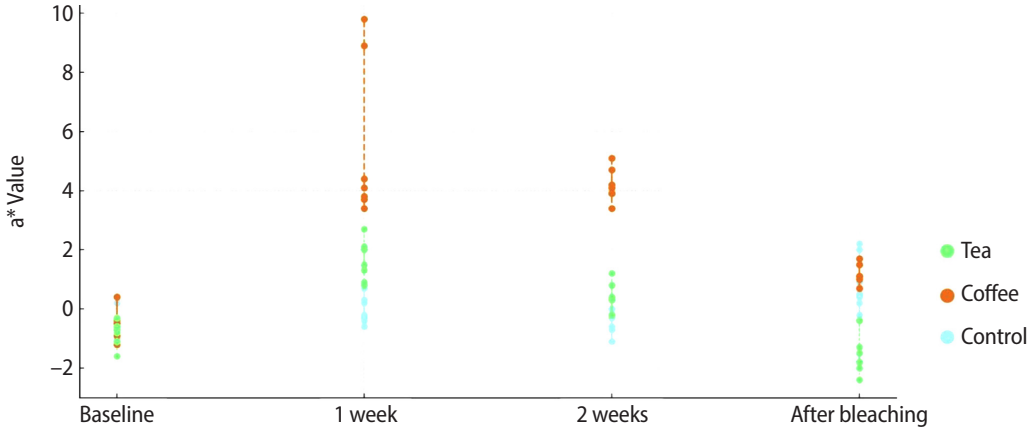

Figure 4. Changes in a* values of composite samples at baseline, after 1 week, 2 weeks of staining, and following bleaching for tea, coffee, and control groups. An increase in a* indicates a shift toward red, while a decrease represents a shift toward green.

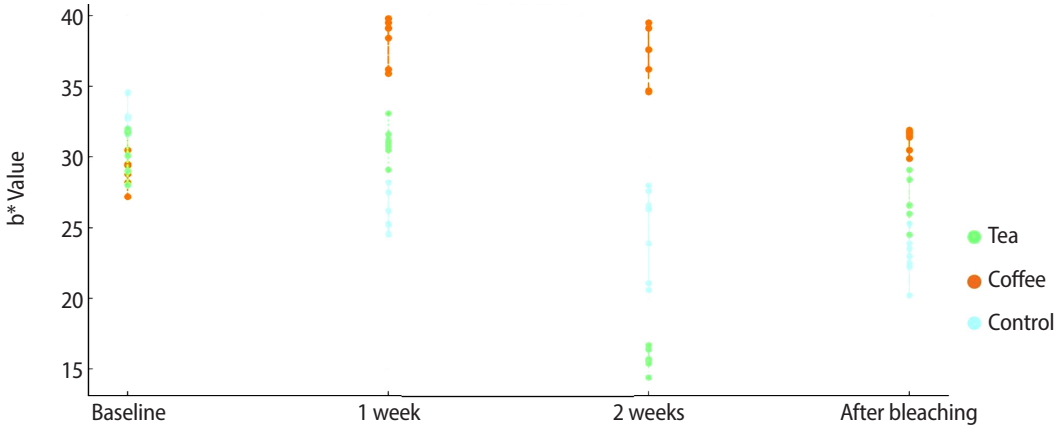

Figure 5. Changes in b* values of composite samples at baseline, after 1 week, 2 weeks of staining, and following bleaching for tea, coffee, and control groups. An increase in b* indicates a shift toward yellow, while a decrease represents a reduction in yellow hue after bleaching.

cantly, indicating a reduction in the yellowish tint. This is contrary to the behavior observed in the coffee group and suggests that tea might have a different interaction with the sample material over extended exposure. This could be due to various factors, such as chemical interactions between tea components and the sample material that inhibit yellowing over time.

The heatmap visually represents the overall color changes for each group over time. Coffee had a pronounced yellowing effect, while tea caused a milder yellowing effect with an unusual reduction at the 2-week mark (Figure 6). Bleaching effectively lightened the color across all groups, with the tea group returning closer to baseline after bleaching. The control group remained relatively stable with a slight lightening effect over time. This visualization highlights the impact of different staining agents and bleaching treatments on the overall color of the samples.

When the Whiteness Index values were examined after bleaching in Figure 7, it was determined that the coffee groups showed statistically lower values than the control group. The whiteness values of the tea groups

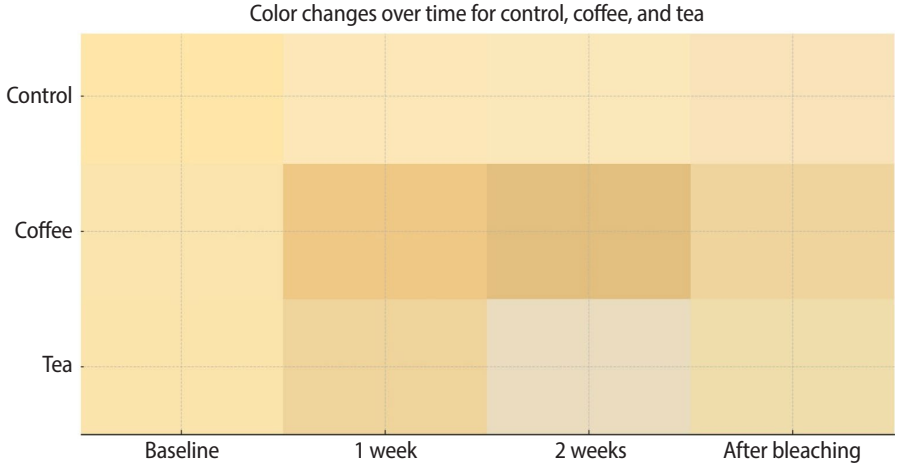

Figure 6. The visualization of the color changes over time for control, coffee, and tea samples. Each cell represents the average color at each time point for each group, converted from Lab* to RGB values.

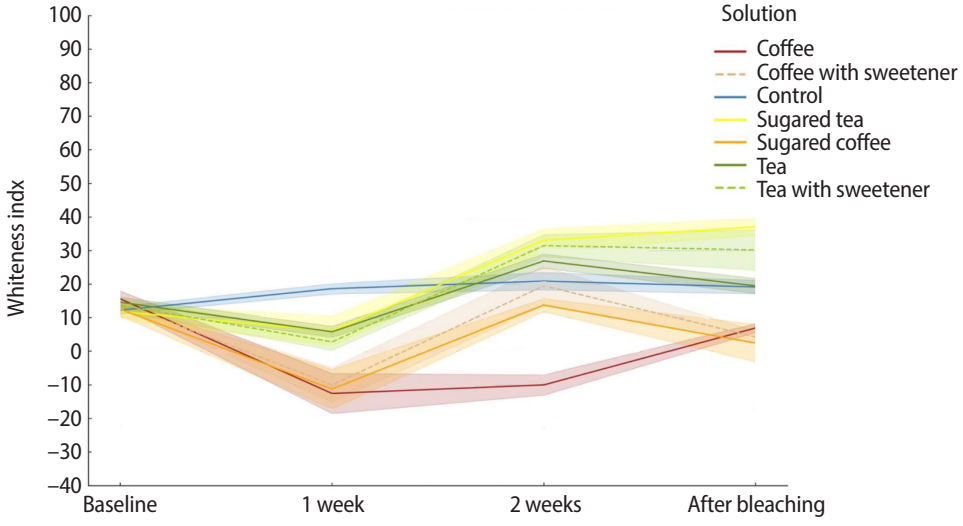

Figure 7. Whiteness index values with 95% confidence intervals.

https://doi.org/10.5395/rde.2026.51.e16

were similar and partially higher than those of the control group. Tea groups showed higher values than the coffee groups.

DISCUSSION

The present study investigated the staining susceptibility of dental composites to commonly consumed beverages and their response to bleaching treatment, with particular attention to the novel aspect of sugar and sweetener additives. The findings demonstrate that both coffee and tea significantly compromise the color stability of composite resins, with staining effects persisting even after bleaching procedures, thus leading to the rejection of the first hypothesis.

The significant discoloration observed in all beverage groups compared to the control can be attributed to the complex interaction between chromogenic compounds and the composite matrix. Coffee-containing solutions demonstrated more pronounced staining effects after 1 week of immersion ($p < 0.001$), which aligns with previous research indicating that coffee contains higher concentrations of tannins and chromogenic compounds compared to tea [15]. The polyphenolic compounds in these beverages can penetrate the resin matrix through micro-porosities and form chemical bonds with the polymer chains, resulting in staining [16].

The staining durations of 1 and 2 weeks were selected to represent both short-term and extended exposure models, enabling the evaluation of progressive discoloration patterns under conditions that approximate daily beverage consumption. It has been reported that 24 hours of *in vitro* immersion corresponds to approximately 1 month of *in vivo* aging, supporting the assumption that the 1-week immersion period used in the present study roughly simulates 6–8 months of clinical beverage exposure [17], whereas extending the exposure to 2 weeks provides a more intensified model that mimics long-term consumption habits [1,15,16]. This design allows assessment of both the initial discoloration potential and the saturation stage of staining over time. Therefore, the 1-week duration was chosen to observe early color changes, while the 2-week duration was included to investigate whether color stabilization or further pigment accumulation would occur with prolonged exposure. Similarly, a 1-week bleaching period using 16% carbamide peroxide for 6 hours daily reflects a commonly recommended home bleaching protocol, which has been reported to achieve effective color recovery without compromising composite integrity [8,14]. Therefore, the chosen durations were designed to balance experimental efficiency with clinical relevance, allowing reliable comparison of staining and bleaching behavior within a controlled timeframe.

The differential staining patterns observed between coffee and tea groups reflect their distinct chemical compositions. Coffee's more immediate and pronounced effect on the L* values (lightness) indicates greater penetration of dark-colored compounds, while the unique behavior of tea at the 2-week mark—where b* values decreased significantly—suggests a complex interaction possibly involving tannin precipitation over extended exposure periods. This finding warrants further investigation using spectroscopic analysis to elucidate the underlying chemical mechanisms.

A key finding of this study is that the addition of sugar or stevia-based sweetener did not significantly affect the staining potential of either coffee or tea ($p > 0.05$), leading to acceptance of our second hypothesis. This result is particularly relevant given the cultural context where these beverages are commonly consumed with additives. Several factors may explain this finding: The sugar concentration used (5 g per 200 mL) may not be sufficient to alter the physical properties of the staining solutions significantly, neither sucrose nor stevia appears to interfere with the chromogenic compounds responsible for staining, the molecular size of sugar and stevia compounds may not significantly alter the diffusion pathways of staining agents into the composite matrix. This finding has important clinical implications, suggesting that patients need not avoid sweeteners in their beverages specifically to prevent composite staining, though the beverages themselves remain problematic.

The bleaching protocol using 16% carbamide peroxide demonstrated variable success across different staining agents. While the treatment effectively increased L* values (lightness) in all groups, indicating successful removal of chromogenic compounds, the coffee groups showed persistently lower Whiteness Index values compared to controls after bleaching ($p < 0.05$), leading to

rejection of our third hypothesis.

Coffee-induced stains may penetrate deeper into the composite matrix or form stronger chemical bonds that are more resistant to oxidative bleaching agents or the 16% carbamide peroxide concentration, while appropriate for home bleaching protocols, may be insufficient for complete removal of deeply embedded stains. Higher concentrations or alternative bleaching agents might yield better results, though this requires investigation of potential adverse effects on composite properties.

The slight decrease in L* values observed in the control group after bleaching may be attributed to surface alterations induced by the bleaching agent rather than pigment removal. Although no staining agents were present, exposure to carbamide peroxide can cause superficial dehydration or changes in surface roughness and refractive index, which can temporarily reduce brightness perception [4,5]. In addition, microscopic surface irregularities formed by oxidative reactions might scatter light differently, leading to a minor reduction in measured L* values despite the absence of external staining. Similar findings have been reported by Rodrigues *et al.* [6] and Karataş *et al.* [8], who noted that bleaching agents may induce subtle optical or microstructural changes even in unstained composite materials.

The staining and bleaching behaviors of resin composites are strongly influenced by their intrinsic material characteristics, particularly the resin matrix composition, filler type, and filler load. Composites with a higher proportion of hydrophilic monomers such as triethylene glycol dimethacrylate exhibit greater water sorption and pigment uptake compared to those with more hydrophobic matrices like bisphenol A-glycidyl methacrylate or urethane dimethacrylate [18,19]. Increased filler content and smaller particle size improve surface smoothness and reduce microvoids, thereby minimizing stain penetration and facilitating more efficient bleaching [9]. Conversely, composites with lower filler loading or irregular filler distribution tend to have higher surface roughness, promoting adsorption of chromogenic molecules and limiting the penetration of bleaching agents [8]. Overall, materials with dense filler packing, reduced water sorption, and a highly cross-linked, hydrophobic resin matrix generally demonstrate superior stain resistance and more predictable bleaching outcomes.

The present study employed Neo Spectra ST (Dentsply Sirona), a nanohybrid composite resin incorporating SphereTEC filler technology, which is designed to provide improved handling characteristics, high filler loading, and enhanced optical blending with natural dentition. According to previous investigations, this material demonstrates satisfactory clinical and esthetic performance; however, some studies have indicated that its color stability and surface properties may vary depending on the staining medium and finishing protocols used. For instance, a recent *in vitro* study comparing Neo Spectra ST high viscosity with other universal composites reported significantly higher ΔE values after immersion in coffee and tea solutions, suggesting a moderate susceptibility to extrinsic discoloration [20]. Similarly, Shah *et al.* [21] observed that Neo Spectra ST exhibited slightly lower microhardness values than other nanohybrid composites, which may contribute to its surface roughness and potential for stain accumulation. Nevertheless, long-term clinical studies have shown that Neo Spectra ST provides acceptable overall performance, with only minor increases in surface wear or discoloration over time [22,23].

Given this evidence, the use of Neo Spectra ST in the current study is justified, as it represents a widely used, clinically relevant material with well-documented mechanical and optical characteristics. The absence of comparable studies examining the influence of sweetener or sugar additives on the staining behavior of this composite highlights the novelty of the present research. Therefore, while findings from other materials may not be directly extrapolated, the results obtained here contribute valuable insight into the color stability of Neo Spectra ST under conditions simulating common beverage consumption habits. Future research comparing different composite systems and sweetener types would further clarify whether these findings are material-specific or represent a broader trend among nanohybrid resin composites.

The persistent staining observed even after bleaching treatment has several important clinical implications: Patients should be informed that dietary habits significantly impact the longevity of composite restorations' aesthetic properties, and that bleaching may not com-

https://doi.org/10.5395/rde.2026.51.e16

pletely restore original coloration. In patients with high consumption of staining beverages, alternative restorative materials with superior stain resistance or more frequent replacement schedules should be considered. While sugar and sweetener additives do not increase staining risk, the base beverages themselves remain problematic. Patients might benefit from strategies such as using straws, limiting contact time, or immediately rinsing after consumption. The findings suggest that preventive measures are more effective than corrective bleaching, emphasizing the importance of patient education and dietary counseling.

Several limitations must be acknowledged when interpreting these findings: The study examined only one composite system. Different resin matrices, filler compositions, and surface treatments may respond differently to staining and bleaching protocols. Future studies should investigate multiple composite systems to establish broader clinical applicability. The *in vitro* design, while providing controlled conditions, cannot replicate the complex oral environment. Factors such as saliva flow, pH fluctuations, masticatory forces, and oral hygiene practices significantly influence staining patterns in clinical settings. The daily renewal of staining solutions may not accurately represent typical beverage consumption patterns.

Future studies—particularly *in vivo* and in situ investigations—are necessary to confirm these findings under clinically relevant conditions.

CONCLUSIONS

This study demonstrates that coffee and tea consumption significantly compromises the color stability of dental composites, with coffee showing more pronounced and persistent staining effects. Importantly, the addition of sugar or stevia-based sweeteners does not exacerbate staining, providing valuable information for patient counseling. However, the limited efficacy of bleaching treatments, particularly for coffee stains, emphasizes the importance of preventive strategies over corrective interventions. These findings should inform clinical decision-making regarding material selection, patient counseling, and maintenance protocols for composite restorations in patients with high consumption of chromogenic beverages.

CONFLICT OF INTEREST

No potential conflict of interest relevant to this article was reported.

FUNDING/SUPPORT

The authors have no financial relationships relevant to this article to disclose.

AUTHOR CONTRIBUTIONS

Conceptualization, Project administration: Harorlı OT, Bayraktar N. Formal analysis, Supervision, Validation: Harorlı OT. Investigation, Methodology, Resources: Karaca OKA, Ekşili Y, Yıldırım MF. Writing - original draft: Harorlı OT, Bayraktar N. Writing - review & editing: Harorlı OT, Bayraktar N. All authors read and approved the final manuscript.

DATA SHARING STATEMENT

The datasets are not publicly available but are available from the corresponding author upon reasonable request.

REFERENCES

1. Alhotan A, Abdelraouf RM, Alhijji S, De Vera MA, Sufyan A, Matinlinna JP, *et al.* Colour parameters and changes of tea-stained resin composite exposed to whitening pen (in vitro study). Polymers (Basel) 2023;15:3068.
2. Nasoohi N, Hadian M, Hoorizad M, Hashemi S, Naziri Saeed SH. In vitro effect of alcohol and non-alcohol mouthwash on color change of two types of bleach shade composite. J Res Dent Maxillofac Sci 2019;4:1-6.
3. Ardu S, Duc O, Di Bella E, Krejci I, Daher R. Color stability of different composite resins after polishing. Odontology 2018;106:328-333.
4. Taher NM. The effect of bleaching agents on the surface hardness of tooth colored restorative materials. J Contemp Dent Pract 2005;6:18-26.
5. Polydorou O, Mönting JS, Hellwig E, Auschill TM. Effect of in-office tooth bleaching on the microhardness of six dental esthetic restorative materials. Dent Mater 2007;23:153-158.
6. Rodrigues JA, Marchi GM, Ambrosano GM, Heymann HO, Pimenta LA. Microhardness evaluation of in situ vital bleaching on human dental enamel using a novel study design. Dent Mater 2005;21:1059-1067.
7. Majeed A, Farooq I, Grobler SR, Rossouw RJ. Tooth-bleaching: a review of the efficacy and adverse effects of various tooth whitening products. J Coll Physicians Surg Pak

2015;25:891-896.
8. Karatas O, Gul P, Akgul N, Celik N, Gundogdu M, Duymus ZY, *et al*. Effect of staining and bleaching on the microhardness, surface roughness and color of different composite resins. Dent Med Probl 2021;58:369-376.
9. Hamdy TM, Abdelnabi A, Othman MS, Bayoumi RE, Abdelraouf RM. Effect of different mouthwashes on the surface microhardness and color stability of dental nanohybrid resin composite. Polymers (Basel) 2023;15:815.
10. Paravina RD, Ghinea R, Herrera LJ, Bona AD, Igiel C, Linninger M, *et al*. Color difference thresholds in dentistry. J Esthet Restor Dent 2015;27 Suppl 1:S1-S9.
11. Karagöz Ş, Demirdöven A. Stevia rebaudiana bitkisinin tatlandırıcı, antioksidan ve antimikrobiyal özellikleri. Akademik Gıda 2018;16:431-438.
12. Wu Z, Tian J, Wei D, Zhang Y, Lin Y, Di P. Effects of thickness and polishing treatment on the translucency and opalescence of six dental CAD-CAM monolithic restorative materials: an in vitro study. BMC Oral Health 2023;23:579.
13. Ntovas P, Masouras K, Lagouvardos P. Efficacy of non-hydrogen peroxide mouthrinses on tooth whitening: an in vitro study. J Esthet Restor Dent 2021;33:1059-1065.
14. Hasani E, Baghban AA, Sheikh-Al-Eslamian SM, Sadr A. Effect of bleaching on color change of composite after immersion in chlorhexidine and coffee. J Conserv Dent 2019;22:529-532.
15. Jaâfoura S, Kikly A, Fejjeri M, Nasri S, Brini M, Kammoun D. Color stability of microhybrid composite resins depending on the immersion medium. Eur J Dent 2025;19:500-512.
16. Sarembe S, Kiesow A, Pratten J, Webster C. The impact on dental staining caused by beverages in combination with chlorhexidine digluconate. Eur J Dent 2022;16:911-918.
17. Cinelli F, Scaminaci Russo D, Nieri M, Giachetti L. Stain susceptibility of composite resins: pigment penetration analysis. Materials (Basel) 2022;15:4874.
18. Yazdi HK, Nasoohi N, Benvidi M. In vitro efficacy of Listerine whitening mouthwash for color recovery of two discolored composite resins. Front Dent 2019;16:181-186.
19. Alharbi A, Ardu S, Bortolotto T, Krejci I. In-office bleaching efficacy on stain removal from CAD/CAM and direct resin composite materials. J Esthet Restor Dent 2018;30:51-58.
20. Kareem AS, Abdel-Fattah WM, El Gayar MI. Evaluation of color stability and surface roughness of smart monochromatic resin composite in comparison to universal resin composites after immersion in staining solutions. BMC Oral Health 2025;25:1211.
21. Shah SS, Patel NK, Yagnik KP, Vyas A, Doshi P, Keshrani PR. Comparative evaluation of microhardness of three restorative materials after immersion in chlorhexidine mouthwash: an *in vitro* study. J Conserv Dent Endod 2024;27:520-523.
22. Kondipudi N, Palla L, Borugadda R, Neelima UL, Manchem A, Nawaz MA. Evaluating the colour stability of esthetic resin composite: a study of NeoSpectra ST under different staining conditions. Int J Dent Mater 2024;6:81-86.
23. Bahig SM, El Sherbiney HH, Zayed MM, Ibrahim SH. A comparative 48 month randomized trial of clinical performance and wear of BISGMA based and BISGMA free nanoceramic resin composites. Sci Rep 2025;15:31167.

https://doi.org/10.5395/rde.2026.51.e16

RDE Restorative Dentistry & Endodontics

Research Article

eISSN 2234-7666
Restor Dent Endod. 2026 May;51(2):e17
https://doi.org/10.5395/rde.2026.51.e17

Clinical outcomes of tooth autotransplantation: a systematic review and meta-analysis of survival

Jasmine Wong[1,*], **Elise Hoi Wan Fok**[1], **Kar Yan Li**[2], **Chengfei Zhang**[1], **Gary Shun Pan Cheung**[3,*]

[1]Restorative Dental Sciences (Endodontics), Faculty of Dentistry, The University of Hong Kong, Hong Kong SAR, China
[2]Clinical Research Centre, Faculty of Dentistry, The University of Hong Kong, Hong Kong SAR, China
[3]Department of Dental Surgery, The University of Hong Kong–Shenzhen Hospital, Shenzhen, China

ABSTRACT

Objectives: Autotransplantation is a procedure that involves the extraction and transplantation of a tooth from one site to another within the same individual. This systematic review and meta-analysis aimed to investigate how clinical outcomes of autotransplanted teeth evolve over time and the principal reasons for extraction.

Methods: Studies were identified from five databases. A meta-analysis was performed to estimate the survival rates in the short-term (1 to ≤4 years), medium-term (>4 to ≤8 years), and long-term (>8 years) periods. Subgroup analysis was performed for age and root development. Risks of bias, reasons for extraction, and patient-reported outcome measures were evaluated.

Results: Of the 3,941 reports initially identified, 46 were included. The estimated short-, medium-, and long-term survival rates were 96.31% (95% confidence interval [CI], 94.80–97.82), 88.23% (95% CI, 85.59–90.87), and 84.80% (95% CI, 76.70–92.91), respectively. There were no significant differences in outcomes between age and root development groups. The most common reason for tooth loss was root resorption. High patient satisfaction rates were reported.

Conclusions: Autotransplanted teeth exhibit high survival rates in the short- to medium-term. Minimizing root surface damage and excluding pulpal contaminants may promote longevity. The procedure appeared equally successful for teeth at different stages of root development and across various age groups.

Keywords: Autotransplantation; Treatment outcome; Meta-analysis; Survival; Systematic review

Received: August 31, 2025 **Revised:** October 6, 2025 **Accepted:** November 11, 2025

Citation
Wong J, Fok EHW, Li KY, Zhang C, Cheung GSP. Clinical outcomes of tooth autotransplantation: a systematic review and meta-analysis of survival. Restor Dent Endod 2026;51(2):e17.

***Correspondence to**
Jasmine Wong, BDS (HK), MDS (Endo) (HK), MFDS RCPS (Glasg), MFDS RCSEd, M Endo RCSEd, F Endo RCSEd
Restorative Dental Sciences (Endodontics), Faculty of Dentistry, The University of Hong Kong, Division of Restorative Dental Sciences 3/F, The Prince Philip Dental Hospital, 34 Hospital Road, Sai Ying Pun, Hong Kong SAR, China
Email: jwong1@hku.hk

Gary Shun Pan Cheung, PhD, BDS (HK), MDS (Cons) (HK), MSc (London), FHKAM (Dental Surgery), FCDSHK (Endo), FAMS, FDS RCSEd, SFHEA
Department of Dental Surgery, University of Hong Kong–Shenzhen Hospital, 1 Haiyuan 1st Road, Futian District, Shenzhen 518053, China
Email: spcheung@hku.hk

Jasmine Wong and Gary Shun Pan Cheung contributed equally to this work as co-corresponding authors.

INTRODUCTION

Autotransplantation is a surgical procedure that involves the extraction and transplantation of a tooth from one site to another within the same individual [1]. It serves as a viable option for the replacement of teeth that are missing or need to be extracted due to traumatic injuries, poor restorability, and/or severe developmental defects [2,3].

Due to the preservation of the periodontal ligament (PDL), autotransplantation offers distinct advantages over other types of fixed prostheses, particularly for younger patients undergoing skeletal growth and developmental changes [4], as well as those who require orthodontic treatment [5]. Other biological advantages include the preservation of proprioception and the ability to remodel in conjunction with the alveolar bone [6]. Whilst autotransplanted immature teeth can benefit from revascularization and continued root development, autotransplantation procedures have also been carried out using mature teeth [7].

Considerations for the donor tooth include a favorable root form to facilitate atraumatic extraction, extent of root development, and sufficient periodontal support prior to extraction [1]. Patient factors, such as age, as well as clinician-related factors, such as surgical techniques, have similarly been reported to influence autotransplantation outcomes [2]. Conversely, damage to the root surface and PDL may result in complications, including external inflammatory root resorption (EIRR) and external replacement root resorption (ERRR), potentially compromising the clinical outcome [8].

Clinical outcomes can be evaluated by determining the healing events, i.e., 'success,' and/or functional retention, i.e., 'survival,' of the autotransplanted tooth. Whilst 'success' typically takes into account biological complications, 'survival' refers to the functional presence of the autotransplanted tooth in the mouth [9]. Functional retention of these teeth is particularly relevant to patients and is an important aspect of patient-reported outcome measures (PROMs) [10].

The outcome of autotransplantation has been examined across various time frames; however, the impact of short-, medium-, and long-term follow-up remains unaddressed in prior studies [11–13]. Furthermore, the reasons for extraction and PROMs related to autotransplantation have been largely overlooked in previous reviews [11,12,14,15]. This study aimed to evaluate the survival rate of autotransplanted teeth over different time frames, reasons for extraction, PROMs, and explore key potential influencing factors, namely age and root development.

METHODS

This review was performed in accordance with the PRISMA (Preferred Reporting Items for Systematic Reviews and Meta-Analyses) guidelines. The protocol was registered on the PROSPERO database (ID: CRD42024513534). The PICO question was: what are the short-, medium-, and long-term (C) survival rates (O) of autotransplanted teeth (I) in patients (P)?

Search of the literature

A literature search was conducted to identify relevant studies from the databases PubMed, Embase, Scopus, Web of Science, and Cochrane Central Register of Controlled Trials. The search was conducted in January 2025 with no initial time limit. Table 1 outlines an example of the search strategy employed.

After removal of duplicates, two reviewers (JW and EF) independently screened titles and abstracts to as-

Table 1. Search strategy used for PubMed

#	Search strategy for PubMed
#1	("transplantation, autologous"[MeSH Terms] AND ("Tooth"[MeSH Terms] OR "dent*"[Title/Abstract] OR "teeth"[Title/Abstract] OR "Tooth"[Title/Abstract] OR "incisor*"[Title/Abstract] OR "canine*"[Title/Abstract] OR "cuspid*"[Title/Abstract] OR "bicuspid*"[Title/Abstract] OR "premolar*"[Title/Abstract] OR "molar*"[Title/Abstract] OR "wisdom teeth"[Title/Abstract] OR "wisdom tooth"[Title/Abstract])) OR "tooth/transplantation"[MeSH Terms]
#2	("dent*"[Title/Abstract] OR "teeth"[Title/Abstract] OR "tooth"[Title/Abstract] OR "incisor*"[Title/Abstract] OR "canine*"[Title/Abstract] OR "cuspid*"[Title/Abstract] OR "bicuspid*"[Title/Abstract] OR "premolar*"[Title/Abstract] OR "molar*"[Title/Abstract] OR "wisdom teeth"[Title/Abstract] OR "wisdom tooth"[Title/Abstract]) AND ("transplant*"[Title/Abstract] OR "autotransplant*"[Title/Abstract])
#3	#1 OR #2
#4	"Survival Rate"[MeSH Terms]
#5	"survival"[Title/Abstract] OR "outcome"[Title/Abstract]
#6	#4 OR #5
#7	#3 AND #6

https://doi.org/10.5395/rde.2026.51.e17

sess their suitability using predefined inclusion and exclusion criteria in Covidence systematic review software (Veritas Health Innovation, Melbourne, VIC, Australia). Full texts were then reviewed. Additional studies identified from references were also considered. Disagreements were resolved by consulting a third reviewer (GC) to achieve a consensus.

The inclusion criteria were: (1) intervention was autotransplantation, (2) ≥1 year follow-up, (3) permanent dentition, (4) reported survival rate and/or number of teeth extracted, (5) outcomes determined by clearly defined clinical/radiographic criteria, (6) English language, and (7) clinical studies involving humans. The exclusion criteria were: (1) *in-vitro*/animal studies, (2) case reports/series, (3) intervention included intentional replantation, and (4) review/opinion articles. If multiple studies had investigated the same or overlapping sample populations, only one representative study, i.e., the one with the largest sample size, was included.

Risk of bias assessment

Two reviewers (JW and EHWF) assessed the risk of bias of the included studies using the Risk Of Bias In Non-randomized Studies of Interventions, ver. 2 (ROBINS-I V2) tool [16]. A third reviewer (GC) was consulted to resolve any disagreements.

Data extraction

Survival rate, defined as the proportion of autotransplanted teeth present at follow-up, was extracted from the included studies. If not explicitly stated, it was calculated based on the number of teeth lost compared to the initially recruited sample. Average follow-up time, or observation period, was recorded. When not stated, the survival rates corresponding to specific time points were recorded instead. Other data collected included the mean/median ages of patients undergoing autotransplantation, the type of donor tooth, and the proportion of teeth with complete or incomplete root development. When declared, PROMs and reasons for extraction were recorded and categorized. If multiple reasons were stated for a single tooth, this would be reflected in the applicable categories.

Statistical analysis

A meta-analysis was performed in Stata software ver. 16.1 (StataCorp LLC, College Station, TX, USA) using the metaprop_one command [17] to estimate pooled survival rates. Study-specific confidence intervals (CIs) were calculated using the exact method, incorporating a continuity correction of 0.5 to prevent the exclusion of studies reporting 0% or 100% survival rates and ensure computational stability. Pooled survival estimates were derived using Wald CIs by random-effects meta-analysis [18], with significance set at $p < 0.05$. A random-effects model was selected a priori due to the expected clinical and methodological heterogeneity across studies, including differences in patient populations and study designs, and the intention of generalizability. To account for temporal variations, separate meta-analyses were performed, stratified by follow-up duration. Follow-up periods were grouped into short-term (1 to ≤4 years), medium-term (4 to ≤8 years), and long-term (>8 years). Pooled survival estimates were calculated for each period. Data lacking clear follow-up times were excluded from meta-analyses.

Whenever appropriate data were available, meta-regression and subgroup analysis were conducted using Stata's metareg and metaprop one commands, respectively, to evaluate the following potential confounders: patient age (≤18 years vs >18 years) and root development (completed vs incomplete). For the latter, only those studies that had involved all donor teeth with either completed root formation or incomplete root development were included in the subgroup analysis to prevent excessive heterogeneity of results. Substantial heterogeneity among studies was quantified using the I^2 statistic (I^2 >50%) or the chi-square test with a *p*-value of <0.01 [19]. The random-effects model was used to estimate survival rates [19], with significance set at $p < 0.05$. All statistical analysis was performed under the guidance of a qualified statistician (KYL).

RESULTS

A total of 3,941 records were identified. After removal of duplicates, retracted studies, and corrupted files, 2689 records remained. Initial screening with the addition of hand-searched articles resulted in 224 articles eligible

for full-text screening. Of these, 178 studies were excluded, whilst 46 studies were included in this review (Figure 1).

The characteristics of the included studies are summarized in Table 2 [3–10,20–57]. The risk of bias of individual studies is shown in Figure 2. The majority were associated with a moderate (n = 21) to serious (n = 20) risk of bias.

The reported overall survival rates ranged from 67.9% to 100%. The average follow-up period ranged from 1 to 26.4 years, with an average patient age between 10 and 39 years. Most studies were classified as having a short-term observation period of 1 to ≤4 years (n = 20), while fewer studies observed autotransplantation outcomes for medium-term (n = 12) and long-term (n = 14) observation periods. The short-term survival rate was 96.31% (95% CI, 94.80–97.82). The medium- and long-term survival rates were 88.23% (95% CI, 85.59–90.87) and 84.80% (95% CI, 76.70–92.91), respectively (Figure 3). Substantial heterogeneity was observed between studies across all time periods (I^2 > 50%, p < 0.01).

Subgroup analysis using single-factor meta-regressions revealed no significant association between age and the survival of autotransplanted teeth (p > 0.05). The proportion difference, CIs, and p-values are reflected in Table 4. Half of the studies investigated autotransplanted teeth in patients ≤18 years (n = 23). The short-, medium-, and long-term survival rates for these patients were 96.92% (95% CI, 94.79–99.05), 87.56% (95% CI, 84.74–90.38), and 89.77% (95% CI, 83.37–96.17), respectively. For those over 18 years, survival rates were slightly lower, i.e., 95.92% (95% CI, 93.40–98.44), 88.94% (95% CI, 84.62–93.25), and 82.20% (95% CI, 69.97–94.44), respectively, although these differences were not

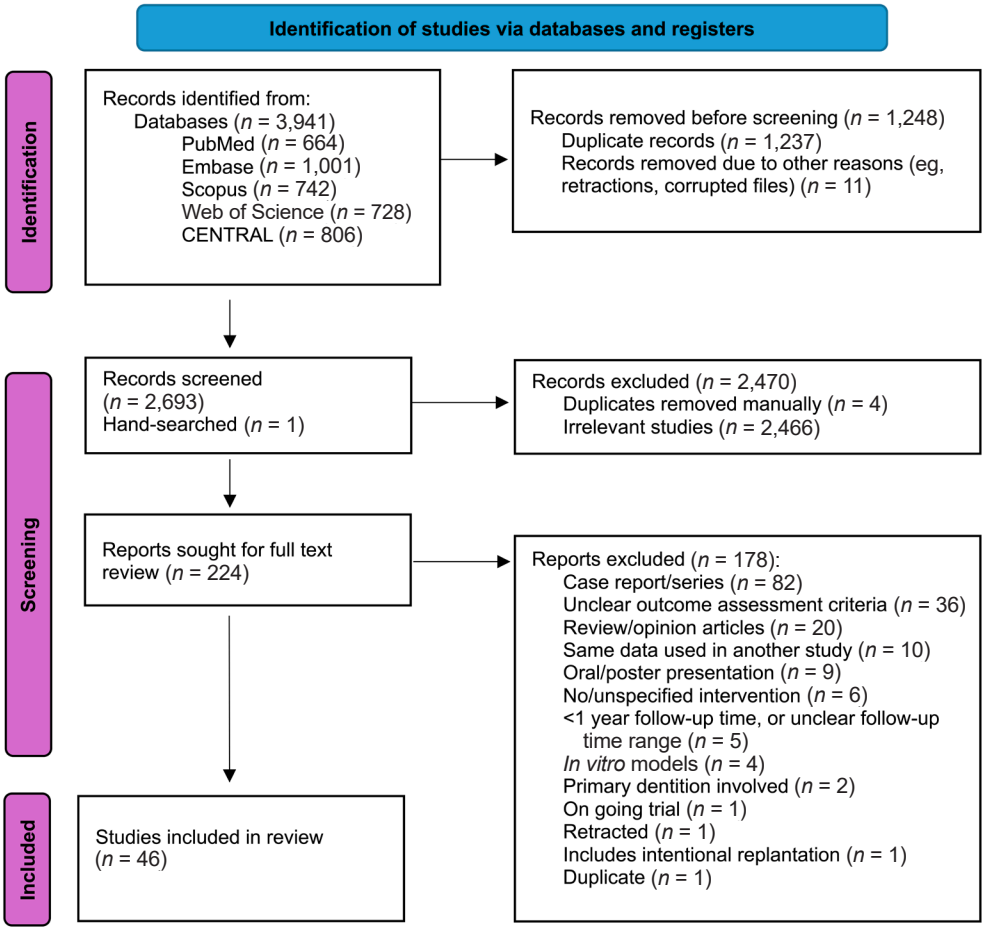

Figure 1. Flow diagram of study selection.

https://doi.org/10.5395/rde.2026.51.e17

Table 2. Included studies and their main characteristics

Study	Year	Number of autotransplanted teeth	Mean/median[a)] follow-up time	Mean/median[a)] age at the time of surgery	Root development of donor tooth	Donor tooth type	Overall survival rate	Reasons for extraction (number of teeth)
Abela *et al.* [20]	2019	329	3.51 years	19.4 years	Not reported	Canines, third molars, premolars, and central incisors	96.96%	Periodontal attachment loss (10)
Ainiwaer *et al.* [21]	2024	96	47.63 months	29.9 years for the surgically-created socket group; 31.7 years for the fresh socket group	All complete	Third molars	95.83%	Periodontal attachment loss (1); crack (1)
Akhlef *et al.* [22]	2025	153	17.1 years	12.7 years	Incomplete = 69%	Premolars	76%	Not reported
Albalooshy *et al.* [8]	2023	144	3.7 years	12.2 years	Incomplete = 53.4%	Premolars	93%	Root resorption (unspecified) (10)
Andreasen *et al.* [6]	1990	370	1 to 13 years	Not reported	Incomplete = 85.68%	Premolars	99.19%	Root resorption (unspecified) (1); orthodontic reasons (1)
Arikan *et al.* [23]	2008	32	5.87 years	34.32	All complete	Canines	93.5%	Root resorption (unspecified) (2)
Barendregt *et al.* [3]	2023	1,654	14.5 years	14.5	Incomplete = 71.94%	Premolars	99.33%	External replacement root resorption (8); External cervical root resorption (1); surgical complication (2)
Bauss *et al.* [24]	2004	91	4 years	17.3	All incomplete	Third molars	100%	Nil
Boschini *et al.* [25]	2020	20	11.9 years	33.6	All complete	Molars	95%	Surgical complication (infection) (1)
Cui *et al.* [26]	2021	29	36 months	Not reported	All completed	Not reported	72.41%	Not reported – but all extracted teeth did not receive root canal treatment
Czochrowska *et al.* [27]	2002	33	26.4 years	11.5	All incomplete	Incisors, premolars, canines, and supernumeraries	90%	External replacement root resorption (2); other (1)
de Carvalho *et al.* [28]	2014	33	7 years	18	Incomplete = 64%	Molars, premolars, canines, and incisors	82%	Not reported
de Freitas Coutinho *et al.* [29]	2021	43	9.68 years	11.47	All incomplete	Premolars and canines	97.67%	Orthodontic reasons (1)
Denys *et al.* [30]	2013	136	4.9 years	13	Incomplete = 84.67%	Molars, premolars, canines, and incisors	86.8%	Not reported
EzEldeen *et al.* [31]	2019	100	4.5 years	10.6 for the guided group, 10.7 for the conventional group	All incomplete	Premolars	92% for the guided group, 84% for the conventional group	External replacement root resorption (5), periapical infection (1); external inflammatory root resorption (5); external cervical root resorption (1)
Gilijamse *et al.* [32]	2016	59	17.35 months	12.5 years	Incomplete = 96.61%	Incisors, premolars, molars	100%	Nil

(Continued on the next page)

https://doi.org/10.5395/rde.2026.51.e17

Table 2. Continued

Study	Year	Number of autotransplanted teeth	Mean/median[a] follow-up time	Mean/median[a] age at the time of surgery	Root development of donor tooth	Donor tooth type	Overall survival rate	Reasons for extraction (number of teeth)
Grisar *et al.* [33]	2019	84	21 years	20.7	Complete = 69.05%	Canines	67.9%	Not reported – but loss was significantly associated with ankylosis and damage to the PDL during surgical removal
Han *et al.* [34]	2025	167	28.5 months	Not reported (ranged between 18 and 60 years)	All closed or semi-closed apices	Third molars	98.8%	Periodontal attachment loss (2)
Huth *et al.* [35]	2013	57	1.6 years	17	Incomplete = 64%	Incisors, canines, premolars, and molars	96%	Periodontal attachment loss (1); surgical complication (1)
Jang *et al.* [7]	2016	105	Up to 12 years	Not reported	All complete	Varied	88% at 3 years and 68.2% at 12 years	Not reported
Jonsson *et al.* [36]	2024	57	18.9 years	13.3 years	Incomplete = 87.72	Premolars	84.2%	Not reported
Josefsson *et al.* [37]	1999	110	1 to 4 years	13.5 years for premolar group; 16.8 years for molar group	Incomplete = 90%	Premolars and molars	91%	External replacement root resorption (3), external inflammatory root resorption (3); root fracture (2); surgical complication (2)
Kafourou *et al.* [4]	2017	89	2.6 years	13.2 years	Incomplete = 50.56%	Mostly premolars	94.4%	Not reported
Kokai *et al.* [5]	2015	100	5.8 years	29.1 years	All completed	Incisors, premolars, molars, and supernumerary teeth	93%	External replacement root resorption and inflammatory root resorption (2); external replacement root resorption and root fracture (2); periodontal attachment loss (2); periodontal attachment loss and root resorption (1)
Kvint *et al.* [38]	2010	215	4.8 years[a]	15.2 years[a]	Not reported	Canines, premolars, and molars	88.37%	Not reported
Li *et al.* [39]	2025	30	14.85 months for the experimental group; 14.23 months in the control group	Not reported	Not reported	Not reported	100%	Nil
Liao *et al.* [40]	2023	27	29.74 months	28.78 years	All completed	Molars	100%	Nil
Lin *et al.* [41]	2020	1,811	8.33 years	Not reported	Not reported	Third molars	74.49%	Not reported
Louropoulou *et al.* [42]	2024	910	Up to 17 years	16 years	Incomplete = 54.18%	Premolars	99.78% at 10 years	External cervical root resorption (1); other (1)
Lucas-Taulé *et al.* [43]	2021	36	29.42 months	30.2 years	Complete = 66.67%	Third molars	97.2%	Not reported
Mertens *et al.* [10]	2016	25	14.3 years	17.1 years	All incomplete	Third molars and premolars	96%	Surgical complication (1)
Myrlund *et al.* [44]	2004	132	1 to 4 years	Not reported	All incomplete	Premolars	98.6% at 4 years	Not reported

(Continued on the next page)

https://doi.org/10.5395/rde.2026.51.e17

Table 2. Continued

Study	Year	Number of autotransplanted teeth	Mean/median[a] follow-up time	Mean/median[a] age at the time of surgery	Root development of donor tooth	Donor tooth type	Overall survival rate	Reasons for extraction (number of teeth)
Plakwicz *et al.* [45]	2013	23	35 months	12 years 8 months	All incomplete	Premolars	100%	Nil
Raabe *et al.* [46]	2021	35	3.4[a] years	13[a] years	Incomplete = 71.42%	Premolars, canines, and molars	91.4%	External inflammatory root resorption (1); external replacement root resorption and cervical root resorption (2)
Restrepo-Restrepo *et al.* [9]	2024	128	1 to 30.11 years	34.34 years for males; 37.57 years for females	Complete = 93.75%	Incisors, canines, premolars, and molars	85.9%	External inflammatory root resorption (14); external replacement root resorption (2); external cervical root resorption (1); other (1)
Strbac *et al.* [47]	2017	66	Minimum of 5 years	19.64 years	All incomplete	Molars	89.39%	Not reported
Sugai *et al.* [48]	2010	117	40.9 months	39 years	All complete	Canines, premolars, and molars	88%	Surgical complications (6); external replacement root resorption (5); root fracture (1); periapical infection (1); other (1)
van Westerveld *et al.* [49]	2019	74	9.7[a] years	12.9 years	All incomplete	Premolars and third molars	95.4%	Root resorption (4); other (1)
Verweij *et al.* [50]	2016	111	19.4 months	13.1 years	All incomplete	Premolars and molars	98.2%	Not reported
Vilhjálmsson *et al.* [51]	2011	41	55.1 months	14.8 years	Completed = 63.41%	Incisors, canines, premolars, and molars	87.80%	Periodontal attachment loss and root resorption (5)
Watanabe *et al.* [52]	2010	38	9.2 years	24.1 months	All completed	Incisors, premolars, and molars	86.80%	External replacement root resorption (3); external inflammatory root resorption (1); periodontal attachment loss (1)
Xia *et al.* [53]	2025	168	5.21 years	29.6 years	All completed	Third molars	91.1%	External inflammatory root resorption (10); periodontal attachment loss (5)
Yan *et al.* [54]	2010	35	5.2 years	24 years	Complete = 54.29%	Third molars	94.29%	Root resorption (2)
Yang *et al.* [55]	2019	82	49.9 months	22.5 years	Incomplete = 15.9%	Anterior, premolars and molars	88% at 1 year, 78% at 5 years, and 74% at 10 years	Not reported
Yoshino *et al.* [56]	2012	614	63.8 months	44.1 years	Complete = 97.56%	Incisors, canines, premolars, and molars	83.39%	Periodontal attachment loss (56); root resorption (27); caries (4); root fracture (3); others (12)
Yu *et al.* [57]	2017	65	9.9 years	33.1 years	All complete	Third molars	90.8%	Not reported

https://doi.org/10.5395/rde.2026.51.e17

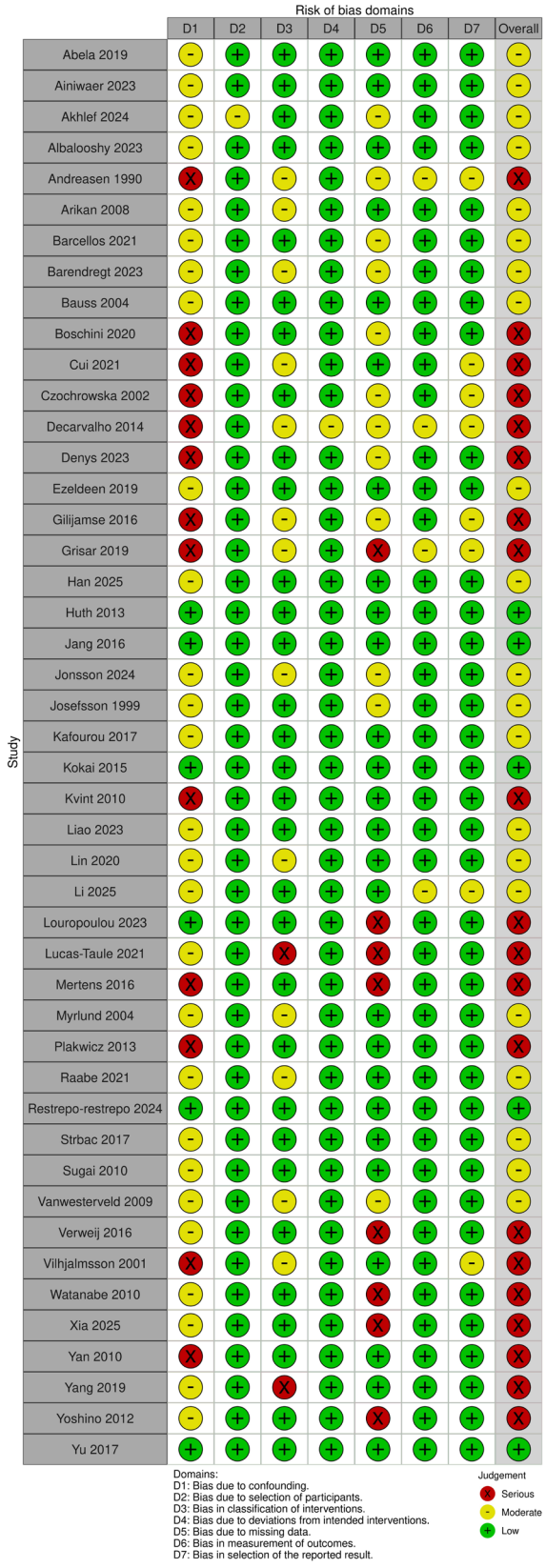

Figure 2. Risk of bias of included studies.

statistically significant (Figure 4).

Similarly, the extent of root development was not significantly associated with the survival of the autotransplanted teeth ($p > 0.05$). The proportion difference, CIs, and p-values are reflected in Table 5. Short, medium, and long-term survival rates for mature teeth were 91.38% (95% CI, 85.29–97.47), 92.14% (95% CI, 89.10–95.18), and 85.30% (95% CI, 73.78–96.81). For teeth with incomplete root development, survival rates were 99.50% (95% CI, 98.31–100.70), 88.59% (95% CI, 83.76–93.43), and 96.39% (95% CI, 92.77–100.00), respectively. Except for medium-term outcomes, which had the fewest applicable studies for both groups, teeth with incomplete root formation showed slightly better survival (Figure 5).

Substantial heterogeneity was observed amongst all subgroups ($I^2 > 50\%$, $p < 0.01$), except for studies investigating the medium-term survival rate for patients 18 years of age or younger ($I^2 = 0.0\%$, $p = 0.92$) and the short-term survival rate for teeth with incomplete root development ($I^2 = 0.0\%$, $p = 0.51$).

Regarding donor tooth type, almost half of the studies ($n = 22$) investigated a variety of donor teeth, whilst the remainder evaluated a single tooth type. Molar teeth were most commonly studied ($n = 11$), followed by premolars ($n = 9$) and canines ($n = 2$). Although this factor was not included in the subgroup analysis, the overall impression from qualitative evaluation suggested that donor tooth type was not a major prognostic factor. Few studies reported that specific tooth types, i.e., molar teeth [30], mandibular teeth [7], and multirooted teeth [5], could be associated with poorer survival rates.

Of the 259 teeth that had been extracted after autotransplantation, nearly half were extracted due to various types of root resorption ($n = 128$), the most prevalent form being EIRR ($n = 36$), followed by ERRR ($n = 34$). A minority ($n = 6$) had suffered external cervical root resorption, and the resorption type in the remaining teeth was unspecified ($n = 52$). About one-third were lost due to periodontal reasons ($n = 84$). Other factors, such as compromised coronal structure (i.e., cracks or caries beyond restoration) ($n = 5$), periapical infection ($n = 2$), and root fracture ($n = 8$), contributed to less than 10%. Only 5% failed due to immediate post-surgical complications ($n = 13$), including failure of initial heal-

https://doi.org/10.5395/rde.2026.51.e17

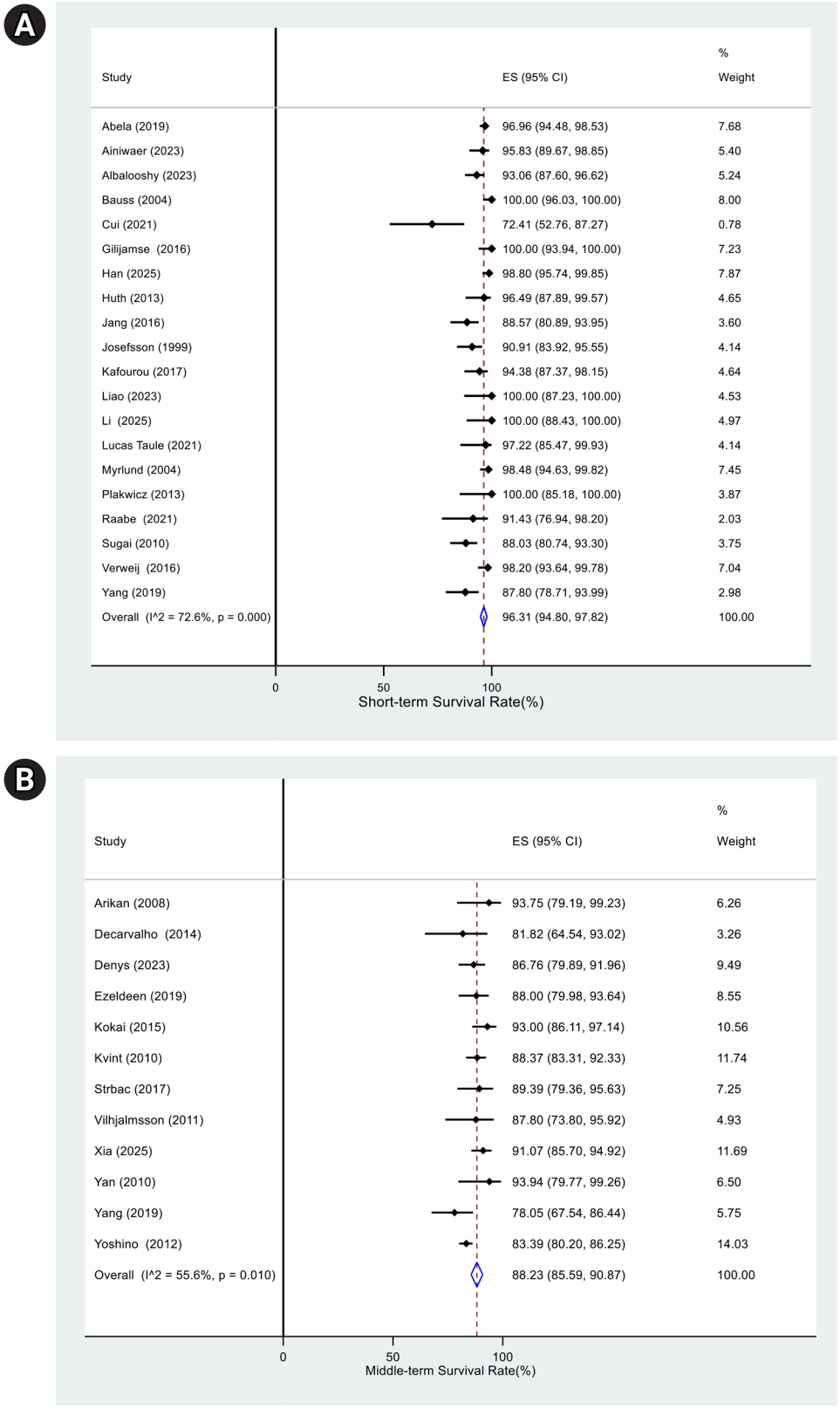

Figure 3. Forrest plots of overall estimated survival rate of autotransplanted teeth in the (A) short-term, (B) medium-term, and (C) long-term. CI, confidence interval; ES, effect size. (Continued on the next page)

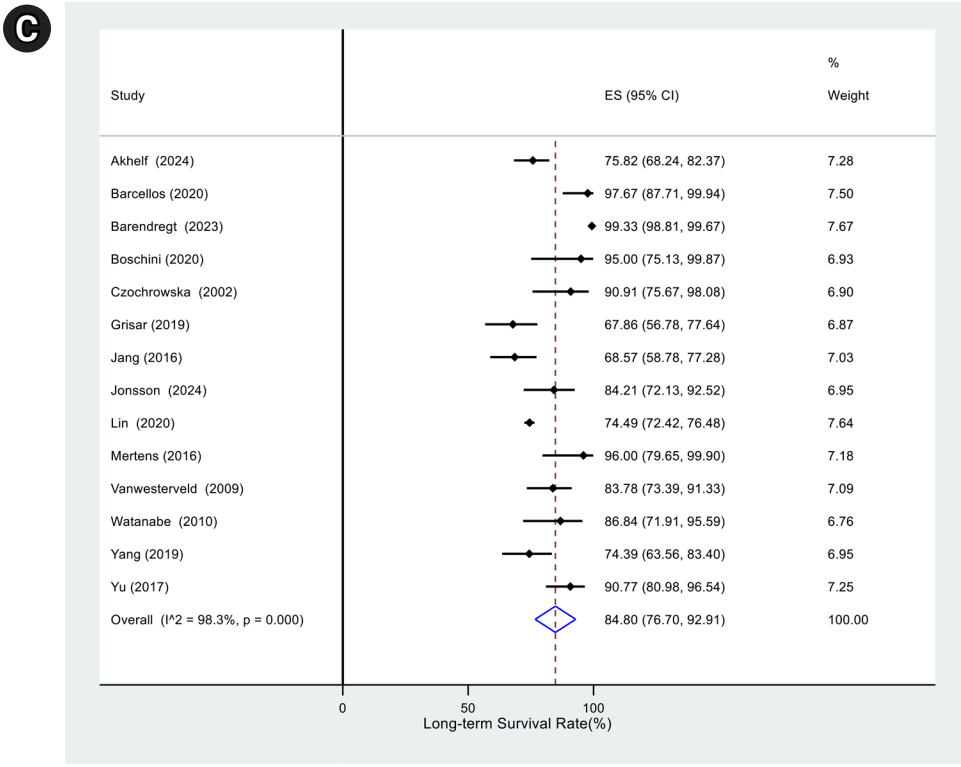

Figure 3. Continued.

ing and acute infections (Figure 6).

Eight studies evaluated PROMs. Various short-form questionnaires were used to evaluate patient satisfaction, functionality, and/or symptoms (Table 3 [21,22,40,43-45,47,49]). The surveys were either designed specifically for the study or were modified from existing instruments [27,58,59]. The majority of patients experienced minimal intra- and postoperative discomfort associated with the surgery [10,40,43,45]. Patients were generally pleased with the aesthetic outcome [22]. One study remarked that the most common postoperative inconvenience was food trapping [40]. Overall, studies reported high levels of patient satisfaction, and most autotransplanted teeth were functional and well-received [10,43,45].

DISCUSSION

Over the last decade or so, the increased interest in tooth autotransplantation has led to the publication of multiple studies [9,41,45,58], literature reviews [60,61], as well as a position statement by the European Society of Endodontics [62]. Given the considerable body of evidence, summarizing and analyzing the research pertaining to clinical outcomes would enhance our understanding of this treatment modality. The primary objective of this study was to synthesize the available data regarding survival rates of autotransplanted teeth via meta-analysis, whilst supplementing these findings with subgroup analysis of the key influencing factors, i.e., age and root development, as well as a qualitative evaluation of the reasons for extraction and PROMs.

In total, 46 studies were included in this review, which suggests tooth autotransplantation is a well-documented treatment modality. The studies identified for this review spanned various time frames, with almost half classified as having a short-term observation period (i.e., 1 to ≤4 years) [20,21,24,26], whilst the remaining were generally evenly distributed between medium- and long-term observation periods. A few large-scale, long-term observational studies were also identified [3,41]. Nevertheless, each study represents an important contribution to this systematic review because it facilitated a comprehensive analysis of how survival rates evolve

https://doi.org/10.5395/rde.2026.51.e17

Table 3. Studies reporting patient-reported outcome measures (PROMs) and a summary of the findings

Study	Year	PROM instrument used/method of evaluation	Findings
Ainiwaer *et al.* [21]	2024	10-item questionnaire assessing the satisfaction of the procedure and signs or symptoms; postoperative pain was evaluated using the visual analogue scale	- The majority of patients were satisfied with the appearance and function of the tooth and would recommend this treatment - Complaints were expressed about the length of the surgical time and the treatment cost - Postoperative pain was greatest at day 1, and gradually reduced to nearly zero over the week
Akhlef *et al.* [22]	2025	13-item questionnaire assessing the aesthetic outcome of the transplanted tooth, with questions modified from previous studies [27,59]	- Almost 90% were satisfied or fairly satisfied with the aesthetic outcome
Liao *et al.* [40]	2023	Questionnaire assessing the usage, presence of discomfort or symptoms, and satisfaction of the autotransplanted tooth	- 90% reported the ability to chew normally without discomfort - Most common unwanted side effect was food impaction, making up almost 50% of the complaints - Over 90% were satisfied with the surgery, whilst all participants reported the surgery had almost or completely met their expectations
Lucas-Taulé *et al.* [43]	2021	8-item questionnaire evaluating patient satisfaction and opinions on the operation, modified from a previous study [27]	- All patients reported that the surgery was not painful and vaguely remember the operation - The position of autotransplanted teeth was well perceived, and maintenance was comparable with that of other teeth
Myrlund *et al.* [44]	2004	12-item questionnaire assessing patient satisfaction	- Over three-quarters experienced low discomfort during the procedure - Over 80% reported integrating well in their dental arch - All patients were satisfied with the function and aesthetics, and would do the same surgery again if needed
Strbac *et al.* [47]	2017	Single question on the patients' satisfaction	- Only one patient out of 53 reported dissatisfaction with the autotransplanted tooth due to a negative aesthetic result
Plakwicz *et al.* [45]	2013	7-item questionnaire evaluating patient satisfaction and opinions on the operation, modified from a previous study [27]	- Over 80% reported positive responses to all items to items asking about the fit, position, maintenance, and surgical discomfort
van Westerveld *et al.* [49]	2019	Questionnaire evaluating the procedure and presence of an autotransplanted tooth	- Most were very satisfied with both procedure and outcome - Individual items were not reported

Table 4. Proportion difference, 95% confidence intervals, and *p*-values for subgroup analysis of age (≤18 years vs >18 years)

Age (yr), ≤18 vs >18	Proportion difference (%)	95% confidence interval	*p*-value
Short-term	0.96	–3.32 to 5.25	0.638
Medium-term	–1.59	–7.80 to 4.36	0.582
Long-term	7.40	–6.34 to 21.13	0.258

Table 5. Proportion difference, confidence intervals, and *p*-values for subgroup analysis of root development (completed vs incomplete)

Root development, completed vs incomplete	Proportion difference (%)	95% confidence interval	*p*-value
Short-term	–5.25	–13.23 to 2.73	0.168
Medium-term	3.55	–5.73 to 12.82	0.311
Long-term	–7.09	–23.17 to 8.99	0.322

over time.

This review demonstrated that autotransplantation of teeth yields favorable survival rates, with 96.31% of teeth retained in the oral cavity for up to 4 years. This dropped to 88.23% when autotransplanted teeth were observed for a period between 4 and 8 years, and decreased further to 84.80% when observed for more than 8 years. Unsurprisingly, a reduction in survival rates corresponded with longer observation periods, as more complications are likely to occur over time [20]. The survival rates were comparable to other forms of surgical endodontic treatment, such as intentional replantation

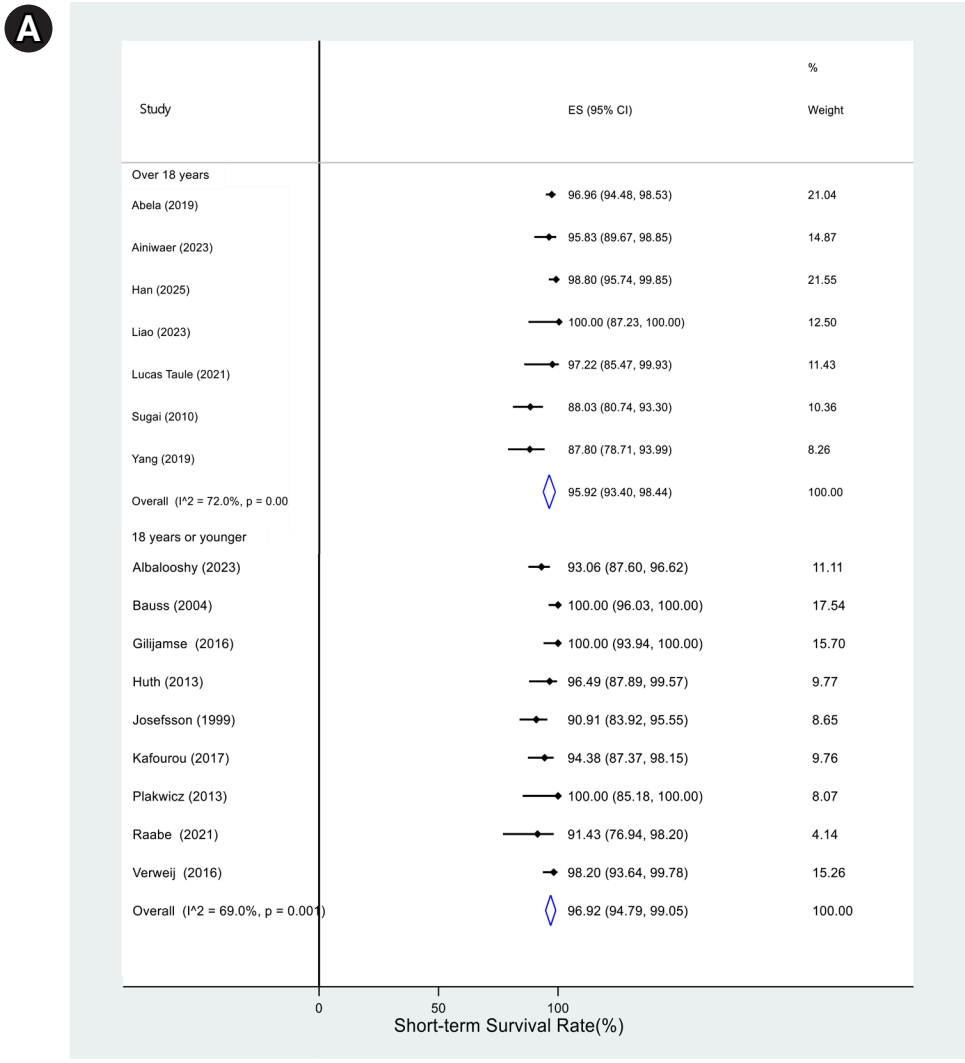

Figure 4. Comparison of estimated survival rates of autotransplanted teeth in patients 18 years or younger compared to patients over 18 years old, in the (A) short-term, (B) medium-term, and (C) long-term. CI, confidence interval; ES, effect size. (Continued on the next page)

[63] and apical surgery [64]. Hence, with careful case selection and adherence to evidence-based practices, autotransplantation should be considered as a viable and predictable treatment option. It is important to note that survival rates express the functional retention of teeth, but do not reveal information about specific clinical outcomes, such as the continuation of root development, revascularization, presence or absence of resorptive defects, and other pathologies [6,8]. Nevertheless, functional retention is a key component of the patients' experience [65,66]. Criteria for 'success,' i.e., the supposed lack of biological complications, do not only vary widely across different studies [22], but may also be too strict to judge the outcome from a patient's perspective [27]. Hence, survival analysis remains a meaningful clinical determinant of treatment effectiveness [67].

Whilst the characteristics of the individual studies differed across a variety of dimensions, such as tooth type, observation periods, surgical techniques, and age (Table 2), it was noted that the majority of studies were observational in nature, therefore exhibited a moderate to serious risk of bias due to the effect of uncontrolled confounders. The authors acknowledge that this limits the generalizability and reliability of the findings of this review, a shortcoming of the study. However, recent efforts to standardize surgical protocols [60,62] and core

https://doi.org/10.5395/rde.2026.51.e17

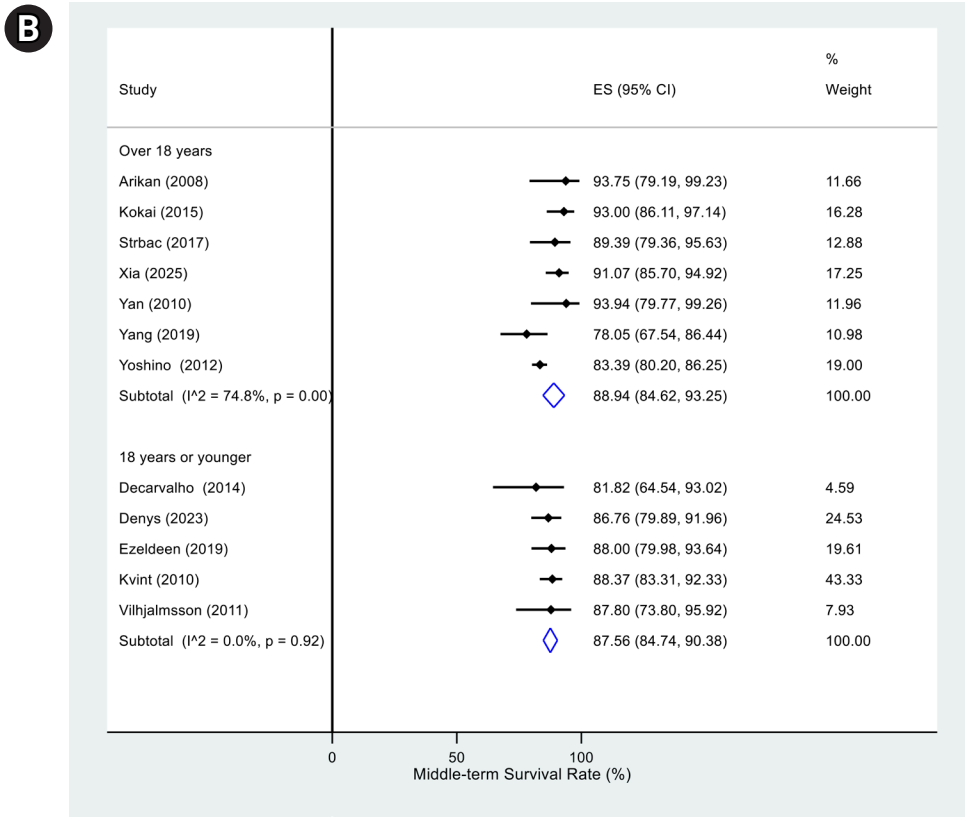

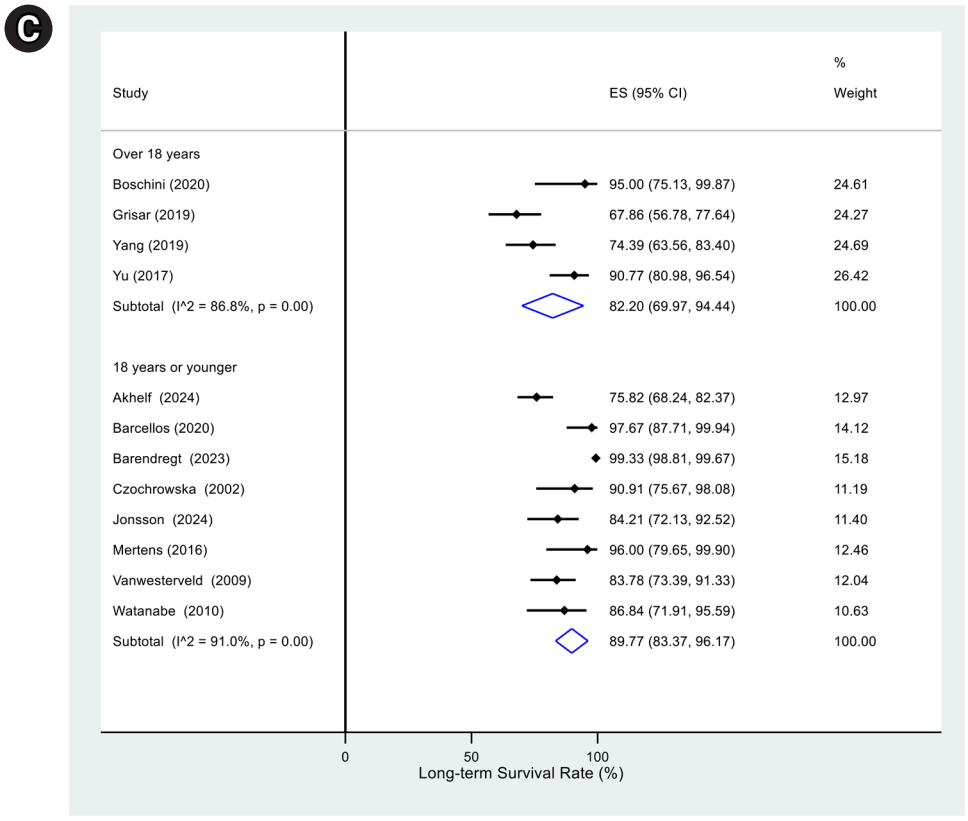

Figure 4. Continued.

Figure 5. Comparison of estimated survival rates of autotransplanted teeth with completed root development compared incomplete root development, in the (A) short-term, (B) medium-term, and (C) long-term. CI, confidence interval; ES, effect size. (Continued on the next page)

outcome sets [68] may improve the consistency and quality of future research.

Despite the application of select inclusion and exclusion criteria, high levels of heterogeneity were observed amongst studies, especially regarding the tooth type, age, root development status, and the surgical technique [7,9,30]. There appeared to be a large variability in the reported parameters [3,12], with most studies primarily focused on reporting the outcomes, with secondary evaluation of selected variables [6,23,26,31]. This heterogeneity complicates meta-analyses, risking potentially unreliable and unrepresentative results. Furthermore, stratifying the period of observation into short-, medium-, and long-term for this review further limited the number of studies within each subgroup. Subgroup analysis and meta-regression were attempted to account for the heterogeneity present and investigate potential influencing factors. However, a comprehensive analysis of all confounding variables was not feasible, which is a recognized limitation of this study. That said, after evaluating the available data, this review was able to analyze the effect of two key factors: root development and age [2,6,12,42]. Although most studies included in our analysis did not report within-study survival rate data stratified by age groups or root development types, precluding a meta-analysis of effect sizes (e.g., odds ratios or hazard ratios) for these subgroups, the approach of comparing groups across studies via subgroup analysis and meta-regression nevertheless allowed for the investigation of the influence of age and root development using the available study-level covariates. However, this approach may result in reduced precision compared to within-study comparisons due to potential ecological bias, which is a limitation of our re-

https://doi.org/10.5395/rde.2026.51.e17

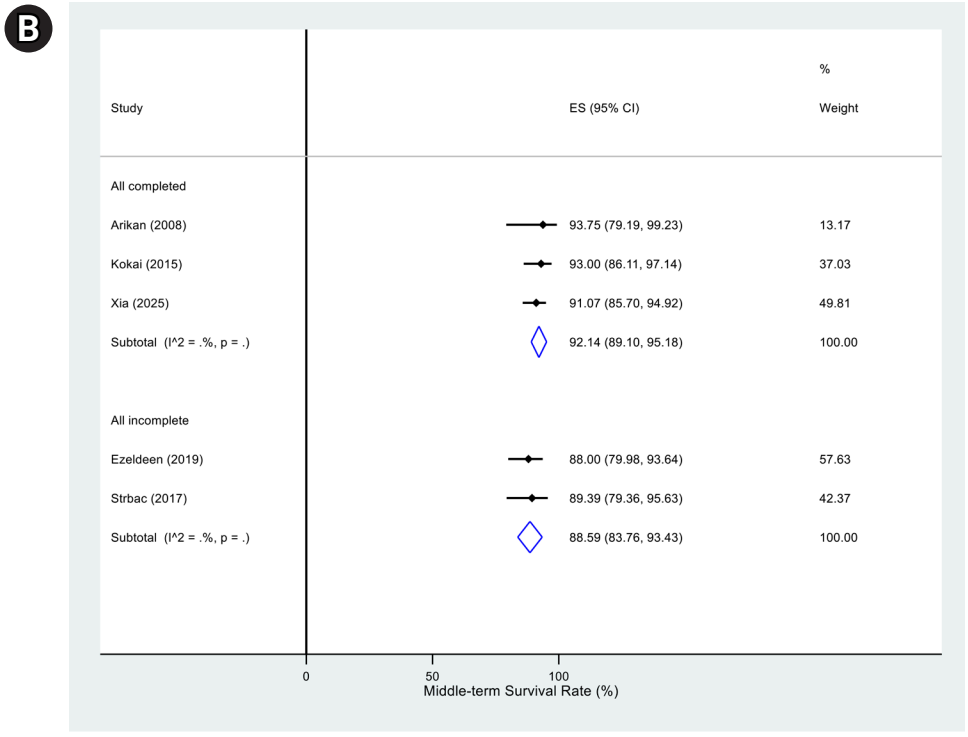

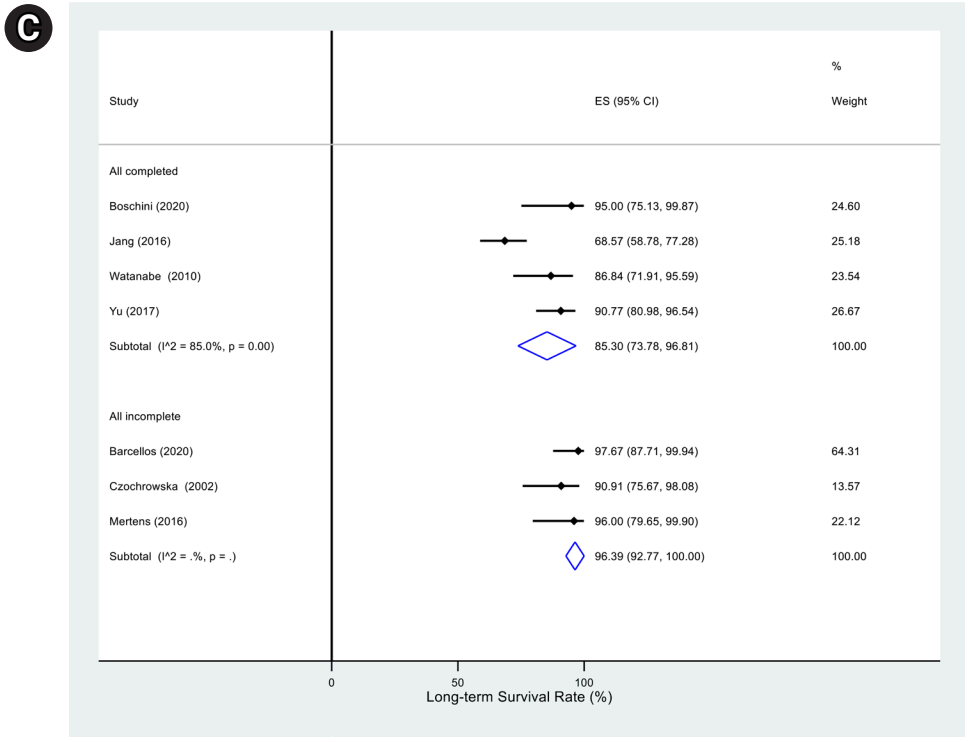

Figure 5. Continued.

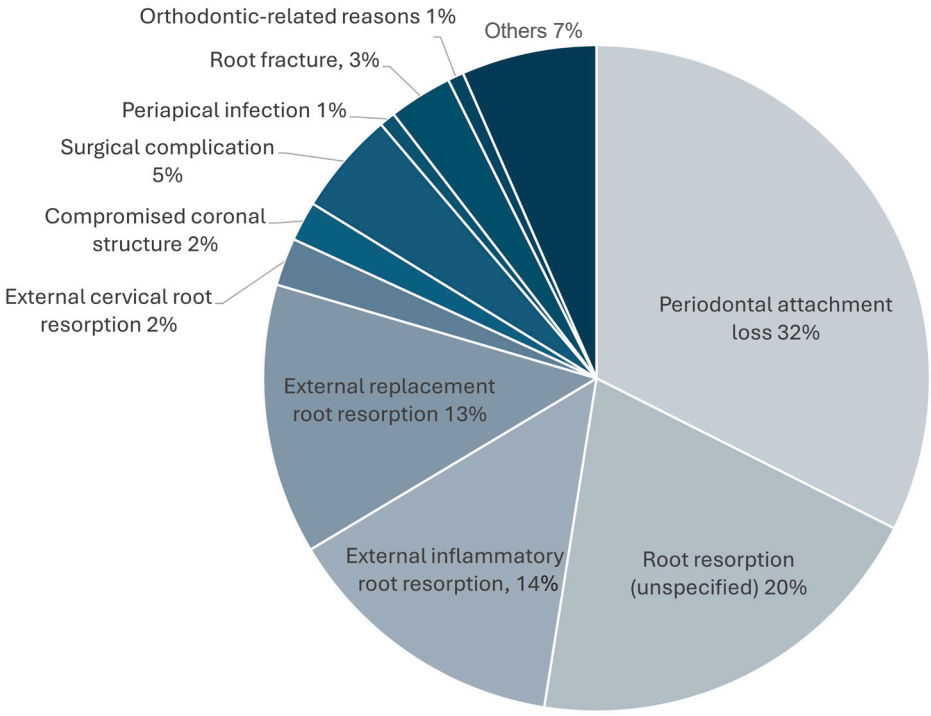

Figure 6. Proportion of autotransplanted teeth extracted ($n = 259$) for various reasons.

view. Future studies should consider reporting stratified survival data to enable more robust subgroup analyses.

The extent of root development has been suggested to affect autotransplantation outcomes for several reasons. Shorter root-forms allow for easier manipulation during surgery [1], and with the presence of the Hertwig epithelial root sheath, immature teeth have greater potential for continued root growth and regeneration of periodontal support [69]. Several studies found that teeth with incomplete root development were less likely to be extracted or experience complications compared to their fully developed counterparts [3,30]. A previous review concluded that the stage of root development significantly influenced the outcome of autotransplanted teeth, but the authors cautioned the interpretation of the results due to substantial inconsistencies amongst the pooled data [12]. Hence, to facilitate subgroup analysis and minimize heterogeneity, root development was dichotomized into 'incomplete' and 'completed' and was analyzed according to each observation time frame. The results of the present study indicated that root development was not associated with survival of the autotransplanted teeth ($p > 0.05$). Nevertheless, biological considerations may still steer clinicians towards using immature teeth for autotransplantation, if available.

Patient age may have an impact on the survival of autotransplanted teeth, as studies suggest younger patients experience fewer biological complications [7,38,48]. Younger individuals exhibit higher regenerative potential [2,48] and more favorable bone mineral density for extractions [7]. However, some studies have found that age did not influence the outcome [9,57]. The results of this review suggested that patients aged 18 years or younger seemed to experience slightly better outcomes compared to older individuals, although the association was not statistically significant ($p > 0.05$). An ideal age for autotransplantation has not been identified per se, but autotransplantation should be considered as an effective treatment option for younger patients, especially given the limitations of prosthodontic replacement options in these age groups [9,60].

Although our study was unable to investigate the influence of donor tooth type on survival rates in subgroup analysis, given the heterogeneity of the data, multirooted donor teeth and mandibular appeared to be associated with poorer outcomes, which was attributed

https://doi.org/10.5395/rde.2026.51.e17

to difficulties during extraction and more challenging endodontic treatment [5,7,30]. Although not necessarily a major prognostic factor, careful case selection focusing on ease of extraction and appropriate tooth dimensions can provide a more favorable environment to promote healing [1,8,38].

Regarding the reasons for loss of autotransplanted teeth, about half of the teeth were extracted due to various forms of resorption, the most common being EIRR, followed by ERRR. Bacterial ingress into the root canal system, coupled with root surface damage, is responsible for the onset of EIRR [70,71]. Although limited evidence suggests that systemic antibiotics may have a protective effect against EIRR [9], current guidelines emphasize that antibiotics should be prescribed only to medically compromised patients [62,72,73]. Therefore, maintaining an aseptic field, reducing surgical trauma, and timely root canal treatment may improve survival outcomes [1,26,34].

Unlike EIRR, which tends to manifest as an early complication [3], the physiological processes leading to ERRR are more gradual, especially in older individuals with lower cell turnover rates [74]. Hence, the affected teeth can be functionally retained for many years [75]. However, particularly in children undergoing rapid developmental changes, ERRR can quickly lead to stunted dentoalveolar growth and tooth loss [4,74]. Ultimately, ERRR is still fundamentally a pathological process and should therefore be mitigated whenever possible. Preservation of viable PDL is universally considered a major protective factor [76]. Extra-oral time within 15 minutes [8,9], digitally assisted techniques, use of three-dimensional printed replicas [21,31,60], and appropriate functional loading have been suggested to be beneficial for the regeneration of periodontal tissues and for reducing the risk of ERRR [3,6].

Periodontal attachment loss was the next most significant reason for extraction. Untreated periodontal disease is a well-established risk factor for tooth loss [77,78], and this is no different for autotransplanted teeth. Deficient recipient bone level and poor initial stability were associated with periodontal defects and poorer healing outcomes [8,9]. Endodontic and restorative-related conditions, such as periapical infections, root fractures, and unrestorable caries, accounted for around 10% of teeth lost. Lapses in surgical technique and post-surgical complications played an equal, yet minor role in survival outcomes. Therefore, as resorption appears to be the most significant reason for the extraction of the autotransplanted tooth, followed by periodontal attachment loss, future research could prioritize strategies to reduce the likelihood of root resorption and encourage periodontal healing.

A comprehensive understanding of clinical outcomes is incomplete without the evaluation of PROMs [66,68]. The present review found only eight of the 46 studies assessed PROMs [10,21,22,40,43,45,49]. The studies utilized a variety of custom instruments, making cross-study comparisons challenging. To circumvent this, studies could choose to implement previously validated and widely used instruments to improve the comparability between studies, particularly regarding the impact of different treatment options on patients' well-being [59,67,79,80]. Nevertheless, there were high levels of satisfaction reported in all eight studies. Several studies reported that minimal discomfort was experienced by patients during and after the surgery [10,21,43]. One study reported that although achieving optimal aesthetic outcomes could be highly technique-sensitive, patients were still largely satisfied with their appearance [22]. Overall, patients were satisfied with the function of the autotransplanted tooth, with minor inconveniences, such as food trapping [21,40,43]. A recent review has echoed the significant evidence gap concerning PROMs in autotransplantation treatments, underscoring the need to standardize future clinical research by incorporating appropriate and validated instruments [80].

CONCLUSIONS

The survival rates of autotransplanted teeth are 96%, 88%, and 84% in the short-, medium-, and long-term, respectively. The longevity of autotransplanted teeth decreases with longer periods of observation. The procedure seemed equally successful for teeth with different stages of root development and age groups. However, the heterogeneity amongst studies limits the generalizability and reliability of these findings. Patients are generally satisfied with the outcome and the functionality of their transplanted teeth. The most common reason

for extraction was root resorption. Curating strategies to reduce the risk of resorption, such as ensuring minimal damage to the PDL, atraumatic extraction, and excluding any pulpal contaminants, could optimize outcomes and improve the survival of autotransplanted teeth.

CONFLICT OF INTEREST

No potential conflict of interest relevant to this article was reported.

FUNDING/SUPPORT

The authors have no financial relationships relevant to this article to disclose.

ACKNOWLEDGMENTS

We would like to thank Ms. Chloe Cheung for her valuable assistance in formulating the search strategy for this review. The authors deny any conflicts of interest related to this study.

AUTHOR CONTRIBUTIONS

Conceptualization, Methodology: Wong J, Cheung GSP. Investigation, Data curation: Wong J, Li KY, Fok EHW. Resources: Wong J, Li KY. Supervision: Cheung GSP. Project administration: Zhang C, Cheung GSP. Writing - original draft: Wong J. Writing - review & editing: Wong J, Cheung GSP, Zhang C, Fok EHW. All authors read and approved the final manuscript.

DATA SHARING STATEMENT

The datasets are not publicly available but are available from the corresponding author upon reasonable request.

REFERENCES

1. Tsukiboshi M. Autotransplantation of teeth: requirements for predictable success. Dent Traumatol 2002;18:157-180.
2. Tsukiboshi M, Yamauchi N, Tsukiboshi Y. Long-term outcomes of autotransplantation of teeth: a case series. Dent Traumatol 2019;35:358-367.
3. Barendregt D, Andreasen JO, Leunisse M, Eggink E, Linssen M, Van der Weijden F, *et al*. An evaluation of 1654 premolars transplanted in the posterior region: a retrospective analysis of survival, success and complications. Dent Traumatol 2023;39 Suppl 1:50-62.
4. Kafourou V, Tong HJ, Day P, Houghton N, Spencer RJ, Duggal M. Outcomes and prognostic factors that influence the success of tooth autotransplantation in children and adolescents. Dent Traumatol 2017;33:393-399.
5. Kokai S, Kanno Z, Koike S, Uesugi S, Takahashi Y, Ono T, *et al*. Retrospective study of 100 autotransplanted teeth with complete root formation and subsequent orthodontic treatment. Am J Orthod Dentofacial Orthop 2015;148:982-989.
6. Andreasen JO, Paulsen HU, Yu Z, Bayer T, Schwartz O. A long-term study of 370 autotransplanted premolars: part II: tooth survival and pulp healing subsequent to transplantation. Eur J Orthod 1990;12:14-24.
7. Jang Y, Choi YJ, Lee SJ, Roh BD, Park SH, Kim E. Prognostic factors for clinical outcomes in autotransplantation of teeth with complete root formation: survival analysis for up to 12 years. J Endod 2016;42:198-205.
8. Albalooshy A, Duggal M, Vinall-Collier K, Drummond B, Day P. The outcomes of auto-transplanted premolars in the anterior maxilla following traumatic dental injuries. Dent Traumatol 2023;39 Suppl 1:40-49.
9. Restrepo-Restrepo FA, Uribe-Jaramillo DF, Villa-Machado PA, Mejía-Cardona JL, Abella-Sans F, Morales-Quezada RK, *et al*. Retrospective follow-up assessment of risk variables influencing the outcome of autologous tooth transplantation. J Endod 2024;50:747-757.
10. Mertens B, Boukari A, Tenenbaum H. Long-term follow up of post-surgical tooth autotransplantation: a retrospective study. J Investig Clin Dent 2016;7:207-214.
11. Akhlef Y, Schwartz O, Andreasen JO, Jensen SS. Autotransplantation of teeth to the anterior maxilla: a systematic review of survival and success, aesthetic presentation and patient-reported outcome. Dent Traumatol 2018;34:20-27.
12. Almpani K, Papageorgiou SN, Papadopoulos MA. Autotransplantation of teeth in humans: a systematic review and meta-analysis. Clin Oral Investig 2015;19:1157-1179.
13. Tan BL, Tong HJ, Narashimhan S, Banihani A, Nazzal H, Duggal MS. Tooth autotransplantation: an umbrella review. Dent Traumatol 2023;39 Suppl 1:2-29.
14. Atala-Acevedo C, Abarca J, Martínez-Zapata MJ, Díaz J, Olate S, Zaror C. Success rate of autotransplantation of teeth with an open apex: systematic review and meta-analysis. J Oral Maxillofac Surg 2017;75:35-50.
15. Chung WC, Tu YK, Lin YH, Lu HK. Outcomes of autotransplanted teeth with complete root formation: a systematic review and meta-analysis. J Clin Periodontol 2014;41:412-423.
16. Cochrane Bias Methods Group. ROBINS-I V2 tool [Internet]. Risk of bias tools; 2024 [cited 2025 Jan 28]. Available from: https://www.riskofbias.info/welcome/robins-i-v2
17. Nyaga VN, Arbyn M, Aerts M. Metaprop: a Stata command to perform meta-analysis of binomial data. Arch Public Health 2014;72:39.

https://doi.org/10.5395/rde.2026.51.e17

18. DerSimonian R, Laird N. Meta-analysis in clinical trials. Control Clin Trials 1986;7:177-188.
19. Higgins JPT, Thomas J, Chandler J, Cumpston M, Li T, Page MJ, *etal*. Cochrane handbook for systematic reviews of interventions, version 6.5 [Internet]. Cochrane; 2024 [cited 2025 Jan 28]. Available from: www.training.cochrane.org/handbook
20. Abela S, Murtadha L, Bister D, Andiappan M, Kwok J. Survival probability of dental autotransplantation of 366 teeth over 34 years within a hospital setting in the United Kingdom. Eur J Orthod 2019;41:551-556.
21. Ainiwaer A, Gong Z, Zuolipahaer Z, Wang L. Midterm outcomes of autogenous mature third molars transplantation into surgically created sockets: a retrospective cohort study. Dent Traumatol 2024;40:573-585.
22. Akhlef Y, Hosseini M, Schwartz O, Andreasen JO, Gerds TA, Jensen SS. Autotransplantation of premolars to the anterior maxilla: a long-term retrospective cohort study of survival, success, esthetic, and patient-reported outcome with up to 38-year follow-up. Dent Traumatol 2025;41:322-337.
23. Arikan F, Nizam N, Sonmez S. 5-year longitudinal study of survival rate and periodontal parameter changes at sites of maxillary canine autotransplantation. J Periodontol 2008;79:595-602.
24. Bauss O, Schwestka-Polly R, Kiliaridis S. Influence of orthodontic derotation and extrusion on pulpal and periodontal condition of autotransplanted immature third molars. Am J Orthod Dentofacial Orthop 2004;125:488-496.
25. Boschini L, Melillo M, Berton F. Long term survival of mature autotransplanted teeth: a retrospective single center analysis. J Dent 2020;98:103371.
26. Cui X, Cui N, Li X, Du X, Zhang S, Wu C, *et al*. Effect of root canal therapy on the success rate of teeth with complete roots in autogenous tooth transplantation. Scanning 2021;2021:6675604.
27. Czochrowska EM, Stenvik A, Bjercke B, Zachrisson BU. Outcome of tooth transplantation: survival and success rates 17-41 years posttreatment. Am J Orthod Dentofacial Orthop 2002;121:110-119, 193.
28. de Carvalho VM, de Carvalho CM, de Carvalho AM, *et al*. Statistical analysis of teeth autotransplantation in Portugal's region of Chaves. Acta Odontol Scand 2014;72:179-186.
29. de Freitas Coutinho NB, Nunes FC, Gagno Intra JB, *et al*. Success, survival rate, and soft tissue esthetic of tooth autotransplantation. J Endod 2021;47:391-396.
30. Denys D, Shahbazian M, Jacobs R, Laenen A, Wyatt J, Vinckier F, *et al*. Importance of root development in autotransplantations: a retrospective study of 137 teeth with a follow-up period varying from 1 week to 14 years. Eur J Orthod 2013;35:680-688.
31. EzEldeen M, Wyatt J, Al-Rimawi A, Coucke W, Shaheen E, Lambrichts I. Use of CBCT guidance for tooth autotransplantation in children. J Dent Res 2019;98:406-413.
32. Gilijamse M, Baart JA, Wolff J, Sándor GK, Forouzanfar T. Tooth autotransplantation in the anterior maxilla and mandible: retrospective results in young patients. Oral Surg Oral Med Oral Pathol Oral Radiol 2016;122:e187-e192.
33. Grisar K, Nys M, The V, Vrielinck L, Schepers S, Jacobs R, *et al*. Long-term outcome of autogenously transplanted maxillary canines. Clin Exp Dent Res 2019;5:67-75.
34. Han B, Liu L, Jiang Z, Ye L, Cao Y, Pan J. Efficacy of root canal treatment for autotransplanted third molars: a 6-Year cohort study of 167 teeth in southern China. PeerJ 2025;13:e18824.
35. Huth KC, Nazet M, Paschos E, *et al*. Autotransplantation and surgical uprighting of impacted or retained teeth: a retrospective clinical study and evaluation of patient satisfaction. Acta Odontol Scand 2013;71:1538-1546.
36. Jonsson T, Jonsdottir HB, Aspelund T, Sigurdsson A, Sigurdsson TJ. Long-term survival of 57 premolars consecutively transplanted to premolar sites. Am J Orthod Dentofacial Orthop 2024;166:480-489.e3.
37. Josefsson E, Brattström V, Tegsjö U, Valerius-Olsson H. Treatment of lower second premolar agenesis by autotransplantation: four-year evaluation of eighty patients. Acta Odontol Scand 1999;57:111-115.
38. Kvint S, Lindsten R, Magnusson A, Nilsson P, Bjerklin K. Autotransplantation of teeth in 215 patients: a follow-up study. Angle Orthod 2010;80:446-451.
39. Li Y, Lin Z, Liu Y, Chen G, Li C, Wu H, *et al*. Fully guided system for position-predictable autotransplantation of teeth: a randomized clinical trial. Int Endod J 2025;58:550-565.
40. Liao F, Wang H, Zhao J, Zhang B, Zhong H. Effectiveness evaluation of autotransplanted teeth after performing extraoral endodontic surgery instead of conventional root canal therapy. BMC Oral Health 2023;23:1005.
41. Lin PY, Chiang YC, Hsu LY, Chang HJ, Chi LY. Endodontic considerations of survival rate for autotransplanted third molars: a nationwide population-based study. Int Endod J 2020;53:733-741.
42. Louropoulou A, Andreasen JO, Leunisse M, Eggink E, Lins-

sen M, Van der Weijden F, *et al*. An evaluation of 910 premolars transplanted in the anterior region: a retrospective analysis of survival, success, and complications. Dent Traumatol 2024;40:22-34.
43. Lucas-Taulé E, Llaquet M, Muñoz-Peñalver J, Nart J, Hernández-Alfaro F, Gargallo-Albiol J. Mid-term outcomes and periodontal prognostic factors of autotransplanted third molars: a retrospective cohort study. J Periodontol 2021;92:1776-1787.
44. Myrlund S, Stermer EM, Album B, Stenvik A. Root length in transplanted premolars. Acta Odontol Scand 2004;62:132-136.
45. Plakwicz P, Wojtowicz A, Czochrowska EM. Survival and success rates of autotransplanted premolars: a prospective study of the protocol for developing teeth. Am J Orthod Dentofacial Orthop 2013;144:229-237.
46. Raabe C, Bornstein MM, Ducommun J, Sendi P, von Arx T, Janner SFM. A retrospective analysis of autotransplanted teeth including an evaluation of a novel surgical technique. Clin Oral Investig 2021;25:3513-3525.
47. Strbac GD, Giannis K, Mittlböck M, Fuerst G, Zechner W, Stavropoulos A, *et al*. Survival rate of autotransplanted teeth after 5 years - a retrospective cohort study. J Craniomaxillofac Surg 2017;45:1143-1149.
48. Sugai T, Yoshizawa M, Kobayashi T, Ono K, Takagi R, Kitamura N, *et al*. Clinical study on prognostic factors for autotransplantation of teeth with complete root formation. Int J Oral Maxillofac Surg 2010;39:1193-1203.
49. van Westerveld KJ, Verweij JP, Toxopeus EE, Fiocco M, Mensink G, van Merkesteyn JP. Long-term outcomes 1-20 years after autotransplantation of teeth: clinical and radiographic evaluation of 66 premolars and 8 molars. Br J Oral Maxillofac Surg 2019;57:666-671.
50. Verweij JP, Toxopeus EE, Fiocco M, Mensink G, van Merkesteyn JP. Success and survival of autotransplanted premolars and molars during short-term clinical follow-up. J Clin Periodontol 2016;43:167-172.
51. Vilhjálmsson VH, Knudsen GC, Grung B, Bårdsen A. Dental auto-transplantation to anterior maxillary sites. Dent Traumatol 2011;27:23-29.
52. Watanabe Y, Mohri T, Takeyama M, Yamaki M, Okiji T, Saito C, *et al*. Long-term observation of autotransplanted teeth with complete root formation in orthodontic patients. Am J Orthod Dentofacial Orthop 2010;138:720-726.
53. Xia J, Ge Z, Zhang Y, Shi J, Xie Z. Prognostic factors for autotransplanted third molars with completely formed roots: a retrospective cohort study. J Am Dent Assoc 2025;156:46-56.
54. Yan Q, Li B, Long X. Immediate autotransplantation of mandibular third molar in China. Oral Surg Oral Med Oral Pathol Oral Radiol Endod 2010;110:436-440.
55. Yang S, Jung BY, Pang NS. Outcomes of autotransplanted teeth and prognostic factors: a 10-year retrospective study. Clin Oral Investig 2019;23:87-98.
56. Yoshino K, Kariya N, Namura D, Noji I, Mitsuhashi K, Kimura H, *et al*. A retrospective survey of autotransplantation of teeth in dental clinics. J Oral Rehabil 2012;39:37-43.
57. Yu HJ, Jia P, Lv Z, Qiu LX. Autotransplantation of third molars with completely formed roots into surgically created sockets and fresh extraction sockets: a 10-year comparative study. Int J Oral Maxillofac Surg 2017;46:531-538.
58. Czochrowska EM, Stenvik A, Zachrisson BU. The esthetic outcome of autotransplanted premolars replacing maxillary incisors. Dent Traumatol 2002;18:237-245.
59. Slade GD, Spencer AJ. Development and evaluation of the oral health impact profile. Community Dent Health 1994;11:3-11.
60. Plotino G, Abella Sans F, Duggal MS, Grande NM, Krastl G, Nagendrababu V, *et al*. Clinical procedures and outcome of surgical extrusion, intentional replantation and tooth autotransplantation: a narrative review. Int Endod J 2020;53:1636-1652.
61. Plotino G, Abella Sans F, Duggal MS, Grande NM, Krastl G, Nagendrababu V, *et al*. Present status and future directions: surgical extrusion, intentional replantation and tooth autotransplantation. Int Endod J 2022;55 Suppl 3:827-842.
62. Plotino G, Abella Sans F, Duggal MS, Grande NM, Krastl G, Nagendrababu V, *et al*. European Society of Endodontology position statement: surgical extrusion, intentional replantation and tooth autotransplantation: European Society of Endodontology developed by. Int Endod J 2021;54:655-659.
63. Mainkar A. A systematic review of the survival of teeth intentionally replanted with a modern technique and cost-effectiveness compared with single-tooth implants. J Endod 2017;43:1963-1968.
64. Iqbal A, Khattak O, Almutairi H, Almaktoom I, Alanazi G, Alruwaili K, *et al*. Endodontic surgery and post-treatment apical periodontitis: a systematic review. Open Dent J 2024;18:e18742106296829.
65. McGrath C, Newsome PR. Patient-centred measures in dental practice: 2. Quality of life. Dent Update 2007;34:41-42, 44.

https://doi.org/10.5395/rde.2026.51.e17

66. Wong J, Cheung GS, Lee AHC McGrath C, Neelakantan P. PROMs following root canal treatment and surgical endodontic treatment. Int Dent J 2023;73:28-41.
67. Friedman S, Mor C. The success of endodontic therapy: healing and functionality. J Calif Dent Assoc 2004;32:493-503.
68. El Karim I, Duncan HF, Cushley S, Nagendrababu V, Kirkevang LL, Kruse CL, *et al*. An international consensus study to identify "what" outcomes should be included in a core outcome set for endodontic treatments (COSET) for utilization in clinical practice and research. Int Endod J 2024;57:270-280.
69. Andreasen JO, Kristerson L, Andreasen FM. Damage of the Hertwig's epithelial root sheath: effect upon root growth after autotransplantation of teeth in monkeys. Endod Dent Traumatol 1988;4:145-151.
70. Patel S, Saberi N, Pimental T, Teng PH. Present status and future directions: root resorption. Int Endod J 2022;55 Suppl 4(Suppl 4):892-921.
71. Abbott PV. Prevention and management of external inflammatory resorption following trauma to teeth. Aust Dent J 2016;61 Suppl 1:82-94.
72. Segura-Egea JJ, Gould K, Şen BH, Jonasson P, Cotti E, Mazzoni A, *et al*. European Society of Endodontology position statement: the use of antibiotics in endodontics. Int Endod J 2018;51:20-25.
73. American Association of Endodontists (AAE). AAE position statement: AAE guidance on the use of systemic antibiotics in endodontics. J Endod 2017;43:1409-1413.
74. Andersson L, Bodin I, Sörensen S. Progression of root resorption following replantation of human teeth after extended extraoral storage. Endod Dent Traumatol 1989;5:38-47.
75. Müller DD, Bissinger R, Reymus M, Bücher K, Hickel R, Kühnisch J. Survival and complication analyses of avulsed and replanted permanent teeth. Sci Rep 2020;10:2841.
76. Andreasen JO, Kristerson L. The effect of limited drying or removal of the periodontal ligament: periodontal healing after replantation of mature permanent incisors in monkeys. Acta Odontol Scand 1981;39:1-13.
77. Carvalho R, Botelho J, Machado V, Mascarenhas P, Alcoforado G, Mendes JJ, *et al*. Predictors of tooth loss during long-term periodontal maintenance: an updated systematic review. J Clin Periodontol 2021;48:1019-1036.
78. Chambrone L, Chambrone D, Lima LA, Chambrone LA. Predictors of tooth loss during long-term periodontal maintenance: a systematic review of observational studies. J Clin Periodontol 2010;37:675-684.
79. Adulyanon S, Vourapukjaru J, Sheiham A. Oral impacts affecting daily performance in a low dental disease Thai population. Community Dent Oral Epidemiol 1996;24:385-389.
80. Saccomanno S, Valeri C, Di Giandomenico D, Fani E, Marzo G, Quinzi V. What is the impact of autotransplantation on the long-term stability and patient satisfaction of impacted canines?: a systematic review. Saudi Dent J 2024;36:1268-1277.

RDE Restorative Dentistry & Endodontics

Research Article

eISSN 2234-7666
Restor Dent Endod. 2026 May;51(2):e20
https://doi.org/10.5395/rde.2026.51.e20

Initial attachment, viability, proliferation, and migration of osteoblast-like SaOS-2 cells on two resorbable xenogeneic membranes for guided tissue regeneration: an *in vitro* experimental study

Rafael Fernández-Grisales[1,*], Giovanna García-Suárez[2], Ximena Guerrero-Rodríguez[2], Carolina Berruecos-Orozco[1], Marco Calle-Jaramillo[1], Wilder Javier Rojas[1], Vanessa Esmeralda Duque[1], Daniela Serna-Guisao[1], Néstor Ríos-Osorio[1,3]

[1]Department of Endodontics, CES University, Medellin, Colombia
[2]Department of Endodontics, Institución Universitaria Colegios de Colombia UNICOC, Bogotá, Colombia
[3]PhD Program Biomedical Sciences, Universidad el Bosque, Bogotá, Colombia

ABSTRACT

Objectives: This study evaluated the biocompatibility of a new xenogeneic resorbable membrane derived from porcine esophagus membrane (Quirumatrix, Cells Tech Co.) and compared it with a porcine pericardium membrane (Straumann Jason, Straumann Holding AG.) traditionally used for guided tissue regeneration. The parameters investigated were the viability, migration, and adhesion of SaOS-2 osteoblast-like cells derived from osteosarcoma on both membranes.

Methods: The cells were cultured in 100 mm plates in RPMI 1640 medium (40 mL), supplemented. They were incubated at 37°C in a humidified atmosphere with 95% air and 5% to 10% CO_2. Cell morphology and adhesion were evaluated using phase contrast optical microscopy and scanning electron microscope. Cell viability and proliferation were evaluated using a fluorometric resazurin reduction assay, with fluorescence intensity measured at 48, 72, and 96 hours. Cell migration was evaluated using staining with Alexa Fluor 555 Phalloidin (Cell Signaling Technology) and DAPI, with a reference line. Cell migration was analyzed by measuring displacement within the delineated area using an Axio Imager M2 fluorescence microscope (Carl Zeiss). Each membrane was photographed. The statistical analysis was performed using GraphPad Prism ver. 10.2.3 (GraphPad Software). A p-value <0.05 was considered significant between experimental groups.

Results: Both membranes were shown to be biocompatible. The porcine pericardium membrane showed greater cell adhesion and proliferation compared to the porcine esophagus membrane. Cell migration was significantly greater in the Jason membrane.

Conclusions: The results revealed that both evaluated membranes are biocompatible and non-cytotoxic; further research is needed to understand their long-term behavior, interactions with other types of cells, and performance in specific therapeutic situations.

Keywords: Biocompatibility; Cell migration; Cell proliferation; Cell viability; Guided tissue regeneration

Received: July 15, 2025 **Revised:** December 29, 2025 **Accepted:** January 2, 2026

Citation
Fernández-Grisales R, García-Suarez G, Guerrero-Rodríguez X, Berruecos-Orozco C, Calle-Jaramillo M, Rojas WJ, Duque VE, Serna-Guisao D, Ríos-Osorio N. Initial attachment, viability, proliferation and migration of osteoblast-like SaOS-2 cells on two resorbable xenogeneic membranes for guided tissue regeneration: an *in vitro* experimental study. Restor Dent Endod 2026;51(2):e20.

***Correspondence to**
Rafael Fernández-Grisales, DDS, MSc
Department of Endodontics, CES University, Calle 10A #22-04, Medellin, Colombia
Email: rfernandez@ces.edu.co

INTRODUCTION

Endodontic surgery is indicated for teeth presenting with persistent apical periodontitis (AP) in which non-surgical root canal treatment has failed or is not feasible [1]. The initiation and progression of AP result from a dynamic interplay between persistent antigenic stimuli—primarily toxins and bacterial by-products originating from an infected root canal system—and the host immune response [2]. Consequently, the principal objective of endodontic surgery is to eliminate or effectively isolate the source of infection, thereby creating biological conditions conducive to periapical tissue healing [1,2].

Histological outcomes of periapical healing following successful endodontic surgery may be categorized as repair or regeneration, depending on lesion characteristics, the availability of resident stem/progenitor cells and growth factors, and the local microenvironmental cues at the surgical site [1,3]. Regeneration entails the reconstitution of periapical tissues—namely bone, periodontal ligament, and root cementum—thereby restoring native architecture and function, whereas repair represents a non-specific healing response characterized by fibrosis and scar formation. Healing by repair frequently fails to restore full tissue function and may result in residual structural irregularities at the injury site [1,3]. Although regeneration constitutes the preferred surgical outcome, its attainment remains challenging, as it is critically dependent on the cellular, molecular, and behavioral properties of periapical tissues throughout the healing cascade [4,5].

Periapical sites—particularly large endodontic lesions—managed by conventional endodontic surgery are frequently repopulated by fibrous connective tissue, a histological correlate of incomplete periapical healing [5]. The ingrowth of non-osteogenic tissues into the post-surgical osseous defect, together with epithelial down-growth along the root surface, may bias healing towards repair rather than true regeneration [4,5]. Accordingly, if colonization of the defect by gingival connective tissue or oral epithelium can be sufficiently delayed to permit the establishment of cells with regenerative capacity—most notably periodontal ligament- and bone-derived cells, epithelial migration may be restrained, and regenerative healing facilitated [4–6].

Currently, there is growing interest in the application of guided tissue regeneration (GTR) strategies as adjuncts to endodontic surgery, incorporating bone grafts and barrier membranes to modulate the local microenvironment in favor of tissue and bone regeneration within periapical defects [1,7]. Notably, a recent systematic review and meta-analysis demonstrated that regenerative protocols employing collagen membranes in combination with bovine-derived hydroxyapatite significantly enhance periapical lesion healing following endodontic surgery [1].

Barrier membranes are designed to inhibit the apical migration of epithelial cells into the surgical defect. An ideal membrane should combine ease of handling with bioabsorbability and biofunctionality [1,8]. Nevertheless, currently available resorbable membranes often fail to achieve complete periapical tissue regeneration, largely due to inflammatory responses arising from insufficient microenvironmental isolation [8]. Consequently, the use of high-biocompatibility barrier membranes is critical for optimizing GTR outcomes and overcoming these limitations [8]. In addition, barrier membranes should support cell adhesion and progenitor cell migration [9]. Osteoblastic progenitor cells must adhere to an appropriate substrate before initiating the wound-healing cascade, including proliferation, differentiation, and subsequent tissue maturation. This attachment process proceeds through four sequential stages: (i) adsorption of glycoproteins onto the substrate surface, (ii) initial cell contact, (iii) stable attachment, and (iv) cell spreading, after which cellular replication is initiated [9]. Despite this, the influence of barrier membrane composition on osteoblastic attachment and behavior remains incompletely understood.

In light of the foregoing, the present *in vitro* study was designed to investigate the biocompatibility of two commercially available xenogeneic resorbable barrier membranes—Straumann Jason (Straumann Holding AG., Basel, Switzerland) and Quirumatrix (Cells Tech Co., Medellín, Colombia)—derived from native collagen and extracellular matrix (ECM), respectively. Specifically, the study sought to provide a comparative biological appraisal by evaluating: (i) the ability of osteoblast-like SaOS-2 cells to adhere to each membrane, (ii) cell vi-

https://doi.org/10.5395/rde.2026.51.e20

ability and proliferative capacity following membrane contact, and (iii) the migratory behavior of SaOS-2 cells across the membrane surfaces.

METHODS

Membranes examined

Two commercially available GTR membranes were evaluated: Quirumatrix (an ECM-derived membrane obtained from decellularized porcine esophagus) and Straumann Jason (a native porcine collagen pericardium-derived membrane) (Figure 1).

Cell culture on barrier membranes

Osteosarcoma-derived Osteoblast-like cells, SaOS-2 (ATCC HTB-85) were purchased from American Type Culture Collection- ATCC Inc. (Manassas, VA, USA). Cells were cultivated in 100-mm culture dishes, ingrown in RPMI 1640 (40 mL) medium (Sigma-Aldrich R4130; Sigma-Aldrich, St. Louis, MO, USA) supplemented with fetal bovine serum (FBS; GE Healthcare Life Sciences, cat. #SH30088.03) and 1% penicillin-streptomycin-amphotericin B (HyClone, Logan, UT, USA; Ref. #SV30079.01). Cells were incubated at 37°C in a humidified atmosphere of 95% air, and 5%–10% CO_2. The medium was changed every 2 days.

First, we followed a standardization protocol to provide optimal conditions for cell attachment and viability assays for both barrier membranes. Initially, the hydration of the membranes was evaluated with DMEM/F12 (Biowest, Nuaillé, France; Ref. #L0090-500) medium, supplemented with different concentrations (10%, 20%) of FBS (GE Healthcare Life Sciences, cat. #SH30088.03) or 100% FBS, before cells were seeded. Better attachment and cell viability were observed on membranes with 100% FBS hydration for 48 hours prior to cell seeding (see cell attachment and viability below).

Once the most appropriate method of hydrating the

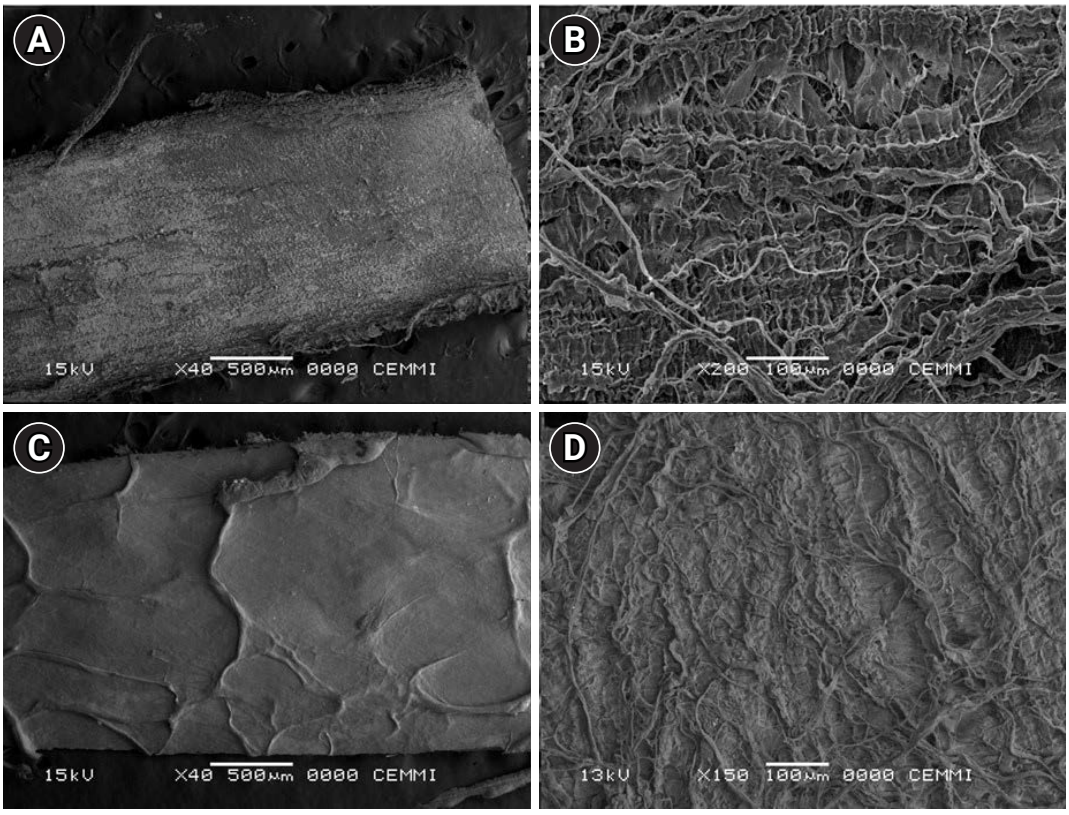

Figure 1. Surface morphology (structure and mesh) scanning electron micrographs of the examined bioabsorbable membranes. (A, B) Jason (Straumann Holding AG., Basel, Switzerland) and (C, D) Quirumatrix (Cells Tech Co., Medellín, Colombia). Magnification bar, 100 µm.

membranes was standardized to allow the maximum percentage of viability and cell attachment, membranes were cut into discs 5 × 3 mm in area, placed into 12-well culture plates with a polyvinyl chloride surgical tape (Micropore; 3M, St. Paul, MN, USA) and hydrated with 100% FBS (GE Healthcare Life Sciences, cat. #SH30088.03) for 48 hours before cell seeding. SaOS-2 cultured in 100-mm culture dishes were trypsinized (0.25% trypsin, SV30037.01, GE Healthcare Life Sciences), and 40,000 cells (in 1 mL of fresh medium) per well were seeded in triplicate onto the 12-well culture plates with or without membranes (control group/cells) (Figure 2).

Visualization of cell attachment and morphological changes

Morphological/phenotypic changes were monitored daily up to 5 days after cell seeding, using phase contrast-light microscopy (Zeiss Axio Imager M2 inverted microscope; Carl Zeiss, Jena, Germany) and compared to control cells (cells seeded directly into each well without a membrane).

Upon completion of a 5-day seeding period, barrier membranes (Jason and Quirumatrix) were prepared for examination under a scanning electron microscope (SEM) to evaluate cell morphology and attachment. Cells were fixed with 2.5% glutaraldehyde (Sigma-Aldrich) for 2 hours, then rinsed three times with phosphate-buffered saline (PBS, Ref. #158127; Sigma-Aldrich). Secondary fixation was carried out using 1% osmium tetroxide. Thereafter, the samples were dehydrated for 30 minutes using a graded series of ethanol (50%, 70%, 90%, and 100%) for 20 minutes each. The samples were subsequently sputtered (gold/palladium sputter-coated) and analyzed with Vega-TEScan (Tescan USA Inc., Warrendale, PA, USA) at an accelerating voltage of 20 kV.

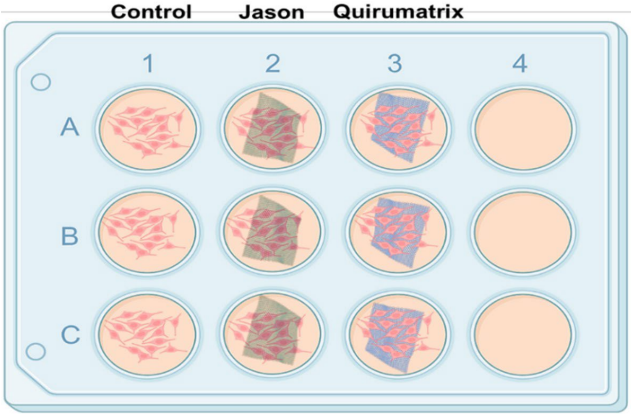

Figure 2. Both membranes (discs 5 × 3 mm in area) were prepared for cell culture. SaOS-2 cells (40,000 cells/mL) were seeded in triplicate into a new 12-well plate containing 1 mL of fresh medium per well. (A) Control group. B) Jason (Straumann Holding AG., Basel, Switzerland). (C) Quirumatrix (Cells Tech Co., Medellín, Colombia).

Representative SEM images were randomly selected from multiple fields of view, prioritizing those that displayed the most common cell morphologies and attachment patterns for each membrane type. Images with artefacts or atypical features were excluded to ensure accurate representation of the experimental findings.

Fluorometric resazurin reduction assay for cell viability

The viability and proliferation of SaOS-2 cells were assessed by fluorometric resazurin reduction assay. Briefly, Resazurin (7-hydroxy-3H-phenoxazin-3-one 10-oxide) is a non-fluorescent molecule that may infiltrate cells, be reduced to highly fluorescent resorufin in the intracellular space and detect changes in oxidation state using fluorometric techniques. This test allowed us to make conclusions on metabolic activity (mitochondrial activity), as the reducing environment can only be sustained with an active intermediate metabolism.

Cells seeded in multiwell plates were spiked with 4.4 µg/well of resazurin solution and incubated at 37°C for four hours. Thereafter, the fluorescence intensity was measured at 48, 72, and 96 hours, using a Tecan Infinite M2000 Pro reader (Tecan, Männedorf, Switzerland) at 535-595 nm wavelengths [10]. Each membrane was removed from the culture well to assess the fluorescence produced by cells adherent to the well versus those adherent to the membrane individually. After each fluorescence reading, each membrane was returned to its corresponding well until a new fluorescence reading was recorded. To evaluate whether the fluorescence measurement obtained by reduced resazurin was proportional to the number of live cells present, a correlation between the quantity of resorufin produced by known concentrations of SaOS-2 cells was established. Cells were serially diluted (80,000, 40,000, 20,000, and

https://doi.org/10.5395/rde.2026.51.e20

10,000). The fluorescence measurements showed that resorufin production was proportional to the number of viable cells. The linear regression analysis indicated a high correlation coefficient (R^2 = 0.993) within the 10,000–80,000 cell range (Figure 3).

Cell migration

The migration assay was performed as previously reported by Takata *et al.* [11]. Membranes were prepared and placed into 12-well culture plates as previously described. The membranes were hydrated with 100% FBS (GE Healthcare Life Sciences, Cat #SH30088.03) for 48 hours. Membranes were then washed with PBS (Sigma-Aldrich, Ref. #P4417). Half of each membrane was covered with sterile surgical tape (Micropore) (Figure 4A, B). A total of 40,000 osteoblast-like SaOS-2 cells were seeded on the non-covered half and allowed to attach for 24 hours. Thereafter, the wells were rinsed with PBS (Sigma-Aldrich, Ref. #P4417) and the surgical tape was removed to allow cell migration (for 3 days). The boundary between the covered and uncovered areas of barrier membranes was marked as a reference line for cell migration. Three days later, the membranes were fixed with 4% paraformaldehyde (Sigma-Aldrich, Ref. #158127) and stained with Alexa Fluor 555 Phalloidin (Cell Signaling Technology #8953) and 4′,6-diamidino-2-phenylindole (DAPI; Cell Signaling Technology). Phalloidin fluorescently stains the cell cytoskeleton through the binding of phalloidin to F-actin. DAPI allows the visualization of nuclear DNA in fixed cells. Having the reference line, cell migration was analyzed by measuring cell displacement through the delimited area. The number of cells was counted under an Axio Imager M2 fluorescence microscope. Each membrane was photographed with an AxioCam HR camera (Carl Zeiss). The visual field for cell counting was selected randomly (Figure 5).

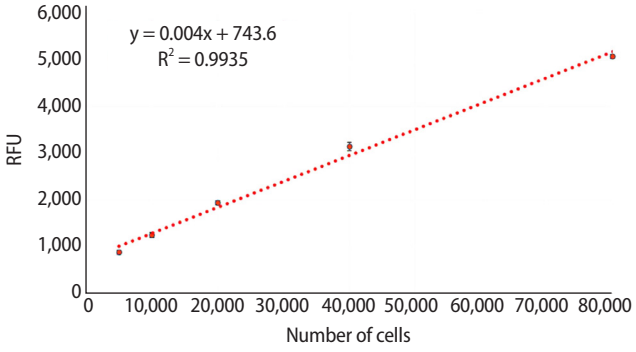

Figure 3. Calibration curve that shows the relationship between the number of SaOS-2 cells and resorufin synthesis via resazurin reduction. RFU, relative fluorescence unit.

Statistical analysis

All experiments were performed at least three times independently, with each condition analyzed in triplicate within each experiment, resulting in a total of nine independent measurements per condition (n = 9). Data

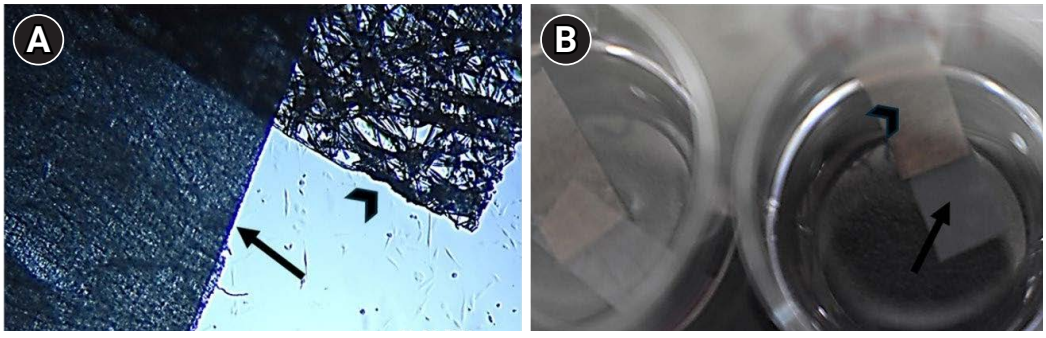

Figure 4. SaOS-2 cell migration assay on Jason (Straumann Holding AG., Basel, Switzerland) and Quirumatrix (Cells Tech Co., Medellín, Colombia) membranes. The membranes (arrow) were placed in 12-well plates with surgical tape (arrowhead), hydrated for 48 hours with 100% fetal bovine serum, and then washed with phosphate-buffered saline. Half of each membrane was covered with sterile surgical tape. 40,000 osteoblast-like SaOS-2 cells were seeded on the non-covered side and allowed to adhere for 24 hours before the surgical tape was removed, thus allowing cell migration. (A) A photomicrograph of the Jason membrane and surgical tape fixing under a microscope. (B) A photograph of the culture well, showing the membrane with a section covered in surgical tape.

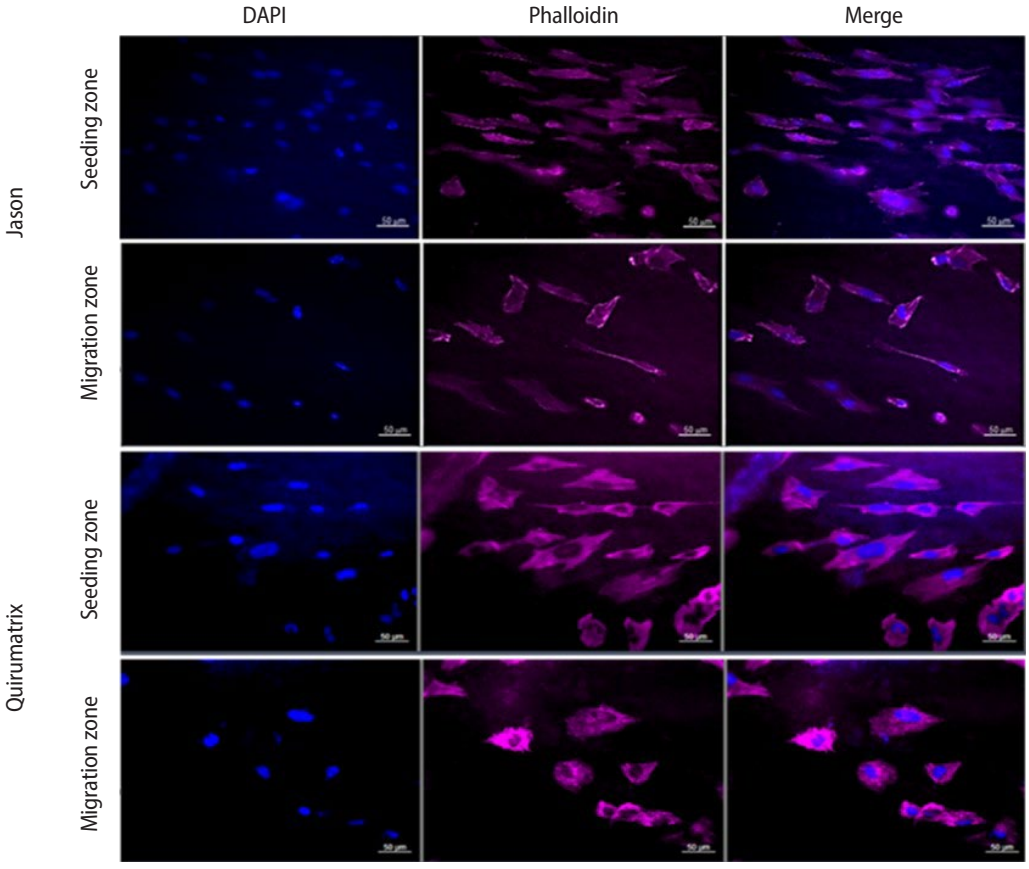

Figure 5. Staining of SaOS-2 cells with Alexa Fluor 555 Phalloidin (Cell Signaling Technology, Danvers, MA, USA) and 4′,6-diamidino-2-phenylindole (DAPI) on barrier membranes to evaluate cell migration. Staining was performed on nine membranes of each type, and cell counts were collected from 10 pictures of each membrane at 20× magnification. Magnification bar 50 µm. Jason: Straumann Holding AG., Basel, Switzerland; Quirumatrix: Cells Tech Co., Medellín, Colombia.

are presented as mean ± standard deviation. Prior to statistical comparison, data distributions were assessed for normality using the Shapiro-Wilk test and for homogeneity of variances using the Levene test. For datasets fulfilling parametric assumptions, comparisons between two experimental groups were performed using the Student *t*-test, whereas comparisons involving more than two groups were analyzed using one-way analysis of variance. When the data did not meet the assumptions of normality and/or homoscedasticity, the nonparametric Mann-Whitney *U* test was used for pairwise comparisons. A p-value <0.05 was considered statistically significant. All statistical analyses were conducted using GraphPad Prism (ver. 10.2.3; GraphPad Software, San Diego, CA, USA).

RESULTS

Visualization of cell attachment and morphological changes

Phase contrast-light microscopy did not provide any evidence of any influence from membrane hazardous residues or the glue from the double-sided adhesive tape throughout the first 5 days of the experiment after cell seeding. There was no interference with the proliferation of cells on the culture plates next to the barrier membranes and tape. There was no evidence of cell detachment or death. SEM examination after 5 days of cell seeding revealed a smaller number of cells attached to Quirumatrix membranes compared to cells on Jason membranes.

Under SEM examination, cells attached to the Jason

https://doi.org/10.5395/rde.2026.51.e20

membrane were elongated and star-shaped, whereas cells attached to the Quirumatrix membrane were more triangular. Furthermore, cells on Jason membranes were observed to emit protrusions from the cell membrane known as "Blebs" (Figures 6–8).

Cell proliferation

Values from the previously provided calibration curves (Figure 3) were used to calculate the number of cells for each fluorescence measurement: membrane, well, and total number of cells (well + membrane) at different times (48, 72, and 96 hours) (Figure 9A–C).

As shown in Figure 9A, the number of cells on the Jason membrane is significantly higher than that on the Quirumatrix membrane after 72 and 96 hours of seeding. Figure 9B indicates that the number of cells in the wells of the culture plate with the Jason membrane and the Quirumatrix is lower than in the wells without the membrane (control). The differences were significant ($p < 0.05$) at 96 hours following seeding.

At 96 hours, when the number of cells identified on the membranes was added up with the number of cells adhered to the corresponding well, it was shown that both Jason and Quirumatrix membranes had considerably more total cells than the control group ($p < 0.05$) (Figure 9C).

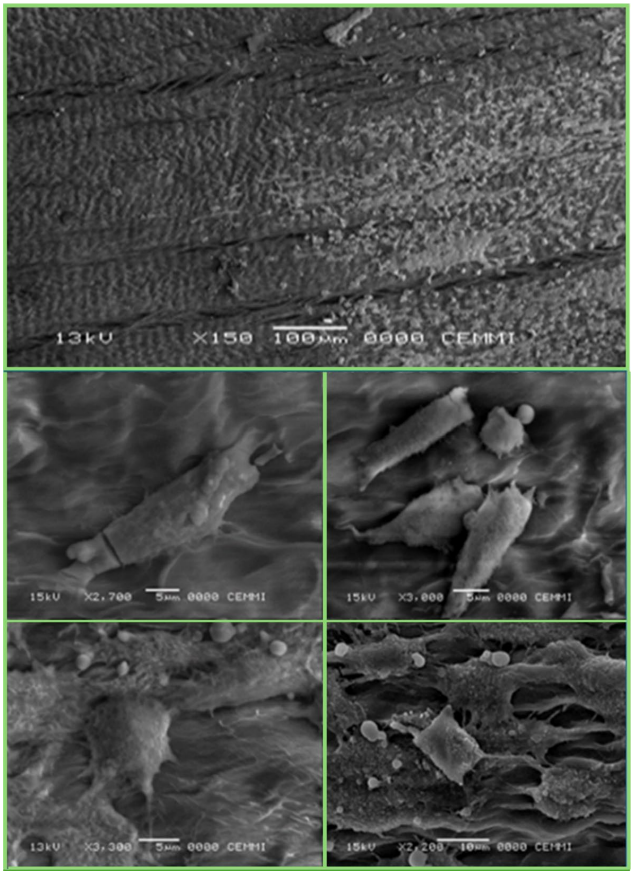

Figure 6. Scanning electron micrographs of SaOS-2 osteoblast-like cells attached to the surface of the Jason membrane (Straumann Holding AG., Basel, Switzerland). The cells have an expanded morphology, with many cytoplasmic extensions interacting directly with the membrane's collagen fibers.

Cell migration

After 3 days of culture, SaOS-2 cells adhered to the bottom of the culture plate and to the membranes; cell migration through the membranes was observed to different degrees (cell photographs) (Figure 9A–C). In the Jason membranes, more cells were observed in the migration zone than in the Quirumatrix membranes; this difference was statistically significant ($p < 0.05$). The seeding zone showed no significant differences between the two membranes (Figure 10).

DISCUSSION

This *in vitro* study evaluated the biocompatibility of two xenogeneic porcine-derived barrier membranes—a novel ECM-derived membrane obtained from decellularized porcine esophagus (Quirumatrix) and a native porcine pericardium collagen membrane (Straumann Jason)—by analyzing osteoblast-like SaOS-2 cell attachment, proliferation, migratory, and viability, behavior [1,9,11,12]. The selection of SaOS-2 osteoblast-like cells as the experimental model warrants consideration. While primary periodontal ligament cells or bone marrow-derived mesenchymal stem cells would more closely recapitulate the physiological regenerative environment, SaOS-2 cells offer distinct advantages for preliminary biocompatibility screening [13,14]. This cell line is well-characterized, exhibits key osteoblastic features including alkaline phosphatase activity and mineralization capacity, and has been extensively validated for evaluating cell–material interactions in biomaterial research [15]. Importantly, the use of a standardized cell line ensures reproducibility and eliminates donor-re-

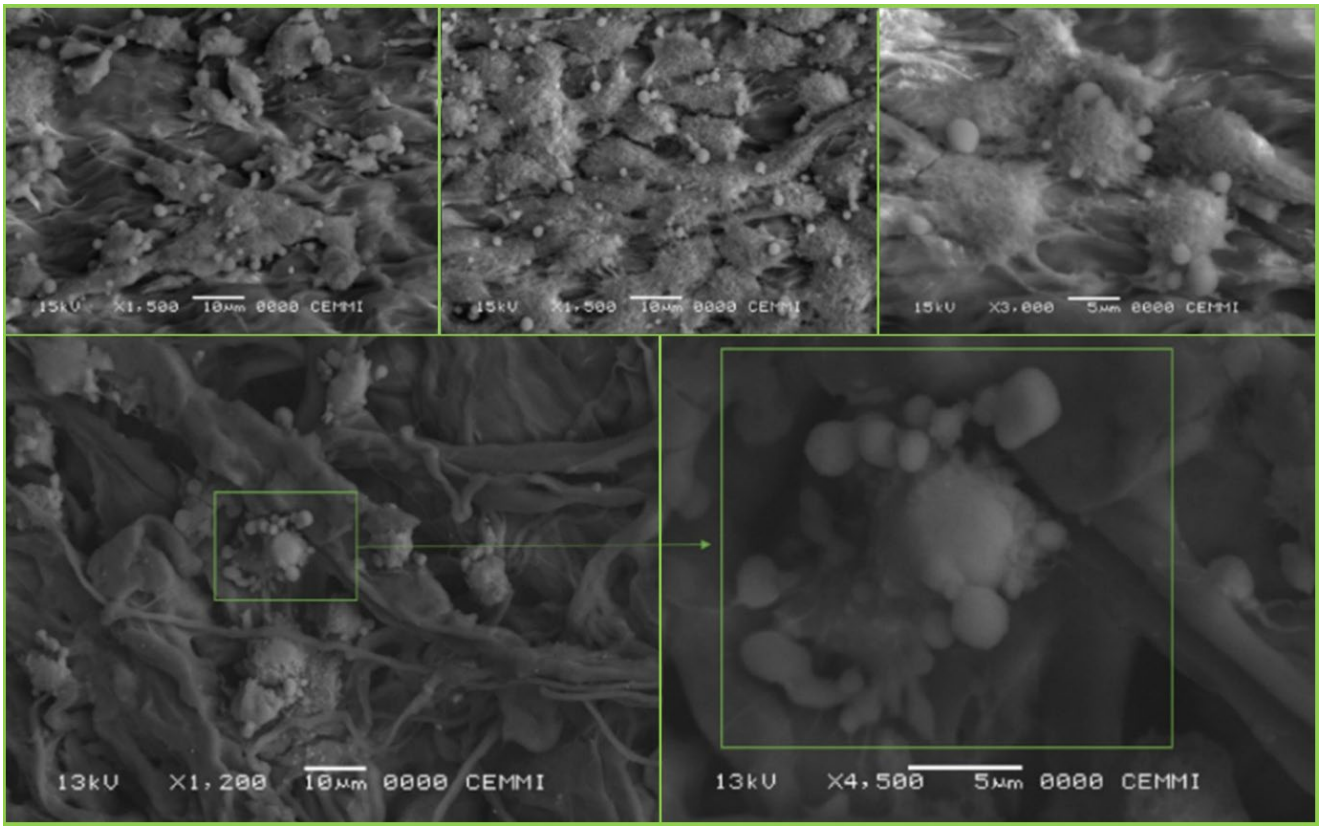

Figure 7. Scanning electron micrographs of SaOS-2 osteoblast-like cells attaching to the surface of the Jason membrane (Straumann Holding AG., Basel, Switzerland), exhibiting visible bleb development on their plasma membrane. The cells have an expanded morphology, with many cytoplasmic extensions and plainly visible blebs, indicating active cell–material interaction.

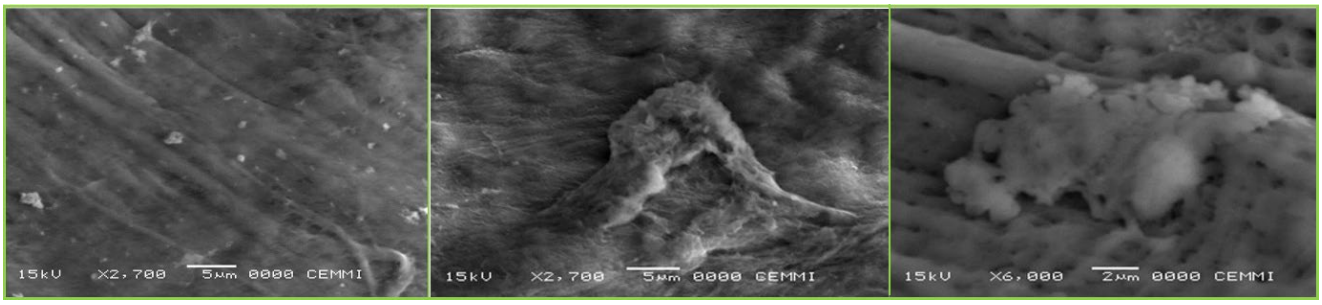

Figure 8. Scanning electron micrographs of SaOS-2 osteoblast-like cells attaching to the surface of the Quirumatrix membrane (Cells Tech Co., Medellín, Colombia). Compared with cells on the Jason membrane (Straumann Holding AG., Basel, Switzerland), the Quirumatrix cells have a more triangular morphology, defined borders, and fewer cytoplasmic extensions. The membrane has a decreased cell density, indicating less proliferation under these conditions.

lated variability inherent to primary cultures, enabling rigorous comparative assessment under controlled conditions [15]. Nevertheless, it must be acknowledged that SaOS-2 cells exhibit altered proliferative kinetics compared to primary osteoblasts and do not fully replicate the cellular heterogeneity or complex signaling networks present during *in vivo* tissue regeneration [16]. Therefore, while these findings provide valuable prelim-

https://doi.org/10.5395/rde.2026.51.e20

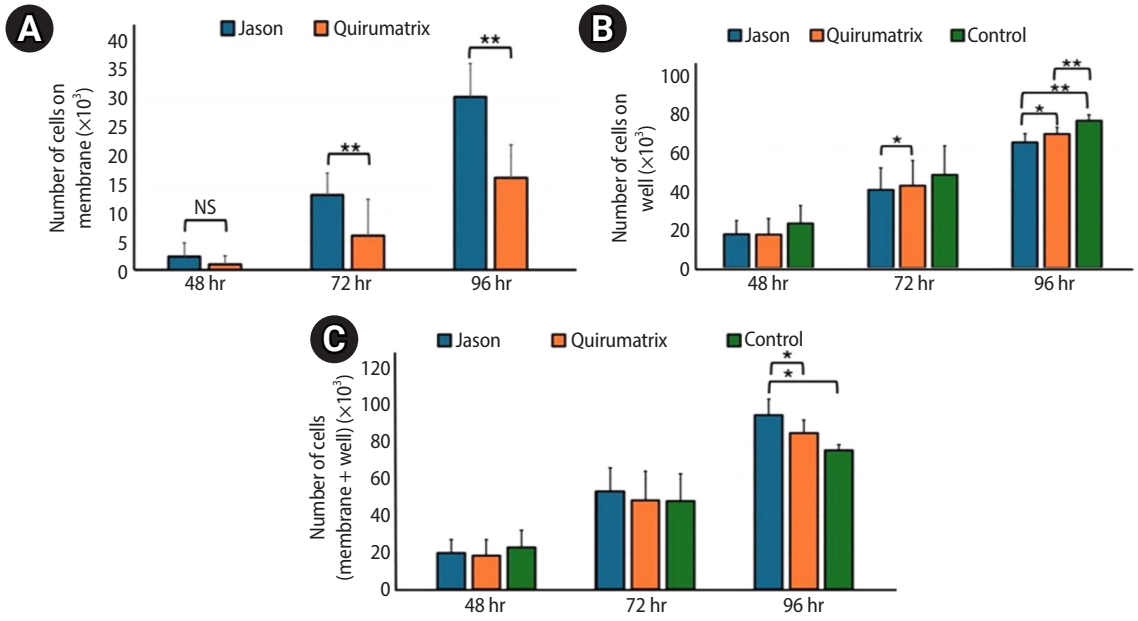

Figure 9. Viability and proliferation of SaOS-2 cells adhered on (A) membrane, (B) well, and (C) total number of cells (well + membrane) at different times (48, 72, and 96 hours). The control group corresponds to cells seeded directly in the well without the presence of the membrane (*$p < 0.05$, **$p < 0.01$). Data are expressed as averages ± standard deviation ($n = 9$). NS, not significant. Jason: Straumann Holding AG., Basel, Switzerland; Quirumatrix: Cells Tech Co., Medellín, Colombia.

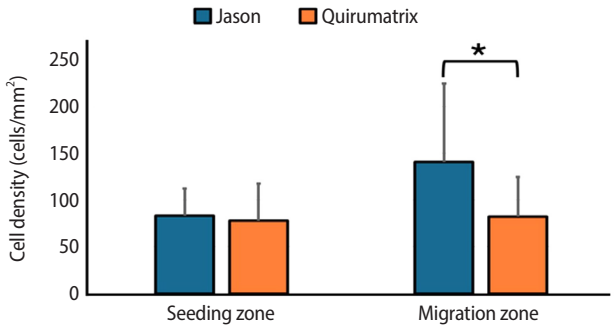

Figure 10. Number of cells/mm^2 counted in the seeding zone and in the cell migration zone of the Jason (Straumann Holding AG., Basel, Switzerland) and Quirumatrix (Cells Tech Co., Medellín, Colombia) membranes after 3 days of culture (*$p < 0.05$). Data are expressed as averages ± standard deviation ($n = 30$).

inary evidence of membrane biocompatibility, future studies incorporating primary cells and *in vivo* models are essential to validate the clinical applicability of these membranes, as discussed in the Study Limitations section.

GTR has been advocated as an adjunct to endodontic surgical procedures to promote complete periapical regeneration by preventing connective tissue collapse within the defect [12]. Barrier membranes are central to this approach, as their shielding function preserves the regenerative space while selectively favoring the repopulation of the defect by periodontal ligament-derived cells and osteogenic precursors [17]. Moreover, semi-permeable membranes contribute to the regulation of the local microenvironment by modulating the diffusion of key biomolecules, including pro-angiogenic growth factors, cytokines, and essential nutrients required for tissue regeneration [8].

Most barrier membranes used in GTR are manufactured from xenogeneic porcine collagen, predominantly type I and/or type III. Native collagen derived from porcine dermis or pericardium has been shown to provide effective barrier function and mechanical stability in regenerative procedures [18]. Beyond its structural role, collagen exhibits chemotactic properties that support fibroblast recruitment and the differentiation, proliferation, and migration of specialized cell populations. Moreover, collagen plays a central role in wound healing, particularly by facilitating platelet activation and angiogenesis [19]. Notably, only in the past decade has

research begun to elucidate the mechanisms governing membrane–host interactions in GTR. Accumulating evidence suggests that barrier membranes may actively contribute to tissue regeneration, as cellular and molecular responses to the membrane surface are intrinsically linked to regenerative outcomes [18,20]. Accordingly, membrane biocompatibility has emerged as a critical determinant of successful tissue regeneration [18].

Decellularized ECM-derived membranes have gained increasing attention as biologically active scaffolds for regenerative applications. The ECM constitutes a complex three-dimensional network composed of structural and signaling macromolecules, including collagen, elastin, fibronectin, laminin, glycosaminoglycans, and proteoglycans, which collectively recapitulate key features of native tissue architecture [21]. Following decellularization, many of the ECM's physicochemical cues and bioactive molecules can be preserved, thereby providing a biologically instructive three-dimensional substrate that supports cell adhesion, migration, proliferation, and differentiation [21]. In addition, ECM-based scaffolds contribute to the maintenance of local tissue homeostasis, facilitate the ingrowth of stem and progenitor cells, and promote regenerative processes through matrix-mediated signaling [21,22]. Accordingly, ECM-derived membranes may offer biologically relevant cues that mimic native signaling events and support the regeneration of damaged periodontal and periapical tissues [21,23].

In this study, a hydration approach was standardized before conducting the biocompatibility assessment of the two membranes to achieve optimal attachment, viability, proliferation, and migration in each membrane. The membranes were hydrated for 48 hours prior to cell seeding using 100% FBS (GE Healthcare Life Sciences, cat. #SH30088.03). This protocol was adopted after preliminary experiments showed that hydration of Quirumatrix membranes in PBS for 24 hours hindered initial cell attachment, with the few adherent cells detaching and undergoing cell death within 12 hours after seeding. One possible explanation for this observation may relate to membrane processing-associated factors inherent to ECM-derived scaffolds. In this context, the potential presence of residual traces of sodium dodecyl sulphate (SDS), an ionic detergent commonly used during decellularization procedures, has been proposed in the literature as a factor that may influence cell–material interactions. Decellularization is performed to minimize adverse host responses, including immune activation, inflammation, and implant rejection, by removing cellular remnants from tissue-derived biomaterials. However, detergents such as SDS are known to denature proteins and alter matrix ultrastructure, and incomplete removal has been associated with cytotoxic effects in some experimental models [24–26]. Importantly, residual SDS content was not directly quantified in the present study; therefore, its potential contribution should be considered hypothetically rather than as a confirmed mechanistic explanation. Notably, FBS has been reported to enhance cell colonization of decellularized tissues [27,28], potentially through protein adsorption and serum-detergent interactions that may facilitate the neutralization or removal of detergent residues [29]. Following optimization of the hydration protocol using 100% FBS, biocompatibility assays were subsequently conducted on both membranes.

Results from this study revealed that both membranes permitted cell attachment, viability, proliferation, and migration, indicating their potential clinical value. Jason outperformed Quirumatrix in terms of biocompatibility. Native collagen in Jason membranes has a robust fibrillar structure, providing exceptional mechanical stability. This natural structure not only provides appropriate strength at the implantation site but also serves as an efficient barrier to epithelial cell invasion, which is necessary for bone and gingival regeneration [30]. This could directly impact its use in patients by enabling faster, more effective regeneration of bone and gingival tissues, thereby improving long-term clinical outcomes [31,32].

Turri *et al.* [33] demonstrated that ECM-based membranes offer significant advantages for guided bone regeneration because their composition is rich in structural proteins, growth factors, and bioactive elements that facilitate cellular integration and the formation of new bone tissue. These membranes release growth factors, including vascular endothelial growth factor and transforming growth factor beta, which promote angiogenesis and bone healing. They attract progenitor cells and stimulate osteoblast differentiation. Its natural

https://doi.org/10.5395/rde.2026.51.e20

structure resembles the human ECM, providing a favorable environment for cell adhesion and proliferation while eliciting no substantial immunological response [33]. The above suggests that Quirumatrix membranes are a promising alternative for GTR; however, the current study's results must be interpreted with caution, although only some aspects of biocompatibility were evaluated. Quirumatrix is an experimental membrane that requires additional studies with more analysis variables. The differences in results between the two membranes could be attributed to a variety of factors, the first of which could be the presence of residual SDS on the Quirumatrix membranes, as previously noted [26,28,29]. Membranes treated with 100% FBS have been shown to increase cellular colonization of decellularized tissues by enriching them with adhesion proteins, growth hormones, and critical nutrients that aid in the early interaction between cells and the substrate [28]. After standardizing appropriate hydration regimens with 100% FBS, biocompatibility testing of both membranes showed that they can be used therapeutically.

Under the parameters of this *in vitro* study, more cells attached to Jason membranes than to Quirumatrix membranes. However, both membranes allowed cell adhesion, which is required for processes such as cell proliferation and migration. This supports other studies suggesting that cells' capacity to adhere to the substrate drives cell proliferation and migration [34]. The attachment of cells to substrates involves a four-step sequence: adsorption of glycoproteins to the substrate surface, cell contact, attachment, and spreading. In general, cell migration and proliferation begin only after these events have occurred. Proper adhesion provides physical anchorage, allowing cells to reorganize their cytoskeleton and extend projections, facilitating their movement toward specific areas of the tissue [35]. This could explain how cells linked to Jason membranes extend and create protrusions known as blebs on their cell membranes. Blebs, which are dynamic protrusions of the plasma membrane driven by intracellular pressure and cytoskeletal remodeling, enable cells to explore their environment and make initial contact with collagen fibers in the ECM. These interactions promote cell adhesion by activating receptors, such as integrins, which bind to collagen's bioactive regions. Furthermore, blebs act as temporary anchoring points for cell migration, generating mechanical forces that propel movement in specific directions [36].

Bleb formation is favored under conditions with low substrate adhesion, a dense or poorly degradable ECM, and high intracellular contractility [37]. Biomaterials used in GTR are typically designed with porous or micro-structured architectures that direct cell migration and proliferation toward the area to be regenerated [38]. However, these structures can represent physically restrictive environments where conventional mesenchymal migration is limited. In this scenario, blebbing-mediated amoeboid migration allows cells to advance without relying on strong adhesion or enzymatic matrix degradation, mechanically adapting to confinement and promoting efficient colonization of the scaffold [37]. This migration modality not only improves cell distribution within the biomaterial but also enhances cell–material interactions and promotes localized secretion of pro-regenerative factors, which are essential for effective tissue repair.

No bleb development was observed in cells adhering to Quirumatrix, unlike on the Jason membrane. This could be due to structural and physical-chemical variations between the two membranes. Jason membranes retain their natural honeycomb-shaped collagen type III structure, characterized by high porosity and multilayered organization. Its porous surface can provide bioactive areas and sufficient mechanical pressure to induce bleb formation, which is required for cell adhesion and migration. On the other hand, the Quirumatrix membrane, while rich in collagen, has a less porous structure, which may limit cell–material interaction and, as a result, bleb formation. These differences highlight the importance of the material's physical and chemical properties in the cellular response, implying that the Jason membrane may provide a more favorable environment for key cellular processes in GTR [38].

It should be noted that, while bleb formation was observed on cells adhering to Jason membranes, the presence of blebs alone does not provide definitive evidence of the cell migration mode. SEM images reveal cell morphology but cannot confirm whether cells are employing amoeboid-like migration or other motility mechanisms. Functional assays, such as live-cell imag-

ing or migration inhibition studies, would be required to determine the actual migration behavior in response to substrate properties. Therefore, the observations presented here should be interpreted as indicative of potential cellular adaptations rather than as conclusive evidence of a specific migration mode.

The decreased number of cells attached to Quirumatrix membranes may also explain the slower pace of cell migration and proliferation compared to the Jason membranes. However, when cell viability was assessed, the total number of cells observed in the membranes and wells was significantly higher in both Jason and Quirumatrix than in the control group, indicating that both membranes significantly stimulated the proliferation of SaOS-2 preosteoblastic cells. Takata *et al*. [35] found that changes in collagen fibril cross-linking, surface roughness, and collagen molecule structure could explain the varying effects on cell adhesion and proliferation. These findings support our SEM observations, which revealed differences in porosity and surface roughness among collagen membranes.

Several limitations of the present *in vitro* investigation should be acknowledged. The biological responses reported herein were derived from the osteoblast-like SaOS-2 cell line, which originates from osteosarcoma and therefore exhibits adhesion, proliferation, and migratory characteristics that may differ from those of primary human osteoblasts, periodontal ligament stem cells, or other progenitor cell populations directly involved in physiological bone and periodontal regeneration. Consequently, the observed cellular behaviors should be interpreted as indicative of relative biocompatibility and cell–material interaction rather than as a direct surrogate for clinical bone regeneration outcomes. In addition, the simplified *in vitro* experimental environment does not fully recapitulate the complex cellular, molecular, and immunological interactions that occur *in vivo*, including inflammatory signaling, vascularization, and multicellular crosstalk. It should be clarified that the terms "biocompatible" and "non-cytotoxic" refer specifically to *in vitro* experimental conditions. While these findings indicate that the material does not adversely affect cell viability under controlled laboratory settings, they do not necessarily predict the *in vivo* biological response, which may be influenced by complex factors such as immune reactions, tissue integration, and long-term material degradation. Therefore, *in vitro* assessments provide initial indications of safety, but further *in vivo* studies are required to fully establish the material's biocompatibility. These limitations underscore the need for complementary studies using primary cells and *in vivo* models to further validate the translational relevance of the present findings.

CONCLUSIONS

Within the constraints of this *in vitro* experimental model, both xenogeneic resorbable membranes exhibited adequate biocompatibility, supporting osteoblast-like cell survival, attachment, and migration. However, clear material-dependent differences in cellular behavior were observed. The Straumann Jason native porcine pericardium collagen membrane demonstrated superior capacity to promote osteoblast-like cell adhesion, proliferation, and directional migration, suggesting a more permissive microenvironment for early osteogenic events.

These findings highlight that membrane performance in GTR extends beyond passive barrier function and is critically influenced by the molecular and structural properties of the biomaterial. Features such as collagen organization, surface topography, and biochemical composition appear to modulate cell–material interactions at the level of cytoskeletal organization, adhesion dynamics, and migratory mechanisms, which are essential determinants of regenerative competence.

Collectively, the results support the concept that barrier membranes actively participate in the regulation of cellular behavior during the early phases of tissue regeneration. While the Quirumatrix ECM-derived membrane represents a biologically promising strategy, its regenerative performance appears to be highly sensitive to processing-related factors that may influence matrix integrity and cell-substrate signaling. Further mechanistic and translational studies are therefore required to elucidate how material-driven molecular cues modulate host cell responses and to define their clinical relevance in regenerative endodontic and periodontal applications.

https://doi.org/10.5395/rde.2026.51.e20

CONFLICT OF INTEREST

No potential conflict of interest relevant to this article was reported.

ACKNOWLEDGMENTS

The authors would like to thank Dr. Lina Escobar, Dr. Zita Bendahan, and Dr. Jaime Castellanos from Universidad del Bosque for their valuable expertise in the execution of this project.

AUTHOR CONTRIBUTIONS

Conceptualization, Visualization: Fernández-Grisales R, Berruecos-Orozco C. Data curation: Fernández-Grisales R, Berruecos-Orozco C, Duque VE, Serna-Guisao D. Formal analysis, Investigation: Fernández-Grisales R, Berruecos-Orozco C, Duque VE, Serna-Guisao D, Rojas WJ, Ríos-Osorio N. Methodology, Software: Duque VE, Serna-Guisao D. Project administration: Fernández-Grisales R. Resources: Ríos-Osorio N. Supervision: Fernández-Grisales R, Berruecos-Orozco C, Calle-Jaramillo M, Rojas WJ. Validation: Fernández-Grisales R, Berruecos-Orozco C, Ríos-Osorio N. Writing - original draft: Ríos-Osorio N. Writing - review & editing: Fernández-Grisales R, Berruecos-Orozco C, Ríos-Osorio N. All authors read and approved the final manuscript.

DATA SHARING STATEMENT

The datasets are not publicly available but are available from the corresponding author upon reasonable request.

REFERENCES

1. Liu TJ, Zhou JN, Guo LH. Impact of different regenerative techniques and materials on the healing outcome of endodontic surgery: a systematic review and meta-analysis. Int Endod J 2021;54:536-555.
2. Rios Osorio N, Caviedes-Bucheli J, Mosquera-Guevara L, Adames-Martinez JS, Gomez-Pinto D, Jimenez-Jimenez K, *et al*. The paradigm of the inflammatory radicular cyst: biological aspects to be considered. Eur Endod J 2023;8:20-36.
3. Lin L, Chen MY, Ricucci D, Rosenberg PA. Guided tissue regeneration in periapical surgery. J Endod 2010;36:618-625.
4. Melcher AH. On the repair potential of periodontal tissues. J Periodontol 1976;47:256-260.
5. Karamifar K, Tondari A, Saghiri MA. Endodontic periapical lesion: an overview on the etiology, diagnosis and current treatment modalities. Eur Endod J 2020;5:54-67.
6. Deng Y, Zhu X, Yang J, Jiang H, Yan P. The effect of regeneration techniques on periapical surgery with different protocols for different lesion types: a meta-analysis. J Oral Maxillofac Surg 2016;74:239-246.
7. Alkandari FA, Alotaibi MK, Al-Qahtani S, Alajmi S. The use of guided tissue regeneration in endodontic microsurgery: setting a threshold. Saudi Dent J 2024;36:461-465.
8. Bashutski JD, Wang HL. Periodontal and endodontic regeneration. J Endod 2009;35:321-328.
9. Yoo CK, Jeon JY, Kim YJ, Kim SG, Hwang KG. Cell attachment and proliferation of osteoblast-like MG63 cells on silk fibroin membrane for guided bone regeneration. Maxillofac Plast Reconstr Surg 2016;38:17.
10. Wang HL, Miyauchi M, Takata T. Initial attachment of osteoblasts to various guided bone regeneration membranes: an in vitro study. J Periodontal Res 2002;37:340-344.
11. Takata T, Wang HL, Miyauchi M. Migration of osteoblastic cells on various guided bone regeneration membranes. Clin Oral Implants Res 2001;12:332-338.
12. Anoopkumar-Dukie S, Carey JB, Conere T, O'sullivan E, van Pelt FN, Allshire A. Resazurin assay of radiation response in cultured cells. Br J Radiol 2005;78:945-947.
13. Czekanska EM, Stoddart MJ, Richards RG, Hayes JS. In search of an osteoblast cell model for in vitro research. Eur Cell Mater 2012;24:1-17.
14. Rodan SB, Imai Y, Thiede MA, Wesolowski G, Thompson D, Bar-Shavit Z, *et al*. Characterization of a human osteosarcoma cell line (Saos-2) with osteoblastic properties. Cancer Res 1987;47:4961-4966.
15. Declercq H, Van den Vreken N, De Maeyer E, Verbeeck R, Schacht E, De Ridder L, *et al*. Isolation, proliferation and differentiation of osteoblastic cells to study cell/biomaterial interactions: comparison of different isolation techniques and source. Biomaterials 2004;25:757-768.
16. Pautke C, Schieker M, Tischer T, Kolk A, Neth P, Mutschler W, *et al*. Characterization of osteosarcoma cell lines MG-63, Saos-2 and U-2 OS in comparison to human osteoblasts. Anticancer Res 2004;24:3743-3748.
17. Zubizarreta-Macho Á, Tosin R, Tosin F, Velasco Bohórquez P, San Hipólito Marín L, Montiel-Company JM, *et al*. Influence of guided tissue regeneration techniques on the success rate of healing of surgical endodontic treatment: a systematic review and network meta-analysis. J Clin Med 2022;11:1062.
18. Sasaki JI, Abe GL, Li A, Thongthai P, Tsuboi R, Kohno T, *et al*. Barrier membranes for tissue regeneration in dentistry. Biomater Investig Dent 2021;8:54-63.
19. Lindner C, Alkildani S, Stojanovic S, Najman S, Jung O, Barbeck M. In vivo biocompatibility analysis of a novel barrier membrane based on bovine dermis-derived collagen for

Guided Bone Regeneration (GBR). Membranes (Basel) 2022;12:378.
20. Alqahtani AM, Moorehead R, Asencio IO. Guided tissue and bone regeneration membranes: a review of biomaterials and techniques for periodontal treatments. Polymers (Basel) 2023;15:3355.
21. Omar O, Elgali I, Dahlin C, Thomsen P. Barrier membranes: more than the barrier effect? J Clin Periodontol 2019;46 Suppl 21(Suppl Suppl 21):103-123.
22. Liang C, Liao L, Tian W. Advances focusing on the application of decellularized extracellular matrix in periodontal regeneration. Biomolecules 2023;13:673.
23. Liu C, Pei M, Li Q, Zhang Y. Decellularized extracellular matrix mediates tissue construction and regeneration. Front Med 2022;16:56-82.
24. Mendibil U, Ruiz-Hernandez R, Retegi-Carrion S, Garcia-Urquia N, Olalde-Graells B, Abarrategi A. Tissue-specific decellularization methods: rationale and strategies to achieve regenerative compounds. Int J Mol Sci 2020;21:5447.
25. Alizadeh M, Rezakhani L, Soleimannejad M, Sharifi E, Anjomshoa M, Alizadeh A. Evaluation of vacuum washing in the removal of SDS from decellularized bovine pericardium: method and device description. Heliyon 2019;5:e02253.
26. Gratzer PF, Harrison RD, Woods T. Matrix alteration and not residual sodium dodecyl sulfate cytotoxicity affects the cellular repopulation of a decellularized matrix. Tissue Eng 2006;12:2975-2983.
27. Long C, Galvez MG, Legrand A, Joubert LM, Wang Z, Chattopadhyay A, *et al*. Intratendinous injection of hydrogel for reseeding decellularized human flexor tendons. Plast Reconstr Surg 2017;139:1305e-1314e.
28. Porzionato A, Stocco E, Barbon S, Grandi F, Macchi V, De Caro R. Tissue-engineered grafts from human decellularized extracellular matrices: a systematic review and future perspectives. Int J Mol Sci 2018;19:4117.
29. Jafari M, Mehrnejad F, Rahimi F, Asghari SM. The molecular basis of the sodium dodecyl sulfate effect on human ubiquitin structure: a molecular dynamics simulation study. Sci Rep 2018;8:2150.
30. Cho YD, Kim KH, Lee YM, Ku Y, Seol YJ. Periodontal wound healing and tissue regeneration: a narrative review. Pharmaceuticals (Basel) 2021;14:456.
31. Opris H, Baciut M, Moldovan M, Cuc S, Petean I, Opris D, *et al*. Comparison of the eggshell and the porcine pericardium membranes for guided tissue regeneration applications. Biomedicines 2023;11:2529.
32. Sbricoli L, Guazzo R, Annunziata M, Gobbato L, Bressan E, Nastri L. Selection of collagen membranes for bone regeneration: a literature review. Materials (Basel) 2020;13:786.
33. Turri A, Elgali I, Vazirisani F, Johansson A, Emanuelsson L, Dahlin C, *et al*. Guided bone regeneration is promoted by the molecular events in the membrane compartment. Biomaterials 2016;84:167-183.
34. Merino-Casallo F, Gomez-Benito MJ, Hervas-Raluy S, Garcia-Aznar JM. Unravelling cell migration: defining movement from the cell surface. Cell Adh Migr 2022;16:25-64.
35. Takata T, Wang HL, Miyauchi M. Attachment, proliferation and differentiation of periodontal ligament cells on various guided tissue regeneration membranes. J Periodontal Res 2001;36:322-327.
36. Paluch EK, Raz E. The role and regulation of blebs in cell migration. Curr Opin Cell Biol 2013;25:582-590.
37. Schick J, Raz E. Blebs-formation, regulation, positioning, and role in amoeboid cell migration. Front Cell Dev Biol 2022;10:926394.
38. Ren Y, Fan L, Alkildani S, Liu L, Emmert S, Najman S, *et al*. Barrier membranes for guided bone regeneration (GBR): a focus on recent advances in collagen membranes. Int J Mol Sci 2022;23:14987.

https://doi.org/10.5395/rde.2026.51.e20

RDE Restorative Dentistry & Endodontics

Research Article

eISSN 2234-7666
Restor Dent Endod. 2026 May;51(2):e21
https://doi.org/10.5395/rde.2026.51.e21

Fracture resistance of regenerated immature teeth in different simulated stages of root development: an *in vitro* cyclic loading study

Kyveli-Artemis Polydora[1,*], **Konstantinos Kodonas**[1], **Anastasia Fardi**[2], **Christos Gogos**[1]

[1]Department of Endodontology, School of Dentistry, Aristotle University of Thessaloniki, Thessaloniki, Greece
[2]Department of Dentoalveolar Surgery, Surgical Implantology and Radiology, School of Dentistry, Aristotle University of Thessaloniki, Thessaloniki, Greece

ABSTRACT

Objectives: This *in vitro* study aimed to assess the fracture resistance of simulated stages of root maturation following regenerative endodontic treatment using a cyclic loading method.

Methods: Ninety extracted maxillary central incisors were randomly allocated into three experimental groups representing different stages of root development, following revitalization: Group A for completely immature teeth immediately after treatment; Group B for teeth with apical closure, and Group C for teeth with apical closure and wall thickening. Two control groups were also included: Group D for intact teeth and Group E for simulated immature teeth without the bioceramic material. Following simulation of immature apices and treatment with a bioceramic material, all specimens were subjected to cyclic loading using a step-stress fatigue protocol until failure. The number of cycles to fracture and the peak load were recorded and statistically analyzed.

Results: Statistically significant differences in loading forces were observed between the negative control group (Group D) and Groups A, B, and E ($p < 0.05$). However, no statistically significant differences were detected among the experimental groups. These results indicate that apical closure and dentinal wall thickening alone did not substantially improve mechanical reinforcement under cyclic loading conditions.

Conclusions: Although intact teeth exhibited superior mechanical performance, apical closure and wall thickening alone were insufficient to enhance reinforcement under cyclic loading.

Keywords: Tooth fractures; Fracture strength; Regenerative endodontics; In vitro techniques

INTRODUCTION

Pulpal necrosis in immature teeth, often caused by trauma, caries, or developmental disorders, presents significant clinical challenges. Incomplete root formation results in thin dentinal walls and open apices, making

Received: August 22, 2025 **Revised:** November 27, 2025 **Accepted:** December 2, 2025

Citation
Polydora KA, Kodonas K, Fardi A, Gogos C. Fracture resistance of regenerated immature teeth in different simulated stages of root development: an *in vitro* cyclic loading study. Restor Dent Endod 2026;51(2):e21.

***Correspondence to**
Kyveli-Artemis Polydora, DDS
Department of Endodontology, School of Dentistry, Aristotle University of Thessaloniki, Campus Dentistry Building, Thessaloniki 54124, Greece
Email: Kyvepoly@dent.auth.gr

these teeth more susceptible to fractures, particularly in the cervical region [1]. Finite element analyses have shown that the highest stress concentrations occur in the coronal portion of the root when subjected to masticatory or traumatic forces [2]. Consequently, fractures frequently develop at the level of the crestal bone, rendering restoration impossible and compromising the long-term prognosis of the tooth [3].

For immature non-vital teeth, current treatment options include regenerative endodontic procedures (REPs) and apexification, typically achieved using a mineral trioxide aggregate (MTA) plug or calcium hydroxide [$Ca(OH)_2$]-induced apical barrier formation [4]. However, the use of MTA apexification has declined due to its high cost, complex handling characteristics, retreatability challenges, and risk of overfilling [5]. Clinical studies comparing the survival and success rates of REPs and apexification have shown similar overall outcomes [6].

Nevertheless, neither $Ca(OH)_2$ nor MTA apexification supports continued root development [7]. In contrast, REPs aim to restore pulp vitality and promote root maturation by stimulating increases in root length, dentinal wall thickness, and apical closure. Furthermore, REPs offer an advantage by allowing for potential retreatment if the initial procedure fails [8,9]. Despite these benefits, the long-term effects of REPs on the structural integrity of treated teeth remain uncertain. In particular, the relationship between the degree of root maturation and the fracture resistance of healing or healed immature teeth remains unclear.

Therefore, this study aims to evaluate the fracture resistance of revascularized teeth at three simulated stages of root development: completely immature, with apical closure, and with apical closure and dentine wall thickening, under cyclic loading conditions. The null hypothesis tested was that apical closure, with or without dentinal wall thickening, does not significantly influence the fracture resistance of the tooth.

METHODS

Study design

The study was conducted in compliance with the ethical standards of the Aristotle University of Thessaloniki Research Committee (approval number: 222/13-03-2024) and the 1964 Helsinki Declaration and its later amendments. The manuscript was prepared following the Preferred Reporting Items for Laboratory Studies in Endodontology 2021 guidelines [10]. All teeth were collected with informed consent from patients undergoing extraction for reasons unrelated to this study, ensuring patient confidentiality throughout the research process.

Sample selection and preparation

A sample size calculation was performed using G*Power software (ver. 3.1.9.7, Heinrich-Heine-Universität Düsseldorf, Düsseldorf, Germany), as indicated by previous published studies comparing fracture resistance with various regenerative endodontic protocols [11,12]. Accordingly, a sample size of 15 teeth per experimental group and 10 per control group was determined to achieve 80% power at a significance level of 0.05. The number of samples increased by five in each group (×5 groups) to account for potential laboratory processing errors.

Ninety freshly extracted intact maxillary central incisors were collected for the study. Calculus and soft tissue deposits were removed with an ultrasonic device (Woodpecker Ultrasonic Scaler; Guilin Woodpecker, Guilin, China). The teeth were sterilized in an autoclave (Lisa; W&h, Bürmoos, Austria) for 40 minutes at 134°C under 20 psi, then stored in distilled water at 4°C [13]. Prior to experimentation, the teeth were carefully examined under magnification (SmartOPTIC; Seliga Microscopes, Lodz, Poland) to ensure they were free from resorption, caries, cracks, or deformities. Teeth from the same individual were excluded.

To ensure specimen homogeneity prior to group allocation, all teeth were measured using a digital caliper (Mitutoyo 150 mm Digital Caliper; Mitutoyo, Hampshire, UK) in three dimensions—buccolingual, mesiodistal, and corono-apical (height)—to establish mean values for the sample. Specimens deviating more than 20% from the mean in any dimension or exhibiting canal curvature greater than 20° were excluded to minimize variation in root size and dentinal wall morphology that could influence stress distribution during fracture testing. The final sample demonstrated consistent morphology, with mean mesiodistal dimensions

https://doi.org/10.5395/rde.2026.51.e21

of 6.5 ± 0.5 mm and buccolingual dimensions of 6.0 ± 0.5 mm. Mesiodistal and buccolingual measurements were recorded at the cementoenamel junction (CEJ), whereas the corono-apical dimension corresponded to the straight line connecting the incisal edge to the apical tip. Each measurement was performed five times; the highest and lowest values were discarded, and the remaining three were averaged to ensure accuracy.

All specimens were radiographed in buccolingual and mesiodistal projections using a digital sensor (Planmeca ProSensor; Planmeca, Helsinki, Finland) at three stages: before instrumentation to verify root length, assess canal morphology, and screen for differences in dentinal wall thickness or pre-existing defects; after bioceramic placement to verify material thickness and homogeneity; and after fracture testing to confirm failure patterns. This imaging-based verification further minimized anatomical variability that could affect stress distribution and fracture resistance. The combination of morphometric caliper measurements and radiographic evaluation ensured consistent root dimensions and dentinal wall thickness across specimens, thereby reducing anatomical variability that could influence fracture resistance outcomes. After confirming anatomical comparability, the specimens were randomly assigned to five groups—three experimental groups (n = 20 each) and two control groups (n = 15 each)—using computer-generated randomization software (QuickCalcs, GraphPad Software, San Diego, CA, USA).

Simulation of immature teeth

Experimental groups were instrumented in order to represent three different stages of root development: completely immature teeth (Group A), teeth with apical closure (Group B), and teeth with apical closure and wall thickening (Group C). Intact teeth served as negative controls (Group D), while teeth with simulated immature roots without material placement served as positive controls (Group E) (Figure 1). The completely immature groups were classified as stage 3 according to Cvek's classification [14].

The apices of the teeth in the positive control and Group A (completely immature) were cut by a low-speed diamond disc (Superflex HP 405; Edenta AG, Pfungen, Austria) such that the remaining root length was 12 mm [15,16]. Immature teeth were simulated according to the study of Elnaghy and Elsaka [16]. Briefly, specimens were enlarged from the coronal to apical direction using long-neck round burs at high-speed rotation with continuous air-water spray. Peeso reamers

Figure 1. Representative radiographic images of the five study groups. (A) Completely immature teeth immediately after treatment (Group A). (B) Teeth with apical closure (Group B). (C) Teeth with apical closure and wall thickening (Group C). (D) Intact teeth (negative control, Group D). (E) Simulated immature teeth without material placement (positive control, Group E).

(Dentsply Maillefer, Ballaigues, Switzerland) of size 1–6 were inserted into varying root canal lengths depending on the experimental group: Groups A and E were instrumented until size 6 Peeso to root length; for Group B, 3 mm coronal to the apex; and for Group C, 3 mm apical to the CEJ. Instrumentation was performed by a single experienced operator using Peeso reamers with fixed, standardized diameters to ensure reproducible enlargement patterns across all specimens [12,15]. Each canal was prepared following a predefined depth-specific protocol to produce uniform tapering and to maintain consistent dentinal wall thickness within and between groups. The use of dimensionally calibrated reamers and a single operator minimized procedural variability and maximized specimen homogeneity, ensuring that differences in dentinal wall size did not confound the experimental outcomes.

Treatment procedures

The treatment procedures were conducted in accordance with the protocol recommended by the European Society of Endodontology (ESE) [17]. Following access cavity preparation, the root canals were rinsed with 1.5% sodium hypochlorite (20 mL, 5 minutes), using a side-vented needle, followed by 5 mL sterile saline and 20 mL 17% ethylenediaminetetraacetic acid (EDTA) (CanalPro EDTA 17%; COLTENE Group, Cuyahoga Falls, OH, USA). The canals were dried with paper points (Diadent Paper Points; Diadent Europe B.V., Almere, The Netherlands) and filled with calcium hydroxide as an intracanal medicament following the protocol of Jamshidi *et al*. [15]. Access cavities were provisionally restored using a temporary filling material (Cavit; 3M ESPE, St Paul, MN, USA).

The teeth were then incubated at 37°C and 100% humidity for 3 weeks. After the incubation period, the calcium hydroxide paste was removed using 1.5% sodium hypochlorite. The root canals were then irrigated with 17% EDTA and distilled water, then dried with paper points. A foam was placed in the root canal up to the working length to simulate the blood clot, standardize the coronal barrier thickness, and facilitate material condensation, following the methodology described by Gunal *et al*. [12].

A 3-mm layer of the bioceramic material (Angelus Bio-C Repair; Angelus, Londrina, Brazil) was applied according to the manufacturer's instructions in all three experimental groups below the CEJ. Teeth were temporally restored with Cavit. To simulate clinical conditions, all specimens were stored in 100% humidity at 37°C until fracture testing. After 12 hours of incubation to allow the bioceramic putty to set, access cavities were restored with glass ionomer cement (Ionoseal; Voco, Cuxhaven, Germany) and light-cured flowable composite (Spectrum; Dentsply Sirona, Constanz, Germany).

Fracture resistance testing

For periodontal ligament (PDL) simulation, teeth were coated with a latex liquid spacing agent (Erkoskin; Erkodent, Pfalzgrafenweiler, Germany) according to the method described by Mello *et al*. [11]. Each tooth was coated with four layers of Erkoskin, with 10 minutes of drying between layers. The specimens were then embedded perpendicularly in self-curing acrylic resin (BMS Light-curing orthodontic resin; BMS Dental, Capannoli, Italy), leaving a 2-mm gap between the top of the acrylic and the CEJ to mimic the bone-tooth relationship. For fracture testing, a custom jig was prepared to fix the acrylic cubes at a 45° angle [18]. Samples were then subjected to cyclic loading using a 2-mm spherical stainless-steel tip mounted on a pneumatic cylinder (SDA; Airblock, Thessaloniki, Greece), controlled by a precision pressure regulator (Regtronic; Metal Work, Consecio, Italy). The pneumatic loading system was operated via a single-board computer running custom Python-based control software and was calibrated using a Universal Testing Machine (Testometric, Rochdale, UK). The pneumatic loading system was calibrated at regular intervals throughout the experimental procedure. Calibration checks were performed after every 10 specimens, and no deviations beyond acceptable tolerance limits were detected. This maintained consistent and reliable loading throughout the experiment. To ensure constant moisture conditions during testing, all samples were covered with a wet gauze throughout the procedure [19].

Fracture resistance was evaluated using the step-stress method described by Lin *et al*. [19] (Supplementary Table 1), in which cyclic loads were progressively increased until specimen failure. The loading cycles

https://doi.org/10.5395/rde.2026.51.e21

followed a sinusoidal waveform at 1 Hz, with the minimum load set to 0. The test commenced with a load amplitude of 200 N, followed by 300 N, each applied for 1,000 cycles. Subsequently, the load amplitude was increased to 400 N and further raised in 50 N increments up to 850 N, with 3,000 cycles at each level. Specimens that withstood these cycles were loaded to 850 N until fracture occurred. A high-sensitivity sensor (G-Sensor; Creality, Shenzhen, China) was employed to detect subtle positional displacements of the cylinder tip indicative of fracture. Data on the number of cycles to failure and the final load at failure were recorded for analysis.

Statistical analysis

Descriptive statistics, including means and standard deviations, were calculated for fracture resistance values in each group. The normality of data distribution was assessed using the Kolmogorov-Smirnov and Shapiro-Wilk tests. Since the data were not normally distributed, non-parametric tests were applied. Differences among the five experimental groups were analyzed using the Kruskal-Wallis test, followed by Bonferroni-adjusted Dunn's *post hoc* comparisons for pairwise analysis. A p-value of <0.05 was considered statistically significant. Statistical analyses were performed using IBM SPSS ver. 28.0 (IBM Corp., Armonk, NY, USA).

RESULTS

Normality tests (Shapiro-Wilk and Kolmogorov-Smirnov) revealed that the data for cyclic load, fracture resistance, and number of cycles were not normally distributed ($p < 0.05$). The Kruskal–Wallis test followed by Bonferroni-adjusted Dunn's *post hoc* comparisons was used to evaluate differences among the five experimental groups.

Fracture resistance

Descriptive statistics for mean load (N), fracture resistance (MPa), and coefficient of variation (CV%) are presented in Table 1. The Kruskal-Wallis test revealed significant differences among the groups ($H(4) = 20.270$, $p < 0.05$). *Post hoc* pairwise comparisons using Bonferroni-adjusted Dunn's tests showed that the negative control (Group D) exhibited significantly higher fracture resistance than Groups A ($p < 0.05$), B ($p < 0.05$), and E ($p < 0.05$). No statistically significant differences were detected among the experimental groups (A–C) or between Group C and the negative control (Group D).

Group C displayed the highest mean fracture resistance among the experimental groups (5,019.05 ± 4,968.58 MPa) and was comparable to the negative control (15,513.33 ± 13,244.33 MPa). However, this observation should be interpreted cautiously, as differences among the experimental groups were not statistically significant ($p > 0.05$).

Load at failure

Mean load values per cycle also varied significantly among groups ($H(4) = 20.332$, $p < 0.05$). Group D (573.33 ± 186.96 N) had significantly higher load capacity compared with Groups A (377.5 ± 105.72 N, $p < 0.05$), B (362.5 ± 153.79 N, $p < 0.05$), and E (316.67 ± 109.65 N, $p < 0.05$). No significant differences were found between Groups A, B, and C.

Number of cycles to fracture

The number of cycles to failure did not differ significantly among groups ($H(4) = 5.468$, $p > 0.05$). The highest mean number of cycles was recorded for the negative

Table 1. Load at failure, fracture resistance, and number of cycles to fracture across groups

Group	Load at failure (N)	Fracture resistance (MPa)	Number of cycles
A	377.50[d] ± 105.72 (28.00)	3,686.65[d] ± 3,300.58 (89.53)	788.65 ± 1,128.80 (143.13)
B	362.50[d] ± 153.79 (42.42)	4,507.25[d] ± 7,863.23 (174.46)	1,009.30 ± 1,438.13 (142.49)
C	387.50 ± 132.66 (34.23)	5,019.05 ± 4,968.58 (98.99)	821.50 ± 893.79 (108.80)
D	573.33[abe] ± 186.96 (32.61)	15,513.33[abe] ± 13,244.33 (85.37)	2,972.33 ± 3,334.44 (112.18)
E	316.67[d] ± 109.65 (34.63)	2,513.00[d] ± 2,797.44 (111.32)	514.33 ± 549.95 (106.93)

Values are presented as mean ± standard deviation, with coefficient of variation (%) in parentheses.
Different superscript letters indicate statistically significant differences between groups ($p < 0.05$). [a]Significantly different from Group A. [b]Significantly different from Group B. [c]Significantly different from Group C. [d]Significantly different from Group D. [e]Significantly different from Group E.

control (2,972.33 ± 3,334.44), followed by Group C (821.50 ± 893.79). The lowest values were observed in the positive control (514.33 ± 549.95).

The distribution of mechanical parameters among the experimental groups is illustrated in Figure 2. Boxplots show the variability in load at failure (Figure 2A), fracture resistance (Figure 2B), and number of cycles to fracture (Figure 2C) across all five groups.

DISCUSSION

REPs offer a promising alternative to traditional root canal treatment, allowing for the regeneration of functional dental pulp [20]. The effectiveness of REPs is assessed based on criteria established by the ESE and the American Association of Endodontists (AAE) [17,21]. The ESE defines success as clinical and radiographic healing, continued root development, a positive pulp sensibility response, absence of root resorption, and absence of crown discoloration [17]. The AAE categorizes outcomes as primary (symptom resolution), secondary (root development), and tertiary (pulp sensibility) [21]. To integrate these perspectives, the ESE criteria describe the observable clinical and radiographic manifestations of success, while the AAE framework contextualizes these changes within biologically driven stages of regeneration. Together, they provide a unified and comprehensive basis for evaluating treatment outcomes in REP cases.

Numerous studies report that REPs frequently result in apical closure, often accompanied by continued root development, including an increase in root length and wall thickness. However, variability exists: while some cases show complete maturation, others exhibit only apical closure without significant root elongation [22,23]. This variability highlights the need to understand which specific components of root development contribute meaningfully to mechanical reinforcement.

This *in vitro* study investigated the impact of different simulated stages of root development, specifically apical closure or a combination of apical closure and wall thickening, on the fracture resistance of simulated immature teeth treated with REP. The results demonstrated no statistically significant differences among the experimental groups, supporting the acceptance of the null hypothesis. Specifically, neither apical closure alone nor apical closure combined with wall thickening resulted in a statistically significant increase in fracture resistance compared with completely immature teeth. These findings help clarify the contribution of individual simulated growth elements to fracture resistance under laboratory conditions, an area that has remained ambiguous in previous literature.

The fracture resistance of immature teeth subjected to REPs has been evaluated in a limited number of research studies [12,13,15,16,18,24]. Most studies have shown that treated teeth have lower fracture resistance compared to intact teeth, an observation that aligns with the findings of the present study. Previous research did not find significant differences in fracture resistance based on the stage of root development [15], the material used [24], and material thickness [12] or the presence of material at the critical cervical area [16].

However, simulated immature teeth showed advanced fracture resistance when fully obturated with MTA [12]. This highlights that material-based reinforcement is possible under certain conditions. In the present study, no significant difference was observed between the positive control (Group E) and the completely immature group (Group A), indicating that bioceramic materials placed at the coronal part of the root canal, below the CEJ, may not effectively strengthen canal walls. Only the negative control group exhibited significantly higher values, underscoring the superior integrity of unaltered dentine.

The use of a bioceramic material at the cervical root area is considered essential for the REP protocol. Recently, there has been a push to develop improved biomaterials. Angelus Bio-C Repair, introduced in 2019, is a premixed paste of bioceramic repair material delivered via syringe. In this study, it was selected for its user-friendly handling characteristics and ease of clinical application. Regardless of the material used, a major limitation of REPs is the hindrance to posttreatment growth of pericervical dentine caused by the placement of bioceramic material. Pericervical dentine growth is crucial for safely transferring load from the occlusal table to the root [25]. This fact is emphasized by the emerging long-term literature data that have identified cervical fractures as a notable cause of posttreatment

https://doi.org/10.5395/rde.2026.51.e21

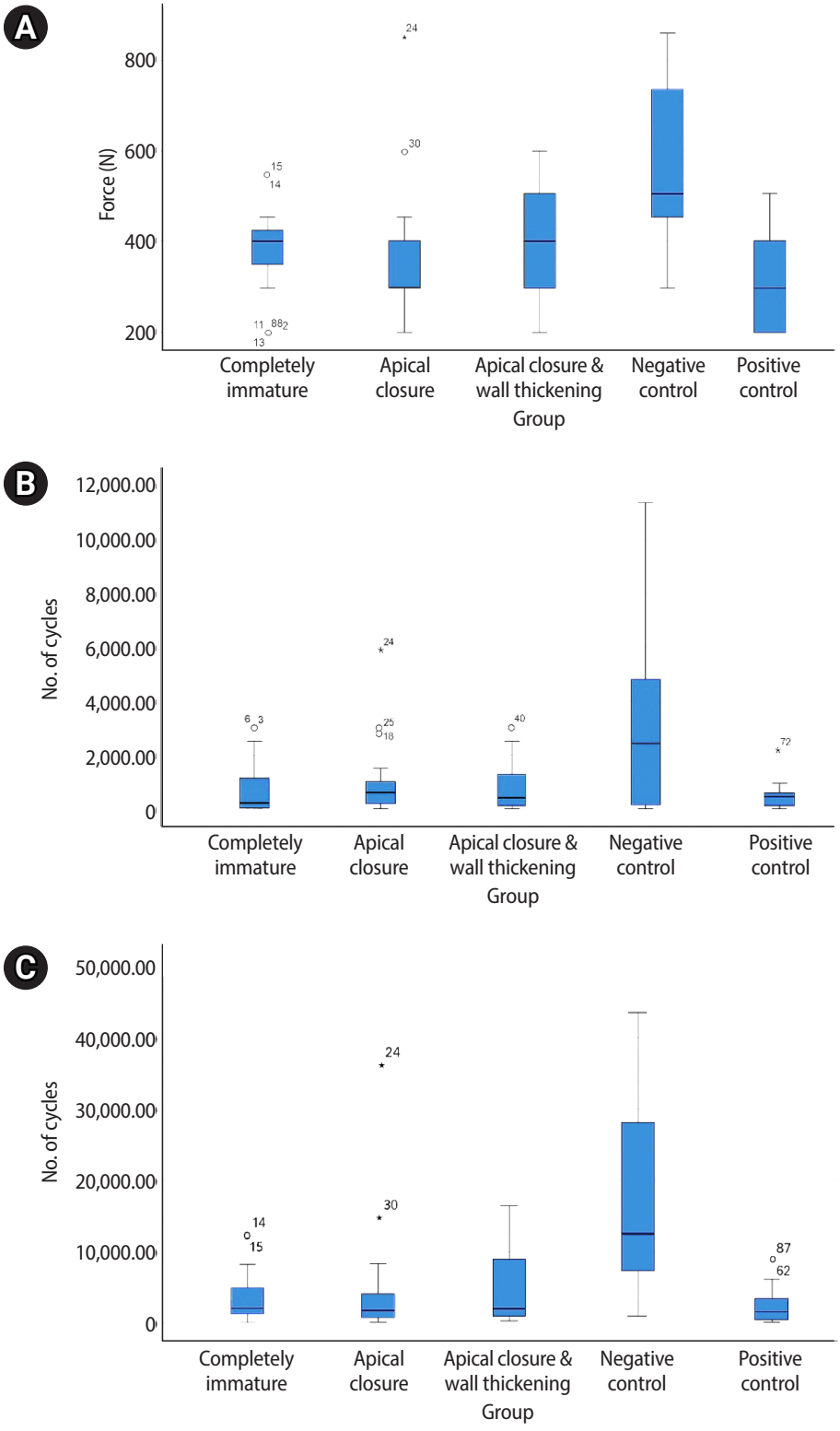

Figure 2. Boxplot representation of mechanical performance across experimental groups. Boxplots illustrate the distribution of (A) load at fracture (N), (B) cycle number to failure, and (C) number of cycles for the five experimental groups: completely immature, apical closure, apical closure with wall thickening, negative control, and positive control. The boxes represent the interquartile range (IQR), with horizontal lines indicating the median values. Whiskers denote 1.5 × IQR, and outliers are shown as individual points.

failure [26,27].

Numerous studies have investigated the fracture resistance of teeth treated with regenerative protocols using static loading tests [15,28]. However, there is no consensus in the literature on the most accurate method for assessing fracture resistance. Static loading tests often overestimate fracture resistance [29], whereas cyclic loading, which simulates oral mastication conditions, is limited by time and cost constraints. Accelerated life testing, such as step-stress testing, is commonly used to identify potential failure modes by subjecting specimens to extreme conditions. Step-stress testing involves applying a constant load for a period before increasing it until failure occurs [30]. This approach has been successfully used to generate longitudinal cracks in endodontically treated teeth, providing a realistic model for investigating the initiation, progression, contributing factors, and management of cracked teeth [19,29].

This study presents limitations related to specimen selection and laboratory conditions for cyclic load measurements [11]. Human maxillary central incisors were specifically chosen for this study as they are the type of teeth most susceptible to trauma [31]. As the use of immature teeth was not feasible, mature teeth were modified to simulate stages of root development, acknowledging the inherent differences in tissue composition [18].

Histological evaluations of teeth treated with REPs have shown the presence of intracanal ectopic bone, cementum-like tissue, disorganized fibrous connective tissue, and PDL in various combinations [26,32]. However, reproducing such biological healing patterns *in vitro* is not possible, as natural revascularization cannot be replicated under laboratory conditions. Therefore, root development was mechanically simulated to approximate these clinical scenarios. Protocols for REPs vary widely, particularly regarding the use of scaffolds [6,8]. Since blood clot formation is important for tissue regeneration [8], a foam material was used in this study to simulate a clot under controlled laboratory conditions. Its uniform structure helps standardize the coronal barrier and isolate the mechanical effect of root development. However, foam does not reproduce the complex, viscoelastic, and fibrin-based architecture of a natural blood clot [8]. Real clots exhibit non-linear, time-dependent behavior and can deform via fibrin stretching or microcrack formation, whereas foam mostly compresses uniformly and collapses under load. Additionally, natural clots can adhere to small dentinal irregularities, whereas foam cannot, a factor that may influence how stresses develop along the canal walls. Finally, blood clots change their mechanical properties over time, while foam remains static, meaning it cannot fully mimic the dynamic nature of clot maturation [33,34].

Including a biomaterial control group could potentially enhance external validity; however, the primary objective of this study was to isolate and examine the influence of simulated root development rather than compare materials. Teeth and restorations are naturally exposed to complex oral conditions, including humidity, temperature, pH, and biofilm activity, which contribute to failures [29,35]. In this setup, only humidity was controlled using a wet gauze; incorporating additional variables would enhance realism but add complexity and cost.

In vitro PDL simulation remains non-standardized, with variability in materials, application techniques, and layer thickness. No studies have demonstrated a consistent viscoelastic layer capable of producing standardized, clinically relevant tooth mobility during testing [36]. Heintze *et al.* [37] further questioned the use of artificial periodontium, citing their observation of high variability in silicone layer thickness (300–700 μm), which compromises standardization and leads to uncontrolled tooth mobility under loading. In the present experiment, the use of Erkoskin mitigated these issues. The material can be applied uniformly as a varnish, forming a homogeneous and adherent layer around the tooth root. This root–PDL simulation complex acted as a monoblock, which was then embedded in acrylic resin. This ensured stable fixation without risk of tooth dislocation during testing. This simple and practical approach, however, remains a methodological limitation, as the material's biomechanical and biological properties require further validation [36].

The experimental conditions in this study were standardized to match those of previous studies. This included the applied load, the number of loading cycles, test geometries, and instrumentation [19]. However, fracture resistance testing can be influenced by various

https://doi.org/10.5395/rde.2026.51.e21

factors such as the type of loading device, antagonist material, crosshead speed, tooth embedding technique, and angle of force application [38,39]. While masticatory forces vary in direction and intensity, a single 45° oblique force was applied to simulate a typical occlusal function [11,24]. Though anatomically shaped metallic antagonists may provide more clinically relevant results, [39] their high cost and complexity of fabrication make them impractical. In this study, a 2-mm-diameter stainless steel sphere was employed as the loading applicator [35]. Though the range of normal chewing force has been estimated from 50 to 190 N in the frontal area and 300 to 800 N in the molar area, the initial load used in this study was set at 200 N, representing a subcritical force that exceeds normal masticatory loads but remains below the threshold for catastrophic fracture [19,29]. This load level was selected to promote accelerated initiation of microcracks while maintaining a clinically relevant loading condition and an efficient testing duration.

The large standard deviations and high variability observed in this study, with coefficients of variation exceeding 100% in some groups, likely reflect specimen heterogeneity. Despite careful selection, extracted human teeth naturally differ in root morphology, canal anatomy, dentinal thickness, and mineral content. Such variability, along with slight differences in simulated maturation stages, may have affected stress distribution and fatigue behavior during cyclic loading. Additionally, Step-stress fatigue testing is inherently probabilistic, as crack initiation and propagation depend on specimen-specific microscopic flaws. Consequently, wide dispersion in cycles-to-failure and fracture load values is expected. The variability observed thus reflects intrinsic limitations in specimen standardization and may have reduced statistical power to detect subtle intergroup differences. In this study, caliper/radiographic measurements were used to reduce morphological variability; however, the use of micro-computed tomography for full three-dimensional (3D) assessment of canal geometry would provide even more precise matching and is a recommended approach for future studies.

Utilizing 3D-printed standardized samples may further reduce geometric variability and improve reproducibility. Studies should also investigate novel materials to reinforce the cervical area and prevent root fractures. Additionally, incorporating oral environment factors—such as biofilm exposure during cyclic loading—would enhance experimental relevance, as such conditions have been shown to significantly reduce the fatigue resistance of coronal dentine [40].

CONCLUSIONS

Within the limitations of the present *in vitro* study, the findings suggest that the stage of root development following REPs does not significantly influence the mechanical reinforcement of immature teeth. Nonetheless, given that this investigation was performed under controlled laboratory conditions, direct extrapolation of these findings to clinical scenarios should be undertaken with caution.

CONFLICT OF INTEREST

No potential conflict of interest relevant to this article was reported.

FUNDING/SUPPORT

The authors have no financial relationships relevant to this article to disclose.

AUTHOR CONTRIBUTIONS

Conceptualization, Methodology: Gogos C, Kodonas K, Polydora KA. Data curation, Supervision: Gogos C, Kodonas K. Formal analysis, Investigation: all authors. Funding acquisition, Project administration: Gogos C, Kodonas K. Software: Gogos C, Fardi A. Writing-original draft: all authors. Writing-review & editing: all authors. All authors read and approved the final manuscript.

DATA SHARING STATEMENT

The datasets are not publicly available but can be obtained from the corresponding author upon reasonable request.

SUPPLEMENTARY MATERIALS

Supplementary Table 1. Loading amplitudes and corresponding numbers of cycles for the accelerated fatigue test.

REFERENCES

1. Cvek M. Prognosis of luxated non-vital maxillary incisors treated with calcium hydroxide and filled with gutta-percha: a retrospective clinical study. Endod Dent Traumatol 1992;8:45-55.

2. Cetinkaya A, Ayrancı LB. Evaluation of stress distribution by applied different forces on immature maxillary central teeth with different treatment options: a laboratory finite element stress analysis. BMC Oral Health 2025;25:3.
3. Andreasen FM, Andreasen JO, Bayer T. Prognosis of root-fractured permanent incisors: prediction of healing modalities. Endod Dent Traumatol 1989;5:11-22.
4. Araújo PR, Silva LB, Neto AP, Almeida de Arruda JA, Álvares PR, Sobral AP, *et al*. Pulp revascularization: a literature review. Open Dent J 2017;10:48-56.
5. Parirokh M, Torabinejad M. Mineral trioxide aggregate: a comprehensive literature review: part III: clinical applications, drawbacks, and mechanism of action. J Endod 2010;36:400-413.
6. Panda P, Mishra L, Govind S, Panda S, Lapinska B. Clinical outcome and comparison of regenerative and apexification intervention in young immature necrotic teeth: a systematic review and meta-analysis. J Clin Med 2022;11:3909.
7. Huang GT. Apexification: the beginning of its end. Int Endod J 2009;42:855-866.
8. Wei X, Yang M, Yue L, Huang D, Zhou X, Wang X, *et al*. Expert consensus on regenerative endodontic procedures. Int J Oral Sci 2022;14:55.
9. Priya B L, Singh N, Mangalam KK, Sachdev R, P A, Jain HN, *et al*. Success and complication rates of revascularization procedures for immature necrotic teeth: a systematic review. Cureus 2023;15:e51364.
10. Nagendrababu V, Murray PE, Ordinola-Zapata R, Peters OA, Rôças IN, Siqueira JF, *et al*. PRILE 2021 guidelines for reporting laboratory studies in Endodontology: explanation and elaboration. Int Endod J 2021;54:1491-1515.
11. Mello I, Michaud PL, Butt Z. Fracture resistance of immature teeth submitted to different endodontic procedures and restorative protocols. J Endod 2020;46:1465-1469.
12. Gunal E, Bezgin T, Ocak M, Bilecenoglu B. Effects of various thicknesses and levels of mineral trioxide aggregate coronal plugs on nanoleakage and fracture resistance in revascularization: an in vitro study. Aust Endod J 2021;47:608-615.
13. Mello I, Michaud PL, Tanner N. Resistance to fracture of extracted teeth used for pre-clinical endodontic procedures: influence of storage conditions. Eur J Dent Educ 2020;24:272-275.
14. Cvek M, Andreasen JO, Borum MK. Healing of 208 intra-alveolar root fractures in patients aged 7-17 years. Dent Traumatol 2001;17:53-62.
15. Jamshidi D, Homayouni H, Moradi Majd N, Shahabi S, Arvin A, Ranjbar Omidi B. Impact and fracture strength of simulated immature teeth treated with mineral trioxide aggregate apical plug and fiber post versus revascularization. J Endod 2018;44:1878-1882.
16. Elnaghy AM, Elsaka SE. Fracture resistance of simulated immature teeth filled with Biodentine and white mineral trioxide aggregate: an in vitro study. Dent Traumatol 2016;32:116-120.
17. Galler KM, Krastl G, Simon S, Van Gorp G, Meschi N, Vahedi B, *et al*. European Society of Endodontology position statement: revitalization procedures. Int Endod J 2016;49:717-723.
18. Tanalp J, Dikbas I, Malkondu O, Ersev H, Güngör T, Bayırlı G. Comparison of the fracture resistance of simulated immature permanent teeth using various canal filling materials and fiber posts. Dent Traumatol 2012;28:457-464.
19. Lin F, Ordinola-Zapata R, Xu H, Heo YC, Fok A. Laboratory simulation of longitudinally cracked teeth using the step-stress cyclic loading method. Int Endod J 2021;54:1638-1646.
20. Li XL, Fan W, Fan B. Dental pulp regeneration strategies: a review of status quo and recent advances. Bioact Mater 2024;38:258-275.
21. American Association of Endodontists (AAE). Clinical considerations for a regenerative procedure: revised 2021 [Internet]. Chicago, IL: AAE; 2021 [cited 2025 Aug 22]. Available from: https://www.aae.org/specialty/wp-content/uploads/sites/2/2021/08/ClinicalConsiderationsApprovedByREC062921.pdf
22. Lenzi R, Trope M. Revitalization procedures in two traumatized incisors with different biological outcomes. J Endod 2012;38:411-414.
23. Nagy MM, Tawfik HE, Hashem AA, Abu-Seida AM. Regenerative potential of immature permanent teeth with necrotic pulps after different regenerative protocols. J Endod 2014;40:192-198.
24. Ali MR, Mustafa M, Bårdsen A, Bletsa A. Fracture resistance of simulated immature teeth treated with a regenerative endodontic protocol. Acta Biomater Odontol Scand 2019;5:30-37.
25. Sharma B, Chalamalasetty N. Modern concepts in endodontic access preparation: a review. Int J Dent Med Sci Res 2024;6:591-594.
26. Becerra P, Ricucci D, Loghin S, Gibbs JL, Lin LM. Histologic study of a human immature permanent premolar with

https://doi.org/10.5395/rde.2026.51.e21

chronic apical abscess after revascularization/revitalization. J Endod 2014;40:133-139.
27. Shimizu E, Ricucci D, Albert J, Alobaid AS, Gibbs JL, Huang GT, *et al*. Clinical, radiographic, and histological observation of a human immature permanent tooth with chronic apical abscess after revitalization treatment. J Endod 2013;39:1078-1083.
28. Crozet A, Aubeux D, Pérez F, Gaudin A. Fracture resistance of simulated immature maxillary anterior teeth restored with various canal filling materials, with micro-posts or with a fiber post. Dent Mater J 2023;42:368-374.
29. Ordinola-Zapata R, Fok AS. Research that matters: debunking the myth of the "fracture resistance" of root filled teeth. Int Endod J 2021;54:297-300.
30. Jerman E, Lümkemann N, Eichberger M, Hampe R, Stawarczyk B. Impact of varying step-stress protocols on the fatigue behavior of 3Y-TZP, 4Y-TZP and 5Y-TZP ceramic. Dent Mater 2021;37:1073-1082.
31. Lam R. Epidemiology and outcomes of traumatic dental injuries: a review of the literature. Aust Dent J 2016;61 Suppl 1:4-20.
32. Martin G, Ricucci D, Gibbs JL, Lin LM. Histological findings of revascularized/revitalized immature permanent molar with apical periodontitis using platelet-rich plasma. J Endod 2013;39:138-144.
33. Liu D, Nguyen N, Bui TQ, Pocivavsek L. A theoretical framework for multi-physics modeling of poro-visco-hyperelasticity-induced time-dependent fracture of blood clots. J Mech Phys Solids 2025;194:105913.
34. Mane JV, Chandra S, Sharma S, Ali H, Chavan VM, Manjunath BS, *et al*. Mechanical property evaluation of polyurethane foam under quasi-static and dynamic strain rates: an experimental study. Procedia Eng 2017;173:726-731.
35. Lima VP, Machado JB, Zhang Y, Loomans BA, Moraes RR. Laboratory methods to simulate the mechanical degradation of resin composite restorations. Dent Mater 2022;38:214-229.
36. AlZahrani F, Richards L. Micro-CT evaluation of a novel periodontal ligament simulation technique for dental experimental models. Arch Orofac Sci 2018;13:93-103.
37. Heintze SD, Monreal D, Reinhardt M, Eser A, Peschke A, Reinshagen J, *et al*. Fatigue resistance of all-ceramic fixed partial dentures: fatigue tests and finite element analysis. Dent Mater 2018;34:494-507.
38. de Abreu RA, Pereira MD, Furtado F, Prado GP, Mestriner W, Ferreira LM. Masticatory efficiency and bite force in individuals with normal occlusion. Arch Oral Biol 2014;59:1065-1074.
39. Silva GR, Silva NR, Soares PV, Costa AR, Fernandes-Neto AJ, Soares CJ. Influence of different load application devices on fracture resistance of restored premolars. Braz Dent J 2012;23:484-489.
40. Orrego S, Melo MA, Lee SH, Xu HH, Arola DD. Fatigue of human dentin by cyclic loading and during oral biofilm challenge. J Biomed Mater Res B Appl Biomater 2017;105:1978-1985.

RDE Restorative Dentistry & Endodontics

Research Article

eISSN 2234-7666
Restor Dent Endod. 2026 May;51(2):e22
https://doi.org/10.5395/rde.2026.51.e22

Interplay of hypoxia, angiogenesis, and macrophages in pulp and periapical lesions: an immunohistochemical cross-sectional study

Puja Chatterjee[1], **Mala Kamboj**[1,*], **Shweta Mittal**[2], **Anjali Narwal**[1], **Anju Devi**[1]

[1]Department of Oral and Maxillofacial Pathology and Microbiology, Post Graduate Institute of Dental Sciences, Pt B.D. Sharma University of Health Sciences, Rohtak, India
[2]Department of Conservative Dentistry and Endodontics, Post Graduate Institute of Dental Sciences, Pt B.D. Sharma University of Health Sciences, Rohtak, India

ABSTRACT

Objectives: This study evaluated and correlated the immune expression of hypoxia and angiogenesis with macrophages in periapical granuloma (PG), radicular cyst (RC), and healthy pulp (HP).

Methods: An observational study was performed on 51 tissue blocks equally divided among the groups, stained immunohistochemically for hypoxia-inducible factor (HIF)-1α, vascular endothelial growth factor (VEGF), and CD68, and the mean expression was calculated. Data were analyzed using Kruskal-Wallis, Mann-Whitney, Spearman correlation tests ($p < 0.001$), and multiple linear regression analysis ($p \leq 0.05$).

Results: HIF-1α expression was highest in PG than RC and HP ($p < 0.001$). Significant differences were found between HP, PG, and RC (both $p < 0.001$). VEGF expression was highest in RC than in PG and HP ($p < 0.001$), with significant differences between HP and both PG and RC ($p < 0.001$); pairwise comparisons were significant between all groups ($p < 0.001$, $p < 0.001$, $p = 0.018$). Correlation analysis showed significant correlations between VEGF and CD68 in HP and PG ($p = 0.007$ and $p = 0.028$, respectively). Linear regression showed that study groups were significantly associated with mean scores of HIF-1α, VEGF, and CD68 ($p = 0.002$, $p = 0.001$, $p < 0.001$).

Conclusions: HIF-1α, VEGF, and CD68 showed increased expression in PGs and RCs, suggesting an association between hypoxic conditions, enhanced angiogenic activity, and macrophage presence within the periapical inflammatory microenvironment. Future studies exploring HIF-1α and VEGF inhibitors as potential treatment modalities for periapical lesions are warranted.

Keywords: Hypoxia-inducible factor 1α; Macrophages; Periapical granuloma; Radicular cyst; Vascular endothelial growth factor

Received: June 21, 2025 **Revised:** December 18, 2025 **Accepted:** January 13, 2026

Citation
Chatterjee P, Kamboj M, Mittal S, Narwal A, Devi A. Interplay of hypoxia, angiogenesis, and macrophages in pulp and periapical lesions: an immunohistochemical cross-sectional study. Restor Dent Endod 2026;51(2):e22.

***Correspondence to**
Mala Kamboj, MDS, MAMS, MNASc
Department of Oral and Maxillofacial Pathology and Microbiology, Post Graduate Institute of Dental Sciences, Pt B.D. Sharma University of Health Sciences, Rohtak 124001, Haryana, India
Email: malskam@gmail.com

INTRODUCTION

The dental pulp is a highly vascularized and innervated connective tissue located within the pulp chamber, which plays a vital role in dentin formation and tooth vitality [1]. Periapical lesions such as periapical abscess, periapical granuloma (PG), and radicular cyst (RC) arise from pulpal diseases due to untreated caries, trauma, or infection. Bacterial toxins, tissue debris, and immune responses contribute to inflammation, tissue damage, and bone destruction around the root apex [2]. Angiogenesis, epithelial cell proliferation, and autophagy are induced by ischemic hypoxia and nutrient depletion in the central areas of inflamed periapical lesions, leading to cyst formation and progression [3].

Ischemic hypoxia is a condition characterized by reduced blood flow and insufficient oxygen supply to a tissue or organ, leading to cellular oxygen deprivation. In periapical lesions, ischemic hypoxia develops primarily due to infection-induced inflammation. The inflammatory process leads to swelling, increased interstitial pressure, and compression of local blood vessels, which collectively diminish perfusion. As inflammation exacerbates, vascular congestion and impaired microcirculation further limit oxygen delivery, contributing to tissue damage and necrosis, ultimately forming an abscess [3].

At the cellular level, hypoxia triggers a cascade of molecular events. Hypoxia-inducible factor 1 (HIF-1) acts as a central regulator of cellular adaptation to decreased oxygen availability. It consists of two subunits—HIF-1α, which is oxygen-sensitive, and HIF-1β, which is constitutively expressed. Under normoxic conditions, HIF-1α is rapidly degraded; however, under hypoxic conditions, HIF-1α stabilizes and accumulates. This stabilization initiates transcription of multiple genes involved in angiogenesis, cell survival, metabolism, and inflammation [4].

HIF-1α induces several proangiogenic molecules, including vascular endothelial growth factor (VEGF), basic fibroblast growth factor, platelet-derived growth factor-B, and angiopoietins 1 and 2, which collectively promote new blood vessel formation to restore oxygen supply [4]. In addition to angiogenesis, hypoxia and inflammation can stimulate autophagy, an essential cytoprotective mechanism enabling cells to degrade damaged components and recycle energy substrates. Autophagy interacts closely with inflammatory pathways and may contribute to the survival and persistence of cells within hypoxic regions of periapical lesions [3].

Angiogenesis (neovascularization) and vasculogenesis are mediated by signaling proteins such as VEGF. It is a critical factor in promoting new vessel formation and vascular permeability, which helps in wound healing [5,6]. VEGF has several isoforms that exert biological activity via specific tyrosine kinase receptors. The presence of VEGF in periapical lesions indicates the potential for healing and repair of affected tissues. VEGF is also said to attract and activate macrophages, which release cytokines and growth factors that promote angiogenesis [5].

Macrophages play a pivotal role in the pathogenesis of periapical lesions by regulating immune responses and mediating tissue destruction and repair. In response to bacterial invasion from necrotic pulp, they infiltrate periapical tissues and exhibit phenotypic plasticity, transitioning between pro-inflammatory (M1) and anti-inflammatory (M2) states [7]. M1 macrophages arise primarily through classical pathway activation and produce cytokines such as interleukin (IL)-1, IL-6, and tumor necrosis factor alpha (TNF-α), as well as reactive oxygen and nitrogen intermediates. These mediators create a microbicidal environment, support Th1 immune responses, and contribute to sustained inflammation [7,8]. In contrast, M2 macrophages, associated with alternative pathway activation, secrete immunosuppressive cytokines such as IL-10, IL-13, and growth factors like transforming growth factor beta, facilitating immunomodulation, tissue remodeling, angiogenesis, and repair [7,8].

This dynamic M1–M2 balance influences lesion progression and healing potential, making macrophage polarization a relevant therapeutic target. Immunohistochemical studies frequently use CD68 as a general macrophage marker; however, because CD68 identifies both phenotypes, additional polarization-specific markers are essential to distinguish M1 and M2 populations in periapical lesions [8].

Therefore, whether a hypoxic environment enhances angiogenesis and attenuates macrophage activity remains to be determined. To date, no study has evaluated

https://doi.org/10.5395/rde.2026.51.e22

the combined effect of these three parameters in pulp and periapical lesions. The present study was conceived to detect the expression of hypoxia, angiogenesis, and immunogenic potential using immunohistochemical expression of HIF-1α, VEGF, and CD68 in healthy pulp (HP) tissue, PG, and RC. Their correlation, if any, would shed insight into the pathological mechanism and help to establish strategies to improve the success rate of the treatment of pulp and periapical diseases.

METHODS

The present observational cross-sectional study was carried out following approval from the Biomedical Health and Research Committee (approval No. PGIDS/BHRC/23/36). It was conducted in compliance with the ethical principles outlined in the 10th version of the Declaration of Helsinki (October 2013, accessible at www.wma.net). Additionally, this observational study has been written according to the STROBE (STrengthening the Reporting of OBservational studies in Epidemiology) guidelines.

Study design and tissue samples

The study included a descriptive analysis of the immunohistochemical expression of HIF-1α, VEGF, and CD68 in 51 formalin-fixed, paraffin-embedded tissue sections comprising 17 cases each of HP, PG, and RC, obtained from prospective biopsy specimens received from May 2022 to May 2023. The criteria to include and exclude cases that determined the eligibility for participation in this study are outlined in Figure 1. Patient data, including age and sex, were obtained from biopsy records. Pathological diagnoses were confirmed based on clinical, radiographic, and histological criteria. HP tissue was obtained from extracted teeth that were free of caries and apical periodontitis, including those extracted for surgical indications such as third-molar removal.

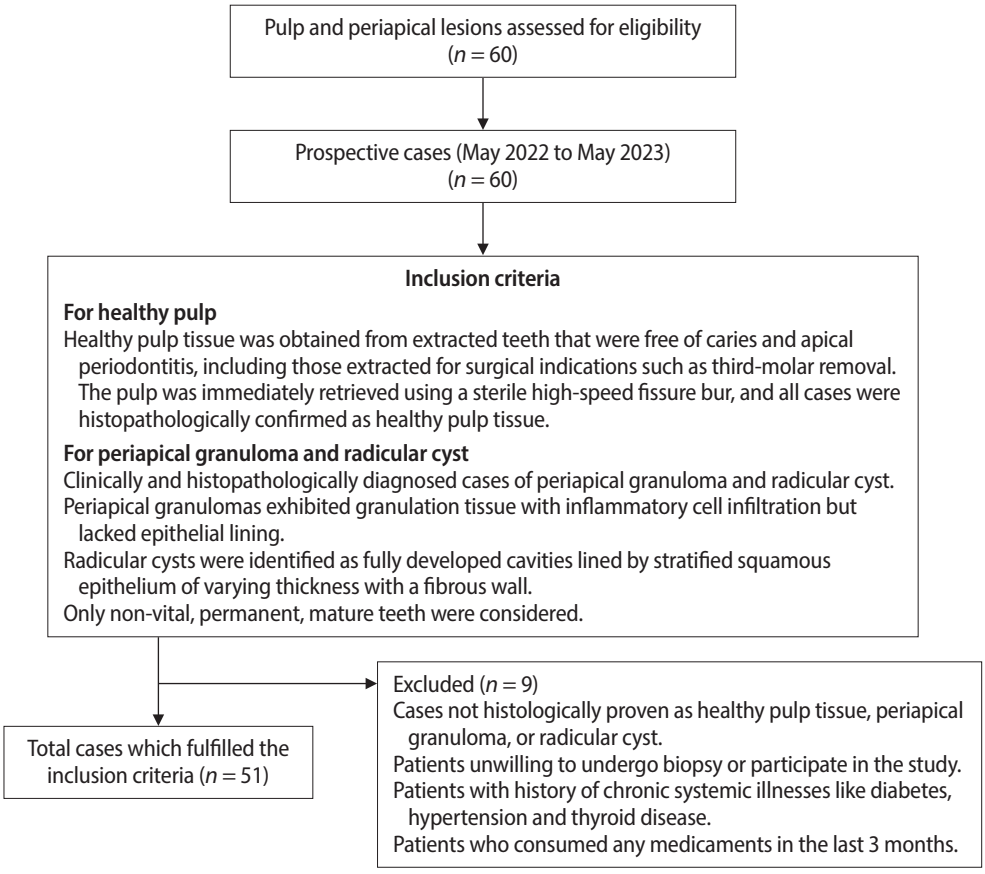

Figure 1. Flow chart depicting the inclusion and exclusion criteria of cases for participation eligibility.

The pulp was immediately retrieved using a sterile high-speed fissure bur, and all cases were histopathologically confirmed as HP tissue. The study included human permanent, mature teeth from all quadrants. All selected specimens were periapical radiolucent lesions of varying sizes associated with non-vital pulp (Figure 2). PG consisted of granulomatous tissue with inflammatory cell infiltration, lacking an epithelial lining. RC was identified as fully developed cavities lined by stratified squamous epithelium of varying thickness with a fibrous wall [8].

Study size

Keeping an effect size of 0.7, an alpha level of 5%, and 90% power of the study using G*Power ver. 3.1 (Heinrich Heine University Düsseldorf, Düsseldorf, Germany), a sample of 14 in each group was calculated [9]. However, keeping in mind the exhaustion of tissues in paraffin blocks or stain failure, 17 cases per group were recruited.

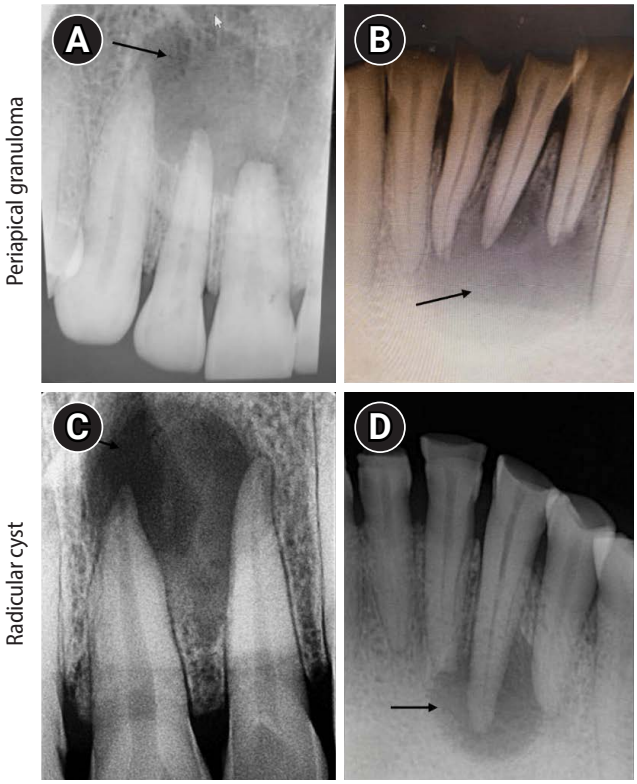

Figure 2. Intraoral periapical radiograph (IOPA) of periapical lesions. (A, B) IOPA of periapical granuloma cases showing well-defined radiolucency with respect to the maxillary right lateral incisor and mandibular right lateral incisor (arrows). (C, D) IOPA of radicular cyst cases showing well-defined radiolucency associated with the root apices of the maxillary left central incisor and mandibular right canine (arrows).

Hematoxylin and eosin staining

All samples underwent macroscopic examination and were appropriately grossed to allow a comprehensive histological analysis of periapical lesions. Tissue sections, 4 μm thick, were prepared from formalin-fixed, paraffin-embedded blocks of HP, PG, and RC. These sections were mounted on glass slides, stained with hematoxylin and eosin, and examined under light microscopy (A, B, and C panels of Figures 3–5). Histopathological evaluation focused on characteristic features such as the epithelial lining, inflammatory cell infiltrate, and connective tissue organization, which formed the basis for the definitive diagnosis of RC, PG, or HP. The histopathologic diagnosis was performed by experienced oral pathologists.

Immunohistochemistry

For immunohistochemical staining, 4-μm-thick tissue sections were obtained from formalin-fixed, paraffin-embedded tissue blocks and mounted on poly-lysine-coated glass slides. Three sections were deparaffinized, rehydrated through a graded alcohol series, and then hydrated with deionized water. Antigen retrieval was performed using Tris-EDTA (pH 9) in a pressure cooker. Sections were then incubated separately for 1 hour at room temperature in a humidified chamber with primary antibodies: monoclonal rabbit anti-human HIF-1α antibody (clone EP118; BioGenex, Fremont, CA, USA; ready-to-use), monoclonal rabbit anti-human VEGF antibody (clone ZR389; ZETA Corporation, Sierra Madre, CA, USA; ready-to-use) and monoclonal mouse anti-human CD68 antibody (clone PG-M1; Diagnostic Biosystems, Pleasanton, CA, USA; ready-to-use). To facilitate primary antibody binding, sections were treated with a supersensitive one-step polymer horseradish peroxidase kit (Biogenex) for 30 minutes following two washes with phosphate-buffered saline.

Peroxidase activity was visualized by immersing sections in diaminobenzidine (HK124-5K; Biogenex) chro-

https://doi.org/10.5395/rde.2026.51.e22

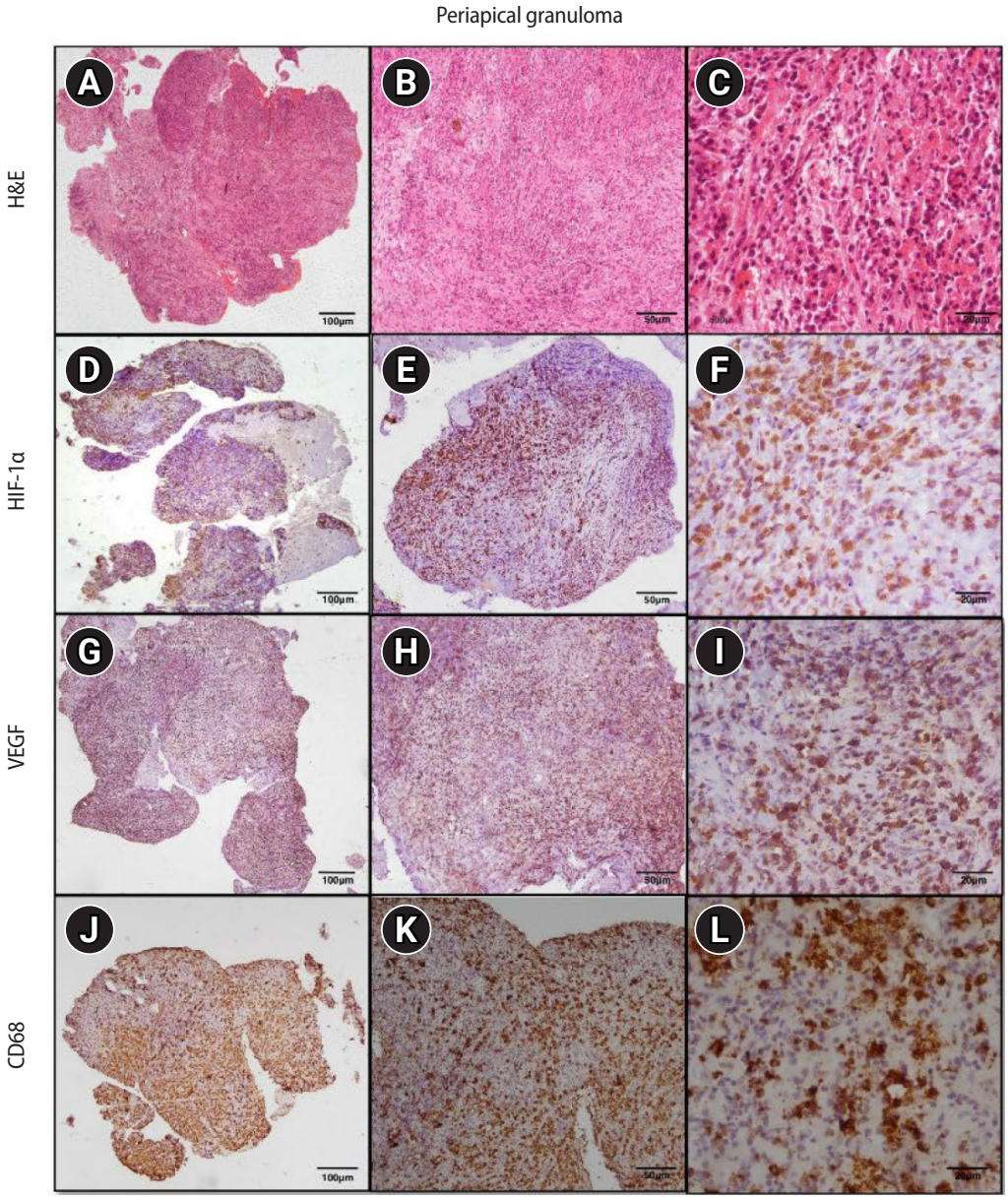

Figure 3. Hematoxylin and eosin (H&E) and immunoexpression of hypoxia-inducible factor 1 alpha (HIF-1α), vascular endothelial growth factor (VEGF), and CD68 in periapical granuloma. (A–C) Periapical granuloma showing fibrocellular connective tissue stroma infiltrated by intense macrophage-rich inflammatory infiltrate. (D–F) Diffuse immunoexpression of HIF-1α in inflammatory cells, endothelial cells, and fibroblasts of periapical granuloma. (G–I) Diffuse immunoexpression of VEGF in blood vessels, inflammatory infiltrate, and stromal cells (fibroblasts) of periapical granuloma. (J–L) Immunoexpression of CD68 in lysosomal granules and the surface of macrophages of periapical granuloma. A–C: H&E staining. D–F: immunohistochemistry (IHC), anti-HIF-1α. G–I: IHC, anti-VEGF. J–L: IHC, anti-CD68. Images were obtained at ×40, ×100, and ×400 magnifications (scale bars: 100, 50, and 20 μm, respectively).

mogen for 10 minutes at room temperature, producing a brown reaction product. The sections were counterstained with Mayer's hematoxylin and cover-slipped. Positive controls included breast carcinoma sections for anti-HIF-1α and VEGF and tonsil sections for anti-CD68. Negative controls consisted of sections where the primary antibody was omitted and replaced with phosphate-buffered saline.

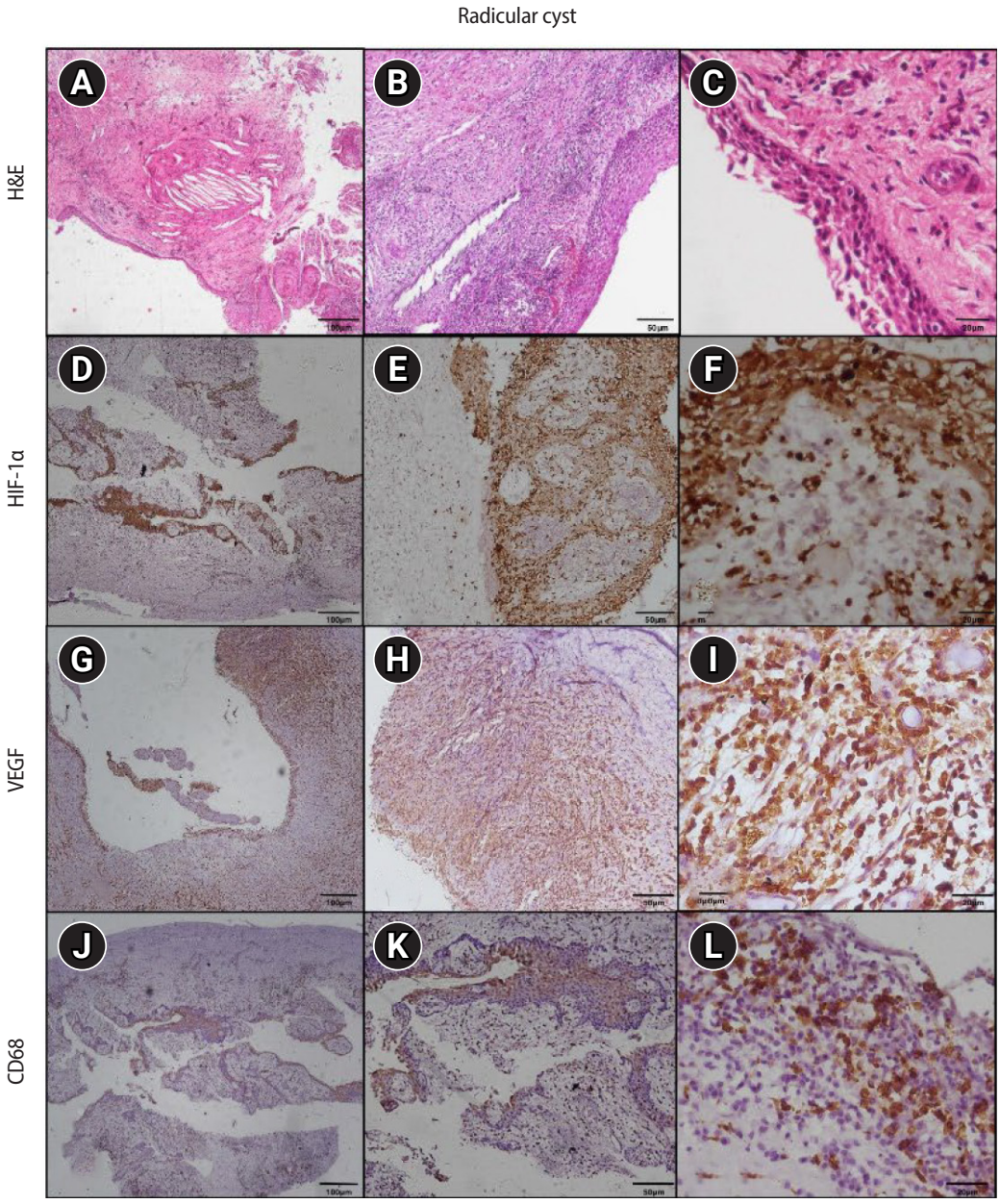

Figure 4. Hematoxylin and eosin (H&E) and immunoexpression of hypoxia-inducible factor 1 alpha (HIF-1α), vascular endothelial growth factor (VEGF), and CD68 in radicular cyst. (A–C) Radicular cyst showing hyperplastic stratified squamous epithelium with an arcading pattern and supporting connective tissue capsule. (D–F) Diffuse immunoexpression of HIF-1α in inflammatory cells, connective tissue, and epithelial lining of radicular cyst. (G–I) Diffuse immunoexpression of VEGF in blood vessels, inflammatory infiltrate, stromal cells (fibroblasts), and epithelial lining of radicular cyst. (J–L) Immunoexpression of CD68 in lysosomal granules and the surface of macrophages of radicular cyst. A–C: H&E staining. D–F: immunohistochemistry (IHC), anti-HIF-1α. G–I: IHC, anti-VEGF. J–L: IHC, anti-CD68. Images were obtained at ×40, ×100, and ×400 magnifications (scale bars: 100, 50, and 20 μm, respectively).

Quantification of immunohistochemistry slides

Immunohistochemical analysis was performed by two independent oral and maxillofacial pathologists (PC and MK). The slides were evaluated under a brightfield research microscope. Photomicrographs were captured using a DS-Fi3 digital camera (Nikon, Tokyo, Japan) and

https://doi.org/10.5395/rde.2026.51.e22

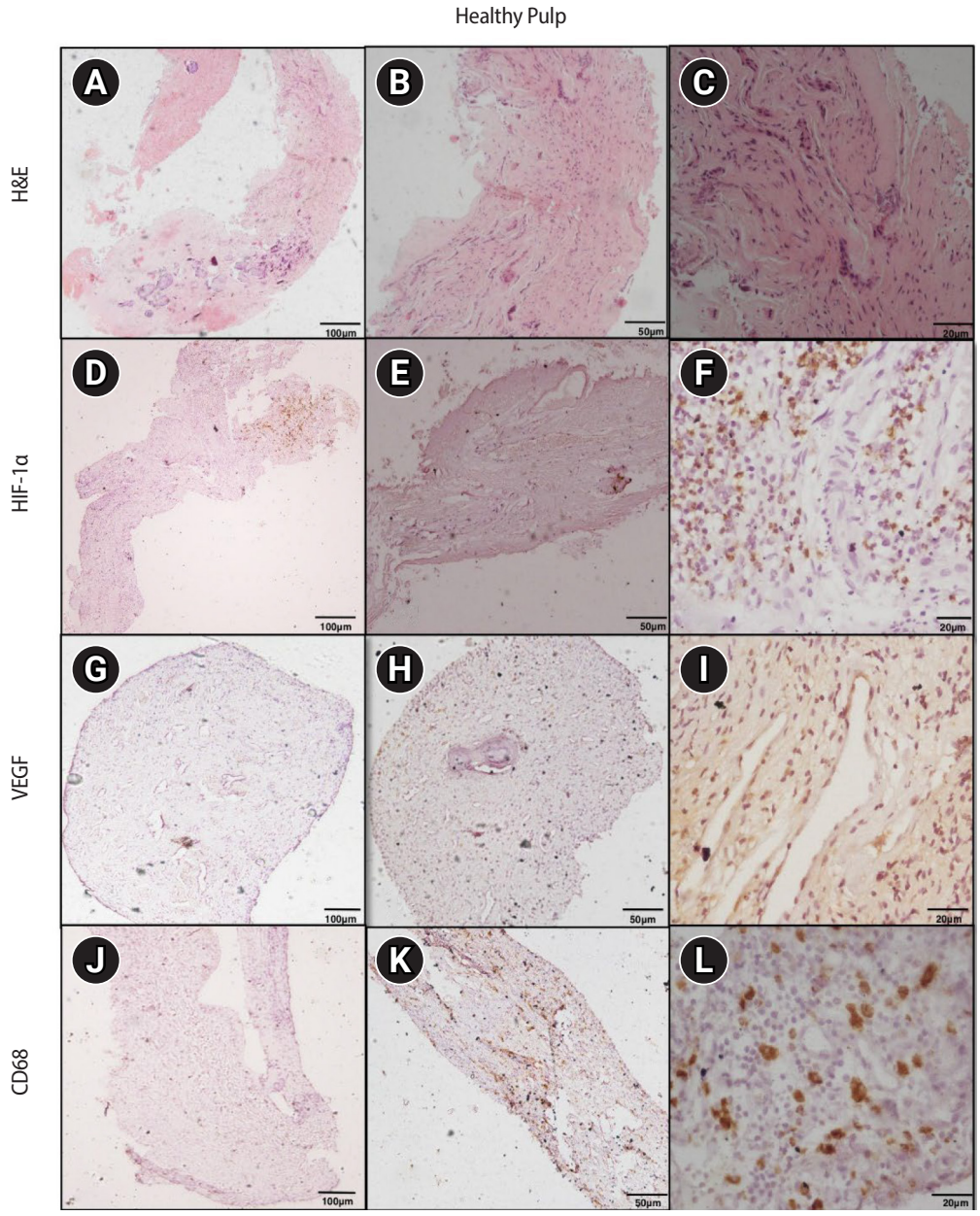

Figure 5. Hematoxylin and eosin (H&E) and immunoexpression of hypoxia-inducible factor 1 alpha (HIF-1α), vascular endothelial growth factor (VEGF), and CD68 in healthy pulp. (A–C) Healthy pulp showing connective tissue stroma with fibroblasts and vascular channels. (D–F) Diffuse immunoexpression of HIF-1α in fibroblasts and endothelial cells. (G–I) Diffuse immunoexpression of VEGF in blood vessels and stromal cells (fibroblasts) of healthy pulp. (J–L) Immunoexpression of CD68 in lysosomal granules and surface of macrophages of healthy pulp. A–C: H&E staining. D–F: immunohistochemistry (IHC), anti-HIF-1α. G–I: IHC, anti-VEGF. J–L: IHC, anti-CD68. Images were obtained at ×40, ×100, and ×400 magnifications (scale bars: 100, 50, and 20 μm, respectively).

analyzed using NIS-Elements imaging software (Nikon) to assess primary antibody expression.

1. Quantification of hypoxia using hypoxia-inducible factor-1α

To evaluate the expression of HIF-1α, the stained

slides were examined under various magnifications (40×, 100×, and 400×) to identify the pattern of positive staining under the microscope. For quantification, six random fields from each immunostained section were selected at 400× magnification. The percentage of positive IHC staining (P) was categorized as follows: 0 (0%–4%), 1 (5%–24%), 2 (25%–49%), 3 (50%–74%), and 4 (75%–100%). The intensity of staining (I) was scored as 0 for no staining, 1 for weak staining (light yellow), 2 for moderate staining (brown), and 3 for strong staining (dark brown). The total score (S) for each section was then calculated as P × I, following the method described by Huang *et al*. [3].

2. Quantification of angiogenesis using vascular endothelial growth factor

VEGF immunohistochemical expression was assessed in the connective tissue of PG, RC, and HP, as well as in the epithelial lining of RC. In the connective tissue, a quantitative evaluation of immunopositive cells, regardless of staining intensity, was conducted following the method by Freitas *et al*. [10]. Tissue sections were examined under light microscopy at 100× magnification to identify five fields with the highest number of immunostained cells. At 400× magnification, immunopositive cells were counted in each field. Cell counts were expressed as the mean number of positive cells in these areas obtained for each sample [6]. The VEGF immunoexpression in the epithelial lining of RCs was evaluated semi-quantitatively using 100× magnification. Based on an adaptation of the method by Leonardi *et al*. [11], epithelial VEGF immunoexpression was classified as follows: no staining in 10% of cells; weak staining in 11%–25% of cells; moderate staining in 26%–75% of cells; and strong staining in more than 76% of cells [6].

3. Quantification of macrophages using CD68

For the quantification of macrophages, CD68 monoclonal antibody staining was performed to confirm the nature of macrophages. For the CD68 antibody, five representative and random fields were selected after identifying the highest immunoreactivity areas at a 100-μm scale. CD68+ cell counts were performed at 400×, and the positivity index (PI) was adopted based on a previously described method [7]. Data were reported as the percentage of positive cells presenting brownish cytoplasmic staining in each sample. The PI was calculated by applying the formula (PI) = (number of immunopositive cells) / (number of counted cells) × 100 [7].

4. Assessment of interobserver agreement

To ensure scoring reliability, two independent oral and maxillofacial pathologists (PC and MK) evaluated all immunostained slides. Interobserver agreement was assessed using Cohen's kappa statistic, which demonstrated excellent reliability across markers—HIF-1α ($\kappa = 0.92$), VEGF ($\kappa = 0.94$), and CD68 ($\kappa = 0.91$)—with all values falling within a 95% confidence interval.

Statistical analysis

Data were analyzed for descriptive statistics and imported into the IBM SPSS ver. 21.0 for Windows (IBM Corp, Armonk, NY, USA) for inferential analysis. The Shapiro-Wilk test for normality indicated a non-normal distribution. Therefore, the nonparametric Kruskal-Wallis H-test was applied to compare the means between the three groups. The Mann-Whitney U-test was used as a *post hoc* test to assess statistical differences between the two groups. Spearman's rho was used to evaluate the relationship among the three parameters within the same group. A p-value of >0.05 was considered nonsignificant, and $p < 0.05$ was considered statistically significant. Multiple linear regression was used to assess the effects of independent variables (age, sex, site, and study groups [HP, PG, and RC]) on the mean scores of HIF-1α, VEGF, and CD68 as dependent variables.

RESULTS

Demographic details of study groups

A total of 30 males and 21 females participated in the study. PG, RC, and HP comprised 13 males (76.5%), four females (23.5%); seven males (41.2%), 10 females (58.8%); and 10 males (58.8%), seven females (41.2%), respectively. The mean age of occurrence was 32.82 years for the three groups. Demographic details, along with lesion location, have been summarized in Table 1.

https://doi.org/10.5395/rde.2026.51.e22

Table 1. Demographic characteristics and lesion site distribution of the study population

Serial No.	Study population	Age (yr)	Sex	Site
	Healthy pulp			
1	PT-3	32	Female	Mandibular right third molar
2	PT-6	28	Female	Mandibular left third molar
3	PT-7	30	Female	Mandibular right third molar
4	PT-10	36	Male	Maxillary left third molar
5	PT-12	35	Male	Maxillary right third molar
6	PT-16	40	Female	Maxillary right third molar
7	PT-17	31	Male	Maxillary left third molar
8	PT-18	29	Male	Mandibular right third molar
9	PT-20	38	Male	Mandibular right third molar
10	PT-23	27	Male	Mandibular left third molar
11	PT-24	26	Male	Maxillary right third molar
12	PT-25	30	Male	Maxillary left third molar
13	PT-26	32	Female	Maxillary left third molar
14	PT-27	33	Female	Maxillary right third molar
15	PT-28	37	Male	Maxillary right third molar
16	PT-29	33	Male	Mandibular left third molar
17	PT-30	28	Female	Mandibular right third molar
	Periapical granuloma			
1	535/21	19	Male	Mandibular left lateral incisor to mandibular right lateral incisor
2	175/22	54	Male	Maxillary right first premolar
3	263/22	18	Female	Maxillary right central incisor
4	281/23	69	Male	Mandibular right lateral incisor
5	285/23	23	Male	Maxillary right and left central incisors
6	313/23	24	Male	Maxillary right and left central incisors
7	314/23	20	Male	Mandibular right central incisor
8	324/23	20	Male	Maxillary left central incisor
9	329/23	26	Male	Mandibular right and left central incisors
10	345/23	20	Male	Maxillary left central incisor
11	374/23	40	Male	Maxillary right and left central incisors
12	441/23	18	Male	Maxillary left central incisor
13	451/23	25	Male	Maxillary right and left central incisors
14	452/23	29	Female	Maxillary right and left central incisors
15	473/23	30	Female	Maxillary right central and lateral incisors
16	480/23	25	Male	Maxillary right first molar
17	85/24	58	Female	Maxillary left lateral incisor
	Radicular cyst			
1	552/21	41	Male	Maxillary left lateral incisor
2	322/21	47	Female	Mandibular right second molar
3	367/21	24	Female	Mandibular left first premolar to mandibular right first premolar
4	466/21	58	Female	Maxillary right central incisor
5	467/21	26	Female	Mandibular right second premolar to mandibular right second molar
6	124/22	51	Male	Maxillary right central incisor to maxillary right canine
7	172/22	36	Female	Maxillary right and left central incisors
8	377/22	17	Male	Maxillary right lateral incisor to maxillary left central incisor
9	71/23	21	Male	Maxillary left central incisor
10	254/23	33	Male	Maxillary right central incisor to maxillary right second premolar
11	337/23	55	Male	Maxillary left second premolar to maxillary left second molar
12	426/23	54	Female	Maxillary left central incisor

(Continued on the next page)

Table 1. Continued

Serial No.	Study population	Age (yr)	Sex	Site
13	438/23	39	Female	Maxillary right and left central incisors
14	442/23	20	Female	Maxillary left central incisor to maxillary left lateral incisor
15	95/24	22	Female	Maxillary right lateral incisor
16	109/24	30	Female	Maxillary right central incisor
17	245/24	37	Male	Maxillary right central incisor

PT, pulp tissue.

Table 2. Mean expression score of HIF-1α, VEGF, and macrophages (CD68) in healthy pulp, periapical granuloma, and radicular cyst

Parameters	Healthy pulp	Periapical granuloma	Radicular cyst	*p*-value[a)]
HIF-1α	10.17 ± 9.01	25.76 ± 9.08	24.65 ± 9.91	<0.001
VEGF	28.04 ± 23.71	88.56 ± 61.69	94.51 ± 49.69	<0.001
CD68	4.16 ± 3.12	16.71 ± 7.38	23.47 ± 10.25	<0.001

Values are presented as mean ± standard deviation.
HIF-1α, hypoxia inducible factor 1 alpha; VEGF, vascular endothelial growth factor.
[a)]Kruskal-Wallis test.

Table 3. Intergroup comparison of HIF-1α, VEGF, and macrophages (CD68) in healthy pulp, periapical granuloma, and radicular cyst

Group	*p*-value		
	HIF-1α expression	VEGF expression	CD68 expression
Healthy pulp and periapical granuloma	<0.001**	<0.001**	<0.001**
Periapical granuloma and radicular cyst	0.865	0.454	0.018*
Healthy pulp and radicular cyst	<0.001**	<0.001**	<0.001**

HIF-1α, hypoxia inducible factor 1 alpha; VEGF, vascular endothelial growth factor.
Post hoc comparisons were performed using the Mann-Whitney U-test: *$p < 0.05$ and **$p < 0.001$, statistically significant.

Immunohistochemical analysis

1. Hypoxia-inducible factor-1α expression

Stronger cytoplasmic and intense nuclear staining of HIF-1α was observed in all samples of PG and RC compared to HP (D, E, and F panels of Figures 3–5). In PG and RC, staining was prominent in inflammatory cells, including macrophages, lymphocytes, and polymorphonuclear neutrophils, as well as in endothelial cells and fibroblasts. Additionally, all layers of the epithelial lining of RC and inflammatory cells within the cystic capsule showed positive staining. However, in HP, HIF-1α staining was limited to fibroblasts and endothelial cells (Figures 3–5). The mean HIF-1α expression was highest in PG, followed by RC and HP, and their comparison was significant ($p < 0.001$) (Table 2). Upon applying the Mann-Whitney test for intergroup comparison, expression of HIF-1α was significantly higher in PG and RC than in HP ($p < 0.001$ for both), while that between PG and RC was not significant ($p = 0.865$) (Table 3).

2. Vascular endothelial growth factor expression

VEGF was evaluated in blood vessels, inflammatory infiltrate (mainly lymphocytes, plasma cells, and neutrophils), and stromal cells (fibroblasts). Overall, VEGF exhibited pronounced cytoplasmic positivity across all study groups. Immunohistochemical assessment was conducted in the connective tissue of PG, RC, and HP, as well as in the epithelial lining of RC (G, H, and I panels of Figures 3–5). VEGF expression was highest in RC than in PG and HP, and this difference was significant ($p < 0.001$) (Table 2). Upon intergroup comparison, the expression of VEGF was significantly higher in PG and RC than in HP ($p < 0.001$ for both); however, the difference between PG and RC was not significant ($p = 0.454$) (Table 3). The analysis of VEGF immunoreactivity in the epithelium of RCs revealed weak expression in one case (5.9%), moderate expression in six (35.3%), and strong expression in 10 cases (58.8%).

3. CD68 expression

Both lysosomal granules and the surface of macrophages expressed the CD68 antibody. Macrophage immunostaining was more prominent in the subepithelial regions of RC and the middle areas of PG (J, K, and L panels of Figures 3–5). The mean CD68 expression was significantly higher for RC than PG and HP ($p < 0.001$)

https://doi.org/10.5395/rde.2026.51.e22

(Table 2). Upon intergroup comparison, the expression of CD68 was significantly higher in RC and PG than in HP, and significantly higher in RC than in PG ($p < 0.001$, $p < 0.001$, and $p = 0.018$, respectively) (Table 3).

4. Correlation of hypoxia-inducible factor-1α with vascular endothelial growth factor expression and macrophages across study groups

Upon application of the Spearman correlation test, HIF-1α in HP, PG, and RC showed a nonsignificant correlation with VEGF ($p = 0.916$, $p = 0.516$, $p = 0.286$) and CD68 ($p = 0.860$, $p = 0.205$, $p = 0.535$), respectively. However, a significant positive correlation between VEGF and CD68 was found in HP (r = 0.630, $p = 0.007$) and PG (r = 0.532, $p = 0.028$), but not in RC ($p = 0.204$) (Table 4). The linear regression results were nonsignificant for the independent variables (age, sex, and site); however, the study groups (HP, PG, and RC) remained significantly associated with the mean scores of HIF-1α, VEGF, and CD68 (Table 5). A summary of the key immunohistochemical findings across the study groups has been provided in Table 6.

DISCUSSION

Periapical lesions are inflammatory responses to anaerobic polymicrobial infections of the dental pulp and root canals [12]. During inflammation, a hypoxic microenvironment activates HIFs, particularly HIF-1α, a key regulator of cellular responses to low oxygen levels [13]. In hypoxic conditions (oxygen concentration ≤2%), HIF-1α stabilizes and alters gene expression, promotes hypoxic adaptation, and influences the inflammatory environment [13]. Hypoxia is linked to processes like proliferation, angiogenesis, and apoptosis, which are essential for the development of a periapical lesion [14]. Elevated HIF-1α levels play a central role and influence macrophage polarization by regulating inducible nitric oxide synthase [12]. The current study was designed to evaluate and correlate the expression of HIF-1α, VEGF, and CD68 (a macrophage marker) in PG, RC, and HP.

The proliferation of cells and formation of cellular aggregates in periapical lesions can restrict oxygen diffusion to the lesion center, leading to hypoxia [15]. In the present study, HIF-1α expression levels were highest in PG, followed by RC, and least in HP, which was significant ($p < 0.001$) (Figures 3–5). The comparison of HIF-1α expression between HP and PG and HP and RC was also significant ($p < 0.001$ for both); however, the intergroup comparison between PG and RC was not significant (Tables 2 and 3).

Huang *et al.* [3] also reported higher HIF-1α expressions in PG and RC compared with HP, with no significant difference between PG and RC. Their values were higher than those in the present study, likely due to differences in lesion size, inflammation, and genetic factors. It could be hypothesized that the elevated HIF-1α in PGs may result from increased inflammatory activity,

Table 5. Multiple linear regression analysis on the association of the independent variables of study groups with the dependent variables of mean scores of HIF-1α, VEGF, and CD68

Dependent variable	B	*p*-value	Beta coefficient	95% CI
HIF-1 α	6.934	0.002	0.478	2.754–11.113
VEGF	32.572	0.001	0.482	13.378–51.767
CD68	10.499	<0.001	0.792	7.583–13.416

B, B coefficient in logistic regression; CI, confidence interval; HIF-1α, hypoxia inducible factor 1 alpha; VEGF, vascular endothelial growth factor.
Age, sex, site, and study groups (healthy pulp, periapical granuloma, and radicular cyst) as the independent variables, $p < 0.05$ (statistically significant).

Table 4. Intragroup correlation of HIF-1α, VEGF, and CD68 expressions in healthy pulp, periapical granuloma, and radicular cyst

Groups	HIF-1α and VEGF		HIF-1α and CD68		VEGF and CD68	
	r	*p*-value	r	*p*-value	r	*p*-value
Healthy pulp	–0.028	0.916	–0.046	0.860	0.630	0.007**
Periapical granuloma	–0.169	0.516	0.324	0.205	0.532	0.028*
Radicular cyst	0.275	0.286	0.162	0.535	0.211	0.417

HIF-1α, hypoxia inducible factor 1 alpha; VEGF, vascular endothelial growth factor.
r, Spearman's rho correlation coefficient.
*$p < 0.05$ and **$p < 0.01$ (two-tailed).

Table 6. Summary of main findings for HIF-1α, VEGF, and CD68 expression across study groups

Parameter	Healthy pulp (HP)	Periapical granuloma (PG)	Radicular cyst (RC)	Statistical significance
HIF-1α expression	Weak staining, limited to fibroblasts and endothelial cells	Strong cytoplasmic + intense nuclear staining Prominent in inflammatory cells, endothelial cells, and fibroblasts	Strong staining in inflammatory cells, fibroblasts, endothelial cells, and all epithelial layers	Significant difference across groups ($p < 0.001$) PG and RC > HP ($p < 0.001$) PG vs RC, not significant ($p = 0.865$)
VEGF expression	Cytoplasmic positivity in vascular, inflammatory and stromal cells	Strong cytoplasmic staining in connective tissue; higher than HP	Highest expression overall; strong epithelial positivity (58.8% cases)	Significant overall ($p < 0.001$) PG and RC > HP ($p < 0.001$) PG vs RC, not significant ($p = 0.454$)
CD68 (macrophages)	Lower macrophage density	Moderate macrophage presence, mainly in the middle connective tissue	Highest macrophage presence, especially subepithelial	Significant overall ($p < 0.001$) PG and RC > HP RC > PG ($p = 0.018$)
Correlation analysis	HIF-1α vs VEGF and CD68: nonsignificant VEGF vs CD68: significant ($r = 0.630$, $p = 0.007$)	HIF-1α correlations are nonsignificant VEGF vs CD68: significant ($r = 0.532$, $p = 0.028$)	Correlations between all markers are nonsignificant	–
Regression analysis	–	–	–	Age, sex, site: nonsignificant Study group remained significantly associated with mean marker expression

HIF-1α, hypoxia-inducible factor 1 alpha; VEGF, vascular endothelial growth factor.

in which macrophages and lymphocytes create a hypoxic microenvironment via cytokine release, particularly IL-1β (Figure 3). In contrast, RCs experience hypoxia due to ischemia from cystic cavity formation but have lower inflammation-driven hypoxia (Figure 4) [3].

Conversely, Alsaegh *et al.* [15] and da Costa *et al.* [14] found significantly higher HIF-1α in RC, attributing it to epithelial proliferation, ischemic microenvironment, and increased metabolic demand. The cystic structure restricts oxygen diffusion, stabilizing HIF-1α. Based on the present study findings, it could be hypothesized that higher HIF-1α expression in PG than RC may be due to the acute and dynamic inflammatory environment in PG, which increases metabolic demand and oxygen consumption, intensifying hypoxia. The intense immune cell infiltration and active tissue remodeling in PG further amplify HIF-1α expression. Also, the fluctuating oxygen levels in PG may drive transient HIF-1α activation, whereas the more stable, chronic hypoxia in RC results in relatively lower expression. The lack of an epithelial lining in PG could also allow broader HIF-1α expression across stromal and inflammatory cells. The expression levels in PG and RC were comparable, with no significant difference, although the PG group showed slightly higher values. Thus, there was a hypoxic environment in both RC and PG, albeit this was slightly higher in PG due to a greater inflammatory response.

HIF-1α is closely linked to the VEGF pathway, with its connection being evident across various physiological and pathological conditions [15]. Activation of HIF-1α directly upregulates VEGF expression, playing a pivotal role in stimulating new blood vessel formation and supporting tissue repair through angiogenesis [15]. VEGF expression levels were highest in RC, followed by PG, and lowest in HP, with a significant difference ($p < 0.001$) (Figures 3–5). The comparison of VEGF expression of HP with PG and RC was significant ($p < 0.001$ for both) and not significant for PG and RC ($p = 0.454$) (Tables 2 and 3).

Similar results were reported by Nonaka *et al.* [6] and Alsaegh *et al.* [15], who observed higher VEGF expression in RC than in PG. Nonaka *et al.* [6] found mean VEGF-positive cells in PGs (564.90), RCs (565.05), and lower in residual RCs (443.90), with strong VEGF expression in the epithelial lining of RCs. This might be due to geographic, genetic, and environmental differ-

https://doi.org/10.5395/rde.2026.51.e22

ences, as well as methodological variations. Alsaegh *et al.* [15] reported significantly higher VEGF in RCs (p = 0.015), with strong expression in 33.3% of RCs vs 11.1% of PGs. However, their study did not quantify VEGF expression, unlike Nonaka *et al.* [6] and the current study. VEGF upregulation in RC may be driven by chronic inflammation, bacterial toxins, and cytokines such as IL-1β and RANTES. In RC, dense inflammatory infiltration stimulates VEGF release from macrophages and neutrophils, while the epithelial lining enhances vascular permeability and lesion growth. Unlike PG, in which VEGF is mainly expressed in inflammatory cells, RC shows stronger epithelial VEGF expression, promoting cyst expansion and chronic inflammation.

In contrast, Fonseca-Silva *et al.* [16] reported higher VEGF expression in PG than in RC, though this difference was not significant. The lower VEGF values in the current study might be due to different evaluation criteria as the former study performed immunohistochemical analysis of VEGF by determining the percentage of positive-staining cells in 10 microscopic fields for each specimen, whereas the present study quantified the mean expression of VEGF in the connective tissue and assessed the semi-quantitative immunoexpression in the epithelial lining of RCs. Leonardi *et al.* [11] found strong VEGF expression in inflammatory cells of non-epithelialized PGS, while epithelialized PGS showed moderate staining in inflammatory cells and strong positivity in epithelial cells. RC exhibited consistent VEGF expression across all epithelial layers with minimal inflammatory staining. Higher VEGF in PG might result from early lesion development, where inflammatory cells drive angiogenesis and vascular hyperpermeability. In RC, epithelial cells become the primary VEGF source, maintaining vascular permeability and cyst growth rather than initiating angiogenesis. Thus, PGs exhibit higher VEGF expression driven by inflammation, whereas RCs rely on epithelial VEGF and exhibit cystic characteristics. The chronicity of inflammation in RCs also contributes to sustained VEGF levels, as prolonged inflammatory processes result in ongoing recruitment and activation of macrophages and other immune cells that further drive angiogenic signaling.

Macrophages play a crucial role in periapical lesions by modulating the immune response and maintaining tissue homeostasis. Due to their plasticity, macrophages adapt to microenvironmental changes, impacting lesion progression and healing [7]. In the present study, CD68 expression was highest in RC, followed by PG, and lowest in HP, with a significant difference (p < 0.001) (Figures 3–5). The intergroup comparison of CD68 expression between all groups showed significant findings (Tables 2, 3). Similar to the present study, França *et al.* [7] and Azeredo *et al.* [17] reported higher CD68 expression in RC than PG, though with no significant difference. Variations in the methodologies could be the probable reason for differences in values. Bolan *et al.* [18] found macrophages diffusely distributed in periradicular lesions, contributing to expansion via IL-1 and TNF-α. de Almeida *et al.* [19] observed higher CD68 expression in cysts and granulomas of younger adults compared to older patients, suggesting a more active immune response in the young, potentially influencing endodontic outcomes. Contrary to the current study, Rodini and Lara [20] and Weber *et al.* [21] reported higher CD68 expression in PG than RC, though the difference was not significant. Increased macrophage recruitment in RC supports tissue remodeling, immune regulation, and lesion expansion through IL-1 and TNF-α, promoting bone resorption and epithelial proliferation [22]. Higher T helper 2 cytokines (IL-6, prostaglandins) enhance macrophage differentiation and chronic inflammation [22]. Predominantly located subepithelially, macrophages aid in antigen presentation and immune modulation. As RC matures, it stabilizes through macrophage-driven inflammation and tissue repair, whereas PGs exhibit a more acute inflammatory response [7,8].

HIF-1α and VEGF are closely interconnected in numerous physiological and pathological processes. Hypoxia was correlated with angiogenesis in the current study to analyze their interrelationship in the study groups, which was found to be nonsignificant for the groups (Table 4). VEGF expression was also correlated with macrophages to assess their interplay in periapical lesions. In the HP and PG groups, VEGF showed a significant positive correlation with CD68 expression (p = 0.007 and p = 0.028, respectively) while in the RC group it was not significant (p = 0.417), indicating an active role of macrophages in VEGF-mediated angiogenesis. This association is likely driven by a hypoxic microen-

vironment that enhances macrophage activation and VEGF production. No study has correlated VEGF with macrophages in periapical lesions. The present study findings could pave the way for future studies that could correlate these expressions for more insight into their role in the pathogenesis of periapical lesions.

HIF-1α and VEGF may serve as potential molecular targets for future investigation in preclinical models of periapical lesions. Exploring the modulation of these pathways could help clarify their role in inflammation, bone resorption, and tissue repair, providing a basis for future translational research. Therapies such as edaravone, which modulates the HIF-1α–VEGF–ANG-1 axis, and VEGF inhibitors like bevacizumab have demonstrated their potential in controlling angiogenesis and bone loss in other inflammatory conditions [15]. Furthermore, combining anti-VEGF treatments with antimicrobials like moxifloxacin has shown rapid lesion regression, suggesting the potential for adaptation in the treatment of periapical lesions to enhance healing outcomes [23].

CONCLUSIONS

This study demonstrated distinct expression patterns of HIF-1α, VEGF, and CD68 across PG, RC, and HP. HIF-1α and VEGF showed significantly higher expression in PG and RC compared to HP, highlighting the role of hypoxia and angiogenesis in lesion progression. Similarly, macrophage density (CD68) was markedly elevated in RC and PG relative to HP, with RC showing the highest levels. Although VEGF and CD68 exhibited a significant positive correlation in HP and PG, no such correlation was observed in RC. Overall, the inter-marker correlations were nonsignificant, and linear regression analysis confirmed that lesion type, rather than demographic factors or site, was significantly associated with expression patterns.

To our knowledge, this is the first study to investigate and correlate the expressions of HIF-1α, VEGF, and macrophages in periapical lesions. The primary strength of the study lies in the precise methodology employed to assess immunohistochemical expression. However, we could not corroborate the correlation between hypoxia, angiogenesis, and macrophages with previous studies, as no prior research has explored this specific interplay. A further limitation is the use of CD68 as a general macrophage marker without incorporating polarization-specific markers (such as CD80/CD86 for M1 or CD163/CD206 for M2), which restricts insights into functional macrophage subsets. Additionally, the heterogeneity in quantification approaches used for different markers, such as variation in scoring methods and expression assessment, may introduce measurement variability. The limited sample size might also be a drawback, impacting the generalizability of the results. However, the findings do highlight the crucial role these factors play in the development and progression of periapical lesions, providing a foundation for novel therapeutic approaches.

CONFLICT OF INTEREST

No potential conflict of interest relevant to this article was reported.

FUNDING/SUPPORT

This research was funded vide letter number R&D/UHSR /2024/974 under the Post Graduate Dissertation Support (PGDS-II) Scheme-II, Research Cell, Pt BD Sharma University of Health Sciences, Rohtak, Haryana-124001, India.

AUTHOR CONTRIBUTIONS

Conceptualization, Project administration: Kamboj M. Data curation, Resources, Funding acquisition: Chatterjee P, Kamboj M. Formal analysis: Chatterjee P. Methodology: Chatterjee P, Mittal S, Devi A. Supervision: Kamboj M, Mittal S, Narwal A. Validation: Kamboj M, Narwal A, Devi A. Writing - original draft: Chatterjee P. Writing - review & editing: Kamboj M, Mittal S, Narwal A, Devi A. All authors read and approved the final manuscript.

DATA SHARING STATEMENT

The datasets are not publicly available but are available from the corresponding author upon reasonable request.

REFERENCES

1. Brizuela M, Bordoni B. Anatomy, head and neck, dental pulp [updated 2025 Dec 9]. In: StatPearls [Internet]. Treasure Island (FL): StatPearls Publishing; 2026 Jan [cited 2025 Jun 21]. Available from: https://www.ncbi.nlm.nih.gov/books/NBK537112/
2. Gopikrishna V. Grossman's endodontic practice. 14th ed. New Delhi: Wolters Kluwer Health; 2021.

https://doi.org/10.5395/rde.2026.51.e22

3. Huang HY, Wang WC, Lin PY, Huang CP, Chen CY, Chen YK. The roles of autophagy and hypoxia in human inflammatory periapical lesions. Int Endod J 2018;51 Suppl 2:e125-e145.
4. Aranha AM, Zhang Z, Neiva KG, Costa CA, Hebling J, Nör JE. Hypoxia enhances the angiogenic potential of human dental pulp cells. J Endod 2010;36:1633-1637.
5. Bletsa A, Virtej A, Berggreen E. Vascular endothelial growth factors and receptors are up-regulated during development of apical periodontitis. J Endod 2012;38:628-635.
6. Nonaka CF, Maia AP, Nascimento GJ, de Almeida Freitas R, Batista de Souza L, Galvão HC. Immunoexpression of vascular endothelial growth factor in periapical granulomas, radicular cysts, and residual radicular cysts. Oral Surg Oral Med Oral Pathol Oral Radiol Endod 2008;106:896-902.
7. França GM, Carmo AFD, Costa Neto H, Andrade AL, Lima KC, Galvão HC. Macrophages subpopulations in chronic periapical lesions according to clinical and morphological aspects. Braz Oral Res 2019;33:e047.
8. Visarnta S, Ratisoontorn C, Panichuttra A, Sinpitaksakul P, Chantarangsu S, Dhanuthai K. Macrophage polarization in human periapical lesions in relation to histopathological diagnosis, clinical features and lesion volume: an ex vivo study. Int Endod J 2024;57:1829-1847.
9. Faul F, Erdfelder E, Lang AG, Buchner A. G*Power 3: a flexible statistical power analysis program for the social, behavioral, and biomedical sciences. Behav Res Methods 2007;39:175-191.
10. Freitas TM, Miguel MC, Silveira EJ, Freitas RA, Galvão HC. Assessment of angiogenic markers in oral hemangiomas and pyogenic granulomas. Exp Mol Pathol 2005;79:79-85.
11. Leonardi R, Caltabiano M, Pagano M, Pezzuto V, Loreto C, Palestro G. Detection of vascular endothelial growth factor/vascular permeability factor in periapical lesions. J Endod 2003;29:180-183.
12. Hirai K, Furusho H, Hirota K, Sasaki H. Activation of hypoxia-inducible factor 1 attenuates periapical inflammation and bone loss. Int J Oral Sci 2018;10:12.
13. He M, Bian Z. Expression of hypoxia-induced semaphorin 7A correlates with the severity of inflammation and osteoclastogenesis in experimentally induced periapical lesions. Arch Oral Biol 2017;75:114-119.
14. da Costa NM, de Siqueira AS, Ribeiro AL, da Silva Kataoka MS, Jaeger RG, de Alves-Júnior SM, *et al*. Role of HIF-1α and CASPASE-3 in cystogenesis of odontogenic cysts and tumors. Clin Oral Investig 2018;22:141-149.
15. Alsaegh MA, Shetty SR, Mahmoud O, Varma SR, Altaie AM, Rawat SS. The expression of HIF-1α and VEGF in radicular cysts and periapical granulomas. Eur J Dent 2025;19:531-539.
16. Fonseca-Silva T, Santos CC, Alves LR, Dias LC, Brito M, De Paula AM, *et al*. Detection and quantification of mast cell, vascular endothelial growth factor, and microvessel density in human inflammatory periapical cysts and granulomas. Int Endod J 2012;45:859-864.
17. Azeredo SV, Brasil SC, Antunes H, Marques FV, Pires FR, Armada L. Distribution of macrophages and plasma cells in apical periodontitis and their relationship with clinical and image data. J Clin Exp Dent 2017;9:e1060-e1065.
18. Bolan M, Lima DA, Figueiredo CP, Di Giunta G, Rocha MJ. Immunohistochemical study of presence of T cells, B cells, and macrophages in periradicular lesions of primary teeth. J Clin Pediatr Dent 2008;32:287-293.
19. de Almeida NF, Brasil SC, Ferreira DC, Armada L. Aging effects in the expression of macrophages in post-treatment apical periodontitis lesions. Spec Care Dentist 2017;37:230-235.
20. Rodini CO, Lara VS. Study of the expression of CD68+ macrophages and CD8+ T cells in human granulomas and periapical cysts. Oral Surg Oral Med Oral Pathol Oral Radiol Endod 2001;92:221-227.
21. Weber M, Schlittenbauer T, Moebius P, Büttner-Herold M, Ries J, Preidl R, *et al*. Macrophage polarization differs between apical granulomas, radicular cysts, and dentigerous cysts. Clin Oral Investig 2018;22:385-394.
22. Bertasso AS, Léon JE, Silva RAB, Silva LA, de Queiroz AM, Pucinelli CM, *et al*. Immunophenotypic quantification of M1 and M2 macrophage polarization in radicular cysts of primary and permanent teeth. Int Endod J 2020;53:627-635.
23. Agarwal M, Gupta C, Mohan KV, Upadhyay PK, Dhawan A, Jha V. Adjunctive intravitreal anti-vascular endothelial growth factor and moxifloxacin therapy in management of intraocular tubercular granulomas. Ocul Immunol Inflamm 2023;31:158-167.

RDE Restorative Dentistry & Endodontics

Research Article

eISSN 2234-7666
Restor Dent Endod. 2026 May;51(2):e23
https://doi.org/10.5395/rde.2026.51.e23

Effect of high irradiance and short exposure curing time on the fracture toughness of bulk-fill resin-based composite: an *in vitro* study

Beatriz Ometto Sahadi[1], **Tainah Oliveira Rifane**[1], **Carolina Bosso André**[2], **Vitaliano Gomes Araújo-Neto**[1,*], **Richard Thomas Bengt Price**[3], **Marcelo Giannini**[1]

[1]Department of Restorative Dentistry, Piracicaba Dental School, University of Campinas, Piracicaba, SP, Brazil
[2]Department of Restorative Dentistry, University of Minas Gerais, Belo Horizonte, MG, Brazil
[3]Department of Dental Clinical Sciences, Dalhousie University, Halifax, NS, Canada

ABSTRACT

Objectives: This study aimed to determine the effect of high irradiance and short exposure time on the fracture toughness of bulk-fill resin-based composites (RBCs).

Methods: Three RBCs were tested: Tetric PowerFill (TPF; Ivoclar Vivadent), Opus Bulk Fill APS (OBF; FGM Dental Group), and Filtek One Bulk Fill (FOB; Solventum). Sixty single-edge-notched disc specimens were prepared using a fracture toughness mold. Each group consisted of 20 samples, divided into two subgroups ($n = 10$). The RBCs were light-cured either for 3 seconds in high-irradiance mode ('3s cure') or for the manufacturer-recommended times (TPF, 10 seconds; OBF, 30 seconds; FOB, 20 seconds) in 'high power' mode using the Bluephase PowerCure (Ivoclar Vivadent). The peak spectral wavelength was measured using a spectrophotometer. Specimens were tested on a universal testing machine, and data were analyzed by two-way analysis of variance and Bonferroni test ($\alpha = 0.05$).

Results: Radiant exposure values (J/cm^2) were 9.5 for the 3-second mode and 12.4, 24.8, and 37.1 for 10, 20, and 30 seconds (high power mode), respectively. FOB (4.22 and 3.79 MPa·m$^{0.5}$ for 20 and 3 seconds) had the highest mean fracture toughness, while OBF showed the lowest (2.01 and 2.10 MPa·m$^{0.5}$ for 30 and 3 seconds). TPF produced intermediate results (2.72 and 2.70 MPa·m$^{0.5}$ for 10 and 3 seconds). Exposure time did not affect TPF and OBF, while the 3-second exposure significantly reduced the fracture toughness for FOB.

Conclusions: The RBCs tested had different fracture toughness values regardless of exposure time. High irradiance and short exposure can reduce fracture toughness depending on the RBC tested.

Keywords: Composite resins; Polymerization; Stress fractures

Received: September 10, 2025 **Revised:** October 14, 2025 **Accepted:** October 14, 2025

Citation
Sahadi BO, Rifane TO, André CB, Araújo-Neto VG, Price RTB, Giannini M. Effect of high irradiance and short exposure curing time on the fracture toughness of bulk-fill resin-based composite: an *in vitro* study. Restor Dent Endod 2026;51(2):e23.

***Correspondence to**
Vitaliano Gomes Araújo-Neto, PhD
Department of Restorative Dentistry, Piracicaba Dental School, University of Campinas, 901, Av. Limeira, Piracicaba, São Paulo 13414-903, Brazil
Email: vitalianoganeto@gmail.com

INTRODUCTION

Some bulk-fill resin-based composites (RBCs) can be light-cured in increments up to 5 mm thick [1,2]. However, not all light-curing units (LCUs) and their exposure modes can be used to cure such composite thickness, as they do not promote adequate photocuring at the deepest layers of bulk-fill composite restorations. Scientific articles have addressed this subject and shown the consequences of the deficient monomeric conversion that can affect some properties of the bulk-fill restorative materials [3,4].

In general, polymerization in the deeper areas of the RBC restoration occurs due to better light transmission through the bulk-fill RBC when compared to incrementally layered conventional composites. Lower light dispersion at the filler-resin matrix interface, reduced filler load, and changes in filler particle type contribute to higher light penetration. Also, bulk-fill RBC includes highly reactive photoinitiators, aromatic dimethacrylate, high-molecular-weight monomers, and fragmentation monomer technology to modulate polymerization shrinkage stress [5,6].

The development of RBCs has been carried out in parallel with high-power light-emitting diode (LED) LCUs that deliver a broad spectrum of blue and violet light, capable of exciting all photoinitiators used in contemporary RBCs. Additionally, many LCUs offer light exposure modes with varying exposure times and power outputs, delivering high irradiance of at least 1,000 mW/cm^2. This high irradiance from LED LCUs has allowed the light exposure time to be reduced from 40 to 10 seconds, or even 3 seconds [7,8].

Some LED LCUs, such as Bluephase PowerCure (Ivoclar Vivadent, Schaan, Liechtenstein) and Valo X-LED Curing Light (Ultradent Products Inc., South Jordan, UT, USA), are equipped with high power and short exposure modes ('3 seconds Cure' and '5 seconds-Xtra Power' modes, respectively) [9–11]. However, studies have shown that short curing times may generate fewer free radicals, compromising the polymerization reaction [12,13], which, in turn, reduces the depth of cure [10,14] and the physical-mechanical properties of bulk-fill RBCs [11,15].

The objective of this study was to investigate the influence of high irradiance and short exposure time from the LED LCU on the fracture toughness of three bulk-fill RBCs. The research hypotheses were: (1) the light exposure mode influences the fracture toughness of bulk-fill RBCs, and (2) the fracture toughness differs among bulk-fill RBCs regardless of the light exposure mode.

METHODS

Three high-viscosity bulk-fill RBCs were tested: Tetric PowerFill (TPF; Ivoclar Vivadent); Opus Bulk Fill APS (OBF; FGM Dental Group), and Filtek One Bulk Fill (FOB; Solventum, St Paul, MN, USA). The compositions and the lot number of bulk-fill RBCs used in this study, as well as their respective recommended light exposure time, are reported in Table 1.

The bulk-fill RBCs were light-polymerized with two light exposure modes ('3s cure' and 'high power') using the Bluephase PowerCure LED LCU. The light output from both light exposure modes of the LCU was measured using a spectrophotometer (MSC15W, SN 37560; Gigahertz-Optik, Amesbury, MA, USA) and the MSC15 measurement software ver. 2019.1.0 (Gigahertz-Optik). The peak spectral wavelength, power output, incident irradiance, and radiant exposure on RBC surfaces from the LED LCUs were determined.

Sixty single-edge-notched disc composite samples (6.5 mm diameter, 2.5 mm thick, and 3.5 mm notch) (Figure 1A) were prepared using a commercial fracture toughness metal mold (Odeme Dental Research, Luzerna, SC, Brazil) that is according to the ASTM Standard E-399-83 [16]. Each group consisted of 20 samples, which were divided into two subgroups (n = 10) according to the three bulk-fill RBCs and two different light exposure modes investigated in this study.

The bulk-fill RBC was inserted into the metal mold in a single increment using a stainless-steel spatula, ensuring complete filling and avoiding air entrapment. After filling, the mold was covered with a polyester strip (KDent, Joinville, SC, Brazil), and the LCU was clamped and positioned perpendicular to the mold. The LCU tip was placed in contact with the polyester strip covering the composite surface, and bulk-fill RBCs were light-cured either using the 3s cure mode or according to the times recommended by the respective manufacturers

https://doi.org/10.5395/rde.2026.51.e23

Table 1. Bulk-fill resin-based composites used, their compositions, and recommended light exposure times according to the manufacturers

Bulk-fill composite (lot number)	Composition	Recommended exposure time
Tetric PowerFill (Z04192)	Bisphenol A glycidyl methacrylate, ethoxylated bisphenol A dimethacrylate, 2,2-bis-(4-(3-methacryloxypropoxy)phenyl)propane, urethane dimethacrylate, tricyclodecane dimethanol dimethacrylate, propoxylated bisphenol A dimethacrylate, addition fragmentation chain transfer, β-allyl sulfone, Ba-Al-Si glass, ytterbium trifluoride, Si-Zr mixed oxide and copolymers (79% by weight)	3 sec or 10 sec[a)]
Opus Bulk Fill APS (171023)	Urethane-dimethacrylate monomers, stabilizers, photoinitiator composition (APS), co-initiators, stabilizers, pigments, and silanized silicon dioxide (79% by weight)	30 sec
Filtek One Bulk Fill (NC88136)	Aromatic urethane dimethacrylate, diurethane dimethacrylate, 1,12-dodecane dimethacrylate, ethyl 4-dimethyl aminobenzoate, silane-treated ceramic, silane-treated silica, ytterbium fluoride and silane-treated zirconia (76.5% by weight)	20 sec

[a)]Three seconds or 10 seconds when using the light-curing units in '3s cure' mode and 'high power mode,' respectively.
Tetric PowerFill: Ivoclar Vivadent, Schaan, Liechtenstein; Opus Bulk Fill APS: FGM Dental Group, Joinville, SC, Brazil; Filtek One Bulk Fill: Solventum, St Paul, MN, USA.

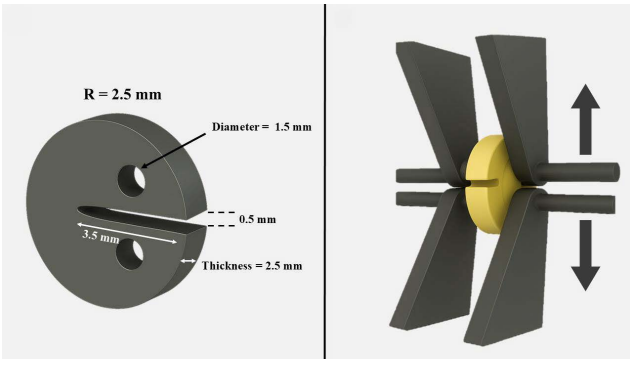

Figure 1. Dimensions and shape of the composite specimen and the fracture toughness testing apparatus.

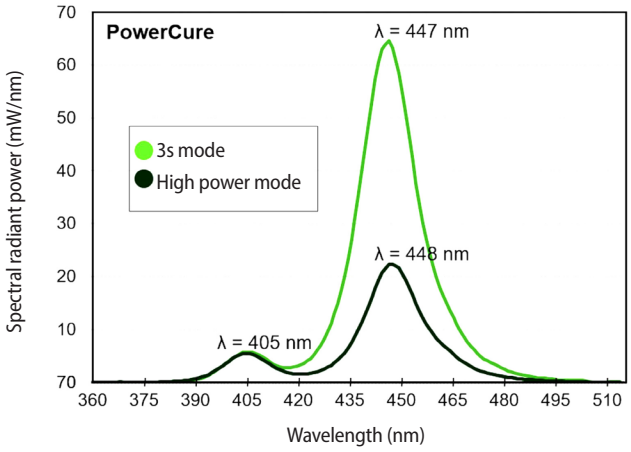

Figure 2. Spectral emissions from the Bluephase PowerCure (Ivoclar Vivadent, Schaan, Liechtenstein) light-curing unit, according to the curing mode.

(TPF, 10 seconds; OBF, 30 seconds; FOB, 20 seconds) in the high power mode, which represented the control groups.

Polymerized specimens were removed from the mold, stored in distilled water at 37°C for 24 hours, and then tested in a universal test machine (Instron 4411; Instron Corp., Norwood, MA, USA) at a 1.0 mm/min crosshead speed (Figure 1B). The fracture load values were acquired and applied to the formula below to calculate the fracture toughness (in $MPa \cdot m^{0.5}$):

Fracture toughness (KIC) = $(PL/BW1.5)\ Y$

where: P, load fracture; L, distance between holes; B, specimen thickness; W, specimen width; Y, geometrical function dependent on a/W, and 'a' is the notch length.

$Y = [2.9(a/w)1/2 - 4.6\ (a/w)3/2 + 21.8\ (a/w)5/2 - 37.6(a/w)7/2 + 38.7(a/w)9/2]$

Fracture toughness data were analyzed for homoscedasticity with Levene test and normality with the Shapiro-Wilks test. Data were analyzed by two-way analysis of variance (ANOVA; factors: 'type of bulk-fill RBC' and 'exposure mode') and Bonferroni test ($\alpha = 0.05$). The SAS software ver. 9.4 (SAS Institute Inc, Cary, NC, USA) was used for all the statistical analyses.

RESULTS

Figure 2 illustrates the emission spectra and the real-time irradiances delivered by the Bluephase PowerCure LCU for each light exposure mode. The emission peaks in the 3s cure mode were at 405 nm (violet) and 447 nm (blue), respectively. In the high power mode, the violet light emission peak remained the same at 405

nm and delivered the same amount of violet light, but the amount of blue light increased (448 nm). This 1-nm change was within the measurement uncertainty of the equipment used in the study. Figure 3 illustrates that 3s cure mode reached irradiance value of 3,178 mW/cm² that was maintained for only 3 seconds, while the high power mode delivered a constant irradiance of approximately 1,238 mW/cm² for 20 seconds in high power mode.

Table 2 reports the power (mW), irradiance (mW/cm²), and the radiant exposure (J/cm²) values from both light exposure modes of Bluephase PowerCure LCU. For the 3s cure mode, the LCU delivered 1,597 mW power output, 3,178 mW/cm² irradiance, and 9.5 J/cm² radiant exposure. The high power mode delivered a power output of 622 mW and an irradiance of 1,238 mW/cm². The exposure times of 10, 20, and 30 seconds delivered radiant exposures of 12.4, 24.8, and 37.1 J/cm², respectively.

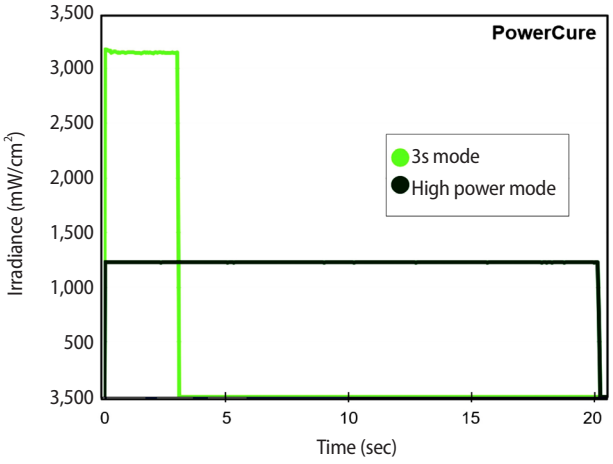

Figure 3. Real-time irradiances delivered from the Bluephase PowerCure (Ivoclar Vivadent, Schaan, Liechtenstein) light-curing unit, according to the light exposure mode.

Table 3 reports the fracture toughness means (MPa·m$^{0.5}$) for bulk-fill RBCs and exposure modes. The two-way ANOVA demonstrated that both 'type of bulk-fill RBC' ($p < 0.001$) and 'exposure mode' ($p < 0.001$) significantly influenced fracture toughness, with no significant interaction between the factors ($p = 0.100$).

The curing modes did not affect the fracture toughness results of TPF ($p = 0.974$) and OBF ($p = 0.632$), while the 3s cure mode significantly reduced the fracture toughness for FOB ($p = 0.020$). On the other hand, the highest fracture toughness means were found for FOB (4.22 and 3.79 MPa·m$^{0.5}$ for 20 and 3 seconds, respectively), while the lowest one was for OBF (2.01 and 2.10 MPa·m$^{0.5}$ for 30 and 3 seconds, respectively), regardless of the light exposure mode. TPF produced intermediate results (2.72 and 2.70 MPa·m$^{0.5}$ for 10 and 3 seconds, respectively).

DISCUSSION

The first research hypothesis that the light exposure mode influences the fracture toughness of bulk-fill RBCs was accepted only for FOB bulk-fill RBC, because the fracture toughness of OBF and TPF cured using the 3s cure or high power modes did not differ statistically. According to the FOB RBC manufacturer, for LCUs that

Table 2. Power output (mW), incident irradiance (mW/cm²), and radiant exposure (J/cm²) values from the '3s cure' and 'high power' modes

Variable	3s cure mode	High power mode
Power output (mW)	1,597	622
Incident irradiance (mW/cm²)	3,178	1,238
Radiant exposure (J/cm²)	9.5[a)]	12.4, 24.8, 37.1[b)]

Exposure time: [a)]3 sec; [b)]10, 20, and 30 sec.

Table 3. Fracture toughness (MPa·m$^{0.5}$) of the bulk-fill RBCs tested according to the exposure modes used

Bulk-fill RBC (recommended exposure time)	3 sec ('3s cure' mode)	Recommended exposure ('high power' mode)
Tetric PowerFill (10 sec)	2.70 ± 0.60^{bA}	2.72 ± 0.37^{bA}
Opus Bulk Fill APS (30 sec)	2.10 ± 0.28^{cA}	2.01 ± 0.19^{cA}
Filtek One Bulk Fill (20 sec)	3.79 ± 0.29^{aB}	4.22 ± 0.53^{aA}

Values are presented as mean ± standard deviation.
Different lowercase letters indicate significant differences among bulk-fill RBCs within the same curing mode ($p < 0.05$).
Different uppercase letters indicate significant differences between curing modes for the same bulk-fill RBC ($p < 0.05$).
Tetric PowerFill: Ivoclar Vivadent, Schaan, Liechtenstein; Opus Bulk Fill APS: FGM Dental Group, Joinville, SC, Brazil; Filtek One Bulk Fill: Solventum, St Paul, MN, USA.

https://doi.org/10.5395/rde.2026.51.e23

deliver an irradiance of 1,000 mw/cm^2 or greater, the light exposure time must be 20 seconds, while for LCUs with lower irradiance (550–1,000 mw/cm^2), the light exposure time must be 40 seconds. Thus, this study used the recommended exposure time (20 seconds), and the FOB composite achieved higher fracture toughness than when exposed for only 3 seconds. The 20-second exposure time in the high power mode delivered a radiant exposure of 24.8 J/cm^2 and irradiance around 1,200 mW/cm^2. In comparison, the '3s cure' mode delivered only 9.5 J/cm^2 radiant exposure and 3,178 mW/cm^2 irradiance. The difference in radiant exposure might explain the difference in fracture toughness between the cure modes used to polymerize the FOB. This contrast highlights two distinct energy-delivery strategies: an ultrashort, high-intensity exposure versus a lower, sustained output (Figure 3).

The 3-second exposure time is the shortest exposure time recommended by any RBC manufacturer. The ability of TPF to be photocured in a short light exposure time is most likely due to the types and concentration of photoinitiators (combination of camphorquinone and Ivocerin) used in this bulk-fill RBC [14,15]. The photoinitiator system in OBF bulk-fill RBC is a proprietary advanced polymerization system (APS), which yielded similar fracture toughness regardless of the light exposure mode used or the radiant exposure delivered to the RBC. The same result was obtained for the TPF bulk-fill RBC; however, this bulk-fill RBC is recommended to be cured in the 3s cure mode on the Bluephase PowerCure LCU. According to its manufacturer, the TPF can also be cured for 10 seconds using the high power mode from the same LCU.

The second research hypotheses that fracture toughness differs among bulk-fill RBCs, regardless of the light exposure mode was accepted because the RBCs showed distinct fracture toughness values and the light exposure mode did not change the order from the highest fracture toughness (FOB: for 20 seconds, 4.22 MPa·m$^{0.5}$ and for 3 seconds, 3.79 MPa·m$^{0.5}$) to the lowest one (OBF: for 20 seconds, 2.01 MPa·m$^{0.5}$ and for 3 seconds, 2.10 MPa·m$^{0.5}$). The TPF composite produced intermediate results (for 20 seconds, 2.70 MPa·m$^{0.5}$ and for 3 seconds, 2.72 MPa·m$^{0.5}$).

The filler content of FOB is a combination of silica, non-agglomerated and cluster fillers, and ytterbium trifluoride particles. The resin matrix contains two methacrylate monomers (aromatic urethane dimethacrylate [AUDMA] and addition-fragmentation methacrylate [AFM] monomers) that help reduce polymerization shrinkage stress. AUDMA is a high-molecular-weight AUDMA that decreases the number of reactive groups in the resin, while the AFM contains a reactive site that cleaves through a fragmentation process during polymerization. The cleaving process tends to reduce the polymerization shrinkage stress, and the monomer fragments can react with each other or with other reactive monomer sites, thereby maintaining the physical properties of FOB bulk-fill RBC due to increased monomer conversion. A study that used single-edge bend bar-shaped specimens and loaded them in a three-point bending test showed that the fracture toughness of FOB was among the highest of the bulk-fill RBCs investigated [17], corroborating this study.

The TPF contains a combination of monomers (bisphenol A glycidyl methacrylate, ethoxylated bisphenol A dimethacrylate, 2,2-bis[4-(3-methacryloxypropoxy) phenyl]propane, urethane dimethacrylate [UDMA], tricyclodecane dimethanol dimethacrylate, propoxylated bisphenol A dimethacrylate) and four types of particles (barium glass, ytterbium trifluoride, mixed oxide, and prepolymers). The polymerization shrinkage stress is controlled by the 'addition fragmentation chain transfer' and the β-allyl sulfone-based dimethacrylate networks. Both are also responsible for improving the polymer's physical properties and enhancing the homogeneity of the network architecture [18], particularly under high irradiance and fast photocuring [19]. However, some studies have recommended longer exposure time and lower irradiance to improve the degree of conversion and the depth of cure of RBCs. Also, the recommendation was to reduce the monomer elution, polymerization shrinkage, and the porosity of TPF [7,8]. On the other hand, a study that compared the fast high irradiance (3s cure mode from Bluephase PowerCure LCU) to conventional curing mode for 20 seconds (irradiance: 1,600 mW/cm^2 from an Elipar LED LCU, TM S10; 3M ESPE, St Paul, MN, USA) showed that the light exposure mode did not affect the mechanical properties (flexural strength, modulus, and fracture toughness) of two RBCs

(TPF and Essentia U, GC Corp., Tokyo, Japan) [20].

The OBF contains UDMA monomer, silanized silicon dioxide as the filler particles and the APS photoinitiator system. This study showed the lowest fracture toughness among the bulk-fill RBCs. A study showed that the flexural strength of OBF was lower than that obtained for X-tra fil (VOCO, Cuxhaven, Germany) [21]. However, another study showed that the OBF light-cured for 40 seconds presented better results for the evaluated mechanical properties than Tetric EvoCeram Bulk Fill (Ivoclar) light-cured for 10 seconds [22]. An *in vitro* study showed that OBF had mechanical performance and reliability similar to those of conventional and incremental RBCs [23].

Thanoon *et al.* [24] showed that the response of bulk-fill composites to a high-irradiation protocol varied with composition and viscosity, with light transmission and degree of conversion occurring more rapidly in low-viscosity materials. Another study indicated that high irradiance and short exposure times can affect the depth of cure of bulk-fill RBCs, and fast curing with high irradiance should be used only for some bulk-fill composites [4]. Ribeiro *et al.* [13] demonstrated that short exposure times (1 to 3 seconds) produced inferior physical-mechanical properties (fracture toughness, energy absorption, and Vickers hardness) in some composites compared to a 10-second exposure at a lower irradiance [13]. On the other hand, the TPF showed superior thermal and monomer conversion results when exposed to high irradiance for a short time (1–5 seconds) compared with the Tetric EvoCeram conventional bulk-fill composite [24].

Most studies have used bar-shaped specimens [25–28], unlike this study, which used disc-shaped ones [13]. The metal mold used in this study produced samples 6.5 mm in diameter and 2.5 mm thick (Figure 1A). Bulk-fill RBCs are recommended to be light-activated to a thickness of up to 4 or 5 mm, but in this study, the composite thickness was lower than their recommended values. The shape and thickness of the composite samples, in addition to the use of contemporary bulk-fill RBCs, may explain their superior fracture toughness values obtained in this study when compared to results (0.4 to 1.6 $MPa{\cdot}m^{0.5}$) reported by previous studies that used conventional RBCs and others that are no longer available [25–29].

The composites tested in this study are indicated for large restorations [30–33] and, when under-polymerized, may result in poor restoration longevity. These composites have been extensively studied regarding exposure time and degree of conversion, hardness, and flexural strength [34–37], but fracture toughness reflects a material's susceptibility to cracking; a higher fracture toughness value indicates that the material is less likely to fracture [38].

The results of this study suggest that the type of bulk-fill RBC and the light exposure mode have a significant influence on the fracture toughness of FOB bulk-fill RBC. This study did not standardize the radiant exposure delivered to all bulk-fill RBCs because different exposure times in high power mode were used to photo-cure the three bulk-fill RBCs. The exposure time was set to the light-activation time recommended by the manufacturers. The same exposure time for the tested bulk-fill RBCs might alter the fracture toughness results.

CONCLUSIONS

Light-curing with short exposure time and high irradiance did not reduce the fracture toughness of OBF and TPF bulk-fill restorative materials. However, this finding cannot be generalized to all bulk-fill composites, because the short high-irradiance protocol yielded lower fracture toughness for FOB.

CONFLICT OF INTEREST

No potential conflict of interest relevant to this article was reported.

FUNDING/SUPPORT

This study was financed in part by the National Council for Scientific and Technological Development (CNPq, process # 308654/2023-4, Brazil - M. Giannini), São Paulo Research Foundation (FAPESP, process # 2021/11972-0, Brazil - M. Giannini), the Coordenação de Aperfeiçoamento de Pessoal de Nível Superior (CAPES, Finance Code 001, Brazil - T.O. Rifane; V.G. Araújo-Neto) and the Dalhousie University, Faculty of Dentistry (Canada - R.T.B. Price).

AUTHOR CONTRIBUTIONS

Conceptualization, Data curation: Sahadi BO, Giannini M. Formal analysis: Sahadi BO, Rifane TO, André CB, Araújo-Neto VG, Price RTB. Funding acquisition, Project administration,

https://doi.org/10.5395/rde.2026.51.e23

Visualization: Giannini M. Giannini M. Investigation: Rifane TO, Araújo-Neto VG, Price RTB. Methodology: Sahadi BO, Rifane TO, Araújo-Neto VG, Price RTB. Supervision: Price RTB, Giannini M. Writing - original draft: Sahadi BO, Rifane TO, Giannini M. Writing - review & editing: Price RTB, Giannini M. All authors read and approved the final manuscript.

DATA SHARING STATEMENT

The datasets are not publicly available but are available from the corresponding author upon reasonable request.

REFERENCES

1. Van Ende A, De Munck J, Lise DP, Van Meerbeek B. Bulk-fill composites: a review of the current literature. J Adhes Dent 2017;19:95-109.
2. Sengupta A, Naka O, Mehta SB, Banerji S. The clinical performance of bulk-fill versus the incremental layered application of direct resin composite restorations: a systematic review. Evid Based Dent 2023;24:143.
3. Fronza BM, Rueggeberg FA, Braga RR, Mogilevych B, Soares LE, Martin AA, *et al*. Monomer conversion, microhardness, internal marginal adaptation, and shrinkage stress of bulk-fill resin composites. Dent Mater 2015;31:1542-1551.
4. Elawsya ME, Montaser MA, El-Wassefy NA, Zaghloul NM. Depth of cure of dual- and light-cure bulk-fill resin composites. Am J Dent 2022;35:185-190.
5. Öztürk AN, Harorli OT. Bulk-fill composite in challenging cavities: conversion rate, solubility, and water absorption analysis. Odontology 2024;112:718-728.
6. Fronza BM, Ayres A, Pacheco RR, Rueggeberg FA, Dias C, Giannini M. Characterization of inorganic filler content, mechanical properties, and light transmission of bulk-fill resin composites. Oper Dent 2017;42:445-455.
7. Al-Zain AO, Ismail EH, Balhaddad AA, Toras O, Alharthy Y, Alsultan R, *et al*. Evaluation of the information provided in the instruction manuals of dental light-curing units. J Esthet Restor Dent 2024;36:1466-1476.
8. Langford DK, Wells MH, Vinall CV, Tantbirojn D, Versluis A. Using bulk-fill composite and high-intensity curing when light tip placement is compromised. Pediatr Dent 2024;46:271-276.
9. Maucoski C, Price RB, Rocha MG, Roulet JF, Sullivan B. Ability of short exposures from laser and quad-wave curing lights to photo-cure bulk-fill resin-based composites. Dent Mater 2023;39:275-292.
10. Dos Santos DB, Romano BC, Pecorari VG, Price RB, Giannini M. Effect of high irradiance and short exposure times on the depth of cure of six bulk-fill resin composites. Eur J Oral Sci 2024;132:e12990.
11. Ribeiro M, Maucoski C, Price RB, Soares CJ. Effect of a 3-second off-label exposure on the depth of cure of eight resin-based composites. Oper Dent 2024;49:421-431.
12. Par M, Marovic D, Attin T, Tarle Z, Tauböck TT. Effect of rapid high-intensity light-curing on polymerization shrinkage properties of conventional and bulk-fill composites. J Dent 2020;101:103448.
13. Ribeiro MT, Price RB, Michaud PL, Soares CJ. Physicomechanical properties of resin-based composites photo-polymerized using laser, polywave and quadwave curing lights. Dent Mater 2025;41:699-707.
14. Randolph LD, Palin WM, Bebelman S, Devaux J, Gallez B, Leloup G, *et al*. Ultra-fast light-curing resin composite with increased conversion and reduced monomer elution. Dent Mater 2014;30:594-604.
15. Rueggeberg FA, Giannini M, Arrais CA, Price RB. Light curing in dentistry and clinical implications: a literature review. Braz Oral Res 2017;31:e61.
16. ASTM International. ASTM E399-83. Standard test method for plane-strain fracture toughness of metallic materials. Annual Book of ASTM Standards. Philadelphia, PA: ASTM International; 1992. p. 676-706.
17. Alshabib A, Silikas N, Watts DC. Hardness and fracture toughness of resin-composite materials with and without fibers. Dent Mater 2019;35:1194-1203.
18. Gorsche C, Griesser M, Gescheidt G, Moszner N, Liska R. β-Allyl sulfones as addition-fragmentation chain transfer reagents: a tool for adjusting thermal and mechanical properties of dimethacrylate networks. Macromolecules 2014;47:7327-7336.
19. Szebeni D, Told R, TolKunsági-Mátéd S, Szalma J, Maróti P, Böddi K, *et al*. Monomer elution and shrinkage stress analysis of addition-fragmentation chain-transfer-modified resin composites in relation to the curing protocol. Dent Mater 2024;40:1611-1623.
20. Garoushi S, Lassila L, Vallittu PK. Impact of fast high-intensity versus conventional light-curing protocol on selected properties of dental composites. Materials (Basel) 2021;14:1381.
21. Kahnamouei MA, Bahari M, Ebrahimi Chaharom ME, Kimyai S, Daneshpooy M, Katebi K, *et al*. The effect of preheating on microhardness and flexural strength of bulk-fill

resin composites: an in-vitro study. Eur Oral Res 2024;58:133-138.
22. Barcelos LM, Braga S, Pereira R, Price RB, Soares CJ. Effect of using manufacturer-recommended exposure times to photo-activate bulk-fill and conventional resin-based composites. Oper Dent 2023;48:304-316.
23. Rosa de Lacerda L, Bossardi M, Silveira Mitterhofer WJ, Galbiatti de Carvalho F, Carlo HL, Piva E, *et al*. New generation bulk-fill resin composites: effects on mechanical strength and fracture reliability. J Mech Behav Biomed Mater 2019;96:214-218.
24. Thanoon H, Price RB, Watts DC. Thermography and conversion of fast-cure composite photocured with quad-wave and laser curing lights compared to a conventional curing light. Dent Mater 2024;40:546-556.
25. Lloyd CH, Iannetta RV. The fracture toughness of dental composites. I. The development of strength and fracture toughness. J Oral Rehabil 1982;9:55-66.
26. Zhao D, Botsis J, Drummond JL. Fracture studies of selected dental restorative composites. Dent Mater 1997;13:198-207.
27. Lohbauer U, Müller FA, Petschelt A. Influence of surface roughness on mechanical strength of resin composite versus glass ceramic materials. Dent Mater 2008;24:250-256.
28. Garoushi S, Säilynoja E, Frater M, Keulemans F, Vallittu PK, Lassila L. A comparative evaluation of commercially available short fiber-reinforced composites. BMC Oral Health 2024;24:1573.
29. Fujishima A, Ferracane JL. Comparison of four modes of fracture toughness testing for dental composites. Dent Mater 1996;12:38-43.
30. Bellinaso MD, Soares FZ, Rocha RO. Do bulk-fill resins decrease the restorative time in posterior teeth?: a systematic review and meta-analysis of in vitro studies. J Investig Clin Dent 2019;10:e12463.
31. Maghaireh GA, Albashaireh ZS, Allouz HA. Postoperative sensitivity in posterior restorations restored with self-adhesive and conventional bulk-fill resin composites: a randomized clinical split-mouth trial. J Dent 2023;137:104655.
32. Elawsya ME, Montaser MA, El-Wassefy NA, Zaghloul NM. Two-year clinical performance of dual- and light-cure bulk-fill resin composites in Class II restorations: a randomized clinical trial. Clin Oral Investig 2024;28:138.
33. Goda B, Hamdi K, Eltoukhy RI, Ali AI, Mahmoud SH. Clinical performance of different bulk-fill composite resin systems in class II cavities: a 2-year randomized clinical trial. J Esthet Restor Dent 2024;36:1122-1137.
34. Almohareb T, Alayed AA, Alzahrani KM, Maawadh AM, Almutairi B, Alhamdan RS, *et al*. Influence of curing duration and mixing techniques of bulk fill resin composites on bi-axial flexural strength and degree of conversion. J Appl Biomater Funct Mater 2020;18:2280800020975721.
35. de Mendonça BC, Soto-Montero JR, de Castro EF, Kury M, Cavalli V, Rueggeberg FA, *et al*. Effect of extended light activation and increment thickness on physical properties of conventional and bulk-filled resin-based composites. Clin Oral Investig 2022;26:3141-3150.
36. Sampaio CS, Abreu JL, Kornfeld B, Silva EM, Giannini M, Hirata R. Short curing time bulk fill composite systems: volumetric shrinkage, degree of conversion and Vickers hardness. Braz Oral Res 2024;38:e030.
37. Marovic D, Par M, Daničić P, Marošević A, Bojo G, Alerić M, *et al*. The role of rapid curing on the interrelationship between temperature rise, light transmission, and polymerisation kinetics of bulk-fill composites. Int J Mol Sci 2025;26.
38. Tantbirojn D, Versluis A, Cheng YS, Douglas WH. Fracture toughness and microhardness of a composite: do they correlate? J Dent 2003;31:89-95.

https://doi.org/10.5395/rde.2026.51.e23

RDE Restorative Dentistry & Endodontics

Research Article

eISSN 2234-7666
Restor Dent Endod. 2026 May;51(2):e24
https://doi.org/10.5395/rde.2026.51.e24

Magnitude of pulp space narrowing over time and contributing factors in teeth with vital pulp therapy: a retrospective cohort study

Akarapong Boontankun[1], Papimon Chompu-inwai[1,*], Chanika Manmontri[1], Nattakan Chaipattanawan[1], Areerat Nirunsittirat[2], Phichayut Phinyo[3,4], Trasapong Thaiupathump[5]

[1]Division of Pediatric Dentistry, Department of Orthodontics and Pediatric Dentistry, Faculty of Dentistry, Chiang Mai University, Chiang Mai, Thailand
[2]Division of Community Dentistry, Department of Family and Community Dentistry, Faculty of Dentistry, Chiang Mai University, Chiang Mai, Thailand
[3]Department of Biomedical Informatics and Clinical Epidemiology (BioCE), Faculty of Medicine, Chiang Mai University, Chiang Mai, Thailand
[4]Center for Clinical Epidemiology and Clinical Statistics, Faculty of Medicine, Chiang Mai University, Chiang Mai, Thailand
[5]Department of Computer Engineering, Faculty of Engineering, Chiang Mai University, Chiang Mai, Thailand

ABSTRACT

Objectives: This study aimed to compare the magnitude of pulp space narrowing over time—measured as the change in pulp/tooth proportion from baseline—between mandibular molars treated with different types of vital pulp therapy (VPT) and their contralateral sound molars (controls). This study also investigated factors influencing the magnitude of pulp space narrowing in molars that have undergone VPT.

Methods: This retrospective cohort study involved the assessment of bitewing radiographs of VPT-treated molars and controls at baseline and follow-up. Using reference points and lines on the radiograph, pulp/tooth proportions were measured by examiners. The intraclass correlation coefficient (ICC) was used to report examiner reliability. The changes in pulp/tooth proportions from baselines were compared between subgroups using multilevel mixed effect linear regression and the Wald test.

Results: A total of 382 bitewing radiographs from 134 teeth were included. The follow-up period ranged from 6 to 84 months (mean, 27.12 ± 17.67 months). ICC values indicated good to excellent examiner reliability. Compared to the controls, changes in pulp/tooth proportion from baselines, indicating pulp space narrowing, were significantly greater in teeth with partial pulpotomy (at pulp chamber width) and coronal pulpotomy (at pulp canal width). Factors affecting the magnitude of pulp space narrowing included the more invasive type of VPT and the more severe preoperative diagnosis.

Conclusions: The magnitude of pulp space narrowing was greater in VPT-treated molars than in controls. The more invasive type of VPT and severe preoperative diagnosis were factors contributing to the magnitude of pulp space narrowing.

Keywords: Dental pulp calcification; Dental pulp cavity; Dental pulp capping; Pulpotomy

Received: October 11, 2025 **Revised:** December 29, 2025 **Accepted:** January 11, 2026

Citation
Boontankun A, Chompu-inwai P, Manmontri C, Chaipattanawan N, Nirunsittirat A, Phinyo P, Thaiupathump T. Magnitude of pulp space narrowing over time and contributing factors in teeth with vital pulp therapy: a retrospective cohort study. Restor Dent Endod 2026;51(2):e24.

***Correspondence to**
Papimon Chompu-inwai, DDS, MS
Division of Pediatric Dentistry, Department of Orthodontics and Pediatric Dentistry, Faculty of Dentistry, Chiang Mai University, 239, Huay Kaew Road, Muang District, Chiang Mai 50200, Thailand
Email: papimon.c@cmu.ac.th

INTRODUCTION

Although vital pulp therapy (VPT) has a high success rate [1–7], one of its most common complications is pulp canal calcification (PCC) [1–4,7]. PCC refers to an increase in the production and deposition of hard tissue in response to several forms of irritation, resulting in a calcified narrowing of the pulp space [8]. Excessive calcification may impede the vitality/function of pulp tissue [9] and complicate endodontic treatment if indicated in the future [10,11]. Radiographically, studies reported a wide range of PCC, from 0% to 45%, in teeth that have undergone VPT [1–7]. However, only one study reported that 5.8% (1 out of 17 teeth) developed periapical radiolucency following total PCC or pulp obliteration in teeth treated with VPT [2]. It is worth noting that previous studies differ in VPT protocol and evaluation method of changes in pulp space. Moreover, pulp space evaluation is quite subjective, cross-sectional, and often a secondary study outcome [1–7].

Objective evaluations of calcified narrowing of the pulp space, based on changes in pulp/tooth ratio or proportion over time measured on radiographs, have been performed in previous studies on age estimation in forensic dentistry [12,13]. In general, factors influencing the narrowing of the pulp space include age, sex, drug use, and dental treatment received [14–16]. However, no study has specifically and objectively studied pulp space narrowing in VPT-treated teeth. Therefore, the objectives of this study were to (1) objectively compare the magnitude of pulp space narrowing over time, based on the change in pulp/tooth proportion values from baseline, between teeth that underwent different types of VPT and their contralateral sound molars (controls) and (2) study factors affecting the magnitude of pulp space narrowing in VPT-treated teeth.

METHODS

Study design and ethics approval

This retrospective cohort study was approved by the Human Experimentation Committee at the Faculty of Dentistry, Chiang Mai University, Chiang Mai, Thailand (registration number 39/2017). The study was conducted in accordance with the Declaration of Helsinki and reported following the Strengthening the Reporting of Observational Studies in Epidemiology (STROBE) guidelines [17].

Study participants

The study focused on the permanent mandibular molars of patients aged 6–18 years who underwent VPT, including a protective liner and base (LB), direct pulp capping (DPC), partial pulpotomy (PP), and coronal pulpotomy (CP), at the Pediatric Dentistry Clinic, Faculty of Dentistry, Chiang Mai University, Thailand from September 2012 to June 2022. The contralateral sound molars of the same patients served as controls.

For comprehensive treatment planning, preoperative bitewing radiographs on both sides were obtained for all patients; these served as the baseline for the control group. VPT was performed on the deep carious tooth within 1 to 2 weeks following the previously described VPT protocol in a published article from the same institution [18,19]. The immediate post-operative radiograph was taken and used as the baseline for the VPT group. Follow-up appointments were scheduled approximately every six months, during which bilateral bitewing radiographs were obtained, consistent with American Academy of Pediatric Dentistry recommendations for high-caries-risk patients [20]. The radiographs were positioned parallel to the crowns of the maxillary and mandibular teeth with the resultant images showing the contact areas as “opened” [21].

Sample size calculation

Sample size calculations were conducted using the program from http://powerandsamplesize.com [22], based on prior studies reporting incidences of pulp space narrowing following VPT: 35% in CP [4] and 5% in PP [1], thus at least 20 teeth was required for each treatment group. However, this study included all mandibular molars that met the inclusion criteria.

Inclusion and exclusion criteria

To be included in this study, the VPT-treated mandibular molars must have (1) a baseline and at least one follow-up bitewing radiograph of good quality; (2) no restorations or devices that interfere with the radiological evaluation of the pulp chamber; (3) all independent

https://doi.org/10.5395/rde.2026.51.e24

variables (predictors) from patient charts, including age (years, months), sex (male, female), follow-up period (recorded at one or more of the following intervals, as available: 6, 12, 18, 24, 30, 36, 48, 60, and 72 months); a preoperative pulpal diagnosis (normal pulp, reversible pulpitis, irreversible pulpitis) [23]; preoperative periapical lesion status (absence, presence); root formation status (mature, immature); type of VPT (LB, DPC, PP, CP); pulp-dressing material (ProRoot MTA, Dentsply Sirona, Tulsa, OK, USA; Biodentine, Septodont, Saint-Maur-des-Fossés, France); type of irrigant (sodium hypochlorite, normal saline solution); site of exposure (mesial, distal); and VPT outcome (success, failure).

Regarding the VPT outcome, treatment was considered successful if the treated tooth demonstrated functional clinical and radiographic survival. Clinically, the tooth did not have pulpitis symptoms, abnormal mobility, or fistula. Radiographically, the tooth showed continued root formation or improved periapical conditions, the absence of prominent lesions, and no internal or external root resorption.

The contralateral sound molars from the same patients with VPT were screened and included as controls if they had (1) the baseline and at least one bitewing radiograph from routine check-ups, and (2) all required independent variables (age, sex, follow-up period, and root formation status).

Bitewing radiographs were excluded if the necessary reference points in Figure 1A, including the cementoenamel junction points on the distal and mesial external tooth surfaces, the highest point of the pulp chamber floor, and the highest point of the furcation of the tooth, were not identifiable by the primary investigator (AB).

Data collection and outcome

The bitewing radiographs that met the inclusion criteria were saved as JPEG files and then randomly placed into sets, each containing 25 radiographs. The blinded, calibrated examiners independently assessed each set of radiographs using the Chiang Mai University–Pulp Space Measurement (CMU–PSM) program on the same computer with the same settings in the same ambient environment. The evaluation duration was limited to 40 minutes per set.

To avoid discrepancies in radiographic image expansion or distortion, the semi-automated CMU–PSM program was specifically developed to linearly measure the pulp space using four pulp/tooth proportion values on bitewing radiographs. When using the CMU–PSM program, the evaluators manually selected the reference points in Figure 1A; the program then automatically created the reference lines in Figure 1B and C. The evaluator checked and manually adjusted the margin of the reference lines as appropriate. Finally, the CMU–PSM program automatically calculated four pulp/tooth proportion values, including pulp chamber width (A1/A0), pulp canal widths (mesial, B1/B0, and distal, B2/B0), and pulpal floor thickness (C1/C0). However, the A1/A0 value was not available for teeth treated with CP because their pulp chamber was completely occupied with pulp-dressing material. All pulp/tooth proportion values were exported to a Microsoft Excel table, and the change (Δ) in these values from the baselines was computed as follows:

ΔA1/A0 = A1/A0 (baseline) – A1/A0 (follow-up)
ΔB1/B0 = B1/B0 (baseline) – B1/B0 (follow-up)
ΔB2/B0 = B2/B0 (baseline) – B2/B0 (follow-up)
ΔC1/C0 = C1/C0 (baseline) – C1/C0 (follow-up)

Sample size for reliability analyses was estimated with an online intraclass correlation coefficient (ICC) calculator (wnarifin.github.io/ssc/ssicc.html) [24] targeting an expected ICC of 0.80 with ± 0.10 precision at the 95% confidence level. This yielded required samples of 51 radiographs for intra-examiner reliability (two ratings per subject) and 29 radiographs for inter-examiner reliability. The radiographs were independently evaluated by four blinded evaluators (three faculty members and one master's student in pediatric dentistry), with reassessment after a 2-week interval for intra-examiner reliability.

The primary investigator (AB) extracted all independent variables from patients' charts. All values were derived from radiographic measurements performed by the calibrated independent evaluators. The dependent variables were the changes from baseline in four pulp/tooth proportion values (ΔA1/A0, ΔB1/B0, ΔB2/B0, ΔC1/C0) assessed at each follow-up. In cases of total PCC, defined in this study as the complete radiographic absence of a discernible pulp space throughout the pulp chamber and root canal, quantitative measurements could not be performed, and these cases were recorded

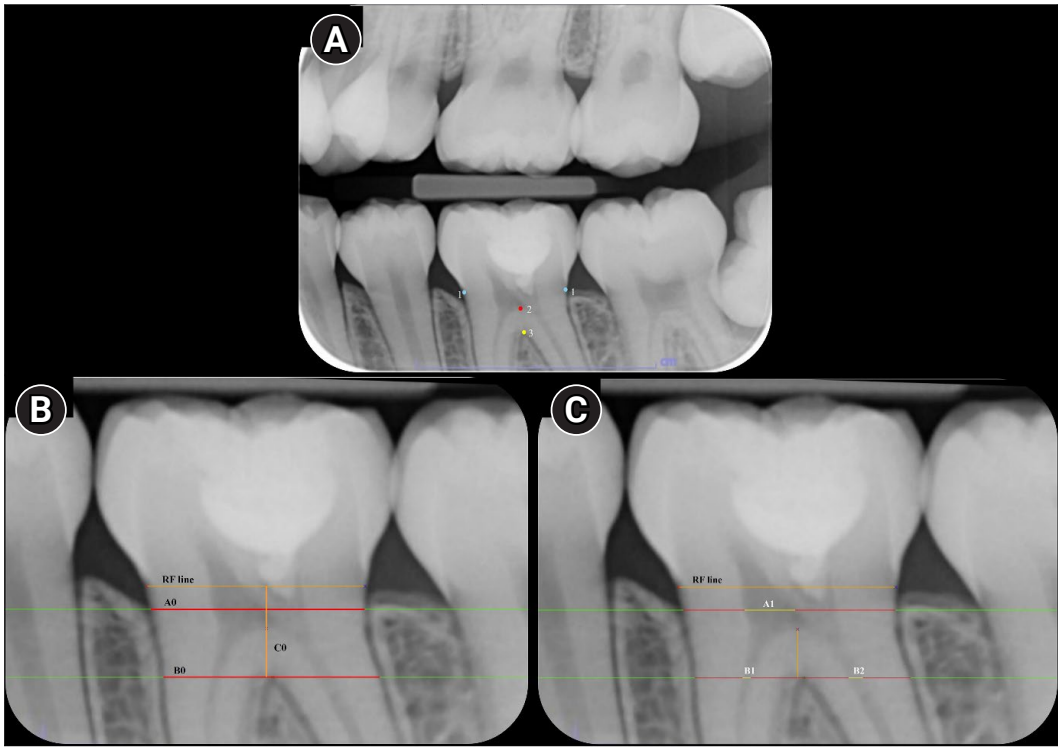

Figure 1. Reference points and lines on a bitewing radiograph used in this study. (A) Reference points: (1) blue points were the cementoenamel junction points on the distal and mesial external tooth surfaces; (2) a red point was the highest point of the pulp chamber floor; and (3) a yellow point was the highest point of the furcation. (B) Reference lines (RF line): the line connecting the mesial and distal cementoenamel junction points; B0 is a horizontal line/distance, paralleling to the RF line, between the mesial and the distal external root surfaces at the level of the fornix of furcation; C0 is the vertical and perpendicular line/distance between the RF line and the B0 line; A0 is the horizontal line/distance, paralleling to the RF line, between the mesial and the distal external root surfaces at the level of the occlusal one fourth of the C0 distance. (C) RF lines: A1 is the horizontal distance of pulp chamber from the mesial to the distal external pulp chamber surfaces at the level of the occlusal one fourth of the C0 distance; B1 is the horizontal distance of the mesial canal at the level of the fornix of furcation; B2 is the horizontal distance of the distal canal at the level of the fornix of furcation and C1 is the vertical distance between the floor of pulp chamber point and the fornix of furcation point.

as total PCC.

The study addressed two main outcomes: (1) differences in changes of pulp space from baseline, by measuring the pulp/tooth proportion at different follow-ups between the VPT-treated and contralateral sound molars and (2) contributing factors associated with changes of the pulp space from baselines in the VPT-treated teeth.

Statistical methods

For intra-examiner reliability, the four pulp/tooth proportion values from the first and second measurements from each evaluator were analyzed using the ICC (two-way mixed model; type, single measurement; definition, absolute agreement). For inter-examiner reliability, the same four proportion values from all evaluators were analyzed using the ICC (two-way random model; type, single measure; definition, absolute agreement). ICCs were calculated using IBM SPSS ver. 19.0 (IBM Corp, Armonk, NY, USA), with an acceptable score set at 0.8 (good reliability), and scores above 0.9 considered excellent reliability [25].

Longitudinal missing data were handled using the last observation carried forward (LOCF) approach [26]. To evaluate the change in pulp/tooth proportion values from baseline, linear mixed-effects models were fitted, assuming a Gaussian distribution for the outcome. The models included fixed effects for treatment type (VPT

https://doi.org/10.5395/rde.2026.51.e24

vs. control), follow-up time (in months, modeled as a continuous variable with both linear and quadratic terms), and their interaction. Additional fixed covariates were included if they were potential confounders of the main determinants. To account for the hierarchical and longitudinal data structure, random effects were specified at the tooth level, with a random slope for time to model repeated measurements within each tooth. No additional patient-level random effects were included because each tooth represented the unit of analysis. Wald tests were applied to assess the statistical significance of associations between independent variables and each outcome at each follow-up time point. Stata software ver. 16.0 (StataCorp LLC, College Station, TX, USA) was used for analysis.

RESULTS

All ICC values were above 0.8, with several exceeding 0.9, indicating good to excellent intra- and inter-examiner reliability.

Demographic data

Of 635 teeth from 400 patients, a total of 134 VPT-treated teeth from 131 patients, with 382 bitewing radiographs, met the inclusion criteria. The follow-up period ranged from 6 to 84 months (mean, 27.12 ± 17.67 months). Missing data amounted to 58.2% of the total. From the same patients who received VPT, 20 contralateral sound molars with 60 bitewing radiographs at different recall periods were included in the control group.

Demographic data of patients with VPT-treated teeth and the control group are summarized in Tables 1 and 2, respectively. Table 3 shows the incidence of total PCC, which was observed in 14/134 teeth (10.4%), involving a higher number of teeth with PP (7/134, 5.2%) and CP (6/134, 4.5%). Only one VPT failure was found in this total PCC group (1/14, 7.1%). This failed tooth also exhibited a fracture in the composite resin restoration.

Comparison of the changes from baseline in pulp/tooth proportion values between molars with different types of vital pulp therapy and controls

Figure 2 illustrates the change from baseline in pulp/tooth proportion between teeth treated with different types of VPT and controls. A general trend of progressive decreases in all four pulp/tooth proportion values

Table 1. Demographic data of the study group with vital pulp therapy-treated teeth

Demographic information	Data
No. of cases	134
Age at treatment (yr)	
Range	6–18
Mean ± SD	9.8 ± 1.9
≥6, ≤8	33 (24.6)
>8, ≤10	46 (34.3)
>10, ≤12	44 (32.8)
>12	11 (8.2)
Sex	
Male	54 (40.3)
Female	80 (59.7)
Follow-up (mo)	
Range	6–84
Mean ± SD	27.12 ± 17.64
Median (IQR)	24 (13.75–37.25)
Root formation status	
Mature	66 (49.3)
Immature	68 (50.7)
Preoperative pulpal diagnosis	
Normal pulp	20 (14.9)
Reversible pulpitis	43 (32.1)
Irreversible pulpitis	71 (52.9)
Preoperative periapical lesion status	
Presence	36 (26.9)
Absence	98 (73.1)
Type of vital pulp therapy	
Protective liner and base	25 (18.7)
Direct pulp capping	27 (20.1)
Partial pulpotomy	51 (38.1)
Coronal pulpotomy	31 (23.1)
Pulp dressing materials (n = 134)	
ProRoot MTA	105 (78.4)
Biodentine	29 (21.6)
Type of irrigants (n = 134)	
Normal saline solution	40 (29.9)
Sodium hypochlorite	94 (70.1)
Site of exposure (n = 103)a)	
Mesial	55 (53.4)
Distal	48 (46.6)
Vital pulp therapy outcome (n = 134)	
Success	127 (94.8)
Failure	7 (5.2)

Values are presented as a number (%) unless otherwise specified.
SD, standard deviation, IQR, interquartile range.

over time was observed. Notably, for ΔA1/A0, the proportion changes were significantly greater in the PP group compared to the control group at 12, 18, 24, 30, 36, and 48 months in Figure 2A. For ΔB1/B0, the changes were significantly greater in the CP group than in the controls at all times, except for 72 months in Figure 2B. For ΔB2/B0, the CP group also showed significantly greater change compared to the controls at all follow-up points in Figure 2C. In contrast, the changes in ΔC1/C0 of each VPT group were not significantly different from those of the control group at 6–60 months; however, the LB group displayed significantly lower change values than the controls at 72 months in Figure 2D. The fixed- and random-effects models for changes from baseline in pulp/tooth proportion values between teeth treated with different types of VPT and controls, including their marginal predictions and pairwise contrast *p*-values, are presented in Supplementary Tables 1–12.

Table 2. Demographic data of the control group

Demographic information	Data
Age at treatment (yr) (*n* = 20)	
Range	6–12
Mean ± SD	9.86 ± 1.47
≥6, ≤8	4 (20.0)
>8, ≤10	7 (35.0)
>10, ≤12	9 (45.0)
>12	0 (0)
Sex (n = 20)	
Male	6 (30.0)
Female	14 (70.0)
Follow-up (mo) (*n* = 20)	
Range	6–52
Mean ± SD	23.80 ± 13.14
Median (Interquartile range)	21 (14.0–32.75)
Root formation status (*n* = 20)	
Mature	10 (50.0)
Immature	10 (50.0)

Values are presented as a number (%) unless otherwise specified.
SD, standard deviation, IQR, interquartile range.

Table 3. Incidence of total pulp canal calcification and failure rate from different types of vital pulp therapy

Type of vital pulp therapy	Total pulp canal calcification (*n* = 134)	Total pulp canal calcification and treatment failure (*n* = 14)
Protective liner and base	0 (0)	0 (0)
Direct pulp capping	1 (0.7)	0 (0)
Partial pulpotomy	7 (5.2)	1 (7.1)
Coronal pulpotomy	6 (4.5)	0 (0)
Total	14 (10.4)	1 (7.1)

Values are presented as a number (%).

Differences in the changes from baseline of pulp/tooth proportion values between the subgroups

The factors that contributed to significant differences between subgroups in change from baseline of pulp/tooth proportion values were VPT type and preoperative pulpal diagnosis.

Type of vital pulp therapy

Figure 3 illustrates changes from baseline in pulp/tooth proportion values in the DPC, PP, and CP groups against those in the LB group. Notably, for the ΔA1/A0 value, changes were significantly greater in the PP group than in the LB group at 12, 18, 24, 30, 36, 48, 60, and 72 months in Figure 3A. In contrast, the changes in ΔB1/B0 of the CP, PP, and DPC groups did not significantly differ from those of the LB group at any follow-up point in Figure 3B. Furthermore, for ΔB2/B0, decreases were significantly greater in the CP group than in the LB group at all follow-up points, except at 6 months (Figure 3C). Finally, for ΔC1/C0, decreases were significantly greater in the PP group than in the LB group at 60 and 72 months in Figure 3D. Figure 4 illustrates different magnitudes of pulp space narrowing over time in different types of VPT cases. The fixed- and random-effects models for changes from baseline in pulp/tooth proportion values (ΔA1/A0) in the DPC, PP, and CP groups compared with those in the LB group, including their marginal predictions and pairwise contrast *p*-values, are presented in Supplementary Tables 13–24.

Preoperative pulpal diagnosis

Figure 5 illustrates changes from baseline of pulp/tooth proportion values in the different groups of preoperative pulpal diagnosis, against the normal pulp group. For the ΔA1/A0 value, changes were significantly greater in the irreversible pulpitis group compared to the normal pulp group at 18, 24, 30, and 36 months in Figure 5A. The changes in ΔB1/B0 for the irreversible and reversible pulpitis groups did not differ significantly from those in the normal pulp group at any follow-up point in Figure

https://doi.org/10.5395/rde.2026.51.e24

5B. For ΔB2/B0, the change was significantly greater in the irreversible pulpitis group compared to the normal pulp group at 72 months in Figure 5C. In terms of ΔC1/C0, the decreases in proportion were significantly greater in the irreversible pulpitis group than in the normal pulp group at 48, 60, and 72 months in Figure 5D. The fixed- and random-effects models for changes from baseline in pulp/tooth proportion values (ΔA1/A0) across different preoperative pulpal diagnosis groups, compared with the normal pulp group, including their marginal predictions and pairwise contrast *p*-values, are presented in Supplementary Tables 25–36.

DISCUSSION

To our knowledge, this study provides a longitudinal and objective evaluation of pulp space narrowing after VPT using pulp/tooth proportion analysis. Unlike previous reports that relied on subjective assessments at single time points, our approach quantified dimensional changes across follow-up periods. Distinct patterns of narrowing were observed. Pulp chamber width (ΔA1/A0) decreased more prominently in teeth that underwent PP, while pulp canal width narrowing (ΔB1/B0 and ΔB2/B0) was greater following CP. These findings highlight that the anatomical level of intervention influences the site of subsequent calcification. In addition, pulp space narrowing was associated with the invasiveness of the VPT procedure and with severe preoperative diagnoses, suggesting that both treatment factors and baseline pathology contribute to the calcification process. Clinically, this indicates the need for long-term radiographic monitoring, particularly in teeth treated with more extensive procedures, as excessive calcification

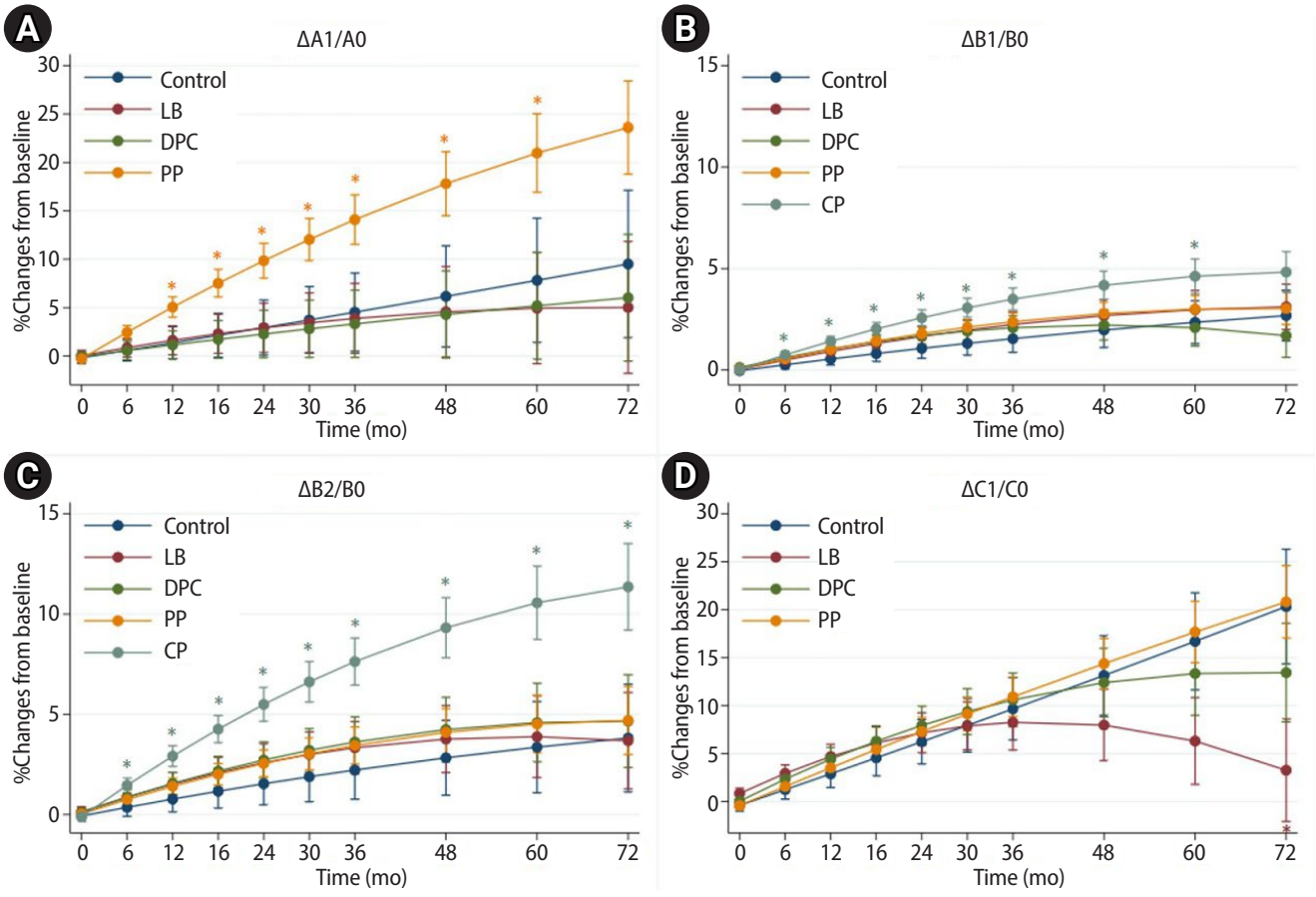

Figure 2. Comparison of the changes from baseline in pulp/tooth proportion values (A–D) between teeth treated with different types of vital pulp therapy and controls. LB, protective liner and base; DPC, direct pulp capping; PP, partial pulpotomy; CP, coronal pulpotomy. *$p < 0.05$, statistically significant.

may increase the complexity of future root canal treatment should it become necessary.

The observation that pulp space also narrows in sound molars aligns with physiological secondary dentin deposition in response to normal stimuli [27]. In sound teeth, secondary dentin deposition is age-dependent; Philippas [14] reported higher rates in younger individuals, with significant slowing at the root canal level after age 20 years. Our study population, aged 6–18 years, reflected this period of heightened activity, yet the differences between sound and treated teeth remained significant. Mechanisms of pulp space narrowing were previously explained for traumatized [28] and restored teeth [16]. Traumatic injuries can disrupt the blood supply, leading to reduced pulpal cellularity due to odontoblast destruction, with replacement by undifferentiated mesenchymal cells that deposit reparative dentin in an unregulated manner [28]. In restored teeth, calcification often occurs in the coronal pulp beneath restorations [16] or near sites of stimulation [29]. The severity of injury influences the rate of PCC, with tertiary dentin deposition occurring significantly faster than primary or secondary deposition [30]. Primary dentin is deposited at 4–8 μm/day until functional occlusion is achieved [31], after which secondary dentin deposition slows to 0.4 μm/day [32]. In contrast, tertiary dentin, often associated with severe injury or inflammation, can be deposited at rates of up to 3.5 μm/day [33].

The type of VPT and the preoperative pulpal diagnosis significantly influenced the magnitude of pulp space narrowing in this study. Our findings align with prior research indicating that more invasive treatments are associated with greater pulp space reduction [30]. The selection of VPT type often reflects the severity of

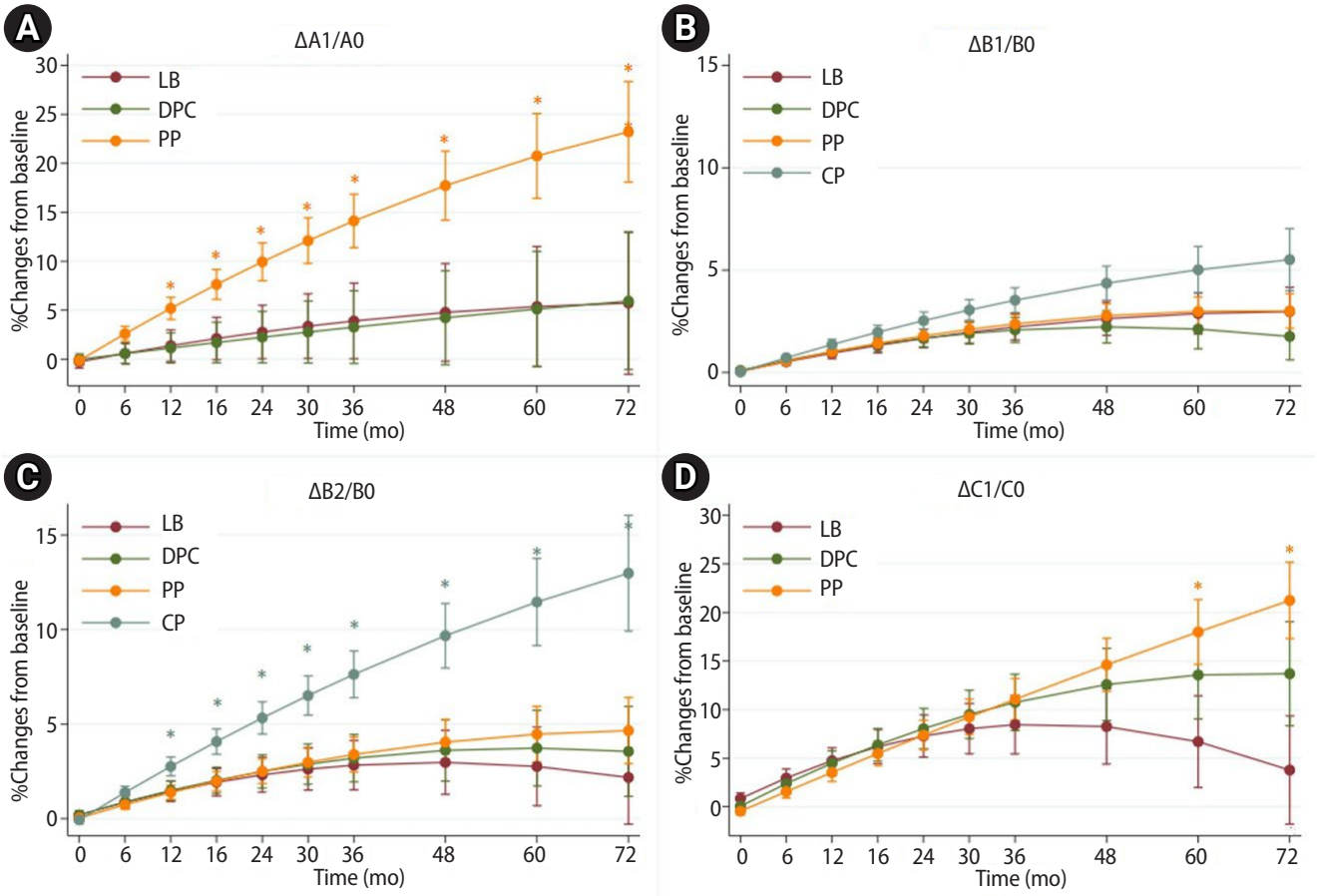

Figure 3. Comparison of the changes from baseline in pulp/tooth proportion values (A–D) in the DPC, PP, and CP groups against those in the LB group. LB, protective liner and base; DPC, direct pulp capping; PP, partial pulpotomy; CP, coronal pulpotomy. *$p < 0.05$, statistically significant.

https://doi.org/10.5395/rde.2026.51.e24

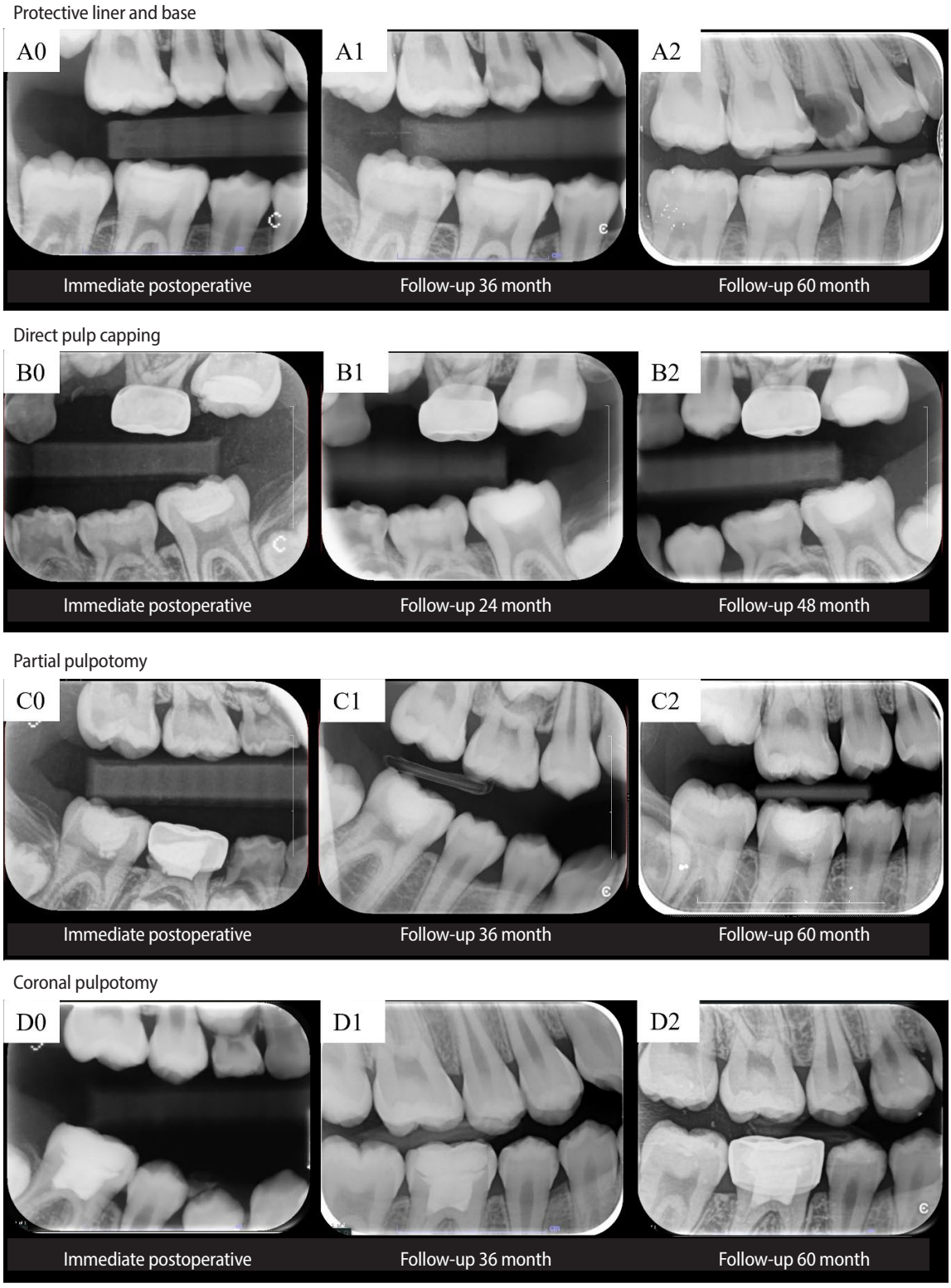

Figure 4. Radiographs demonstrate pulp space narrowing over time following different types of vital pulp therapy. A greater magnitude of pulp space narrowing was observed in teeth treated with partial and coronal pulpotomy.

pulpal injury and inflammation, with more extensively affected teeth receiving more invasive interventions [34]. Additionally, the larger contact area between the pulp tissue and pulp-dressing materials in PP and CP may promote the formation of a calcified barrier beneath the material, thereby increasing the likelihood of PCC [27]. This enhanced contact may also facilitate the release of growth factors involved in the calcification process [27]. However, the specific biological mechanisms linking different VPT procedures to PCC remain unclear and warrant further investigation.

In addition, the changes in proportion at the pulp canal width (ΔB1/B0 and ΔB2/B0) indicated a similar trend between the distal and mesial roots; however, the change in proportion (ΔB1/B0) in the mesial root showed no significant difference across VPT types. This lack of significant differences may be attributed to the smaller diameter of mesial roots compared to distal roots. In mandibular first molars, the distal root exhibits a greater pulp/tooth area ratio than the mesial root, as measured by cone-beam computed tomography (CBCT) [35]. Consequently, the smaller canal diameter in the mesial root may have obscured detectable changes in proportion at the orifice in our study.

Narrowing of the pulp space, typically resulting from PCC, was observed to increase over time in this study. This phenomenon has important clinical implications. Current management practices for PCC include either early endodontic treatment or continuous monitoring [8]. Although histological studies indicate that teeth with PCC do not exhibit pathological pulpal inflammation [9], the condition may nonetheless complicate future root canal procedures. Previous studies reported PCC incidences ranging from 0% to 45% [1–7], but only

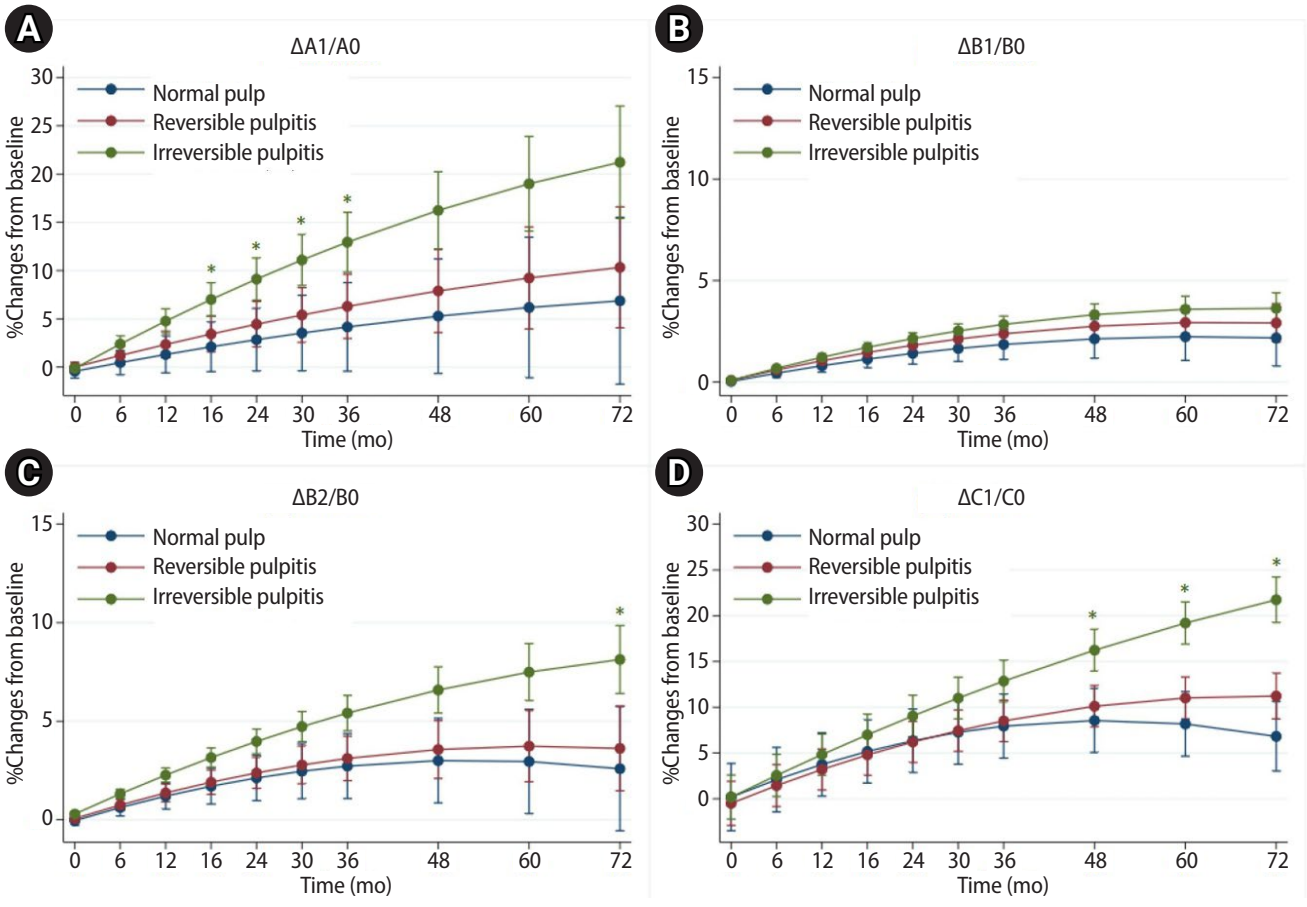

Figure 5. Comparison of the changes from baseline of pulp/tooth proportion values (A–D) in the different groups of preoperative pulpal diagnosis, against the normal pulp group. *$p < 0.05$, statistically significant.

https://doi.org/10.5395/rde.2026.51.e24

one documented pulp necrosis (5.8%) in teeth with complete PCC after CP [2]. In our study, only one out of 14 teeth with total PCC showed VPT failure (7.1%); this case involved a fractured restoration, complicating the attribution of failure specifically to PCC. Further research is needed to determine the true clinical impact of total PCC and establish evidence-based guidelines for the timing of endodontic intervention in VPT-treated teeth.

Although this study provides, to our knowledge, early insights into PCC and the narrowing of pulp space over time in VPT-treated teeth, it has some limitations. First, the retrospective design led to substantial data exclusion due to missing or poor-quality radiographs. Second, the limited diversity of irrigants and pulp-dressing materials, along with the narrow age range of participants, may affect generalizability. Third, the CMU–PSM program used for pulp/tooth proportion measurement is constrained by its reliance on two-dimensional measurements. While CBCT and histological techniques offer more accurate assessments [9,36,37], they are less practical for clinical use due to cost, accessibility, and higher radiation exposure [38]. Fourth, although 58.2% of the data were missing, the trends observed in the raw data were consistent with those obtained using the LOCF method, supporting the reliability of this imputation approach. While LOCF is generally suboptimal due to its assumption of no further change, its use was considered reasonable here given the gradual and biologically plausible progression of pulp/tooth proportion values over time. Lastly, formal simulation-based power estimation was not conducted because it would have required assumptions about unknown parameters; therefore, some residual uncertainty in statistical precision cannot be completely excluded. Future prospective studies with larger and more diverse samples are needed to confirm these findings and improve methodological robustness.

CONCLUSIONS

This study observed that the molars treated with VPT tended to exhibit a greater magnitude of pulp space narrowing over time compared with the contralateral sound molars. The degree of narrowing appeared to be associated with the invasiveness of the VPT procedure and the severity of the preoperative pulpal diagnosis. These observations may provide information that clinicians could consider when interpreting long-term pulpal changes following VPT; however, further prospective studies are needed to better elucidate the clinical significance of these findings and to inform appropriate monitoring or management approaches.

CONFLICT OF INTEREST

No potential conflict of interest relevant to this article was reported.

FUNDING/SUPPORT

This study was financially supported by the Research Fund for Postgraduate Students of the Faculty of Dentistry, Chiang Mai University.

ACKNOWLEDGMENTS

The authors would like to thank Dr. Boonchanit Nophachatsathid, a former master's student in pediatric dentistry, for contributing to the measurement of the pulp space.

AUTHOR CONTRIBUTIONS

Conceptualization, Investigation: Boontankun A, Chompu-inwai P, Manmontri C, Chaipattanawan N. Data curation: Boontankun A, Chompu-inwai P, Manmontri C, Chaipattanawan N, Phinyo P. Formal analysis: Boontankun A, Phinyo P. Funding acquisition: Boontankun A, Chompu-inwai P. Methodology: All authors. Project administration: Boontankun A. Resources: Chompu-inwai P. Software: Thaiupathump T. Supervision: Chompu-inwai P. Validation: Boontankun A, Chompu-inwai P, Phinyo P, Nirunsittirat A. Visualization: Boontankun A, Chompu-inwai P. Writing - original draft: Boontankun A, Chompu-inwai P. Writing - review & editing: All authors. All authors read and approved the final manuscript.

DATA SHARING STATEMENT

The datasets are not publicly available but are available from the corresponding author upon reasonable request.

SUPPLEMENTARY MATERIALS

Supplementary Table 1. Fixed and random-effects model for the changes from baseline in pulp/tooth proportion values (ΔA1/A0) between teeth treated with different types of vital pulp therapy and controls

Supplementary Table 2. Marginal predicted values of the fixed and random-effects model for the changes from baseline in pulp/tooth proportion values (ΔA1/A0) between teeth treated with different types of vital pulp therapy and controls

Supplementary Table 3. Bonferroni-adjusted *p*-values for contrasts of the marginal predicted values of the fixed and random-effects model for the changes from baseline in pulp/tooth proportion values (ΔA1/A0) between teeth treated with

different types of vital pulp therapy and controls
Supplementary Table 4. Fixed and random-effects model for the changes from baseline in pulp/tooth proportion values (ΔB1/B0) between teeth treated with different types of vital pulp therapy and controls
Supplementary Table 5. Marginal predicted values of the fixed and random-effects model for the changes from baseline in pulp/tooth proportion values (ΔB1/B0) between teeth treated with different types of vital pulp therapy and controls
Supplementary Table 6. Bonferroni-adjusted *p*-values for contrasts of the marginal predicted values of the fixed and random-effects model for the changes from baseline in pulp/tooth proportion values (ΔB1/B0) between teeth treated with different types of vital pulp therapy and controls
Supplementary Table 7. Fixed and random-effects model for the changes from baseline in pulp/tooth proportion values (ΔB2/B0) between teeth treated with different types of vital pulp therapy and controls
Supplementary Table 8. Marginal predicted values of the fixed and random-effects model for the changes from baseline in pulp/tooth proportion values (ΔB2/B0) between teeth treated with different types of vital pulp therapy and controls
Supplementary Table 9. Bonferroni-adjusted *p*-values for contrasts of the marginal predicted values of the fixed and random-effects model for the changes from baseline in pulp/tooth proportion values (ΔB2/B0) between teeth treated with different types of vital pulp therapy and controls
Supplementary Table 10. Fixed and random-effects model for the changes from baseline in pulp/tooth proportion values (ΔC1/C0) between teeth treated with different types of vital pulp therapy and controls
Supplementary Table 11. Marginal predicted values of the fixed and random-effects model for the changes from baseline in pulp/tooth proportion values (ΔC1/C0) between teeth treated with different types of vital pulp therapy and controls
Supplementary Table 12. Bonferroni-adjusted *p*-values for contrasts of the marginal predicted values of the fixed and random-effects model for the changes from baseline in pulp/tooth proportion values (ΔC1/C0) between teeth treated with different types of vital pulp therapy and controls
Supplementary Table 13. Fixed and random-effects model for the changes from baseline in pulp/tooth proportion values (ΔA1/A0) in the DPC and PP groups against those in the LB group
Supplementary Table 14. Marginal predicted values of the fixed and random-effects model for the changes from baseline in pulp/tooth proportion values (ΔA1/A0) in the DPC and PP groups against those in the LB group
Supplementary Table 15. Bonferroni-adjusted *p*-values for contrasts of the marginal predicted values of the fixed and random-effects model for the changes from baseline in pulp/tooth proportion values (ΔA1/A0) in the DPC and PP groups against those in the LB group
Supplementary Table 16. Fixed and random-effects model for the changes from baseline in pulp/tooth proportion values (ΔB1/B0) in the DPC, PP, and CP groups against those in the LB group
Supplementary Table 17. Marginal predicted values of the fixed and random-effects model for the changes from baseline in pulp/tooth proportion values (ΔB1/B0) in the DPC, PP, and CP groups against those in the LB group
Supplementary Table 18. Bonferroni-adjusted *p*-values for contrasts of the marginal predicted values of the fixed and random-effects model for the changes from baseline in pulp/tooth proportion values (ΔB1/B0) in the DPC, PP, and CP groups against those in the LB group
Supplementary Table 19. Fixed and random-effects model for the changes from baseline in pulp/tooth proportion values (ΔB2/B0) in the DPC, PP, and CP groups against those in the LB group
Supplementary Table 20. Marginal predicted values of the fixed and random-effects model for the changes from baseline in pulp/tooth proportion values (ΔB2/B0) in the DPC, PP, and CP groups against those in the LB group
Supplementary Table 21. Bonferroni-adjusted *p*-values for contrasts of the marginal predicted values of the fixed and random-effects model for the changes from baseline in pulp/tooth proportion values (ΔB2/B0) in the DPC, PP, and CP groups against those in the LB group
Supplementary Table 22. Fixed and random-effects model for the changes from baseline in pulp/tooth proportion values (ΔC1/C0) in the DPC and PP groups against those in the LB group
Supplementary Table 23. Marginal predicted values of the fixed and random-effects model for the changes from baseline in pulp/tooth proportion values (ΔC1/C0) in the DPC and PP groups against those in the LB group
Supplementary Table 24. Bonferroni-adjusted p-values for contrasts of the marginal predicted values of the fixed and random-effects model for the changes from baseline in pulp/tooth proportion values (ΔC1/C0) in the DPC and PP groups against those in the LB group
Supplementary Table 25. Fixed and random-effects model for the changes from baseline of pulp/tooth proportion values (ΔA1/A0) in the different groups of preoperative pulpal diagnosis, against the normal pulp group
Supplementary Table 26. Marginal predicted values of the fixed and random-effects model for the changes from baseline of pulp/tooth proportion values (ΔA1/A0) in the different groups of pre-operative pulpal diagnosis, against the normal pulp group
Supplementary Table 27. Bonferroni-adjusted p-values for contrasts of the marginal predicted values of the fixed and random-effects model for the changes from baseline of pulp/tooth proportion values (ΔA1/A0) in the different groups of preoperative pulpal diagnosis, against the normal pulp group
Supplementary Table 28. Fixed and random-effects model for the changes from baseline of pulp/tooth proportion values (ΔB1/B0) in the different groups of pre-operative pulpal diagnosis, against the normal pulp group
Supplementary Table 29. Marginal predicted values of the fixed and random-effects model for the changes from baseline of pulp/tooth proportion values (ΔB1/B0) in the different groups of preoperative pulpal diagnosis, against the normal

https://doi.org/10.5395/rde.2026.51.e24

pulp group
Supplementary Table 30. Bonferroni-adjusted *p*-values for contrasts of the marginal predicted values of the fixed and random-effects model for the changes from baseline of pulp/tooth proportion values (ΔB1/B0) in the different groups of preoperative pulpal diagnosis, against the normal pulp group
Supplementary Table 31. Fixed and random-effects model for the changes from baseline of pulp/tooth proportion values (ΔB2/B0) in the different groups of preoperative pulpal diagnosis, against the normal pulp group
Supplementary Table 32. Marginal predicted values of the fixed and random-effects model for the changes from baseline of pulp/tooth proportion values (ΔB2/B0) in the different groups of preoperative pulpal diagnosis, against the normal pulp group
Supplementary Table 33. Bonferroni-adjusted *p*-values for contrasts of the marginal predicted values of the fixed and random-effects model for the changes from baseline of pulp/tooth proportion values (ΔB2/B0) in the different groups of preoperative pulpal diagnosis, against the normal pulp group
Supplementary Table 34. Fixed and random-effects model for the changes from baseline of pulp/tooth proportion values (ΔC1/C0) in the different groups of preoperative pulpal diagnosis, against the normal pulp group
Supplementary Table 35. Marginal predicted values of the fixed and random-effects model for the changes from baseline of pulp/tooth proportion values (ΔC1/C0) in the different groups of preoperative pulpal diagnosis, against the normal pulp group
Supplementary Table 36. Bonferroni-adjusted *p*-values for contrasts of the marginal predicted values of the fixed and random-effects model for the changes from baseline of pulp/tooth proportion values (ΔC1/C0) in the different groups of preoperative pulpal diagnosis, against the normal pulp group

REFERENCES

1. Sharma P, Garg S, Dhindsa A, Jain N, Joshi S, Gupta A. Effect of chlorhexidine gluconate as hemostatic agent in healing and repair after mineral trioxide aggregate vital pulp therapy in young permanent teeth: a clinical study. Indian J Physiol Pharmacol 2021;65:222-228.
2. Linsuwanont P, Wimonsutthikul K, Pothimoke U, Santiwong B. Treatment outcomes of mineral trioxide aggregate pulpotomy in vital permanent teeth with carious pulp exposure: the retrospective study. J Endod 2017;43:225-230.
3. Taha NA, Abdulkhader SZ. Full pulpotomy with biodentine in symptomatic young permanent teeth with carious exposure. J Endod 2018;44:932-937.
4. Eid A, Mancino D, Rekab MS, Haikel Y, Kharouf N. Effectiveness of three agents in pulpotomy treatment of permanent molars with incomplete root development: a randomized controlled trial. Healthcare (Basel) 2022;10:431.
5. Mass E, Zilberman U. Long-term radiologic pulp evaluation after partial pulpotomy in young permanent molars. Quintessence Int 2011;42:547-554.
6. Asgary S, Eghbal MJ. Treatment outcomes of pulpotomy in permanent molars with irreversible pulpitis using biomaterials: a multi-center randomized controlled trial. Acta Odontol Scand 2013;71:130-136.
7. Lipski M, Nowicka A, Kot K, Postek-Stefańska L, Wysoczańska-Jankowicz I, Borkowski L, *et al*. Factors affecting the outcomes of direct pulp capping using Biodentine. Clin Oral Investig 2018;22:2021-2029.
8. Boontankun A, Manmontri C, Chaipattanawan N, Chompu-inwai P. Pulp canal calcification in young permanent teeth that have undergone vital pulp therapy: a review. Pediatr Dent J 2023;33:199-210.
9. Patterson SS, Mitchell DF. Calcific metamorphosis of the dental pulp. Oral Surg Oral Med Oral Pathol 1965;20:94-101.
10. McCabe PS, Dummer PM. Pulp canal obliteration: an endodontic diagnosis and treatment challenge. Int Endod J 2012;45:177-197.
11. American Association of Endodontists (AAE). Treatment standards [Internet]. Chicago, IL: AAE; 2020 [cited 2023 Mar 15]. Available from: https://www.aae.org/specialty/wp-content/uploads/sites/2/2018/04/TreatmentStandards_WhitePaper_v1.pdf?utm_source=chatgpt.com
12. Khojastepour L, Rahimizadeh N, Khayat A. Morphologic measurements of anatomic landmarks in pulp chambers of human first molars: a study of bitewing radiographs. Iran Endod J 2008;2:147-151.
13. Jeon HM, Kim JH, Heo JY, Ok Sm, Jeong SH, Ahn YW. Age estimation by radiological measuring pulp chamber of mandibular first molar in Korean adults. J Oral Med Pain 2015;40:146-154.
14. Philippas GG. Influence of occlusal wear and age on formation of dentin and size of pulp chamber. J Dent Res 1961;40:1186-1198.
15. Chigono Y, Daimon T, Miyagawa M, Miake Y, Moriguchi M, Tanabe Y, *et al*. Dental pulp changes observed in a patient on long-term corticosteroids. J Hard Tissue Biol 2007;16:31-35.
16. Fleig S, Attin T, Jungbluth H. Narrowing of the radicular pulp space in coronally restored teeth. Clin Oral Investig 2017;21:1251-1257.
17. von Elm E, Altman DG, Egger M, Pocock SJ, Gøtzsche PC, Vandenbroucke JP. The Strengthening the Reporting of Observational Studies in Epidemiology (STROBE) statement:

guidelines for reporting observational studies. J Clin Epidemiol 2008;61:344-349.
18. Machareonsap H, Chompu-Inwai P, Chaipattanawan N, Manmontri C, Nirunsittirat A, Phinyo P. Normal saline or sodium hypochlorite irrigation for vital pulp therapy?: a non-inferiority randomized controlled trial. Eur Endod J 2024;9:180-190.
19. Parinyaprom N, Nirunsittirat A, Chuveera P, Na Lampang S, Srisuwan T, Sastraruji T, *et al*. Outcomes of direct pulp capping by using either proroot mineral trioxide aggregate or biodentine in permanent teeth with carious pulp exposure in 6- to 18-year-old patients: a randomized controlled trial. J Endod 2018;44:341-348.
20. American Academy of Pediatric Dentistry. Caries-risk assessment and management for infants, children, and adolescents. Ref Man Pediatr Dentistry 2020;2:66-72.
21. Iannucci JM, Howerton LJ. Dental radiography: principles and techniques. 6th ed. St. Louis, MO: Elsevier; 2021.
22. PowerAndSampleSize.com. Power and sample size calculators [Internet]. PowerAndSampleSize; c2026 [cited 2023 Mar 15]. Available from: http://powerandsamplesize.com/calculators/
23. American Association of Endodontists (AAE). Endodontic diagnosis [Internet]. Chicago, IL: AAE; 2013 [cited 2023 Mar 4] Available from: https://www.aae.org/specialty/wp-content/uploads/sites/2/2017/07/endodonticdiagnosisfall2013.pdf
24. Arifin WN. A web-based sample size calculator for reliability studies. Educ Med J 2018;10:67-76.
25. Koo TK, Li MY. A guideline of selecting and reporting intraclass correlation coefficients for reliability research. J Chiropr Med 2016;15:155-163.
26. Liu X. Methods for handling missing data. In: Liu X, editor. Methods and applications of longitudinal Data Analysis. Oxford: Academic Press; 2016. p. 441-73.
27. Liu X. Methods and Applications of Longitudinal Data Analysis. Amsterdam: Academic Press; 2015.
28. Nanci A. Ten Cate's oral histology: development, structure, and function. 9th ed. St Louis, MO: Elsevier; 2018.
29. Sener S, Cobankara FK, Akgünlü F. Calcifications of the pulp chamber: prevalence and implicated factors. Clin Oral Investig 2009;13:209-215.
30. Walton RE, Torabinejad M. Principles and practice of endodontics. 3rd ed. St Louis, MO: W.B. Saunders; 2002.
31. Kumar GS. Orban's oral histology and embryology. 14th ed. Noida: Elsevier India; 2015.
32. Simon S, Smith AJ, Lumley PJ, Cooper PR, Berdal A. The pulp healing process: from generation to regeneration. Endod Topics 2012;26:41-56.
33. Hegde S, Mallya L. Calcific metamorphosis: an insight. Indian J Med Forensic Med Toxicol 2019;13:199-202.
34. Ghoddusi J, Forghani M, Parisay I. New approaches in vital pulp therapy in permanent teeth. Iran Endod J 2014;9:15-22.
35. Chaleefong M, Prapayasatok S, Nalampang S, Louwakul P. Comparing the pulp/tooth area ratio and dentin thickness of mandibular first molars in different age groups: a cone-beam computed tomography study. J Conserv Dent 2021;24:158-162.
36. Piattelli A, Trisi P. Pulp obliteration: a histological study. J Endod 1993;19:252-254.
37. Krastl G, Zehnder MS, Connert T, Weiger R, Kühl S. Guided endodontics: a novel treatment approach for teeth with pulp canal calcification and apical pathology. Dent Traumatol 2016;32:240-246.
38. Oenning AC, Jacobs R, Pauwels R, Stratis A, Hedesiu M, Salmon B. Cone-beam CT in paediatric dentistry: DIMITRA project position statement. Pediatr Radiol 2018;48:308-316.

https://doi.org/10.5395/rde.2026.51.e24

RDE Restorative Dentistry & Endodontics

Research Article

eISSN 2234-7666
Restor Dent Endod. 2026 May;51(2):e25
https://doi.org/10.5395/rde.2026.51.e25

Comparison of the cyclic fatigue resistance of original and replica-like files: a systematic review and meta-analysis

Mert Unal*, Fatih Cakici

Department of Endodontics, Faculty of Dentistry, Ordu University, Ordu, Türkiye

ABSTRACT

Objectives: This systematic review and meta-analysis aimed to evaluate the existing literature and quantitatively analyze the cyclic fatigue resistance of original and replica-like nickel-titanium endodontic files.

Methods: A comprehensive search was conducted across four electronic databases up to July 6, 2025, following PRISMA guidelines (PROSPERO: CRD420251086699). The methodological quality of included studies was assessed using criteria adapted from previous *in vitro* systematic reviews. Publication bias was evaluated using Egger's test and the trim-and-fill method. A random-effects meta-analysis was performed to compare the cyclic fatigue resistance of original and replica-like files using time to fracture (TTF) and number of cycles to fracture (NCF) as outcomes. These were expressed as standardized mean differences (SMDs) with 95% confidence intervals (CIs). Heterogeneity was analyzed using the I^2 statistic.

Results: A total of 14 studies involving 1,276 endodontic files (nine original and 31 replica-like types) were included. Based on TTF values, replica-like files showed significantly greater cyclic fatigue resistance than original files (SMD, –0.845; 95% CI, –1.268 to –0.423; $p < 0.001$). However, NCF-based analysis revealed no statistically significant difference (SMD, –1.532; 95% CI, –3.615 to 0.550; $p = 0.149$).

Conclusions: Replica-like files exhibited cyclic fatigue resistance comparable to original instruments and may be considered potential alternatives. However, due to high heterogeneity and methodological variability, these findings should be interpreted with caution.

Keywords: Cyclic fatigue; Dental instruments; Endodontics; Nickel-titanium alloy; Instrument fracture

INTRODUCTION

Nickel-titanium (Ni-Ti) endodontic instruments have revolutionized root canal treatment by reducing treatment time, operator fatigue, and procedural errors compared to manual instrumentation [1]. Despite all these advantages, the primary factor limiting the use of Ni-Ti files (65%) has been reported to be cost [2]. Currently,

Received: November 18, 2025 **Revised:** December 21, 2025 **Accepted:** January 2, 2026

Citation
Unal M, Cakici F. Comparison of the cyclic fatigue resistance of original and replica-like files: a systematic review and meta-analysis. Restor Dent Endod 2026;51(2):e25.

***Correspondence to**
Mert Unal, DDS
Department of Endodontics, Faculty of Dentistry, Ordu University, Cumhuriyet Campus, Altınordu, Ordu 52200, Türkiye
Email: mert.unal.011@gmail.com

in order to reduce this cost, clinicians are increasingly turning to more affordable systems that are similar to the well-known brand systems [3].

These systems, commonly referred to as replica-like instruments, are characterized by having the same number of files, similar color coding, and comparable instrument nomenclature to the original system, while being manufactured and distributed by independent companies and marketed under different brand identities [4]. Importantly, replica-like systems differ from counterfeit instruments, which unlawfully replicate original products in terms of design, packaging, and branding. Unlike counterfeit systems, replica-like instruments are legally produced and distributed, despite their intentional similarity to original systems in external design features. For example, while ProTaper Universal (Dentsply Sirona, Ballaigues, Switzerland) represents an original system, instruments such as EdgeTaper (EdgeEndo, Albuquerque, NM, USA), U-File (Dentmark, Ludhiana, India), and Multitaper (Proclinic Expert, Besançon, France) may be considered replica-like alternatives due to their similarity in file sequence, color coding, and nomenclature, but their distribution under different brand names. In contrast, a system marketed under the same name and packaging as ProTaper Universal would be classified as a counterfeit product [3,4]. Despite the increasing popularity of replica-like systems, there is insufficient scientific data on their overall performance and safety [5].

Regardless of whether they are original or replica-like, fractures of these files within the canal during treatment remain a frustrating complication for clinicians [6,7]. Instrument fractures can occur in two distinct ways: torsional or cyclic fatigue [8]. A torsional fracture occurs when the instrument tip becomes locked in the canal while the shaft continues to rotate, leading to plastic deformation and fracture due to exceeding the metal's elastic limit [9,10]. On the other hand, cyclic fatigue occurs during the shaping of curved canals, when the instrument is subjected to repeated cycles of tension and compression, eventually surpassing its maximum flexural capacity [11,12]. Fracture due to cyclic fatigue has been reported to play a more significant role in instrument separation compared to torsional failure [13,14]. In this context, although studies have been conducted on the cyclic fatigue resistance of both original and replica-like files, to the best of our knowledge, no comprehensive review is available.

The aim of this systematic review and meta-analysis is to evaluate the existing literature and quantitatively analyze the cyclic fatigue resistance of original and replica-like Ni-Ti files. The null hypothesis (H_0) tested is that there is no statistically significant difference in cyclic fatigue resistance between original and replica-like endodontic files.

METHODS

Protocol and registration

This systematic review and meta-analysis were conducted in accordance with the PRISMA (Preferred Reporting Items for Systematic Reviews and Meta-Analyses) guidelines [15]. The protocol of this study was registered in the PROSPERO International Prospective Register of Systematic Reviews (CRD420251086699).

Research question and eligibility criteria

This systematic review and meta-analysis focused on comparing the cyclic fatigue resistance of original and replica-like endodontic files. In this context, the PICOS question was structured as follows: Population (P): Ni-Ti endodontic instruments; Intervention (I), instrumentation of the Ni-Ti files within artificial root canals; Comparison (C), original vs replica-like files; Outcome (O), cyclic fatigue resistance; Study Design (S), laboratory studies.

The following criteria were used for the inclusion of studies in this systematic review and meta-analysis:

- Articles providing complete statistical data without inconsistent measurements,
- Articles in which the definition of replica-like files was clearly stated, and the selection criteria were described,
- *In vitro* studies that compared both original and replica-like files within the same experimental setup,
- Articles that compared the cyclic fatigue resistance of original and replica-like files using a standardized testing device.

https://doi.org/10.5395/rde.2026.51.e25

Information sources and search strategy

The search terms were determined by two independent reviewers (EBC, MU) to encompass all terms related to original and replica-like files. The search terms and their equivalent Medical Subject Headings terms were searched in the following databases: MEDLINE (PubMed), Scopus, Web of Science, and Google Scholar. The search was limited to English-language articles published up until July 6, 2025. Additionally, a manual search was conducted by reviewing the references of the included studies (Table 1).

Screening and data extraction

The results from the databases were imported into Mendeley Reference Manager (Elsevier, Amsterdam, Netherlands), and duplicate records were removed. The remaining studies were then transferred to Microsoft Excel (Microsoft, Redmond, WA, USA), where additional duplicates were manually eliminated. Two independent reviewers (EBC and MU) conducted full-text assessments of the articles identified after title and abstract screening. Any discrepancies or questionable evaluations were resolved through consultation with a senior reviewer (F.C.). Following the full-text review, data extraction was performed using a standardized data collection form. The information obtained from the included studies consisted of: author, year of publication, sample size, instrument name, motion type (rotary or reciprocating), taper, tip diameter, speed, torque, the structure and dimensions of the artificial canal (inner diameter, curvature angle, radius of curvature), test temperature, experimental setup (static or dynamic), and outcome (number of cycles to fracture [NCF], time to fracture [TTF]).

Risk of bias assessment

The methodological quality of the included studies was assessed using a modified version of the quality appraisal criteria derived from previous systematic reviews conducted for *in vitro* studies [16,17]. The methodological assessment was performed independently by two reviewers (EBC and MU). In cases of disagreement, an experienced reviewer (F.C.) was consulted to reach a consensus. The evaluation criteria were as follows: (1)

Table 1. Search results

Source	Search strategy	Results
PubMed	#1 ((((((dental instruments) OR (endodontic files)) OR (root canal preparation)) OR (nickel-titanium)) OR (nitinol)) OR (rotary)) OR (reciproc) Filters: English	9
	#2 (replica) OR (replica-like) Filters: English	
	#3 ((((cyclic fatigue) OR (cyclic resistance)) OR (flexural fatigue)) OR (flexural resistance)) OR (stress resistance) Filters: English	
	#4 (((((((dental instruments) OR (endodontic files)) OR (root canal preparation)) OR (nickel-titanium)) OR (nitinol)) OR (rotary)) OR (reciproc) AND (english[Filter])) AND ((replica) OR (replica-like) AND (english[Filter]))) AND (((((cyclic fatigue) OR (cyclic resistance)) OR (flexural fatigue)) OR (flexural resistance)) OR (stress resistance) AND (english[Filter]))	
Web of Science	#1 ((((((ALL=(dental instruments)) OR ALL=(endodontic files)) OR ALL=(root canal preparation)) OR ALL=(nickel titanium)) OR ALL=(nitinol)) OR ALL=(rotary)) OR ALL=(reciproc) and English (Languages)	11
	#2 (ALL=(replica)) OR ALL=(replica-like) and English (Languages)	
	#3 ((((ALL=(cyclic fatigue)) OR ALL=(cyclic resistance)) OR ALL=(flexural fatigue)) OR ALL=(flexural resistance)) OR ALL=(stress resistance) and English (Languages)	
	#4 #1 AND #2 AND #3	
Scopus	#1(ALL (dental AND instruments) OR ALL (endodontic AND files) OR ALL (root AND canal AND preparation) OR ALL (nickel AND titanium) OR ALL (nitinol) OR ALL (rotary) OR ALL (reciproc))	164
	#2(ALL (replica) OR ALL (replica-like))	
	#3(ALL (cyclic AND fatigue) OR ALL (cyclic AND resistance) OR ALL (flexural AND fatigue) OR ALL (flexural AND resistance) AND ALL (stress AND resistance))	
	#4 ((ALL (dental AND instruments) OR ALL (endodontic AND files) OR ALL (root AND canal AND preparation) OR ALL (nickel AND titanium) OR ALL (nitinol) OR ALL (rotary) OR ALL (reciproc))) AND ((ALL (cyclic AND fatigue) OR ALL (cyclic AND resistance) OR ALL (flexural AND fatigue) OR ALL (flexural AND resistance) AND ALL (stress AND resistance))) AND ((ALL (replica) OR ALL (replica-like)))	
Gray literature	Cyclic fatigue replica file original file "cyclic fatigue"	650
Manual search		3

sample size calculation, (2) randomization, (3) standardization of the cyclic fatigue testing model, (4) test temperature, (5) blinding of the operator, (6) standardization of file and artificial root canal dimensions, (7) following the manufacturer's instructions, and (8) appropriate statistical analysis. In this eight-item checklist, a score of 1 indicated low risk of bias and 0 indicated high risk of bias. A score of 6 or higher was considered low risk of bias, 4 or 5 was considered moderate risk, and 3 or lower was considered high risk of bias.

Data synthesis

A random-effects meta-analysis was conducted to compare the cyclic fatigue resistance of original and replica-like endodontic files. All statistical analyses were performed using Comprehensive Meta-Analysis software (CMA, version 2.0; Biostat, Englewood, NJ, USA). The cyclic fatigue resistance of original and replica-like files was evaluated by measuring TTF and NCF. These continuous outcomes (TTF and NCF) were expressed as standardized mean differences (SMDs) with 95% confidence intervals (CIs). The assessment of heterogeneity involved a detailed examination of the characteristics of the included studies and the use of the I^2 statistic. Heterogeneity was classified as low (25%), moderate (50%), and high (75%) based on I^2 values. To investigate potential sources of heterogeneity, subgroup analyses were performed. Publication bias was assessed by visual inspection of funnel plots using the trim-and-fill method and quantitatively evaluated using Egger's regression test, with a significance threshold set at $p < 0.05$.

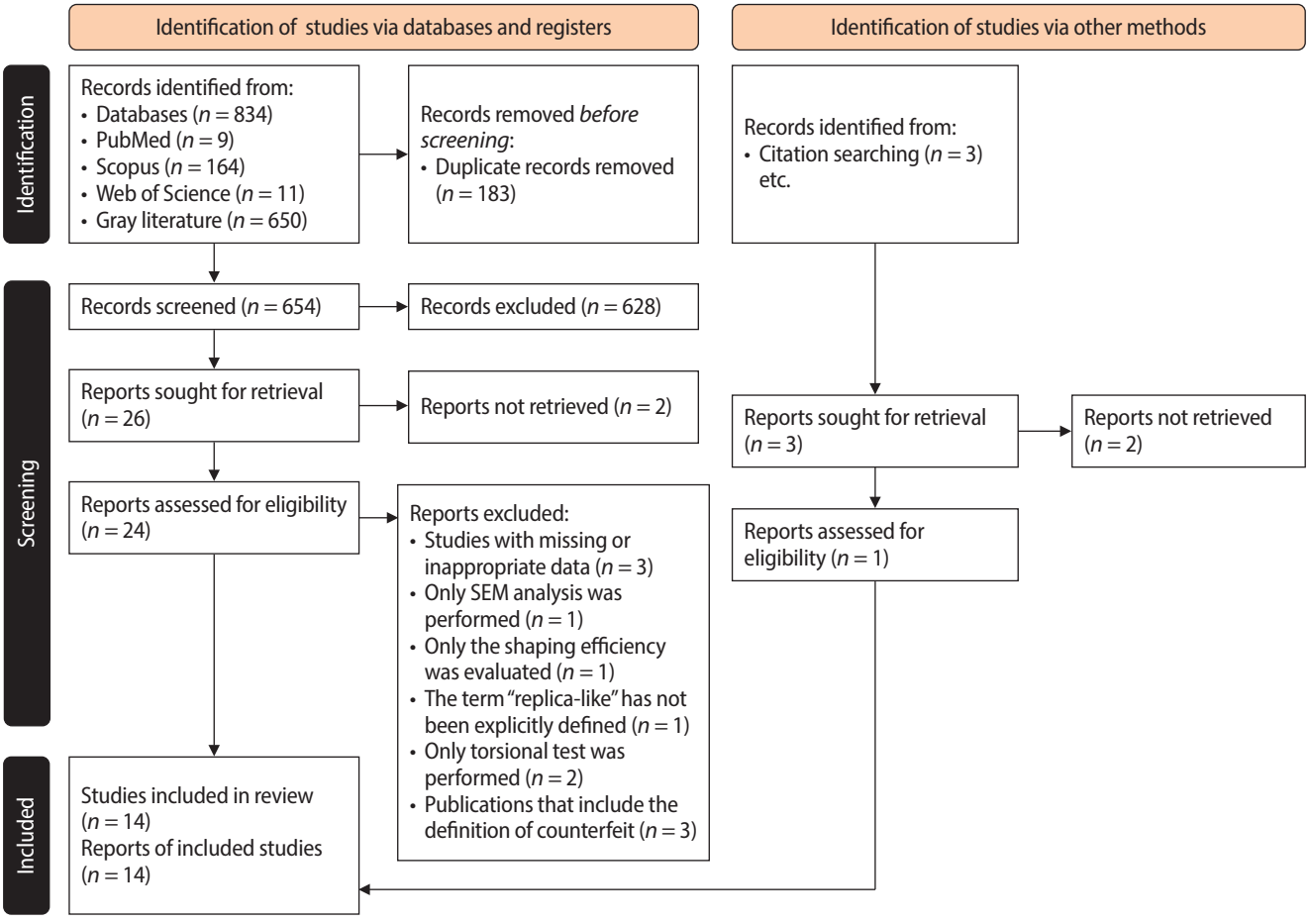

Figure 1. PRISMA (Preferred Reporting Items for Systematic Reviews and Meta-Analyses) flow chart for study selection. SEM, standard error of mean.

https://doi.org/10.5395/rde.2026.51.e25

RESULTS

Search results

The PRISMA flow diagram illustrating the stages of study inclusion and exclusion is shown in Figure 1. A total of 837 records were identified through database searches and manual searching. After removing 183 duplicates, 628 records were excluded during title and abstract screening. Full-text access to four articles could not be obtained. The remaining 25 articles were assessed in full text based on the predefined inclusion criteria.

Three studies were excluded from the analysis due to the absence of standard deviation values, despite reporting mean values [18–20]. One study was excluded because it did not clearly define the term "replica-like" [21]. One study was also excluded because it included only scanning electron microscope (SEM) analysis and did not evaluate cyclic fatigue resistance [22]. Additionally, three studies comparing the shaping efficiency and torsional resistance of replica-like and original instruments were also excluded from the meta-analysis [23–25]. Finally, three studies that used the term "counterfeit" instead of "replica-like" were also excluded [26–28]. As a result, a total of 14 studies were included in the meta-analysis [3–5,29–39].

Study characteristics

The details of the 14 studies included in the meta-analysis are shown in Table 2. A total of 1,276 endodontic files were evaluated across these studies, comprising nine different types of original files and 31 different types of replica-like files. Rotary systems were used in eight studies [3–5,29–31,34,38], while Reciproc files (VDW, Munich, Germany) were used in five studies [32,33,36,37,39]. In one study [35], both Reciproc and rotary original systems were compared with their corresponding replica-like counterparts.

In terms of the ambient temperature at which the experimental setup was conducted, it was observed that five studies performed the cyclic fatigue test at body temperature [29,31,35,37,39], while seven studies carried out the test at room temperature [3–5,30,33,34,38]. In two studies, no information was provided regarding the environmental temperature [32,36].

In all studies, the values of the radius and curvature angle of the artificial canal were reported according to the Pruett method; however, information regarding the inner diameter and taper of the artificial canal was not provided in four studies [3,30,32,35]. A static testing model was used in 12 studies [3–5,29,31–35,37–39], while a dynamic testing model was employed in two studies [30,36].

According to the results of cyclic fatigue resistance, nine studies [3–5,33–37,39] used the TTF as the outcome measure, while one study [31] reported the NCF. Four studies [29,30,32,38] provided both NCF and TTF values. In 12 studies [4,5,29–33,35–39], NCF and TTF data were presented as mean and standard deviation, whereas two studies [3,34] reported the data as median and interquartile range. The data from these two studies were converted into mean and standard deviation values using the formula proposed by Wan *et al.* [40].

Risk of bias

The results of the risk of bias assessment are shown in Table 3. Six studies [5,31,33,34,38,39] were assessed as having a low risk of bias, while eight studies [3,4,29,30,32,35–37] were considered to have a moderate risk of bias. None of the 14 studies included in the meta-analysis reported randomization of files during use, and in all cases, the operator was not blinded.

Data synthesis

1. Time to fracture

Comparison data based on TTF were obtained from 13 studies, encompassing a total of 59 original and replica-like endodontic files. In the analysis comparing SMD, a random-effects model with the inverse variance method revealed a statistically significant difference between the original and replica-like groups ($p < 0.001$), with a summarized SMD of −0.845 (95% CI, −1.268 to −0.423) (Figure 2). Based on the TTF values, the replica-like files exhibited a statistically significantly higher cyclic fatigue resistance compared to the original files.

According to Higgins' I-squared (I^2) statistic, a high level of heterogeneity was observed among the studies ($I^2 = 94.615$). Moreover, while publication bias was detected according to Egger's regression test ($p = 0.003$), no indication of publication bias was observed through

Table 2. The methodological characteristics of the included studies

Study	Year	Sample size	Groups/taper-diameter	Speed/torque	Artificial canal	Test temperature	Curvature of angle/radius of curvature	The size of the artificial canal	Model setup	Outcome	Results
Alcalde *et al.* [29]	2020	*n* = 10 per group (Rotary Systems)	(O) PTG: 25.08 (R) PT: 25.08 (R) FG: 25.08 (R) ETP: 25.06	PTG: 300 rpm/3 N·cm PT: 300 rpm/2 N·cm FG: 500 rpm/3 N·cm ETP: 300 rpm/3 N·cm	Custom made stainless steel block	Body temperature	60º Curvature 5 mm radius	0.40 mm tip diameter 0.06 mm taper	Static	TTF ± SD NCF ± SD 	PTG: 145.2 ± 8.55 PT: 261.5 ± 14.52 FG: 146.5 ± 6.83 ETP: 290.5 ± 12.27 PTG: 732 ± 42.76 PT: 1,307 ± 72.61 FG: 1,210 ± 56.96 ETP: 1,453 ± 61.34
Alnoury [30]	2024	*n* = 15 per group (Rotary Systems)	(O) PTG: 25.08 (R) FVG: 25.08 (R) MG3GP: 25.08	All systems: 350 rpm/2 N·cm	Custom made stainless steel block	Room temperature	60º Curvature 5 mm radius	Not specified	Dynamic	TTF ± SD NCF ± SD 	PTG: 354.3 ± 52.01 FVG: 1,130.3 ± 244.42 MG3GP: 366.3 ± 98.15 PTG: 2,066.75 ± 303.4 FVG: 6,593.42 ± 1,425.79 MG3GP: 2,136.75 ± 572.55
Aydın *et al.* [31]	2024	*n* = 15 per group (Rotary Systems)	(O) PTN: 25.06 (R) PPG: 25.06 (R) ETG: 25.06 (R) FVG: 25.08	All systems: 300 rpm/2 N·cm	Custom made stainless steel block	Body temperature	60º Curvature 3 mm radius	Inner diameter: 1.5 mm	Static	NCF ± SD 	PTN: 589 ± 63 PPG: 507 ± 51 ETG: 316 ± 45 FVG: 341 ± 71
Lima *et al.* [32]	2024	*n* = 10 per group (Reciproc Systems)	(O) RB: 25.08 (R) RCB: 25.08 (R) OOFB: 25.08	All systems: RECIPROC ALL mode	Custom made stainless steel block	Not specified	60º Curvature 5 mm radius	Not specified	Static	TTF ± SD NCF ± SD 	RB: 596.7 ± 57.33 RCB: 348.7 ± 60.74 OOFB: 718.5 ± 47.53 RB: 2,984 ± 286.7 RCB: 1,744 ± 303.7 OOFB: 3,593 ± 283.7
Martins *et al.*[3]	2020	*n* = 12 per group (Rotary Systems)	(O) PTU: 20.07 (R) ET: 20.06 (R) UF: 20.07 (R) GTU: 20.07 (R) SF: 20.07 (R) MT: 20.07 (R) PLT: 20.07	All systems: 300 rpm/2 N·cm	Custom made stainless steel block	Room temperature	86º Curvature 6 mm radius	Not specified	Static	TTF ± SD 	PTU: 44.5 ± 11.32 ET: 83.33 ± 41,51 UF: 67.1 ± 24.15 GTU: 46.1 ± 24.91 SF: 128.03 ± 47.38 MT: 20.17 ± 11.74 PLT: 16.87 ± 6.71

(Continued on the next page)

https://doi.org/10.5395/rde.2026.51.e25

Table 2. Continued

Study	Year	Sample size	Groups/taper-diameter	Speed/torque	Artificial canal	Test temperature	Curvature of angle/radius of curvature	The size of the artificial canal	Model setup	Outcome	Results
Martins *et al.* [4]	2020	*n* = 10 per group (Rotary Systems)	(O) PTU F1: 20.7 (O) PTG F1: 20.07 (R) UF F1: 20.07 (R) SF F1: 20.07 (R) SFB F1: 20.07	All systems: 300 rpm/1.5 N·cm	Custom made stainless steel block	Room temperature	86º Curvature 6 mm radius	Inner diameter: 1.4 mm Nontapered	Static	TTF ± SD	ROT group: PTU F1: 44.5 ± 7.4 PTG F1: 109.7 ± 29.9 UF F1: 66.8 ± 15.2 SF F1: 134.6 ± 34.5 SFB F1 : 343.1 ± 57.4 OTR group: PTU F1: 94.7 ± 13.6 PTG F1: 166.8 ± 26.6 UF F1: 171.5 ± 52.8 SF F1: 222.5 ± 40 SFB F1: 679.4 ± 71
Martins *et al.* [5]	2021	*n* = 10 per group (Rotary Systems)	(O) PTN X1: 17.04 (O) PTN X2: 25.06 (O) PTN X3: 30.07 (R) XF X1: 17.04 (R) XF X2: 25.06 (R) XF X3: 30.07	Not specified	Custom made stainless steel block	Room temperature	86º Curvature 6 mm radius	Inner diameter: 1.4 mm Nontapered	Static	TTF ± SD	PTN X1: 52 ± 5 PTN X2: 45.4 ± 7.2 PTN X3: 37.9 ± 8.1 XF X1: 65.9 ± 21.6 XF X2: 41.5 ± 15.1 XF X3: 34.2 ± 12.5
Martins *et al.* [33]	2021	*n* = 10 per group (Reciproc Systems)	(O) Reciproc: 25.08 (O) RB: 25.08 (O) WOG: 25.07 (R) RS: 25.08 (R) OF: 25.08 (R) OFB: 25.08	All systems: RECIPROC ALL or WAVE ONE AL mode	Custom made stainless steel block	Room temperature	86º Curvature 6 mm radius	Inner diameter: 1.4 mm Nontapered	Static	TTF ± SD	Reciproc: 178.8 ± 29.1 RB: 223.5 ± 35.9 WOG: 160.5 ± 52.6 RS: 94 ± 38.3 OF: 76.8 ± 20.8 OFB: 409.6 ± 44.9
Martins *et al.* [34]	2022	*n* = 12 per group (Rotary Systems)	(O) PTU: 20.07 (O) PTG: 20.07 (R) PreTG: 20.07 (R) GTF: 20.07 (R) ETP: 20.07 (R) SFB: 20.07	All systems: 300 rpm/2 N·cm	Custom made stainless steel block	Room temperature	86º Curvature 6 mm radius	Inner diameter: 1.4 mm Nontapered	Static	TTF ± SD	PTU: 43.53 ± 11.32 PTG: 108.27 ± 50.57 PreTG: 185.53 ± 89.73 GTF: 128.27 ± 34.63 ETP: 124.87 ± 19.29 SFB: 326.27 ± 77.82
Unal and Cakici [39]	2026	*n* = 20 per group (Reciproc Systems)	(O) RB: 25.08 (R) ROB: 25.08	All systems: RECIPROC ALL mode	Custom made stainless steel block	Body temperature	60º Curvature 5 mm radius	0.27 mm tip diameter 0.08 mm taper	Static	TTF ± SD	RB: 257.7 ± 18.1 ROB: 253.1 ± 58.2

(Continued on the next page)

https://doi.org/10.5395/rde.2026.51.e25

Table 2. Continued

Study	Year	Sample size	Groups/taper-diameter	Speed/torque	Artificial canal	Test temperature	Curvature of angle/radius of curvature	The size of the artificial canal	Model setup	Outcome	Results
Uslu *et al.* [35]	2023	*n* = 12 per group (Reciproc and Rotary Systems)	(O) PTN: 25.06 (O) Reciproc: 25.08 (R) XF: 25.06 (R) OOF: 25.08	Reciproc, OOF: RECIPROC ALL mode PTN, XF: 300 rpm/2 N·cm	Custom made ceramic block	Body temperature	60º Curvature 3 mm radius	Not specified	Static	TTF ± SD	PTN: 145.15 ± 49.26 Reciproc: 568.05 ± 50.21 XF: 134.8 ± 41.89 OOF: 267.7 ± 86.43
Ríos-Osorio *et al.* [36]	2025	*n* = 105 per group (Reciproc Systems)	(O) RB: 25.08 (O) OR: 25.06 (O) RM: 25.06 (R) RWG: 25.07 (R) RCS: 25.06	All systems: RECIPROC ALL mode	Custom made stainless steel block	Not specified	60º Curvature 5 mm radius	Inner diameter: 1.4 mm	Dynamic	TTF ± SD	Reciproc: 1,116 ± 350 OR: 741 ± 211 RM: 976 ± 249 RWG: 810 ± 248 RCS: 739 ± 372
Tarragó *et al.* [37]	2025	*n* = 9 per group (Reciproc Systems)	(O) Reciproc: 25.08 (O) RB: 25.08 (R) RS: 25.08 (R) REB: 25.08	All systems: RECIPROC ALL mode	Custom made stainless steel block	Body temperature	60º Curvature 5 mm radius	Inner diameter: 1.5 mm	Static	TTF ± SD	Single curvature Reciproc: 171.5 ± 38.9 RB: 355.4 ± 86.4 RS: 169 ± 104.8 REB: 359.5 ± 102.8 Double curvature Reciproc: 133.4 ± 47.4 RB: 140.5 ± 67.7 RS: 57.8 ± 20 REB: 142.9 ± 69
Zanza *et al.* [38]	2022	*n* = 20 per group (Rotary Systems)	(O) VB: 25.04 (R) ESS: 25.04	All systems: 500 rpm/1 N·cm	Custom made stainless steel block	Room temperature	60º Curvature 5 mm radius	0.05 mm taper	Static	TTF ± SD NCF ± SD	VB: 113.4 ± 13.4 ESS: 75.2 ± 16.3 VB: 945.2 ± 111.6 ESS: 626.7 ± 135.8

ET, EdgeTaper; ETG, EndoArt TouchGold; ETP, EdgeTaper Platinum; ESS, EdgeSequel Sapphire; ES, effect size; FG, Flex Gold; FVG, Fanta V-Taper Gold; GTF, Go Taper Flex; GTU, Go-Taper Universal; MG3GP, MG3 Gold Perfect; MT, Multitaper; NCF, number of cycles to fracture; O, original systems; OF, One Files; OFB, One Files Blue; OOF, Only One File; OOFB, Only One File Blue; OR, One Reci; PLT, Pluri Taper; PPG, Perfect MTF Plus Gold; PreTG, Premium Taper Gold; PT, Pro-T file; PTG, ProTaper Gold; PTN, ProTaper Next; PTU, ProTaper Universal; R, replica-like systems; RB, Reciproc Blue; RCB, RC Blue; RCS, RCS Blue T; REB, Reverso Blue; RM, R Motion; ROB, Recip One Blue; RS, Reverso Silver; RWG, Roll Wave Gold; SD, standard deviation; SF, Super Files; SFB, Super Files Blue; TTF, time to fracture; UF, U-File; VB, Vortex Blue; WOG, WaveOne Gold; XF, X-File.

https://doi.org/10.5395/rde.2026.51.e25

Table 3. Risk of bias assessment of the included studies

Study	Sample size calculation	Randomization	Standardization of cyclic testing model	Test temperature	Blinding of operator	Files and artificial root canal dimensions	Manufacturers instructions	Statistical analysis	Risk of bias
Alcalde *et al.* [29]	1	0	1	1	0	0	1	1	(Moderate) 5
Alnoury [30]	1	0	1	1	0	0	1	1	(Moderate) 5
Aydın *et al.* [31]	1	0	1	1	0	1	1	1	(Low) 6
Lima *et al.* [32]	1	0	1	0	0	0	1	1	(Moderate) 4
Martins *et al.* [3]	1	0	1	1	0	0	1	1	(Moderate) 5
Martins *et al.* [4]	0	0	1	1	0	1	1	1	(Moderate) 5
Martins *et al.* [5]	1	0	1	1	0	1	1	1	(Low) 6
Martins *et al.* [33]	1	0	1	1	0	1	1	1	(Low) 6
Martins *et al.* [34]	1	0	1	1	0	1	1	1	(Low) 6
Unal and Cakici [39]	1	0	1	1	0	1	1	1	(Low) 6
Uslu *et al.* [35]	1	0	1	1	0	0	1	1	(Moderate) 5
Ríos-Osorio *et al.* [36]	1	0	1	0	0	1	1	1	(Moderate) 5
Tarragó *et al.* [37]	0	0	1	1	0	1	1	1	(Moderate) 5
Zanza *et al.* [38]	1	0	1	1	0	1	1	1	(Low) 6

the examination of funnel plots using the trim and fill method (Figure 3A). To explore and reduce the sources of heterogeneity, subgroup analyses were performed based on the type of file motion and the testing temperature.

According to the subgroup analysis based on file kinematics, 36 out of the 59 comparison data sets involved rotary files, while 23 involved comparisons between original and replica-like reciprocating files. The subgroup analysis revealed that file kinematics were significantly associated with the comparison between original and replica-like instruments (Q-value, 36.797; $p < 0.001$) (Figure 4). Replica-like rotary files exhibited a statistically significantly higher cyclic fatigue resistance compared to original rotary files (SMD, –1.819; 95% CI, –2.331 to –1.306; $p < 0.001$, $I^2 = 93.5$). In contrast, original reciprocating files demonstrated a statistically significantly higher cyclic fatigue resistance compared to replica-like reciprocating files (SMD, 0.673; 95% CI, 0.052 to 1.293; $p = 0.034$, $I^2 = 93.8$). While the overall analysis indicated that replica-like instruments exhibited significantly higher TTF values compared to original instruments (SMD, –0.845; $p < 0.001$), this difference lost statistical significance in the subgroup analysis based on kinematic motion (SMD, –0.579; $p = 0.642$). This suggests that the performance of original and replica instruments may vary depending on the type of motion employed, which could be a contributing factor to the heterogeneity observed across studies.

In the overall meta-analysis, among the 59 comparison data sets used for the evaluation of TTF, eight comparison data sets derived from the studies by Lima *et al.* [32] and Ríos-Osorio *et al.* [36] were excluded from the temperature-based subgroup analysis because the experimental testing temperature was not reported. Consequently, a total of 51 comparison data sets were included in the temperature-related subgroup analysis, of which 41 were conducted at room temperature and 10 at body temperature.

The subgroup analysis demonstrated that the testing temperature was not significantly associated with the comparison between original and replica-like instruments (Q-value, 1.126; $p = 0.289$) (Figure 5). Replica-like files exhibited a statistically significantly higher cyclic fatigue resistance than original files under room tem-

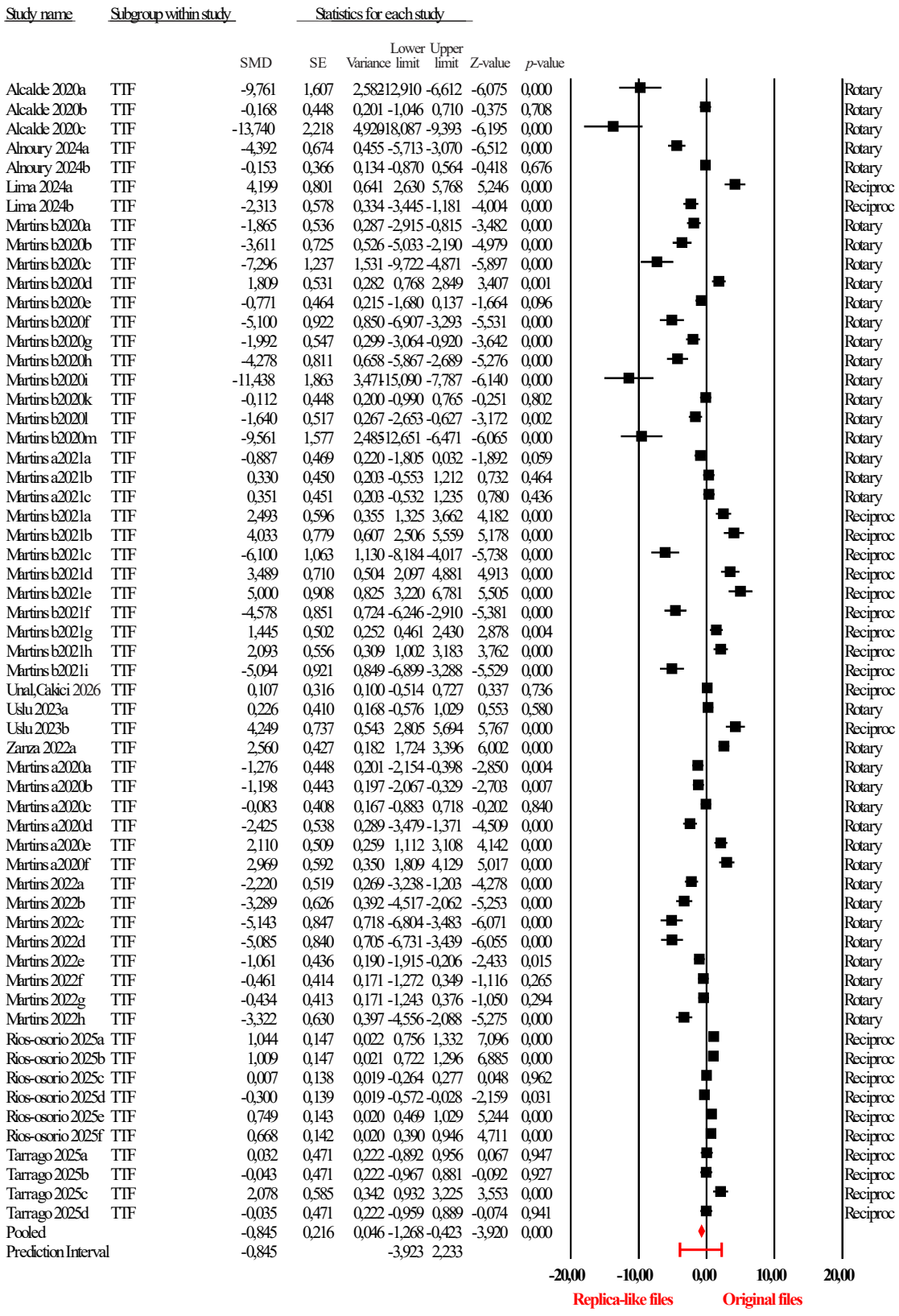

Figure 2. Forest plot analysis based on time to fracture (TTF) values. SE, standard error; SMD, standardized mean difference.

https://doi.org/10.5395/rde.2026.51.e25

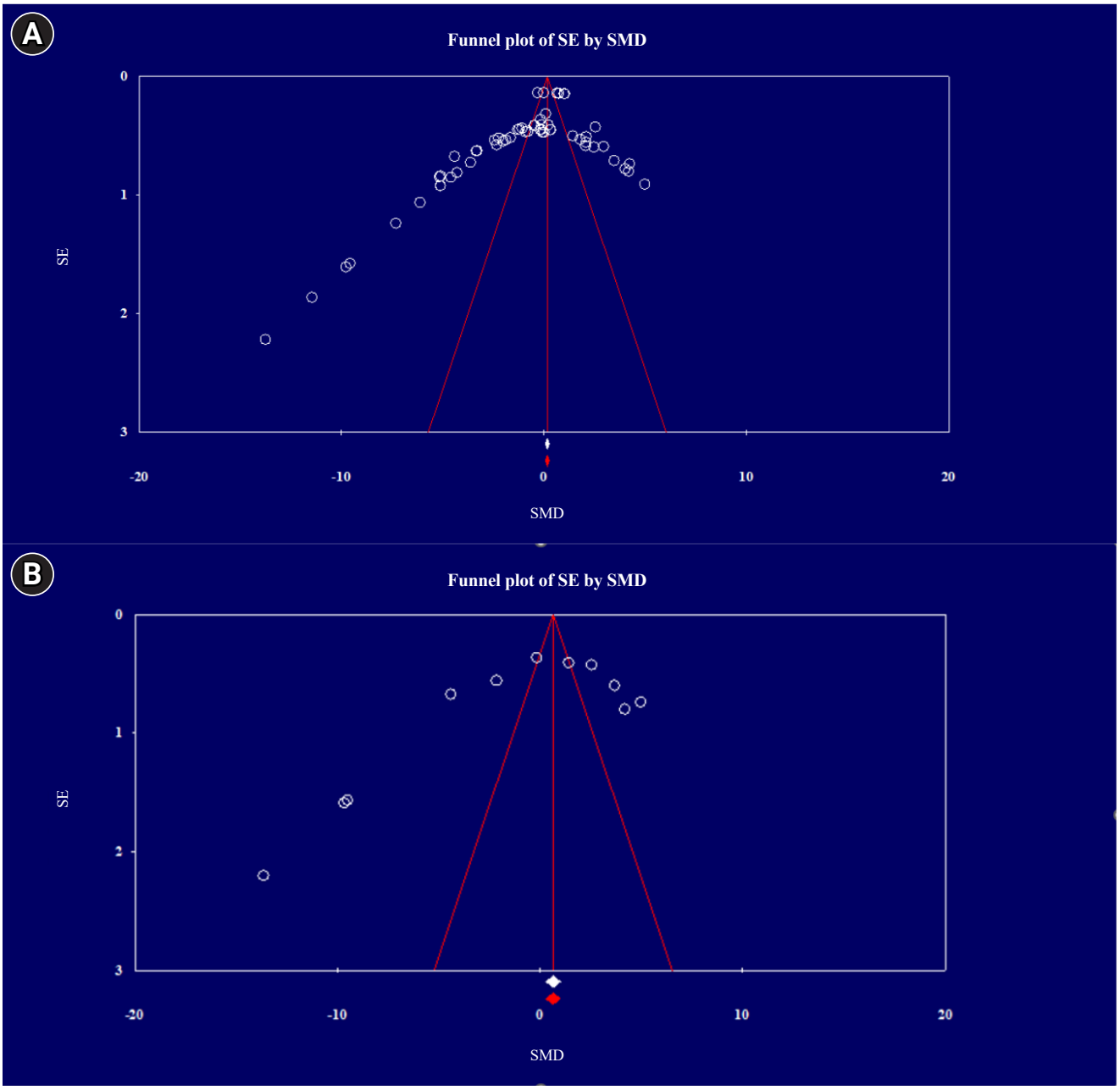

Figure 3. Funnel plot generated following the application of the trim-and-fill method for the assessment of publication bias. (A) Studies containing time to fracture values. (B) Studies containing the number of cycles to fracture values. SE, standard error; SMD, standardized mean difference.

perature conditions (SMD, −1.404; 95% CI, −2.145 to −0.664; $p < 0.001$, $I^2 = 94.4\%$). In contrast, no statistically significant difference in cyclic fatigue resistance was observed between original and replica-like files in comparisons conducted at body temperature (SMD, −0.631; 95% CI, −1.853 to 0.592; $p = 0.312$, $I^2 = 92.4\%$).

2. Number of cycles to fracture

Comparison data based on the NCF were obtained from five studies, encompassing a total of 11 original and replica-like endodontic files. A meta-analysis using a random-effects model and the inverse variance method for the comparison of standardized mean differences revealed no statistically significant difference between

Group by Comparison	Study name	Subgroup within study	SMD	SE	Variance	Lower limit	Upper limit	Z-value	*p*-value	
Reciproc	Lima 2024a	TTF	4,199	0,801	0,641	2,630	5,768	5,246	0,000	Reciproc
Reciproc	Lima 2024b	TTF	-2,313	0,578	0,334	-3,445	-1,181	-4,004	0,000	Reciproc
Reciproc	Martins b2021a	TTF	2,493	0,596	0,355	1,325	3,662	4,182	0,000	Reciproc
Reciproc	Martins b2021b	TTF	4,033	0,779	0,607	2,506	5,559	5,178	0,000	Reciproc
Reciproc	Martins b2021c	TTF	-6,100	1,063	1,130	-8,184	-4,017	-5,738	0,000	Reciproc
Reciproc	Martins b2021d	TTF	3,489	0,710	0,504	2,097	4,881	4,913	0,000	Reciproc
Reciproc	Martins b2021e	TTF	5,000	0,908	0,825	3,220	6,781	5,505	0,000	Reciproc
Reciproc	Martins b2021f	TTF	-4,578	0,851	0,724	-6,246	-2,910	-5,381	0,000	Reciproc
Reciproc	Martins b2021g	TTF	1,445	0,502	0,252	0,461	2,430	2,878	0,004	Reciproc
Reciproc	Martins b2021h	TTF	2,093	0,556	0,309	1,002	3,183	3,762	0,000	Reciproc
Reciproc	Martins b2021i	TTF	-5,094	0,921	0,849	-6,899	-3,288	-5,529	0,000	Reciproc
Reciproc	Rios-osorio 2025a	TTF	1,044	0,147	0,022	0,756	1,332	7,096	0,000	Reciproc
Reciproc	Rios-osorio 2025b	TTF	1,009	0,147	0,021	0,722	1,296	6,885	0,000	Reciproc
Reciproc	Rios-osorio 2025c	TTF	0,007	0,138	0,019	-0,264	0,277	0,048	0,962	Reciproc
Reciproc	Rios-osorio 2025d	TTF	-0,300	0,139	0,019	-0,572	-0,028	-2,159	0,031	Reciproc
Reciproc	Rios-osorio 2025e	TTF	0,749	0,143	0,020	0,469	1,029	5,244	0,000	Reciproc
Reciproc	Rios-osorio 2025f	TTF	0,668	0,142	0,020	0,390	0,946	4,711	0,000	Reciproc
Reciproc	Tarrago 2025a	TTF	0,032	0,471	0,222	-0,892	0,956	0,067	0,947	Reciproc
Reciproc	Tarrago 2025b	TTF	-0,043	0,471	0,222	-0,967	0,881	-0,092	0,927	Reciproc
Reciproc	Tarrago 2025c	TTF	2,078	0,585	0,342	0,932	3,225	3,553	0,000	Reciproc
Reciproc	Tarrago 2025d	TTF	-0,035	0,471	0,222	-0,959	0,889	-0,074	0,941	Reciproc
Reciproc	Unal,Calici 2026	TTF	0,107	0,316	0,100	-0,514	0,727	0,337	0,736	Reciproc
Reciproc	Uslu 2023b	TTF	4,249	0,737	0,543	2,805	5,694	5,767	0,000	Reciproc
Reciproc	Pooled		0,673	0,317	0,100	0,052	1,293	2,125	0,034	
Reciproc	Prediction Interval		0,673			-2,217	3,563			
Rotary	Alcalde 2020a	TTF	-9,761	1,607	2,582	-12,910	-6,612	-6,075	0,000	Rotary
Rotary	Alcalde 2020b	TTF	-0,168	0,448	0,201	-1,046	0,710	-0,375	0,708	Rotary
Rotary	Alcalde 2020c	TTF	-13,740	2,218	4,920	-18,087	-9,393	-6,195	0,000	Rotary
Rotary	Alnoury 2024a	TTF	-4,392	0,674	0,455	-5,713	-3,070	-6,512	0,000	Rotary
Rotary	Alnoury 2024b	TTF	-0,153	0,366	0,134	-0,870	0,564	-0,418	0,676	Rotary
Rotary	Martins 2022a	TTF	-2,220	0,519	0,269	-3,238	-1,203	-4,278	0,000	Rotary
Rotary	Martins 2022b	TTF	-3,289	0,626	0,392	-4,517	-2,062	-5,253	0,000	Rotary
Rotary	Martins 2022c	TTF	-5,143	0,847	0,718	-6,804	-3,483	-6,071	0,000	Rotary
Rotary	Martins 2022d	TTF	-5,085	0,840	0,705	-6,731	-3,439	-6,055	0,000	Rotary
Rotary	Martins 2022e	TTF	-1,061	0,436	0,190	-1,915	-0,206	-2,433	0,015	Rotary
Rotary	Martins 2022f	TTF	-0,461	0,414	0,171	-1,272	0,349	-1,116	0,265	Rotary
Rotary	Martins 2022g	TTF	-0,434	0,413	0,171	-1,243	0,376	-1,050	0,294	Rotary
Rotary	Martins 2022h	TTF	-3,322	0,630	0,397	-4,556	-2,088	-5,275	0,000	Rotary
Rotary	Martins a2020a	TTF	-1,276	0,448	0,201	-2,154	-0,398	-2,850	0,004	Rotary
Rotary	Martins a2020b	TTF	-1,198	0,443	0,197	-2,067	-0,329	-2,703	0,007	Rotary
Rotary	Martins a2020c	TTF	-0,083	0,408	0,167	-0,883	0,718	-0,202	0,840	Rotary
Rotary	Martins a2020d	TTF	-2,425	0,538	0,289	-3,479	-1,371	-4,509	0,000	Rotary
Rotary	Martins a2020e	TTF	2,110	0,509	0,259	1,112	3,108	4,142	0,000	Rotary
Rotary	Martins a2020f	TTF	2,969	0,592	0,350	1,809	4,129	5,017	0,000	Rotary
Rotary	Martins a2021a	TTF	-0,887	0,469	0,220	-1,805	0,032	-1,892	0,059	Rotary
Rotary	Martins a2021b	TTF	0,330	0,450	0,203	-0,553	1,212	0,732	0,464	Rotary
Rotary	Martins a2021c	TTF	0,351	0,451	0,203	-0,532	1,235	0,780	0,436	Rotary
Rotary	Martins b2020a	TTF	-1,865	0,536	0,287	-2,915	-0,815	-3,482	0,000	Rotary
Rotary	Martins b2020b	TTF	-3,611	0,725	0,526	-5,033	-2,190	-4,979	0,000	Rotary
Rotary	Martins b2020c	TTF	-7,296	1,237	1,531	-9,722	-4,871	-5,897	0,000	Rotary
Rotary	Martins b2020d	TTF	1,809	0,531	0,282	0,768	2,849	3,407	0,001	Rotary
Rotary	Martins b2020e	TTF	-0,771	0,464	0,215	-1,680	0,137	-1,664	0,096	Rotary
Rotary	Martins b2020f	TTF	-5,100	0,922	0,850	-6,907	-3,293	-5,531	0,000	Rotary
Rotary	Martins b2020g	TTF	-1,992	0,547	0,299	-3,064	-0,920	-3,642	0,000	Rotary
Rotary	Martins b2020h	TTF	-4,278	0,811	0,658	-5,867	-2,689	-5,276	0,000	Rotary
Rotary	Martins b2020i	TTF	-11,438	1,863	3,471	-15,090	-7,787	-6,140	0,000	Rotary
Rotary	Martins b2020k	TTF	-0,112	0,448	0,200	-0,990	0,765	-0,251	0,802	Rotary
Rotary	Martins b2020l	TTF	-1,640	0,517	0,267	-2,653	-0,627	-3,172	0,002	Rotary
Rotary	Martins b2020m	TTF	-9,561	1,577	2,485	-12,651	-6,471	-6,065	0,000	Rotary
Rotary	Uslu 2023a	TTF	0,226	0,410	0,168	-0,576	1,029	0,553	0,580	Rotary
Rotary	Zanza 2022a	TTF	2,560	0,427	0,182	1,724	3,396	6,002	0,000	Rotary
Rotary	Pooled		-1,819	0,262	0,068	-2,331	-1,306	-6,952	0,000	
Rotary	Prediction Interval		-1,819			-4,687	1,049			
Overall	Pooled		-0,579	1,246	1,552	-3,021	1,862	-0,465	0,642	
Overall	Prediction Interval		-0,808			-3,882	2,266			

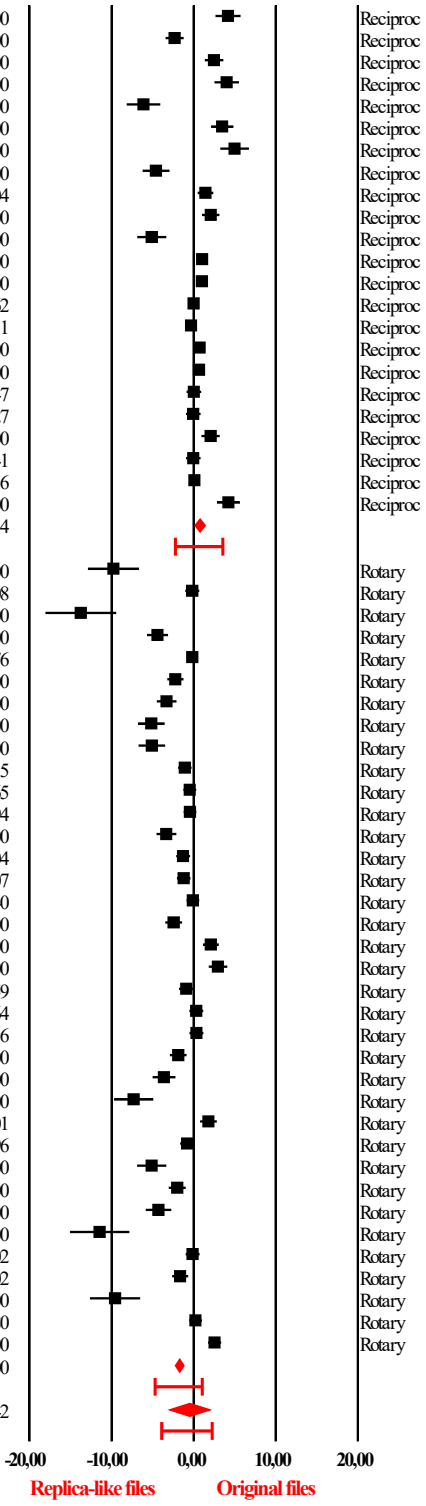

Figure 4. Subgroup analysis of time to fracture (TTF) according to instrument kinematics. SE, standard error; SMD, standardized mean difference.

https://doi.org/10.5395/rde.2026.51.e25

Group by Comparison	Study name	Subgroup within study	Statistics for each study						
			SMD	SE	Variance	Lower limit	Upper limit	Z-value	*p*-value
Body	Alcalde 2020a	TTF	-9,761	1,607	2,582	-12,910	-6,612	-6,075	0,000
Body	Alcalde 2020b	TTF	-0,168	0,448	0,201	-1,046	0,710	-0,375	0,708
Body	Alcalde 2020c	TTF	-13,740	2,218	4,920	-18,087	-9,393	-6,195	0,000
Body	Tarrago 2025a	TTF	0,032	0,471	0,222	-0,892	0,956	0,067	0,947
Body	Tarrago 2025b	TTF	-0,043	0,471	0,222	-0,967	0,881	-0,092	0,927
Body	Tarrago 2025c	TTF	2,078	0,585	0,342	0,932	3,225	3,553	0,000
Body	Tarrago 2025d	TTF	-0,035	0,471	0,222	-0,959	0,889	-0,074	0,941
Body	Unal,Cakici 2026	TTF	0,107	0,316	0,100	-0,514	0,727	0,337	0,736
Body	Uslu 2023a	TTF	0,226	0,410	0,168	-0,576	1,029	0,553	0,580
Body	Uslu 2023b	TTF	4,249	0,737	0,543	2,805	5,694	5,767	0,000
Body	Pooled		-0,631	0,624	0,389	-1,853	0,592	-1,011	0,312
Body	Prediction Interval		-0,631			-5,040	3,779		
Room	Alnoury 2024a	TTF	-4,392	0,674	0,455	-5,713	-3,070	-6,512	0,000
Room	Alnoury 2024b	TTF	-0,153	0,366	0,134	-0,870	0,564	-0,418	0,676
Room	Martins 2022a	TTF	-2,220	0,519	0,269	-3,238	-1,203	-4,278	0,000
Room	Martins 2022b	TTF	-3,289	0,626	0,392	-4,517	-2,062	-5,253	0,000
Room	Martins 2022c	TTF	-5,143	0,847	0,718	-6,804	-3,483	-6,071	0,000
Room	Martins 2022d	TTF	-5,085	0,840	0,705	-6,731	-3,439	-6,055	0,000
Room	Martins 2022e	TTF	-1,061	0,436	0,190	-1,915	-0,206	-2,433	0,015
Room	Martins 2022f	TTF	-0,461	0,414	0,171	-1,272	0,349	-1,116	0,265
Room	Martins 2022g	TTF	-0,434	0,413	0,171	-1,243	0,376	-1,050	0,294
Room	Martins 2022h	TTF	-3,322	0,630	0,397	-4,556	-2,088	-5,275	0,000
Room	Martins a2020a	TTF	-1,276	0,448	0,201	-2,154	-0,398	-2,850	0,004
Room	Martins a2020b	TTF	-1,198	0,443	0,197	-2,067	-0,329	-2,703	0,007
Room	Martins a2020c	TTF	-0,083	0,408	0,167	-0,883	0,718	-0,202	0,840
Room	Martins a2020d	TTF	-2,425	0,538	0,289	-3,479	-1,371	-4,509	0,000
Room	Martins a2020e	TTF	2,110	0,509	0,259	1,112	3,108	4,142	0,000
Room	Martins a2020f	TTF	2,969	0,592	0,350	1,809	4,129	5,017	0,000
Room	Martins a2021a	TTF	-0,887	0,469	0,220	-1,805	0,032	-1,892	0,059
Room	Martins a2021b	TTF	0,330	0,450	0,203	-0,553	1,212	0,732	0,464
Room	Martins a2021c	TTF	0,351	0,451	0,203	-0,532	1,235	0,780	0,436
Room	Martins b2020a	TTF	-1,865	0,536	0,287	-2,915	-0,815	-3,482	0,000
Room	Martins b2020b	TTF	-3,611	0,725	0,526	-5,033	-2,190	-4,979	0,000
Room	Martins b2020c	TTF	-7,296	1,237	1,531	-9,722	-4,871	-5,897	0,000
Room	Martins b2020d	TTF	1,809	0,531	0,282	0,768	2,849	3,407	0,001
Room	Martins b2020e	TTF	-0,771	0,464	0,215	-1,680	0,137	-1,664	0,096
Room	Martins b2020f	TTF	-5,100	0,922	0,850	-6,907	-3,293	-5,531	0,000
Room	Martins b2020g	TTF	-1,992	0,547	0,299	-3,064	-0,920	-3,642	0,000
Room	Martins b2020h	TTF	-4,278	0,811	0,658	-5,867	-2,689	-5,276	0,000
Room	Martins b2020i	TTF	-11,438	1,863	3,471	-15,090	-7,787	-6,140	0,000
Room	Martins b2020k	TTF	-0,112	0,448	0,200	-0,990	0,765	-0,251	0,802
Room	Martins b2020l	TTF	-1,640	0,517	0,267	-2,653	-0,627	-3,172	0,002
Room	Martins b2020m	TTF	-9,561	1,577	2,485	-12,651	-6,471	-6,065	0,000
Room	Martins b2021a	TTF	2,493	0,596	0,355	1,325	3,662	4,182	0,000
Room	Martins b2021b	TTF	4,033	0,779	0,607	2,506	5,559	5,178	0,000
Room	Martins b2021c	TTF	-6,100	1,063	1,130	-8,184	-4,017	-5,738	0,000
Room	Martins b2021d	TTF	3,489	0,710	0,504	2,097	4,881	4,913	0,000
Room	Martins b2021e	TTF	5,000	0,908	0,825	3,220	6,781	5,505	0,000
Room	Martins b2021f	TTF	-4,578	0,851	0,724	-6,246	-2,910	-5,381	0,000
Room	Martins b2021g	TTF	1,445	0,502	0,252	0,461	2,430	2,878	0,004
Room	Martins b2021h	TTF	2,093	0,556	0,309	1,002	3,183	3,762	0,000
Room	Martins b2021i	TTF	-5,094	0,921	0,849	-6,899	-3,288	-5,529	0,000
Room	Zanza 2022a	TTF	2,560	0,427	0,182	1,724	3,396	6,002	0,000
Room	Pooled		-1,404	0,378	0,143	-2,145	-0,664	-3,719	0,000
Room	Prediction Interval		-1,404			-6,144	3,336		
Overall	Pooled		-1,197	0,323	0,104	-1,830	-0,564	-3,705	0,000
Overall	Prediction Interval		-1,197			-5,678	3,284		

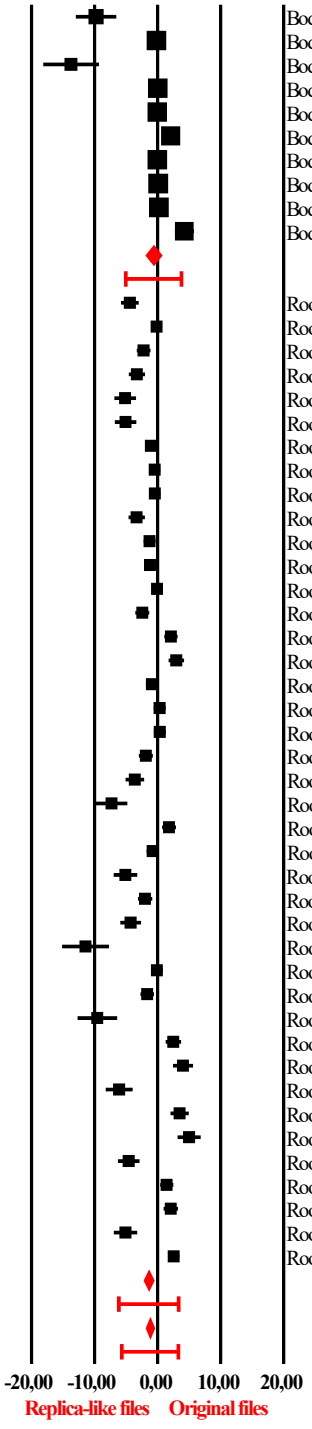

Figure 5. Subgroup analysis of time to fracture (TTF) according to testing temperature. SE, standard error; SMD, standardized mean difference.

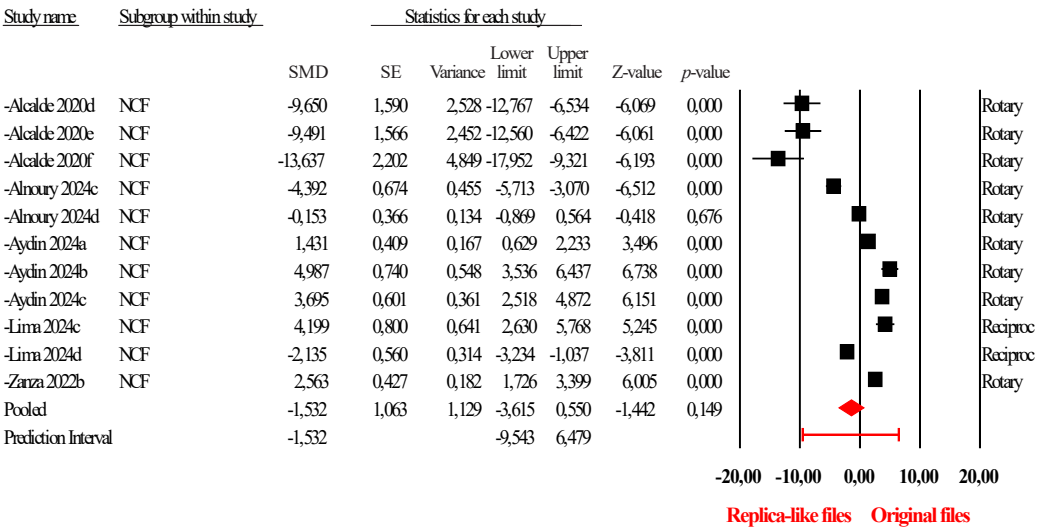

Figure 6. Forest plot analysis based on the number of cycles to fracture (NCF) values. SMD, standardized mean difference; SE, standard error.

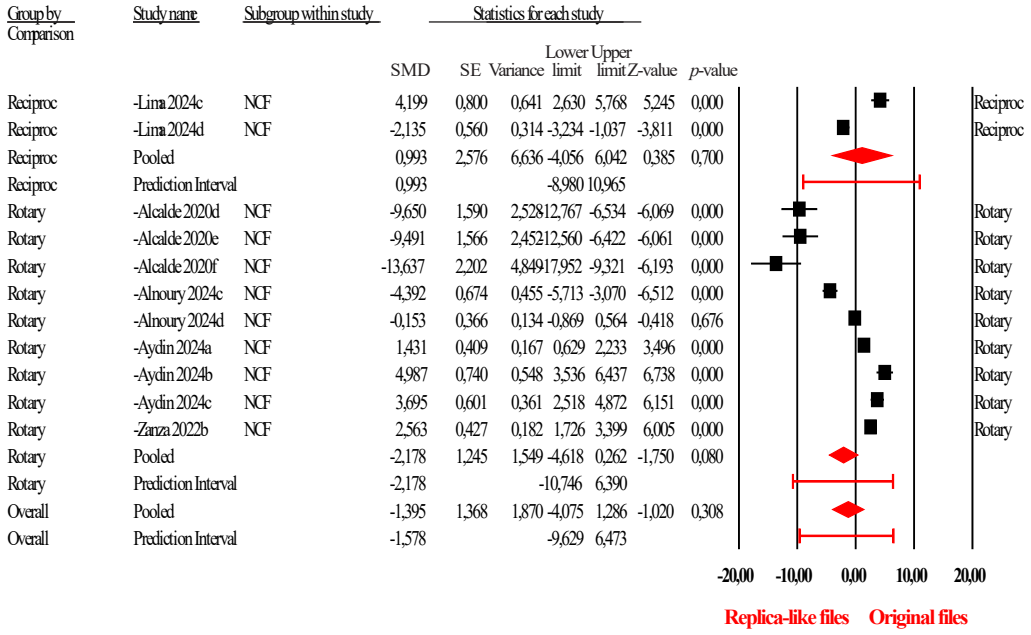

Figure 7. Subgroup analysis of the number of cycles to fracture (NCF) according to instrument kinematics. SE, standard error; SMD, standardized mean difference.

the original and replica-like groups (p = 0.149), with a summarized SMD of −1.532 (95% CI, −3.615 to 0.550) (Figure 6). According to the NCF values, no statistically significant difference in cyclic fatigue resistance was observed between the replica-like and original files.

According to Higgins' I^2 statistic, a high level of heterogeneity was observed among the studies (I^2 = 96.824). However, no evidence of publication bias was detected based on Egger's regression test (p = 0.132) and the examination of funnel plots using the trim and fill method (Figure 3B). To explore and reduce the sources of heterogeneity, subgroup analyses were performed based on the type of file motion and the testing temperature.

According to the subgroup analysis based on file kine-

https://doi.org/10.5395/rde.2026.51.e25

matics, nine out of the 11 comparison datasets involved rotary files, while two involved comparisons between original and replica-like reciprocating files. The subgroup analysis indicated that file kinematics were not significantly associated with the comparison between original and replica-like files (Figure 7) (Q-value, 1.228; $p = 0.268$). No significant difference was observed in cyclic fatigue resistance between replica-like rotary files and original rotary files (SMD, –2.178; 95% CI, –4.618 to 0.262; $p = 0.08$, $I^2 = 97$). Similarly, the comparison between replica-like reciprocating files and original reciprocating files did not yield a statistically significant result (SMD, 0.993; 95% CI, –4.056 to 6.042; $p = 0.70$, $I^2 = 97.6$).

In the overall meta-analysis, among the 11 comparison data sets used for the evaluation of the NCF, two comparison data sets from the study by Lima *et al.* [32] were excluded from the temperature-based subgroup analysis because the experimental testing temperature was not reported. Consequently, nine comparison data sets were included in the temperature-related subgroup analysis, of which three were conducted at room temperature and six at body temperature.

The subgroup analysis indicated that the testing temperature was not significantly associated with the comparison between original and replica-like instruments (Q-value, 1.05; $p = 0.305$) (Figure 8). No statistically significant difference in cyclic fatigue resistance was observed between replica-like and original files in comparisons conducted at either room temperature (SMD, –0.62; 95% CI, –3.926 to 2.685; $p = 0.713$, $I^2 = 97.4\%$) or body temperature (SMD, –3.339; 95% CI, –7.353 to 0.675; $p = 0.103$, $I^2 = 97.2\%$).

DISCUSSION

Endodontic instruments with structural similarities to those manufactured by leading and well-established companies, typically originating from India and China, have been used in endodontics for a considerable period. These instruments were first systematically defined as replica-like by Martins *et al.* [4]. The criteria for classification as replica-like instruments include having the same number of files as the original system, identical color coding, and similar nomenclature to the original brand. In some studies, instruments that entirely mimic the original systems and are marketed under the same name have also been evaluated. These instruments have been defined as counterfeit files by Rodrigues *et al.* [28] and have been shown to exhibit inferior mechanical and metallurgical properties compared to the original systems. Furthermore, the use of such counterfeit systems has been associated with patent infringement and potential risks to patient safety, as consistently reported across multiple studies [26–28]. In the present

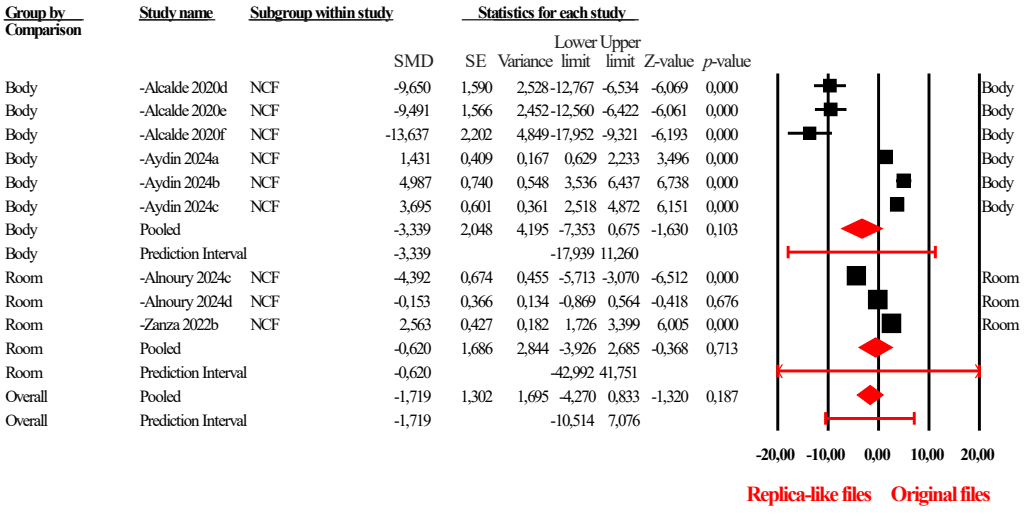

Figure 8. Subgroup analysis of number of cycles to fracture (NCF) according to testing temperature. SE, standard error; SMD, standardized mean difference.

systematic review and meta-analysis, studies evaluating counterfeit files were excluded, whereas only those instruments that met the criteria for replica-like systems were included.

Cyclic fatigue resistance can vary depending on numerous factors, including the type and size of the instrument, testing temperature, experimental setup, and the dimensions of the artificial canal [41–44]. The high number of influencing variables, along with the absence of a universally accepted standardized protocol for cyclic fatigue testing, limits the number of eligible meta-analyses on this topic and contributes to increased heterogeneity among studies. Given that it is not feasible to control all variables simultaneously, only studies that evaluated original and replica-like instruments under internally standardized experimental conditions were included in the present meta-analysis.

Due to the indication of substantial heterogeneity, a random-effects model was applied. To further explore potential sources of heterogeneity, subgroup analyses were performed based on kinematic motion (reciprocating vs. rotary) and testing temperature (room temperature vs. body temperature). In the included studies, cyclic fatigue resistance was reported using two different outcome measures: NCF and TTF. Because these outcome measures are not methodologically equivalent and may differentially influence the interpretation of results, two separate meta-analyses were conducted according to each outcome.

Based on NCF values, no statistically significant difference in cyclic fatigue resistance was observed between original and replica-like instruments. In contrast, the overall analysis based on TTF values suggested that replica-like instruments tended to exhibit higher cyclic fatigue resistance compared to original instruments. Accordingly, the null hypothesis (H_0) was only partially rejected. However, this discrepancy between NCF- and TTF-based findings warrants careful interpretation.

One possible explanation for this inconsistency is the inherent methodological limitation of TTF as an outcome measure. Unlike NCF, TTF values are directly influenced by the rotational speed (rpm) applied during testing. In studies where different rpm values are used for original and replica-like instruments, TTF-based comparisons may be biased, as instruments operating at higher rotational speeds are expected to reach fracture in a shorter time. This limitation is exemplified by the study of Alcalde *et al.* [29], included in the present meta-analysis, in which original and replica-like instruments were tested at different rotational speeds. Under such conditions, TTF outcomes may underestimate cyclic fatigue resistance independently of the intrinsic mechanical properties of the instruments. In contrast, NCF calculations inherently normalize results by accounting for rotational speed and are therefore less susceptible to rpm-related bias. Consequently, NCF-based findings may represent a more standardized and methodologically robust indicator of cyclic fatigue resistance across studies employing different kinematic parameters.

Previous studies have attributed the relatively higher cyclic fatigue resistance observed in some replica-like instruments to factors such as smoother surface morphology and a higher proportion of martensitic phase, as demonstrated by SEM and metallurgical analyses [3–5,33]. A smoother surface finish has been consistently associated with improved cyclic fatigue resistance [45–47]. Additionally, deviations in taper and tip diameter from the original instruments have been reported for replica-like systems [39]. Given that smaller taper and reduced tip size are known to enhance cyclic fatigue resistance [48–50], such dimensional differences may contribute to improved fatigue performance under certain testing conditions. However, these findings should not be interpreted as evidence of universal superiority, but rather as indicators that replica-like instruments may exhibit comparable or, in specific experimental settings, higher cyclic fatigue resistance.

Another noteworthy point is the influence of artificial canal dimensions on cyclic fatigue resistance. While four of the included studies [3,30,32,35] did not provide any information regarding the size of the artificial canal, the remaining 10 studies [4,5,29,31,33,34,36–39] evaluated original and replica-like instruments using a single type of artificial canal. In a study evaluating the cyclic fatigue resistance of the same file type in artificial canals of varying dimensions, it was reported that an increase in canal size was associated with prolonged TTF [51]. In another study, two different instruments with the same taper and tip diameter were tested in an artificial canal that was not dimensionally compatible

https://doi.org/10.5395/rde.2026.51.e25

with their sizes. It was observed that the instruments followed different trajectories due to differences in their bending properties [52]. This resulted in variations in the degree and radius of curvature experienced by each instrument within the artificial canal. Therefore, dimensional discrepancies between original and replica-like instruments and their compatibility with the artificial canal may have influenced the outcomes. It is believed that evaluating original and replica-like instruments in artificial canals specifically designed to match their respective dimensions would provide more consistent and reliable results in future studies.

In the subgroup analysis based on file kinematics, no statistically significant association was observed according to NCF values. However, analysis based on TTF values revealed a significant relationship between file kinematics and the comparison of original and replica-like instruments. In line with the overall results, replica-like instruments demonstrated greater resistance in the rotary group, whereas original instruments exhibited higher resistance compared to their replicas in the reciprocating group. The more complex nature of reciprocating motion compared to rotational motion, along with the greater reliance on proprietary heat treatment protocols, may have prevented replica-like reciprocating systems from keeping pace with such technological advancements. This limitation could have contributed to the observed results favoring original instruments in reciprocating motion. Replica-like systems, which are primarily designed to mimic the appearance of original instruments, may differ from the original systems in several critical aspects, such as cutting-edge design, core diameter, and Ni-Ti alloy composition. These differences, which influence cyclic fatigue resistance [21,53,54], are thought to be more easily compensated for in continuous rotational motion due to its predictable 360° stress distribution. However, in reciprocating motion, where the direction of rotation changes, increased contact with canal walls and higher stress accumulation may occur, making it more difficult for replica-like systems to compensate for such structural differences.

Subgroup analyses based on testing temperature provided further insight into the influence of experimental conditions on cyclic fatigue outcomes. Consistent with the overall findings of the present meta-analysis, NCF-based comparisons revealed no statistically significant difference in cyclic fatigue resistance between original and replica-like instruments at either room temperature or body temperature. In contrast, TTF-based analyses demonstrated that replica-like instruments exhibited higher cyclic fatigue resistance than original instruments under room temperature conditions, whereas this difference was no longer observed when testing was performed at body temperature. This discrepancy may be partly explained by the temperature-dependent mechanical behavior of nickel-titanium alloys. As emphasized by Savitha *et al.* [17], cyclic fatigue tests should preferably be conducted at body temperature in order to better simulate clinical conditions and to enhance the clinical relevance of experimental findings. In this context, the attenuation of TTF-based differences at body temperature observed in the present meta-analysis may reflect a more clinically representative assessment of cyclic fatigue resistance.

According to the Egger regression test applied to evaluate publication bias, a publication bias was detected in studies reporting TTF values ($p < 0.05$), whereas no evidence of publication bias was found in studies reporting NCF values ($p > 0.05$). Although a slight asymmetry was observed in the funnel plots for both TTF and NCF under the random-effects model using the trim-and-fill method, the analysis indicated that no imputation of missing studies was necessary, as confirmed by the absence of filled circles (Figure 3). These findings suggest that the observed asymmetry is more likely attributable to other factors, such as the high heterogeneity and methodological variability among the included studies, rather than to publication bias itself.

The meta-analyses revealed a high level of heterogeneity for both TTF and NCF data ($I^2 > 90\%$), which highlights a key limitation of the present study. Subgroup analyses indicated that this heterogeneity was partially attributable to differences in kinematic motion and testing temperature. However, due to methodological and experimental variability among the included studies, it was not possible to substantially reduce heterogeneity through the exclusion of specific studies. Potential reasons for the high heterogeneity include the wide variation in standard deviations and sample sizes across the included studies, as well as the presence of numer-

ous variables such as differences in testing apparatus, artificial canal parameters, and the diameter, taper, and metallurgical properties of the instruments examined. Taking all of these factors into account, replica-like instruments may be considered potential alternatives to original systems in terms of cyclic fatigue resistance. However, this interpretation should be made with caution in light of the high heterogeneity and methodological variability observed across the included studies. To achieve a more accurate understanding, future research should employ experimental setups designed in accordance with ISO standards, as is currently the case in the evaluation of torsional stress.

CONCLUSIONS

Overall, replica-like instruments exhibited cyclic fatigue resistance comparable to original systems and may be considered potential alternatives rather than superior options; however, due to the high heterogeneity and methodological variability among the included studies, these findings should be interpreted with caution, and further high-quality, well-standardized *in vitro* studies are required to confirm their clinical relevance.

CONFLICT OF INTEREST

No potential conflict of interest relevant to this article was reported.

FUNDING/SUPPORT

The authors have no financial relationships relevant to this article to disclose.

ACKNOWLEDGMENTS

We would like to express our gratitude to Elif Bahar Cakıcı for her contributions to this study.

AUTHOR CONTRIBUTIONS

Conceptualization, Formal analysis, Data curation, Visualization: Unal M. Methodology, Investigation: Unal M, Cakıcı F. Validation: Cakıcı F. Resources: Unal M, Cakıcı F. Supervision, Project administration: Cakıcı F. Writing – original draft: Unal M. Writing – review & editing: Unal M, Cakıcı F. All authors have read and approved the final manuscript.

DATA SHARING STATEMENT

The datasets are not publicly available but are available from the corresponding author upon reasonable request.

REFERENCES

1. Cheung GS, Liu CS. A retrospective study of endodontic treatment outcome between nickel-titanium rotary and stainless steel hand filing techniques. J Endod 2009;35:938-943.
2. Locke M, Thomas MB, Dummer PM. A survey of adoption of endodontic nickel-titanium rotary instrumentation part 1: general dental practitioners in Wales. Br Dent J 2013;214:E6.
3. Martins JN, Silva EJ, Marques D, Pereira MR, Ginjeira A, Silva RJ, *et al*. Mechanical performance and metallurgical features of ProTaper universal and 6 replicalike systems. J Endod 2020;46:1884-1893.
4. Martins JN, Nogueira Leal Silva EJ, Marques D, Ginjeira A, Braz Fernandes FM, De Deus G, *et al*. Influence of kinematics on the cyclic fatigue resistance of replicalike and original brand rotary instruments. J Endod 2020;46:1136-1143.
5. Martins JN, Silva EJ, Marques D, Belladonna F, Simões-Carvalho M, Camacho E, *et al*. Comparison of design, metallurgy, mechanical performance and shaping ability of replica-like and counterfeit instruments of the ProTaper Next system. Int Endod J 2021;54:780-792.
6. Adorno CG, Yoshioka T, Suda H. The effect of root preparation technique and instrumentation length on the development of apical root cracks. J Endod 2009;35:389-392.
7. Kim HC, Lee MH, Yum J, Versluis A, Lee CJ, Kim BM. Potential relationship between design of nickel-titanium rotary instruments and vertical root fracture. J Endod 2010;36:1195-1199.
8. Sattapan B, Nervo GJ, Palamara JE, Messer HH. Defects in rotary nickel-titanium files after clinical use. J Endod 2000;26:161-165.
9. Keskin C, Inan U, Demiral M, Keleş A. Cyclic fatigue resistance of Reciproc Blue, Reciproc, and WaveOne Gold reciprocating instruments. J Endod 2017;43:1360-1363.
10. Sivas Yilmaz Ö, Keskin C, Aydemir H. Comparison of the torsional resistance of 4 different glide path instruments. J Endod 2021;47:970-975.
11. Cheung GS. Instrument fracture: mechanisms, removal of fragments, and clinical outcomes. Endod Topics 2007;16:1-26.
12. Pedullà E, La Rosa GR, Virgillito C, Rapisarda E, Kim HC, Generali L. Cyclic fatigue resistance of nickel-titanium rotary instruments according to the angle of file access and radius of root canal. J Endod 2020;46:431-436.

https://doi.org/10.5395/rde.2026.51.e25

13. Cai JJ, Tang XN, Ge JY. Effect of irrigation on surface roughness and fatigue resistance of controlled memory wire nickel-titanium instruments. Int Endod J 2017;50:718-724.
14. Gambarini G, Grande NM, Plotino G, Somma F, Garala M, De Luca M, *et al*. Fatigue resistance of engine-driven rotary nickel-titanium instruments produced by new manufacturing methods. J Endod 2008;34:1003-1005.
15. Page MJ, McKenzie JE, Bossuyt PM, Boutron I, Hoffmann TC, Mulrow CD, *et al*. The PRISMA 2020 statement: an updated guideline for reporting systematic reviews. BMJ 2021;372:n71.
16. De Pedro-Muñoz A, Rico-Romano C, Sánchez-Llobet P, Montiel-Company JM, Mena-Álvarez J. Cyclic fatigue resistance of rotary versus reciprocating endodontic files: a systematic review and meta-analysis. J Clin Med 2024;13:882.
17. Savitha S, Sharma S, Kumar V, Chawla A, Vanamail P, Logani A. Effect of body temperature on the cyclic fatigue resistance of the nickel-titanium endodontic instruments: a systematic review and meta-analysis of in vitro studies. J Conserv Dent 2022;25:338-346.
18. Ragozzini G, Abu Hasna A, Dos Reis FA, de Moura FB, Campos TM, Bueno CE, *et al*. Effect of autoclave sterilization on the number of uses and resistance to cyclic fatigue of WaveOne Gold and four replica-like endodontic instruments. Int J Dent 2024;2024:6628146.
19. de Bastos RS, da Silva TV, Vieira VT, Silva EJ. Evaluation of mechanical properties of an original and a replica-like reciprocating instruments. Aust Endod J 2024;50:486-492.
20. Dos Reis FA, Abu Hasna A, Ragozzini G, de Moura FB, Campos TM, de Martin AS, *et al*. Assessing the cyclic fatigue resistance and sterilization effects on replica-like endodontic instruments compared to Reciproc Blue. Sci Rep 2023;13:22956.
21. Faus-Llácer V, Hamoud-Kharrat N, Marhuenda Ramos MT, Faus-Matoses I, Zubizarreta-Macho Á, Ruiz Sánchez C, *et al*. Influence of the geometrical cross-section design on the dynamic cyclic fatigue resistance of NiTi endodontic rotary files: an in vitro study. J Clin Med 2021;10:4713.
22. Noenko I, Goncharuk-Khomyn M, Belun V, Biley A. Counterfeit endodontic files features objectified with scanning electron microscopy: comparative study of SOCO SC Pro original and falsified rotary instruments. J Int Dent Med Res 2023;16:565-573.
23. Mumcu AK, Sari S, Özdemir ZY, Kiraz G, Kurnaz S. Comparing the shaping efficiency of original and replica-like endodontic instruments: in vitro study. Turk Klin J Dent Sci 2025;31:51-58.
24. Campos GO, Silva JD, Buono VTL, Santos LA, Peixoto IFC, Viana ACD. In-depth metallurgical, design, and mechanical analysis of Reciproc Blue and four replica-like endodontic systems [Preprint]. Research Square; 2024 [cited 2025 Nov 18]. Available from: https://doi.org/10.21203/rs.3.rs-3822398/v1
25. Martins JN, Silva EJ, Marques D, Arantes-Oliveira S, Caramês J, Versiani MA. Comparison of geometric design, metallurgical features and mechanical behavior of ProTaper Gold SX and two replica-like instruments. Rev Port Estomatol Cir Maxilofac 2021;62:1-8.
26. Madytianos B, Liu E, Marshall A, Mahony E, Liu K, Manogaran J, *et al*. A critical evaluation of physical and manufacturing properties of genuine and counterfeit rotary nickel-titanium endodontic instruments. Aust Dent J 2023;68:179-185.
27. Ertas H, Capar ID, Arslan H, Akan E. Comparison of cyclic fatigue resistance of original and counterfeit rotary instruments. Biomed Eng Online 2014;13:67.
28. Rodrigues CS, Vieira VT, Antunes HS, De-Deus G, Elias CN, Moreira EJ, *et al*. Mechanical characteristics of counterfeit Reciproc instruments: a call for attention. Int Endod J 2018;51:556-563.
29. Alcalde M, Duarte MA, Amoroso Silva PA, Souza Calefi PH, Silva E, Duque J, *et al*. Mechanical properties of ProTaper Gold, EdgeTaper Platinum, Flex Gold and Pro-T rotary systems. Eur Endod J 2020;5:205-211.
30. Alnoury A. Cyclic fatigue resistance of ProTaper Gold and two replicalike rotary systems. An in vitro study. Saudi Endod J 2024;14:25-30.
31. Aydın U, Özdemir M, Çulha E, Baştürk Özer MN, Turan B. Evaluation of cyclic fatigue resistance of novel replica-like instruments in static test model. Appl Bionics Biomech 2024;2024:8842478.
32. Lima TO, Duarte MA, Rosa SJ, Cordova AV, Souza PR, Vivan RR, *et al*. Cyclic and torsional fatigue resistance of two replicalike and original brand reciprocating system. RSBO 2024;21:241-246.
33. Martins JN, Silva EJ, Marques D, Belladonna F, Simões-Carvalho M, Vieira VT, *et al*. Design, metallurgical features, mechanical performance and canal preparation of six reciprocating instruments. Int Endod J 2021;54:1623-1637.
34. Martins JN, Silva EJ, Marques D, Pereira MR, Vieira VT, Arantes-Oliveira S, *et al*. Design, metallurgical features, and

mechanical behaviour of NiTi endodontic instruments from five different heat-treated rotary systems. Materials (Basel) 2022;15:1009.

35. Uslu O, Haznedaroglu F, Keskin C. Comparison of mechanical resistance and standardisation between original brand and replica-like endodontic systems. Aust Endod J 2023;49:149-158.
36. Ríos-Osorio N, Briñez-Rodríguez S, Fernández-Grisales R, Triana-Correa J, Pushaina-Velásquez A, García-Restrepo H, *et al*. Dynamic cyclic fatigue resistance of Reciproc® Blue, One Reci®, R-Motion®, and two replica-like endodontic files after autoclave sterilisation and/or immersion in sodium hypochlorite: a comparative in vitro study. J Clin Exp Dent 2025;17:e542-e551.
37. Tarragó C, Valencia De Pablo O, Loroño G, Conde A, Perez Alfayate R, Rossi Fedele G, *et al*. Cyclic fatigue resistance of 'replica-like" and original reciprocating instruments in single and double curvatures. Eur Endod J 2025;10:237-241.
38. Zanza A, Russo P, Reda R, Di Matteo P, Donfrancesco O, Ausiello P, *et al*. Mechanical and metallurgical evaluation of 3 different nickel-titanium rotary instruments: an in vitro and in laboratory study. Bioengineering (Basel) 2022;9:221.
39. Unal M, Cakici EB. Comparison of design, cyclic fatigue resistance, and metallurgical properties of original, replica-like, and counterfeit nickel-titanium files. Microsc Res Tech 2026;89:87-99.
40. Wan X, Wang W, Liu J, Tong T. Estimating the sample mean and standard deviation from the sample size, median, range and/or interquartile range. BMC Med Res Methodol 2014;14:135.
41. Fukumori Y, Nishijyo M, Tokita D, Miyara K, Ebihara A, Okiji T. Comparative analysis of mechanical properties of differently tapered nickeltitanium endodontic rotary instruments. Dent Mater J 2018;37:667-674.
42. de Vasconcelos RA, Murphy S, Carvalho CA, Govindjee RG, Govindjee S, Peters OA. Evidence for reduced fatigue resistance of contemporary rotary instruments exposed to body temperature. J Endod 2016;42:782-787.
43. Gambarini G. Cyclic fatigue of nickel-titanium rotary instruments after clinical use with low- and high-torque endodontic motors. J Endod 2001;27:772-774.
44. Plotino G, Grande NM, Cordaro M, Testarelli L, Gambarini G. A review of cyclic fatigue testing of nickel-titanium rotary instruments. J Endod 2009;35:1469-1476.
45. Kuhn G, Jordan L. Fatigue and mechanical properties of nickel-titanium endodontic instruments. J Endod 2002; 28:716-720.
46. Anderson ME, Price JW, Parashos P. Fracture resistance of electropolished rotary nickel-titanium endodontic instruments. J Endod 2007;33:1212-1216.
47. Zupanc J, Vahdat-Pajouh N, Schäfer E. New thermomechanically treated NiTi alloys: a review. Int Endod J 2018;51:1088-1103.
48. Rodrigues RC, Lopes HP, Elias CN, Amaral G, Vieira VT, De Martin AS. Influence of different manufacturing methods on the cyclic fatigue of rotary nickel-titanium endodontic instruments. J Endod 2011;37:1553-1557.
49. Silva EJ, Peña-Bengoa F, Ajuz NC, Vieira VT, Martins JN, Marques D, *et al*. Multimethod analysis of large- and low-tapered single file reciprocating instruments: design, metallurgy, mechanical performance, and irrigation flow. Int Endod J 2024;57:601-616.
50. Bahia MG, Buono VT. Decrease in the fatigue resistance of nickel-titanium rotary instruments after clinical use in curved root canals. Oral Surg Oral Med Oral Pathol Oral Radiol Endod 2005;100:249-255.
51. Bürklein S, Maßmann P, Donnermeyer D, Tegtmeyer K, Schäfer E. Need for standardization: influence of artificial canal size on cyclic fatigue tests of endodontic instruments. Appl Sci (Switzerland) 2021;11:4950.
52. Plotino G, Grande NM, Mazza C, Petrovic R, Testarelli L, Gambarini G. Influence of size and taper of artificial canals on the trajectory of NiTi rotary instruments in cyclic fatigue studies. Oral Surg Oral Med Oral Pathol Oral Radiol Endod 2010;109:e60-e66.
53. Pruett JP, Clement DJ, Carnes DL. Cyclic fatigue testing of nickel-titanium endodontic instruments. J Endod 1997;23:77-85.
54. Tripi TR, Bonaccorso A, Condorelli GG. Cyclic fatigue of different nickel-titanium endodontic rotary instruments. Oral Surg Oral Med Oral Pathol Oral Radiol Endod 2006;102:e106-e114.

https://doi.org/10.5395/rde.2026.51.e25

RDE Restorative Dentistry & Endodontics

Research Article

eISSN 2234-7666
Restor Dent Endod. 2026 May;51(2):e26
https://doi.org/10.5395/rde.2026.51.e26

In vitro assessment of geometric characteristics in canal preparation using nickel-titanium files used for minimal invasiveness: an experimental study

EunJin Jang[1], **Hyeon-Cheol Kim**[2,*], **WooCheol Lee**[1,*]

[1]Department of Conservative Dentistry, Dental Research Institute, School of Dentistry, Seoul National University, Seoul, Korea
[2]Department of Conservative Dentistry, Dental Research Institute, Dental and Life Science Institute, School of Dentistry, Pusan National University, Yangsan, Korea

ABSTRACT

Objectives: This study aimed to assess geometric characteristics in canal preparation using nickel-titanium (NiTi) files used for minimal invasiveness.

Methods: Thirty J-shaped simulated canals in resin blocks were instrumented with either TruNatomy (TR; Dentsply Sirona), EndoRoad (ER; Maruchi), or ProTaper Ultimate (PTU; Dentsply Sirona). The simulated canal blocks were scanned using microcomputed tomography before and after instrumentation. The scanned images were reconstructed, and the canal surface area was measured from 0.5 to 6.5 mm from the apex. Three-dimensional representative models of each group were rendered. The data were statistically analyzed using one-way analysis of variance and Kruskal-Wallis test at 95% significance level.

Results: TR showed a superior ability to maintain the canal's center. TR demonstrated comparable apical preparation to PTU. ER showed a smaller and limited apical preparation than other systems, with a tendency for canal preparation toward the inner side of the curvature. PTU featured the largest prepared apical size among the file groups and tended to straighten the curvature by preparing the canal more towards the outward side. The surface area instrumented using each NiTi file showed statistically significant differences among the three groups at all levels except 0.5, 2.0, and 3.5 mm from the apex ($p < 0.05$). There was no statistically significant difference between TR and PTU at a level of 0.5 mm from the apex ($p > 0.05$).

Conclusions: While PTU is suitable for general canal preparation to facilitate irrigation and intracanal medication, TR and ER excel in preserving canal centering with minimal concern for canal transportation by minimally invasive preparation.

Keywords: Root canal preparation; Geometric characteristics; Minimal invasiveness; Nickel-titanium files

Received: November 8, 2025 **Revised:** December 12, 2025 **Accepted:** December 27, 2025

Citation
Jang E, Kim HC, Lee W. *In vitro* assessment of geometric characteristics in canal preparation using nickel-titanium files used for minimal invasiveness: an experimental study. Restor Dent Endod 2026;51(2):e26.

***Correspondence to**
Hyeon-Cheol Kim, DDS, MS, PhD
Department of Conservative Dentistry, Dental Research Institute, School of Dentistry, Pusan National University, 20 Geumo-ro, Mulgeum-eup, Yangsan 50612, Korea
Email: golddent@pusan.ac.kr

WooCheol Lee, DDS, MS, PhD
Department of Conservative Dentistry, Dental Research Institute, School of Dentistry, Seoul National University, 101 Daehak-ro, Jongno-gu, Seoul 03080, Korea
Email: jimin525@snu.ac.kr

Hyeon-Cheol Kim and WooCheol Lee contributed equally to this work as co-corresponding authors.

INTRODUCTION

Proper cleaning and shaping of the root canal system are fundamental aspects of successful endodontic treatment. The primary goal of root canal preparation is to eliminate microorganisms, necrotic tissue, and infected dentin that may lead to pulp and periapical infections [1]. Nickel-titanium (NiTi) instruments have revolutionized root canal preparation due to their unique metallurgical properties, including superelasticity and shape memory, offering superior performance compared to traditional stainless-steel files while minimizing preparation-related complications such as canal transportation, ledge or zip formation, and other aberrations [2]. Recent generations of heat-treated NiTi instruments exhibit increased flexibility, fatigue resistance, and improved canal centering, allowing effective cleaning and shaping with minimal deviation from the original canal anatomy [3].

Current trends in endodontics emphasize a conservative approach to treatment. Modern advancements such as dental operating microscopes, ultrasonic instruments, heat-treated NiTi files, and supplemental irrigating systems have contributed to the shift toward minimally invasive endodontics (MIE). In this context, a conservative treatment approach refers to preserving pericervical and radicular dentin through conservative access cavity design, anatomically centered canal preparation with minimal taper enlargement, and reliance on enhanced irrigation and disinfection rather than excessive mechanical instrumentation [3,4]. MIE aims to preserve tooth structure, enhancing the long-term prognosis of endodontically treated teeth [3,4].

NiTi files with reduced taper and shaft diameter enable effective apical canal enlargement while minimizing file stress and reducing debris extrusion [5]. These design modifications allow for efficient preparation and disinfection up to the apical region without compromising the integrity of the canal or increasing the risk of procedural errors [6].

A critical consideration in assessing file performance is the ability to maintain the instrument's central positioning within the canal, minimizing canal transportation. Especially, the instrumentation of the apical region is considered an essential component for achieving thorough cleaning and shaping. When considering transportation and apical preparation, it is challenging to determine which is more crucial, as there is a potential for conflicting aspects between these two values [2,7].

Manufacturers develop instrument systems to apply the MIE concept to mechanical shaping procedures. Among them, the TruNatomy rotary system (Dentsply Sirona, Ballaigues, Switzerland) features heat-treated instruments with an off-centered rectangular cross-section, regressive taper, and a maximum fluted diameter of 0.8 mm. The instruments have variable tapers, ranging from 0.02 for larger instruments to 0.04 for smaller ones. Previous studies highlight its high cyclic fatigue resistance and ability to preserve the original canal anatomy, attributed to enhanced flexibility from advanced heat treatment during the post-manufacturing process [4,8].

The ProTaper Ultimate (PTU) rotary system (Dentsply Sirona) is the latest addition to this kind of instrument system, utilizing a specialized heat treatment technology to achieve optimal flexibility and strength. Its parallelogram cross-section with distinctive acute angles, a partially off-centered design, and a maximal flute diameter of 1.0 mm allows for conservative dentin removal in critical areas, such as the cementoenamel junction [9,10].

The EndoRoad file system (Maruchi, Wonju, Korea) incorporates an innovative heat treatment known as "memory-triple heat treatment." This process induces the R-phase within the range of body temperature. This leads to a symmetric presence of the R-phase at body temperature, yielding a substantial enhancement in flexibility and cyclic fatigue resistance of the files compared to earlier heat treatment technologies [11,12].

However, despite these advancements, the efficacy and geometric characteristics of these modern NiTi files during canal preparation remain inadequately studied.

The objective of this study was to evaluate the geometric characteristics of canal preparation using three NiTi file systems designed for the minimal invasiveness concept. The null hypothesis was that there would be no significant differences in canal preparation among the tested file systems.

https://doi.org/10.5395/rde.2026.51.e26

METHODS

The flow of this study is summarized in Figure 1. A total of 30 simulated J-shaped root canals in transparent resin blocks (Dentsply Sirona) were used in this study. Each resin block measured 16 mm in length, with a curvature radius of 3.5 mm and an angle of 53º, as measured according to the method described by Pruett *et al.* [13]. The point of maximum flexure was located 3.5 mm from the apical end, and the apical foramen communicated with the exterior of the resin block.

Group designation and Specimen preparation

The specimens were divided into three groups (n = 10 per group). The sample size was determined using pilot data from a preliminary micro-CT analysis and G*Power 3.1.9.2 software (Heinrich-Heine-Universität Düsseldorf, Germany), with an α level of 0.05 and a power of 0.80. This analysis indicated that a minimum of nine specimens per group would be required to detect significant differences in canal geometry among the file systems; therefore, 10 specimens per group were used in the present study. This sample size is also in line with a previous micro-CT study evaluating canal shaping outcomes using standardized models [7].

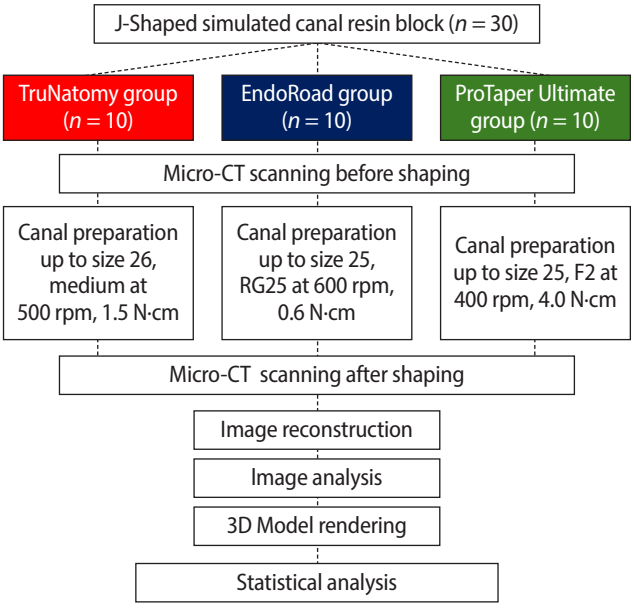

Figure 1. Experimental flow of this study. Micro-CT, micro-computed tomography; 3D, three-dimensional. TruNatomy: Dentsply Sirona, Ballaigues, Switzerland. ProTaper Ultimate: Dentsply Sirona. EndoRoad: Maruchi, Wonju, Korea.

All canal preparations were performed by a single experienced operator (a postgraduate student with over 6 years of clinical experience). The preparation followed the instructions of the manufacturer with minor modifications in which unnecessary steps were omitted. The final instrumentation size of all systems was standardized to approximately #25.

1. TruNatomy group (n = 10)

Working length was measured using a #10 K file, and patency was confirmed. Instrumentation was performed with the TruNatomy system at a speed of 500 rpm and a torque setting of 1.5 N•cm. All instrumentation was performed in the presence of a lubricant (RC prep; Premier Dental, Plymouth Meeting, PA, USA). Initial instrumentation was performed using the TruNatomy Glider file (#17/.02) until the working length was reached. The canal was irrigated with saline, and patency was reconfirmed. As the simulated canal is made of resin material, there was no organic tissue, bacteria, or dentinal tubules. So, only saline was used to clean out the resin debris after instrumentation. Final instrumentation was performed using the TruNatomy Prime file (#26/.04) to the working length. Irrigation with saline and patency checks were repeated throughout the process.

2. ProTaper Ultimate group (n = 10)

Working length was measured with a #10 K file, and patency was confirmed. Instrumentation was performed with the PTU system at a speed of 400 rpm and a torque setting of 4.0 N•cm. The same lubricant was used during all steps. Initial instrumentation was performed with the PTU Slider file (#16/.02v) to confirm the patency. The same saline irrigation protocol was used, followed by the instrumentation with the PTU Shaper file (#20/.04v), with the patency maintained. The instrumentation process continued with the PTU F1 file (#20/.07v) and, subsequently, the PTU F2 file (#25/.08v), both to the working length. The working length was maintained throughout instrumentation. Saline irrigation and patency checks were repeated at each step.

3. EndoRoad group (n = 10)

Working length was measured with a #10 K file, and pa-

tency was confirmed. Instrumentation was performed with the EndoRoad system at a speed of 600 rpm and a torque setting of 0.6 N•cm. The same lubricant was used during all steps. Initial instrumentation was performed using the EndoRoad RP15 file (#15/.02) to confirm the patency. The canal was irrigated with saline, followed by instrumentation with the EndoRoad RP20 file (#20/.03) until the patency was confirmed. Final instrumentation was performed using the EndoRoad RG25 file (#25, variable taper of .06 at less than 3 mm from the tip, and .02 at more than 3 mm from the tip) to the working length. Saline irrigation and patency checks were repeated throughout the process.

Before the experimental tests, all instruments were inspected under a dental operating microscope to confirm the absence of deformation, unwinding, or other defects. All files used in this study for canal preparation showed a normal morphology.

Micro-computed tomography scanning and three-dimensional reconstruction

The resin blocks were scanned before and after canal instrumentation using a micro-computed tomography (micro-CT, SkyScan 1273; Bruker micro-CT, Kontich, Belgium). Each specimen was secured in a cylindrical holder using Parafilm (Sigma-Aldrich, St. Louis, MO, USA), with the access cavity positioned at the top. The holder was placed in the micro-CT scanner, where parameters, file prefixes, and data directories were manually configured. Scanning was conducted individually for each specimen, with 21 minutes and 46 seconds per scan, at 70 kV, 214 μA, with 360° rotation and a 0.3° rotation step. The scans produced images with a voxel size of 24 μm.

Image reconstruction was performed using NRecon software (Bruker micro-CT, ver. 1.7.4.2) with beam hardening correction set at 40% and ring artifact correction at 1, generating 972 cross-sectional images per specimen. The reconstructed datasets were coregistered using DataViewer software (ver. 1.5.6.2, Bruker micro-CT). CTAn software (ver. 1.18.4.1, Bruker micro-CT) was employed to measure the cross-sectional areas of canals. Using CTvol software (ver. 2.3.2.0, Bruker micro-CT), three-dimensional (3D) models of the canals before and after instrumentation were rendered to evaluate the geometrical characteristics of the prepared canals.

Canal levels from 0.5 mm to 6.5 mm from the apex were subdivided into increments of 1.0 mm. The cross-sectional surface areas (mm^2) were measured at the seven levels at each 1-mm incremental level from 0.5 mm to 6.5 mm.

Statistical analysis

The Shapiro-Wilk test was used to assess the normality of the data distribution for all three groups at each measurement level. When the assumptions of normality and homogeneity of variance were satisfied, one-way analysis of variance was used to determine significant differences among the groups, followed by appropriate *post hoc* pairwise comparisons with Bonferroni adjustment. For data that did not meet normality assumptions, the nonparametric Kruskal-Wallis test was applied instead. All statistical analyses were performed using IBM SPSS Statistics software (ver. 26; IBM Corp., Armonk, NY, USA), with a confidence interval of 95% and a significance level set at 0.05.

RESULTS

During instrumentation, no procedural complications, such as instrument fracture, loss of working length, or ledge formation, were observed in any specimen.

In the 3D models, the TruNatomy group showed superior ability in maintaining the center of the canal (Figure 2). The TruNatomy group also demonstrated comparable apical preparation to that of the PTU group. The EndoRoad group, in contrast, showed a more limited apical preparation compared to the other NiTi file systems, with a tendency for canal preparation toward the inner side of the canal curvature (Figure 2). However, this tendency was consistent and presented with minimal aberrations. The PTU group featured the largest apical preparation among the file groups, with a notable tendency to straighten the canal curvature by preparing more toward the outward side.

Statistical analysis of the instrumented surface area revealed differences among the three groups at all levels (Figure 3), except at 0.5 mm, 2.0 mm, and 3.5 mm from the apex. The PTU group showed significantly larger areas than other groups at all levels, while the EndoRoad

https://doi.org/10.5395/rde.2026.51.e26

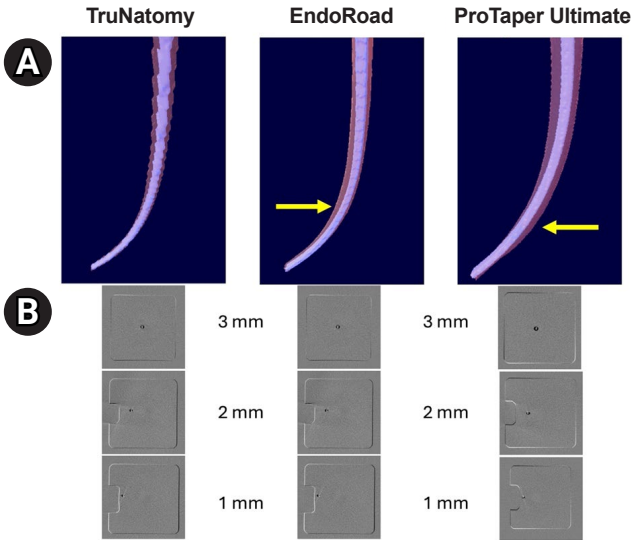

Figure 2. Representative superimposed images show maintaining the center of the canals after instrumentation. (A) Longitudinal superimposed images. The EndoRoad group shows inner side deviation to the canal curvature, while the ProTaper Ultimate group shows outward side deviation apically (yellow arrows). (B) Cross-sectional superimposed images at the 1 mm, 2 mm, and 3 mm levels. TruNatomy: Dentsply Sirona, Ballaigues, Switzerland. ProTaper Ultimate: Dentsply Sirona. EndoRoad: Maruchi, Wonju, Korea.

group shows generally showed smaller surface areas, especially over the 3.5 mm level. The TruNatomy group showed significantly larger areas at the 1 mm level. In comparison, there was no difference between the TruNatomy and EndoRoad groups at 2.0 mm and 3.5 mm levels from the apex.

Significant differences were observed among all groups at the 1 mm and 3 mm levels ($p < 0.05$, Figure 4). The PTU group shows significantly bigger areas than the other groups at the 2 mm level ($p < 0.05$). The TruNatomy and EndoRoad groups do not have a significant difference. Significant differences were observed among all groups at the 1 mm level ($p < 0.05$).

DISCUSSION

This study evaluated the geometric characteristics of canal preparation using three NiTi file systems designed according to the MIE concept. A designated file from each system was selected to standardize the apical tip ISO size of #25 (EndoRoad RG25 file and PTU F2) and #26 (TruNatomy Prime file). It might initially seem that

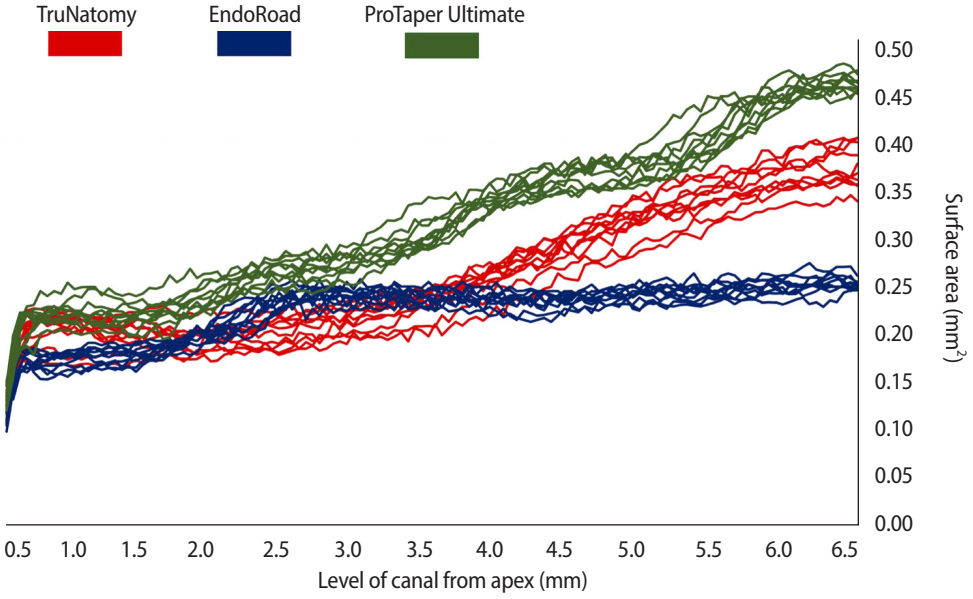

Figure 3. Line graphs of the instrumented surface areas for all specimens of the three groups at levels from 0.5 mm to 6.5 mm from the apex. The ProTaper Ultimate group (green) shows much bigger areas than other groups in all levels, while the EndoRoad group (blue) shows generally a smaller surface area, especially over the 3.5 mm level. The TruNatomy group (red) shows a significantly larger area at the 1 mm level ($p < 0.05$). In comparison, there was no difference between the TruNatomy and EndoRoad groups at 2.0 mm and 3.5 mm levels from the apex. TruNatomy: Dentsply Sirona, Ballaigues, Switzerland. ProTaper Ultimate: Dentsply Sirona. EndoRoad: Maruchi, Wonju, Korea.

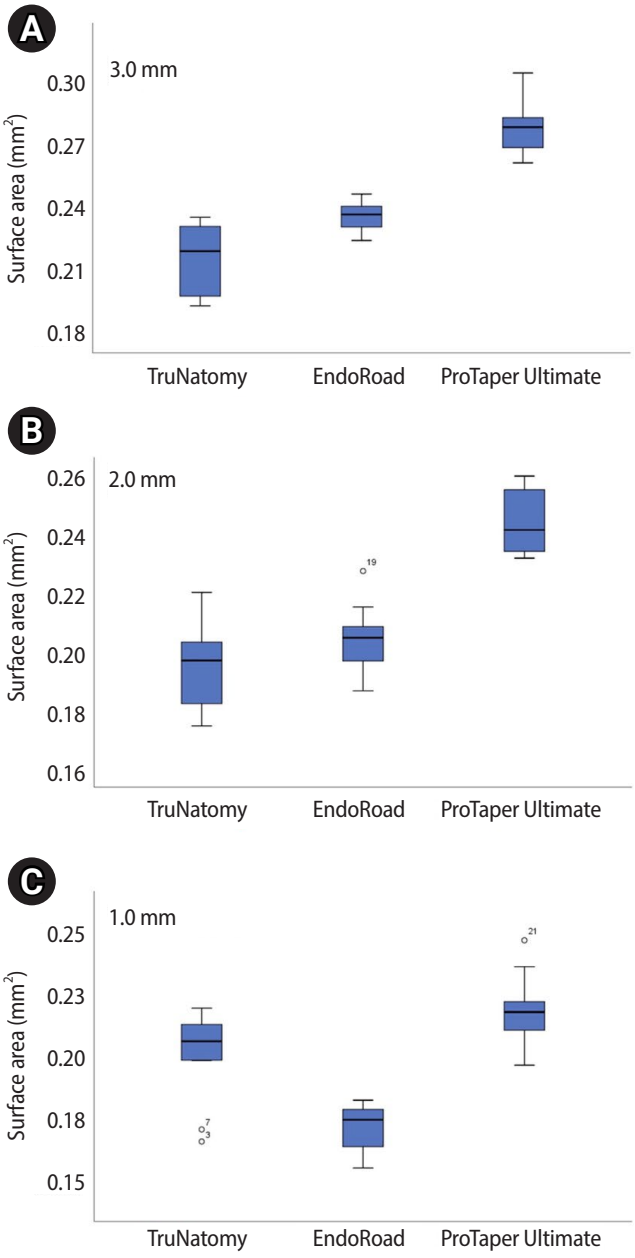

Figure 4. Instrumented surface areas at three levels. (A) All groups show significant differences among the groups at the 1 mm and 3 mm levels. (B) The ProTaper Ultimate group shows significantly bigger areas than the other groups at the 2 mm level. TruNatomy and EndoRoad do not have a significant difference. (C) All groups show significant differences among the groups at the 1 mm level. TruNatomy: Dentsply Sirona, Ballaigues, Switzerland. ProTaper Ultimate: Dentsply Sirona. EndoRoad: Maruchi, Wonju, Korea.

the TruNatomy file, with its slender and narrow appearance, would result in insufficient canal preparation. However, the results showed that the instrumented area at the apical 0.5–3.0 mm prepared with the TruNatomy Prime file was comparable to that of the PTU F2 file [8,9].

The TruNatomy system was originally designed to achieve minimally invasive canal preparation and to preserve a larger portion of the tooth structure, particularly the root dentine [8,9]. The findings of this study partially support this concept, as the canal preparation in the coronal 3.0–6.5 mm region with the TruNatomy file was more limited compared to the larger-taper PTU file system. However, this minimal preparation could raise concerns about the prognosis of the overall treatment, as restricted canal shaping may reduce the accessibility of irrigants and intracanal medicaments. Despite these concerns, the results demonstrated that apical preparation from 0.5 mm to 3.0 mm using the TruNatomy file was comparable to that achieved by the PTU file. This suggests that the core function of instrumentation—removing debris and microorganisms—was not compromised, even with this smaller and more conservative file system [8,9,14,15].

Although the tip size (approximately #25) of the three NiTi file systems was standardized, the cross-sectional areas changed from 0.5 to 6.5 mm from the apex and differed significantly among the systems. The key characteristics of each file system can be summarized as follows: TruNatomy demonstrated apical preparation comparable to PTU, highlighting its effectiveness in shaping the apical region. PTU exhibited the most extensive preparation among the three groups, reflecting its large taper design. EndoRoad showed relatively limited apical preparation compared to the other systems; however, its low standard deviation indicated a consistent preparation trend across specimens [8,9].

Schilder [16] proposed that the final preparation should have a continuous taper with the smallest possible apical foramen. Similarly, Buchanan [17] suggested that apical preparation should be performed to the minimum size possible. However, current instrumentation and irrigation techniques remain insufficient for the complete elimination of debris and bacteria in the apical third [18]. The challenge of removing bacterial debris from this region is attributed to the narrow canal space, complex canal morphology, inadequate irrigant flushing, and variations in the diameter of the root ca-

https://doi.org/10.5395/rde.2026.51.e26

nal [6]. Thus, the debate regarding the optimal extent of apical enlargement for successful endodontic treatment remains unresolved. Although randomized controlled trials are considered the gold standard in clinical research, no such study has been conducted in this regard to date.

The concept of significant apical enlargement is based on the premise that increasing the apical diameter enhances canal debridement [19]. This is justified by evidence that microorganisms can penetrate dentinal tubules to depths of 200–300 μm, where they are difficult to eliminate using conventional methods [20]. Studies by Falk and Sedgley [21] have demonstrated that larger apical preparation improves the efficacy of irrigation solutions and reduces bacterial growth in the apical region. Similarly, Brunson *et al.* [22] reported that larger apical preparation increases the volume of irrigation solution reaching the apical third, enhancing the removal of tissue debris.

Additionally, Fornari *et al.* [23] and Plotino *et al.* [24] observed that apical enlargement reduces the non-instrumented areas within the root canal, potentially improving overall cleanliness. Conversely, a study by Coldero *et al.* [25] found no significant difference in intracanal bacterial reduction with or without apical enlargement preparation. It concluded that removing additional dentine from the apical region is unnecessary when an adequate coronal taper is achieved, as this facilitates effective irrigation throughout the root canal system. Thus, apical enlargement remains controversial to date, and no study has ever shown a direct relationship between apical enlargement and clinical success or failure in endodontic treatment. Additionally, apical enlargement carries several drawbacks, including the risk of canal transportation, weakening of the root structure, and potential over-preparation of the canal [26].

Transportation is defined as the removal of the canal wall structure on the outer curve of the apical half of the canal. This occurs due to the natural tendency of files to return to their original linear shape during canal preparation, potentially resulting in ledge formation or even perforation [2]. Therefore, a more comprehensive definition of root canal transportation describes it as the deviation of the post-instrumentation canal center from its original position compared to the pre-instrumentation canal center.

Canal transportation during instrumentation most commonly occurs at different levels depending on the degree of root canal curvature. As a deviation of the prepared canal from its original path, root canal transportation is a critical factor influencing treatment outcomes [2,27]. Consequently, evaluating the ability of endodontic instruments to remain centered within the canal while minimizing iatrogenic defects is essential.

While small-tapered instruments are commonly believed to possess greater flexibility, allowing them to maintain the original axial direction of the root canal more effectively, recent studies using proper 3D analysis with micro-CT technology have demonstrated comparable canal transportation levels between the XP-endo Shaper (FKG Dentaire) and other systems in mesial canals of mandibular molars [27]. Previous meta-analysis research on the centering ability of NiTi instruments has identified the shaft taper as a significant factor influencing canal transportation, emphasizing the importance of taper selection in minimizing this issue during canal preparation [28].

This study utilized resin blocks simulating root canals as experimental samples, providing advantages and limitations. Using simulated root canals with standardized shapes and dimensions, such as round cross-sections, continuous tapers, and uniform sizes, allows for high reproducibility and a controlled environment to evaluate various instrumentation techniques. One of the primary benefits of using simulated resin blocks is the ability to visualize how canal preparation progresses during instrumentation. This feature is particularly valuable for assessing shaping outcomes, including apical stop formation, taper consistency, and the presence of aberrations such as zips, elbows, or perforations. Additionally, the high degree of standardization in simulated canal block anatomy eliminates anatomical variability, enabling researchers to focus solely on the performance of the instruments under investigation. Such evaluations provide insights into the efficacy and safety of different file systems under controlled conditions [29,30].

Despite their advantages, simulated resin block models have several significant limitations. One major drawback is their inability to evaluate root canal cleanliness, as the resin material does not replicate the

biological presence of pulp tissue, debris, or microbial contamination. Moreover, the mechanical properties of resin differ substantially from those of human dentin, requiring lower forces for instrumentation and potentially underestimating straightening and the incidence of preparation errors, such as ledging or outer widening [30–32]. This discrepancy leads to differences in the forces required for instrumentation, with human dentin requiring approximately twice the force for preparation compared to resin blocks. While resin block models offer valuable insights into instrumentation performance, the results must be interpreted cautiously when extrapolating findings to clinical practice. The simplified anatomy and reduced hardness of resin blocks may underestimate the challenges of preparing natural root canals. Therefore, the findings of this study should be regarded as comparative data obtained under highly standardized *in vitro* conditions rather than as direct predictors of clinical outcomes.

In the present study, the primary objective was to compare subtle differences in shaping behavior and canal geometry among three NiTi file systems designed for MIE. To achieve this aim, it was essential to minimize anatomical variability and confounding factors. Simulated canals in resin blocks with identical curvature, length, and canal diameter were therefore selected, as they provide a highly standardized experimental environment in which the effects of the instruments themselves can be isolated more reliably. While this choice inevitably limits the direct clinical extrapolation of our results, it strengthens the internal validity of the comparison among the three systems.

This study used micro-CT technology, and this imaging technique enables noninvasive, nondestructive, and high-resolution 3D assessments, offering unparalleled insights into various aspects of canal instrumentation. Micro-CT provides the ability to precisely analyze the changes in root canal volume, monitoring changes in the structural integrity of the canal walls [7,32]. Especially in this study, the assessment of shaping performance and maintaining the original anatomy would be effective. As a result, micro-CT findings are reliable only within experiments conducted under identical conditions and parameter settings.

CONCLUSIONS

Based on the results from the present study, PTU may be an ideal option when extensive canal preparation is needed to create sufficient space for irrigation and intracanal medication, with a low tendency for canal transportation under the conditions of this study. TruNatomy seems proper for maintaining canal centering, particularly in severely curved canals, with comparable apical preparation to that of PTU. EndoRoad is a reliable choice for negotiating highly calcified canals, enabling minimal preparation and glide path establishment with reduced risk of procedural accidents.

CONFLICT OF INTEREST

No potential conflict of interest relevant to this article was reported.

FUNDING/SUPPORT

This study was supported by the SNUDH Research Fund (grant No. 04-2022-0121).

AUTHOR CONTRIBUTIONS

Conceptualization, Funding acquisition, Supervision, Project administration: Lee W. Data curation, Software: Jang E. Formal analysis: Jang E, Lee W. Investigation, Visualization: Jang E, Kim HC. Methodology, Validation: Kim HC, Lee W. Writing - original draft: Jang E. Writing - review & editing: Kim HC, Lee W. All authors read and approved the final manuscript.

DATA SHARING STATEMENT

The datasets are not publicly available but are available from the corresponding author upon reasonable request.

REFERENCES

1. Siqueira JF. Aetiology of root canal treatment failure: why well-treated teeth can fail. Int Endod J 2001;34:1-10.
2. Peters OA. Current challenges and concepts in the preparation of root canal systems: a review. J Endod 2004;30:559-567.
3. Silva EJ, De-Deus G, Souza EM, Belladonna FG, Cavalcante DM, Simões-Carvalho M, *et al*. Present status and future directions: minimal endodontic access cavities. Int Endod J 2022;55 Suppl 3:531-587.
4. Kang YJ, Kwak SW, Ha JH, Gambarini G, Kim HC. Fracture resistances of heat-treated nickel-titanium files used for minimally invasive instrumentation. BMC Oral Health 2025;25:126.

https://doi.org/10.5395/rde.2026.51.e26

5. Chaniotis A, Ordinola-Zapata R. Present status and future directions: management of curved and calcified root canals. Int Endod J 2022;55 Suppl 3:656-684.
6. Butcher S, Mansour A, Ibrahim M. Influence of apical preparation size on effective conventional irrigation in the apical third: a scanning electron microscopic study. Eur Endod J 2019;4:9-14.
7. Versiani MA, Leoni GB, Steier L, De-Deus G, Tassani S, Pécora JD, *et al*. Micro-computed tomography study of oval-shaped canals prepared with the self-adjusting file, Reciproc, WaveOne, and ProTaper universal systems. J Endod 2013;39:1060-1066.
8. Elkholy MM, Nawar NN, Ha WN, Saber SM, Kim HC. Impact of canal taper and access cavity design on the life span of an endodontically treated mandibular molar: a finite element analysis. J Endod 2021;47:1472-1480.
9. Song J, Jang JH, Chang SW, Chung SH, Oh S. Comparison of mechanical properties and shaping performance of ProGlider and ProTaper ultimate slider. BMC Oral Health 2025;25:59.
10. Alhayki MM, Eid B, Elemam R, Elsewify T. Evaluation of apically extruded debris during root canal preparation using ProTaper ultimate and ProTaper gold: an ex vivo study. Eur Endod J 2025;10:41-46.
11. Hong J, Kwak SW, Ha JH, Sigurdsson A, Shen Y, Kim HC. Effect of different heat treatments and surface treatments on the mechanical properties of nickel-titanium rotary files. Metals 2023;13:1769.
12. Kim E, Ha JH, Dorn SO, Shen Y, Kim HC, Kwak SW. Effect of heat treatment on mechanical properties of nickel-titanium instruments. J Endod 2024;50:213-219.
13. Pruett JP, Clement DJ, Carnes DL. Cyclic fatigue testing of nickel-titanium endodontic instruments. J Endod 1997;23:77-85.
14. Unno H, Ebihara A, Hirano K, Kasuga Y, Omori S, Nakatsukasa T, *et al*. Mechanical properties and root canal shaping ability of a nickel-titanium rotary system for minimally invasive endodontic treatment: a comparative in vitro study. Materials (Basel) 2022;15:7929.
15. Copelli FA, Oda LY, Rodrigues CT, Batista A, Duarte MA, Cavenago BC. Evaluation of minimally invasive preparation of curved mesial canals of mandibular molars: an in vitro study. J Endod 2024;50:1321-1326.
16. Schilder H. Cleaning and shaping the root canal. Dent Clin North Am 1974;18:269-296.
17. Buchanan LS. The standardized-taper root canal preparation: part 1: concepts for variably tapered shaping instruments. Int Endod J 2000;33:516-529.
18. Siqueira JF, Rôças IN. Clinical implications and microbiology of bacterial persistence after treatment procedures. J Endod 2008;34:1291-1301.e3.
19. Lee OY, Khan K, Li KY, Shetty H, Abiad RS, Cheung GS, *et al*. Influence of apical preparation size and irrigation technique on root canal debridement: a histological analysis of round and oval root canals. Int Endod J 2019;52:1366-1376.
20. Tsesis I, Lokshin M, Littner D, Goldberger T, Rosen E. Depth of bacterial penetration into dentinal tubules after use of different irrigation solutions: a systematic review of in vitro studies. Appl Sci 2022;13:496.
21. Falk KW, Sedgley CM. The influence of preparation size on the mechanical efficacy of root canal irrigation in vitro. J Endod 2005;31:742-745.
22. Brunson M, Heilborn C, Johnson DJ, Cohenca N. Effect of apical preparation size and preparation taper on irrigant volume delivered by using negative pressure irrigation system. J Endod 2010;36:721-724.
23. Fornari VJ, Hartmann MS, Vanni JR, Rodriguez R, Langaro MC, Pelepenko LE, *et al*. Apical root canal cleaning after preparation with endodontic instruments: a randomized trial in vivo analysis. Restor Dent Endod 2020;45:e38.
24. Plotino G, Grande NM, Tocci L, Testarelli L, Gambarini G. Influence of different apical preparations on root canal cleanliness in human molars: a SEM study. J Oral Maxillofac Res 2014;5:e4.
25. Coldero LG, McHugh S, MacKenzie D, Saunders WP. Reduction in intracanal bacteria during root canal preparation with and without apical enlargement. Int Endod J 2002;35:437-446.
26. Lertchirakarn V, Palamara JE, Messer HH. Patterns of vertical root fracture: factors affecting stress distribution in the root canal. J Endod 2003;29:523-528.
27. Cerqueira NM, Louzada VG, Silva-Sousa YT, Raucci-Neto W, Leoni GB. Effect of canal preparation with XP-endo shaper and ProTaper next on root canal geometry and dentin thickness of mandibular premolars with radicular grooves and two canals: a micro-CT study. Clin Oral Investig 2021;25:5505-5512.
28. Gundappa M, Bansal R, Khoriya S, Mohan R. Root canal centering ability of rotary cutting nickel titanium instruments: a meta-analysis. J Conserv Dent 2014;17:504-509.
29. Yang G, Yuan G, Yun X, Zhou X, Liu B, Wu H. Effects of two

nickel-titanium instrument systems, Mtwo versus ProTaper universal, on root canal geometry assessed by micro-computed tomography. J Endod 2011;37:1412-1416.
30. Christofzik D, Bartols A, Faheem MK, Schroeter D, Groessner-Schreiber B, Doerfer CE. Shaping ability of four root canal instrumentation systems in simulated 3D-printed root canal models. PLoS One 2018;13:e0201129.
31. Bürklein S, Poschmann T, Schäfer E. Shaping ability of different nickel-titanium systems in simulated S-shaped canals with and without glide path. J Endod 2014;40:1231-1234.
32. Peters OA, Laib A, Göhring TN, Barbakow F. Changes in root canal geometry after preparation assessed by high-resolution computed tomography. J Endod 2001;27:1-6.

https://doi.org/10.5395/rde.2026.51.e26

RDE Restorative Dentistry & Endodontics

Case Report

eISSN 2234-7666
Restor Dent Endod. 2026 May;51(2):e27
https://doi.org/10.5395/rde.2026.51.e27

Endodontic treatment of a molar-incisor malformation of the maxillary first molar: a case report

Woo-Lim Kim, Se-Hee Park, Kyung-Mo Cho, Jin-Woo Kim*

Department of Conservative Dentistry, College of Dentistry, Kangwon National University, Gangneung, Korea

ABSTRACT

Molar-incisor malformation (MIM) is a developmental dental anomaly primarily affecting permanent first molars, often accompanied by structural irregularities such as cervical mineralized diaphragms (CMDs) and furcal channels. These anatomical complexities present significant challenges for endodontic treatment. This case report presents the endodontic management of a maxillary first molar diagnosed with MIM—a condition for which root canal treatment has rarely been reported. The affected tooth exhibited characteristic features of MIM, including underdeveloped roots, CMD, and an open furcal channel. Initial canal negotiation revealed four buccal canals, but the palatal canal could not be located via conventional access. A separate access approach enabled successful identification, disinfection, and obturation of the palatal canal. Follow-up imaging showed healing of the periapical lesion and favorable clinical outcomes. This case highlights the diagnostic and technical challenges in managing MIM-affected teeth and underscores the importance of advanced imaging, tailored access strategies, and careful material selection to achieve successful endodontic outcomes.

Keywords: Cone-beam computed tomography; Molar-incisor malformation; Root canal therapy; Tooth abnormalities

INTRODUCTION

Molar-incisor malformation (MIM), also known as molar-root incisor malformation, is a developmental dental anomaly affecting the permanent first molars, maxillary central incisors, and second primary molars. In most reported cases, the first permanent molars are predominantly involved, exhibiting normal crown morphology but short, thin roots with atypical pulp chamber structures, constricted into straight form. This condition was first reported in 2014 [1,2].

Although the precise etiology of MIM remains unclear, many cases have been associated with significant systemic medical events during early childhood, potentially disrupting normal root development [3,4].

MIM-affected teeth often present with clinical complications, including periodontal bone loss (52.6%), endodontic lesions (50.0%), and combined endodontic-periodontal lesions (28.9%) [5]. Endodontic treatment can be particularly challenging due to structural

Received: July 27, 2025 **Revised:** October 9, 2025 **Accepted:** October 16, 2025
Citation
Kim WL, Park SH, Cho KM, Kim JW. Endodontic treatment of a molar-incisor malformation of the maxillary first molar: a case report. Restor Dent Endod 2026;51(2):e27.
***Correspondence to**
Jin-Woo Kim, DDS, MSD, PhD
Department of Conservative Dentistry, College of Dentistry, Kangwon National University, 7 Jukheon-gil, Gangneung 25457, Korea
Email: mendo7@gwnu.ac.kr

anomalies such as the cervical mineralized diaphragm (CMD) [2,3,6] and furcal communication [3,7], which may obscure canal pathways or provide alternative routes for bacterial ingress.

The prevalence of MIM remains uncertain; the literature still lacks robust population-level data. However, a recent study conducted in an Australian pediatric dental unit reported a prevalence of 0.47% (5 out of 1,054 children), suggesting that MIM, while rare, may be more common than previously assumed [8].

This report presents the endodontic management of a maxillary first molar diagnosed with MIM, providing new clinical insight into this rare condition.

CASE REPORT

A 17-year-old male patient presented with a chief complaint of noticing a lesion on the gingiva without experiencing any associated pain (Figure 1A). Clinical examination revealed a sinus tract on the palatal gingiva of the maxillary right first molar (#16) (Figure 1B). The tooth exhibited pain to palpation, while percussion and mobility tests were normal.

The patient's medical history was significant for bilateral arteriovenous malformations diagnosed around the age of one. He underwent endovascular stent implantation under general anesthesia at that time. Since the procedure, he has been undergoing routine follow-up with magnetic resonance imaging every 2 or 3 years. There was no significant dental history related to tooth #16, and the patient had not undergone any prior dental treatment involving the tooth.

Although the coronal morphology of all four first molars was normal (Figure 1C and D), all exhibited root malformations (Figure 1E), leading to a diagnosis of MIM. Based on clinical and radiographic findings, the maxillary right first molar (#16) was diagnosed with pulp necrosis and chronic apical abscess, and nonsurgical root canal treatment was planned.

To obtain a more accurate assessment of the root canal morphology, cone-beam computed tomography (CBCT) was performed. The palatal canal was found to be separated from the main pulp chamber (Figure 1F). Three canals were identified in the mesiobuccal root, and one canal each in the distobuccal and palatal roots, totaling five canals (Figure 1G).

At the first visit, following conventional access cavity preparation, pulp extirpation and working length deter-

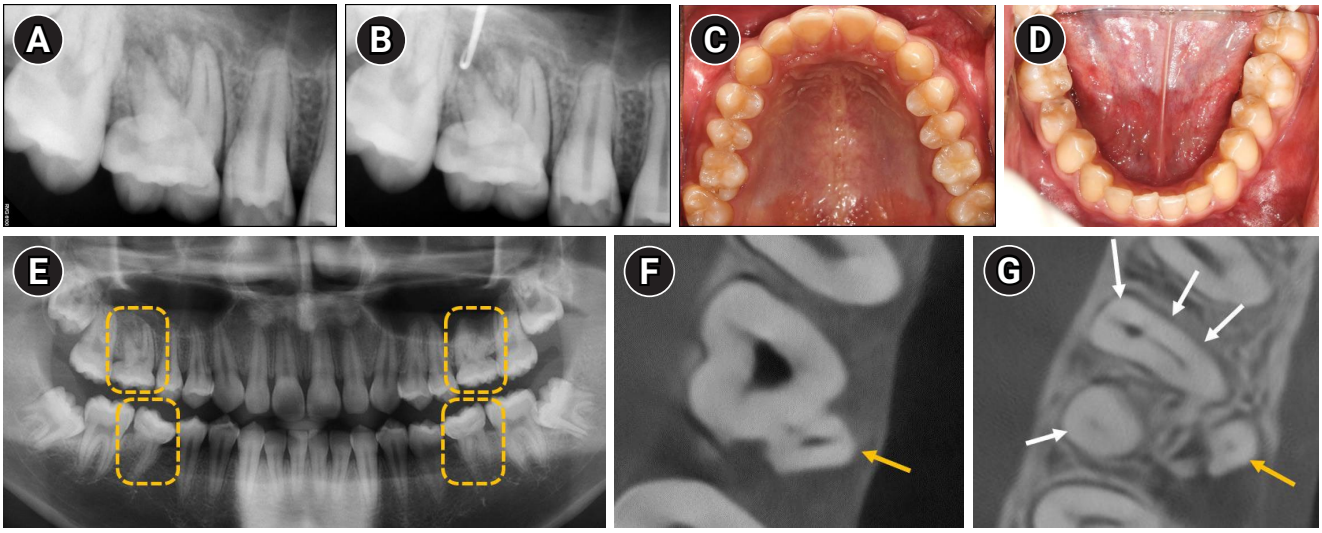

Figure 1. Diagnostic evaluation of maxillary right first molar and overall dentition. (A) Periapical radiograph showing an ill-defined radiolucency associated with tooth #16. (B) Radiograph confirming communication of the sinus tract with the periapical area. (C, D) Intraoral photographs showing normal coronal morphology of all first molars. (E) Panoramic radiograph revealing that all first molars have shortened, tapered roots. Yellow dashed boxes highlight the affected maxillary and mandibular first molars on both sides. (F) Cone-beam computed tomography (CBCT) axial view demonstrating that the palatal canal (yellow arrow) is not in continuity with the pulp chamber. (G) CBCT showing five root canals: three in the mesiobuccal root, and one each in the distobuccal (four white arrows) and palatal roots (yellow arrow).

https://doi.org/10.5395/rde.2026.51.e27

mination were performed for four buccal canals—three within the mesiobuccal root and one within the distobuccal root (Figure 2A–C). A glide path was established using a HyFlex EDM 10/.05 glide path file (Coltène/Whaledent, Altstätten, Switzerland). Canal shaping was subsequently carried out with a HyFlex EDM 20/.05 taper preparation file, followed by enlargement using a 25/~ HyFlex One File and final finishing using the 40/.04 HyFlex EDM finishing file. Irrigation was performed using 2.5% sodium hypochlorite (NaOCl). For intracanal medication, a calcium hydroxide-based paste (Metapaste Plus; Meta Biomed, Cheongju, Korea) was placed into the canals. The access cavity was temporarily sealed with a temporary restorative material (Caviton; GC Corp., Tokyo, Japan).

As the palatal canal was not connected to the main pulp chamber (Figure 1F), a separate access cavity was planned to locate the palatal canal. An attempt was made to access the canal via a cervical approach, which was deemed appropriate given the canal morphology (Figure 2D). However, the palatal canal could not be identified during the procedure, and a perforation occurred (Figure 2E). The perforation site was subsequently repaired using Biodentine (Septodont, Saint-Maur-des-Fossés, France) and resin-modified glass ionomer (Fuji II LC, GC).

At the second visit, intercommunication among the three mesiobuccal canals was confirmed by observing the flow of 2.5% NaOCl during irrigation. After removing the temporary restoration and intracanal medicament, canal patency was reestablished, and the canals were prepared for obturation. Final irrigation was performed using 2.5% NaOCl, followed by passive ultrasonic irrigation (Endosonic Blue 2; Maruchi, Wonju, Korea). Obturation was performed using a sealer-based technique with a calcium silicate sealer (CeraSeal; Meta Biomed). Following master cone fitting in all four buccal canals, root canal obturation was completed (Figure 2F–H).

At the third visit, to find the palatal canal, a second CBCT scan was obtained. The canal was found to be

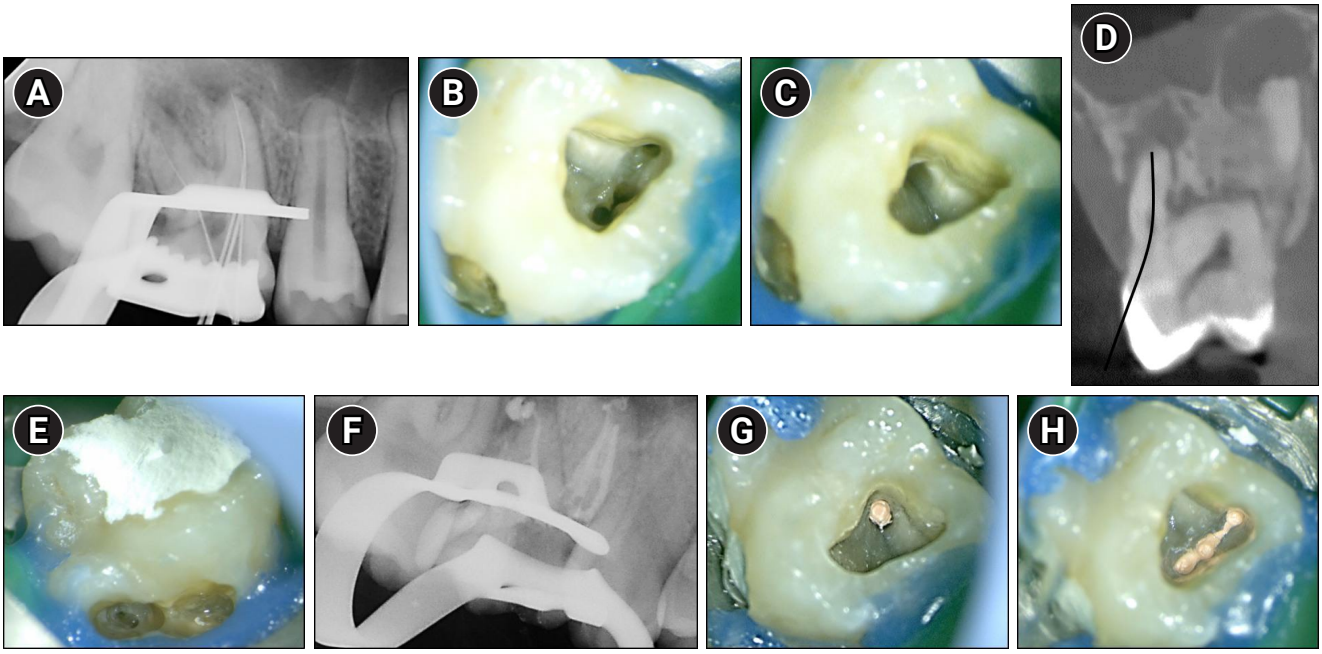

Figure 2. Endodontic management of maxillary right first molar (#16). (A) Working length radiograph taken after conventional access cavity preparation, showing four files in the buccal canals. (B, C) Clinical photographs of the pulp chamber floor showing three canal orifices in the mesiobuccal root and one in the distobuccal root. (D) Cone-beam computed tomography sagittal view showing the cervical access route chosen based on presumed palatal canal location. The black curved line indicates the presumed path for cervical access to the palatal canal. (E) Clinical image showing the perforation area after failed palatal canal identification. (F) Post-obturation radiograph confirming canal filling in three mesiobuccal and one distobuccal canal. (G) Clinical image showing obturation of the distobuccal canal with gutta-percha. (H) Clinical image showing well-condensed gutta-percha filling in the mesiobuccal canals.

located in a more mesio-palatal position than initially anticipated (Figure 3A and B). Working length determination, canal instrumentation, and irrigation were subsequently performed using the same protocol and instruments as those employed for the buccal canals.

At the following visit, obturation of the palatal canal was performed using the same technique and materials as used for the buccal canals using a sealer-based technique. Core buildup was then completed using bonding (Scotchbond Universal Adhesive; 3M ESPE, St. Paul, MN, USA) and resin core (Filtek Fill and Core, 3M ESPE) (Figure 3C–E).

Serial follow-up evaluations revealed progressive healing, as the periapical lesion showed a gradual reduction in size—initially evident at 1 month (Figure 3F) and continuing to further resolution by 5 months (Figure 3G). The patient is scheduled for continued follow-up evaluations.

DISCUSSION

MIM was reported independently by researchers from Korea and Switzerland in the same year, 2014 [1,2]. Over the past 10 years, since 2014, a total of 24 reports on MIM have been published, with half of them (12 reports) originating from Korean researchers [3]. However, the potential association between MIM and regional or ethnic factors remains unclear and warrants further investigation. Furthermore, although numerous reports have documented the clinical presentation of MIM, only three have described its endodontic management: one involving a maxillary incisor [9] and two involving mandibular first molars [7,10], with no cases reported in maxillary molars.

The first permanent molars are the most commonly affected teeth in MIM. Significant medical events occurring within the first 4 years of life—such as neurological conditions, prematurity, low birth weight, surgical interventions, and medication use—have been frequently associated with this condition. These findings support the hypothesis that early childhood medical history may contribute to the development of this dental anomaly [3,4].

This hypothesis is further supported by the developmental timeline of the first permanent molars. The mineralization of the permanent first molars begins around birth, with crown completion occurring at approximately 3 years of age and root initiation commencing at about 4 years [11]. This period of active dental development overlaps with the time during which many

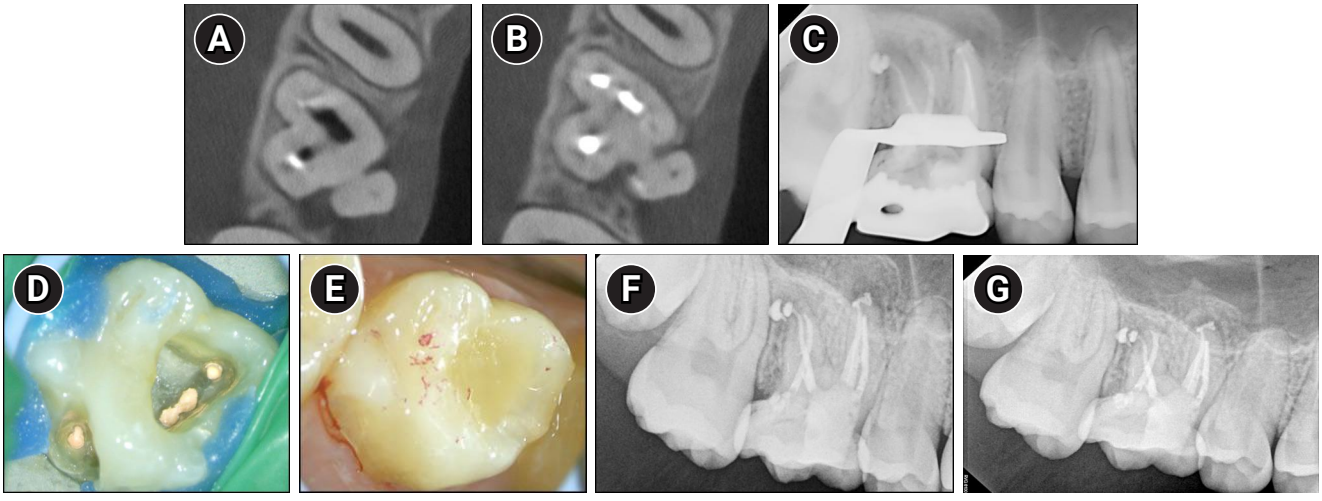

Figure 3. Identification and treatment of the palatal canal through buccal access in maxillary right first molar (#16). (A, B) Retaken cone-beam computed tomography axial views showing the palatal canal located more mesially than initially anticipated. (C) Radiograph taken after obturation of the palatal canal. (D) Clinical view of the completed obturation including the palatal canal. (E) Clinical view of the core buildup, demonstrating proper occlusal contacts. (F) One-month follow-up radiographs demonstrating reduction of the periapical radiolucency. (G) Five-month follow-up radiographs showing a further reduction of the periapical radiolucency.

https://doi.org/10.5395/rde.2026.51.e27

systemic medical events tend to occur, potentially increasing the susceptibility of these teeth to developmental disturbances such as MIM. MIM can manifest with considerable morphological variability, ranging from severely underdeveloped roots to relatively well-formed ones. The present case represents a variant of MIM in which the roots were distinctly separated, highlighting the heterogeneity of this condition and the importance of recognizing its diverse clinical presentations.

One of the common features, and now considered a typical structural anomaly of MIM, is the presence of a CMD—a dense mineralized structure located at the cementoenamel junction [2,3]. Histologically, CMD consists of irregular dentin, osteodentin, or cementum-like tissue, forming a calcified barrier at the cervical region. This structure can obscure the canal pathway or complicate its identification during endodontic treatment. Clinically, CMD hinders access to the root canal system and may lead to misidentification of canal orifices, thereby increasing the risk of iatrogenic errors. Furthermore, numerous microporosities observed within CMD may serve as potential pathways for bacterial ingress and contribute to persistent infection within the pulp chamber, even after treatment [2,3,6].

Another notable feature of MIM is the presence of an open channel in the furcation area. This structure provides direct communication between the external furcation region and the pulp chamber, potentially serving as a pathway for bacterial ingress. Such an anatomical anomaly may increase the risk of persistent infection or reinfection, even after endodontic treatment [3,7]. In addition, the presence of this open communication raises the possibility that immature accessory furcal canals may form at the pulpal floor, further complicating disinfection. These findings highlight the need for careful evaluation of MIM cases when radiolucent lesions persist or recur.

In the present case, both a CMD and an open channel were identified, consistent with previously reported anatomical features of MIM (Figure 4A–C). A periapical lesion developed despite the absence of caries or visible fractures, which are typically associated with pulpal infection. This unusual clinical finding may be explained by the presence of structural anomalies commonly seen in MIM, specifically microporosities within the CMD and an open furcal channel. The CMD-associated microporosities could have acted as microchannels for bacterial ingress, promoting chronic intrapulpal infection. Additionally, the open channel observed in the furcation area may have established a direct connection between the oral environment and the pulp chamber, serving as a potential route for bacterial contamination. Together, these features likely contributed to pulpal pathology and the development of the periapical lesion in the absence of conventional etiological factors.

In the present case, negotiation of the palatal canal was particularly challenging due to the localized presence of a CMD near the palatal region (Figure 5A and

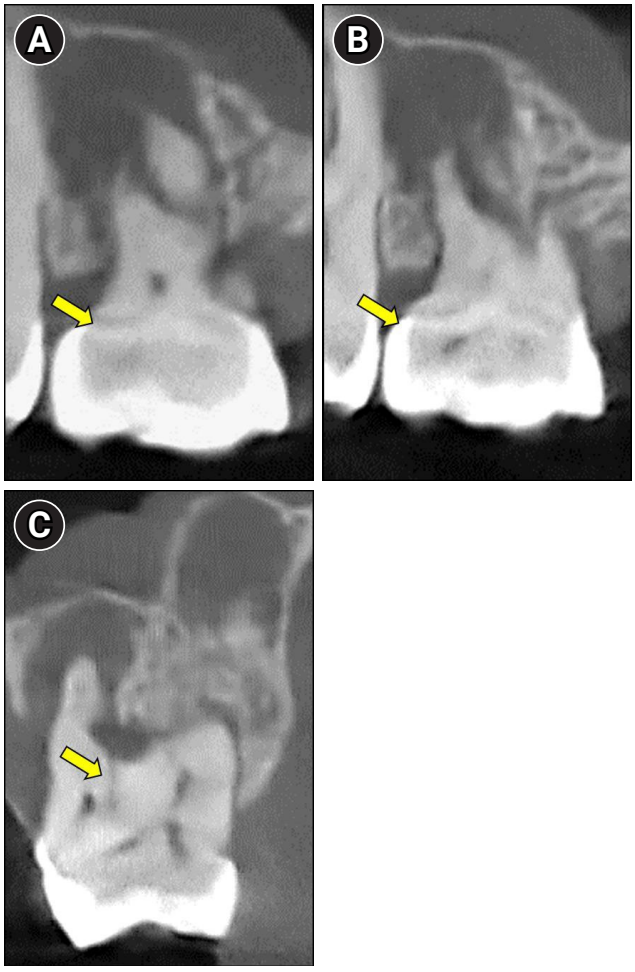

Figure 4. Cone-beam computed tomography images revealing characteristic anatomical features of molar-incisor malformation. (A, B) A dense mineralized structure consistent with a cervical mineralized diaphragm (yellow arrows). (C) An open channel (yellow arrow) connecting the furcation region to the pulp chamber.

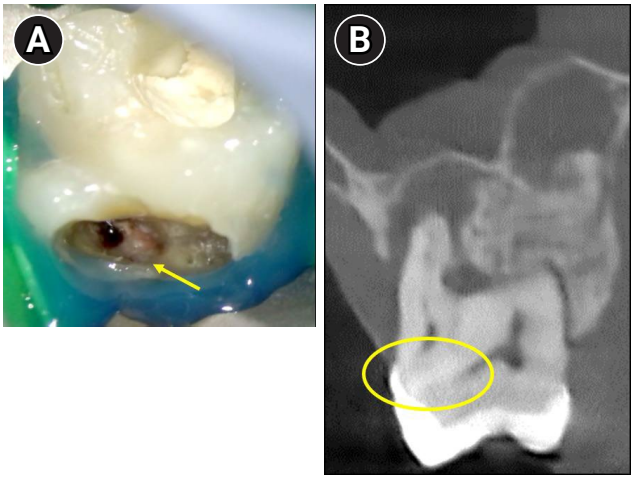

Figure 5. Difficulty in identifying the palatal canal due to the presence of a localized cervical mineralized diaphragm (CMD) near the palatal region. (A) Clinical view showing a mineralized barrier (yellow arrow) obstructing access to the palatal canal. (B) Cone-beam computed tomography image revealing CMD in the palatal area (highlighted with a yellow circle).

B). The mineralized barrier, with microporosity, likely obscured the true canal orifice, leading to an initial file path error. During the initial attempt, the file may have entered an area presumed to be a microporous structure rather than the true canal pathway, resulting in failure to find the true palatal canal. Although alternative strategies such as guided endodontics or three-dimensional-printed guides could have been considered, these technologies were not available in Korea at the time. We contacted international providers, but confirmed that such services were not accessible locally; thus, they could not be applied in this case.

While we recognize that continuous wave compaction (CWC) may achieve superior sealing ability compared to sealer-based techniques [12], the clinical circumstances in our case justified a different approach. Specifically, the patient's young age, the presence of a relatively wide apical foramen at the initiation of root canal treatment, and the need to avoid undue apical pressure all necessitated a more conservative strategy. Therefore, a sealer-based obturation technique with a bioceramic sealer (CeraSeal) was deliberately chosen. Importantly, even if a small amount of sealer extrudes beyond the apex, the favorable biocompatibility of bioceramic sealers minimizes the likelihood of adverse periapical reactions. Moreover, bioceramic sealers exert less apical pressure during obturation, making them particularly advantageous in such cases. This approach not only provided effective sealing in the atypical canal morphology but also leveraged the biological advantages of bioceramic materials in the periapical environment.

Interestingly, the palatal canal was found to be anatomically separated from the main pulp chamber, necessitating access through the palatal cervical region (Figure 2D). Such a configuration, in which the palatal canal is anatomically separated from the main pulp chamber, has not been previously reported in the literature. Therefore, the present case highlights a novel anatomical variation associated with MIM that has not been documented in the existing literature.

Mineral trioxide aggregate (MTA) and Biodentine are widely used for the repair of root perforations due to their biocompatibility and ability to induce hard tissue formation. Compared with MTA, Biodentine has been shown to induce greater RUNX2 (Runt-related transcription factor 2) expression, a key marker of osteoblastic differentiation [13]. It also promotes enhanced hydroxyapatite formation upon contact with tissue fluids, which contributes to improved biological integration and long-term sealing efficacy [13,14]. Clinically, Biodentine offers practical advantages, including a significantly shorter setting time (approximately 12 minutes), higher Vickers microhardness, and superior handling characteristics that improve efficiency and facilitate dentin-like substitution [15,16]. In recent years, premixed MTA putty materials such as EndoSequence Root Repair Material (RRM) Putty (Brasseler USA, Savannah, GA, USA), TotalFill BC RRM Putty (FKG Dentaire Sàrl, Le Crêt-du-Locle, Switzerland), Well-Root PT Putty (VERICOM Co., Ltd., Chuncheon, Korea), and One-Fil PT Putty (MEDICLUS Co., Ltd., Cheongju, Korea) have also been introduced. These newer materials are syringe- or putty-based, user-friendly, set rapidly, and do not induce discoloration. Nevertheless, in the present case, Biodentine was deliberately selected because it is a well-validated material with longstanding clinical validation, offering both favorable handling and biological properties while avoiding tooth discoloration.

https://doi.org/10.5395/rde.2026.51.e27

CONCLUSIONS

To the best of our knowledge, this is the first documented case reporting endodontic treatment in a maxillary first molar affected by MIM. The tooth exhibited characteristic features of MIM, including a CMD and an open furcal channel, which posed significant challenges to canal identification and disinfection. The palatal canal was found to be separated from the main pulp chamber. Early recognition of CMD, cervical constrictions, abnormal pulp chamber morphology, or root developmental disturbances on radiographs is essential for diagnosing MIM. In treatment planning, obtaining a CBCT scan should be prioritized to accurately assess the complex cervical and furcal anatomy, as CMD and furcal channels can obscure canal pathways or allow bacterial ingress. Careful disinfection and the use of bioceramic sealers and calcium silicate-based materials such as Biodentine are recommended. Long-term follow-up remains critical, and overall, MIM-affected teeth require individualized strategies beyond standard endodontic protocols and, when available, guided endodontic techniques to improve outcomes. This report highlights the anatomical complexity and therapeutic challenges associated with MIM-affected teeth, particularly maxillary molars, and emphasizes the importance of advanced imaging and careful canal-negotiation strategies to achieve favorable clinical outcomes.

CONFLICT OF INTEREST

No potential conflict of interest relevant to this article was reported.

FUNDING/SUPPORT

The authors have no financial relationships relevant to this article to disclose.

AUTHOR CONTRIBUTIONS

Conceptualization: Kim WL, Kim JW, Cho KM. Formal analysis: Kim WL, Kim JW, Park SH. Data curation, Methodology, Validation, Visualization: Kim WL, Kim JW. Supervision: Kim JW. Writing - original draft: Kim WL, Kim JW. Writing - review & editing: All authors. All authors read and approved the final manuscript.

DATA SHARING STATEMENT

The datasets are not publicly available but are available from the corresponding author upon reasonable request.

REFERENCES

1. Lee HS, Kim SH, Kim SO, Lee JH, Choi HJ, Jung HS, *et al*. A new type of dental anomaly: molar-incisor malformation (MIM). Oral Surg Oral Med Oral Pathol Oral Radiol 2014;118:101-109.
2. Witt CV, Hirt T, Rutz G, Luder HU. Root malformation associated with a cervical mineralized diaphragm: a distinct form of tooth abnormality? Oral Surg Oral Med Oral Pathol Oral Radiol 2014;117:e311-e319.
3. Jensen ED, Smart G, Poirier BF, Sethi S. Molar-root incisor malformation: a systematic review of case reports and case series. BMC Oral Health 2023;23:576.
4. Vargo RJ, Reddy R, Da Costa WB, Mugayar LR, Islam MN, Potluri A. Molar-incisor malformation: eight new cases and a review of the literature. Int J Paediatr Dent 2020;30:216-224.
5. Kim JE, Hong JK, Yi WJ, Heo MS, Lee SS, Choi SC, *et al*. Clinico-radiologic features of molar-incisor malformation in a case series of 38 patients: a retrospective observational study. Medicine (Baltimore) 2019;98:e17356.
6. Lee HS, Kim SH, Kim SO, Choi BJ, Cho SW, Park W, *et al*. Microscopic analysis of molar--incisor malformation. Oral Surg Oral Med Oral Pathol Oral Radiol 2015;119:544-552.
7. Yue W, Kim E. Nonsurgical endodontic management of a molar-incisor malformation-affected mandibular first molar: a case report. J Endod 2016;42:664-668.
8. Jensen ED, Smart G, Lee N, Tan J, Oliver K, Ha WN, *et al*. Prevalence and morphological features of molar-root incisor malformation in children attending a specialist paediatric dental unit. Int J Paediatr Dent 2023;33:543-552.
9. Byun C, Kim C, Cho S, Baek SH, Kim G, Kim SG, *et al*. Endodontic treatment of an anomalous anterior tooth with the aid of a 3-dimensional printed physical tooth model. J Endod 2015;41:961-965.
10. Park S, Byun S, Kim J, Yang B, Oh S. Treatment of molar incisor malformation and the short term follow-up: case reports. Eur J Paediatr Dent 2020;21:238-242.
11. AlQahtani SJ, Hector MP, Liversidge HM. Brief communication: the London atlas of human tooth development and eruption. Am J Phys Anthropol 2010;142:481-490.
12. Alkahtany SM, AlHussain AA, AlMthen HA, AlDokhi HD, Bukhary SM, Almohaimede AA, *et al*. Obturation quality of bioceramic sealers with different obturation techniques: a micro-CT evaluation. Sci Rep 2024;14:31146.
13. Silva LA, Pieroni KA, Nelson-Filho P, Silva RA, Her-

nandéz-Gatón P, Lucisano MP, *et al*. Furcation perforation: periradicular tissue response to Biodentine as a repair material by histopathologic and indirect immunofluorescence analyses. J Endod 2017;43:1137-1142.
14. Ma X, Xu H, Chen X, Zou Q, Wang J, Da Y, *et al*. Modern methods and materials used to treat root perforation: effectiveness comparison. J Mater Sci Mater Med 2024;35:1.
15. Kaup M, Schäfer E, Dammaschke T. An in vitro study of different material properties of Biodentine compared to ProRoot MTA. Head Face Med 2015;11:16.
16. Misra R, Toprani N, Bhagwat S, Vaishnav A, Dureja A, Bhosale O. Efficacy of mineral trioxide aggregate versus Biodentine as a direct pulp capping material in carious human mature permanent teeth: a systematic review. Cureus 2025;17:e89154.

https://doi.org/10.5395/rde.2026.51.e27

Restorative Dentistry and Endodontics (*Restor Dent Endod, RDE*) is a peer-reviewed and open-access electronic journal providing up-to-date information regarding the research and developments on new knowledge and innovations pertinent to the field of contemporary clinical operative dentistry, restorative dentistry, and endodontics. In the field of operative and restorative dentistry, the journal deals with diagnosis, treatment planning, treatment concepts and techniques, adhesive dentistry, esthetic dentistry, tooth whitening, dental materials, and implant restoration. In the field of endodontics, the journal deals with a variety of topics such as etiology of periapical lesions, outcome of endodontic treatment, surgical endodontics including replantation, transplantation and implantation, dental trauma, intracanal microbiology, endodontic materials (MTA, nickel-titanium instruments, etc), molecular biology techniques, and stem cell biology. *RDE* publishes research articles, review articles and case reports dealing with aforementioned topics from all over the world.

Manuscripts submitted to *RDE* should be prepared according to the instructions below. For issues not addressed in these instructions, the author should refer to the Recommendations for the Conduct, Reporting, Editing, and Publication of Scholarly Work in Medical Journals (http://www.icmje.org/recommendations/) from the International Committee of Medical Journal Editors (ICMJE).

Research and Publication Ethics

All of the manuscripts should be prepared based on strict observation of research and publication ethics guidelines recommended by the Council of Science Editors (https://www.councilscienceeditors.org), International Committee of Medical Journal Editors (ICMJE, https://www.icmje.org), World Association of Medical Editors (WAME, https://www.wame.org), and the Korean Association of Medical Journal Editors (KAMJE, https://www.kamje.or.kr/en/main_en).

All studies involving human subjects or human data must be reviewed and approved by a responsible Institutional Review Board (IRB). Please refer to the principles embodied in the Declaration of Helsinki (https://www.wma.net/policies-post/wma-declaration-of-helsinki-ethical-principles-for-medical-research-involving-human-subjects) for all investigations involving human materials. Animal experiments also should be reviewed by an appropriate committee (IACUC) for the care and use of animals. Also, studies with pathogens requiring a high degree of biosafety should pass review of a relevant committee (Institutional Biosafety Committee). The approval should be described in the Methods section. For studies of humans including case reports, state whether informed consents were obtained from the study participants (or from a parent or legal guardian if the participant is unable to provide consent). The editor of *RDE* may request submission of copies of the documents regarding ethical issues.

The *RDE* will follow the guidelines of the Committee on Publication Ethics (COPE, https://publicationethics.org) for the settlement of any misconduct.

Authorship

Authorship credit should be based on (1) substantial contributions to conception and design, acquisition of data, and analysis and interpretation of data; (2) drafting the article or revising it critically for important intellectual content; (3) final approval of the version to be published; and (4) agreement to be accountable for all aspects of the work in ensuring that questions related to the accuracy or integrity of any part of the work are appropriately investigated and resolved. Authors should meet these four conditions.

Role of Corresponding Author: The corresponding author takes primary responsibility for communication with the journal during the manuscript submission, peer review, and publication process. The corresponding author typically ensures that all of the journal's administrative requirements, such as providing the details of authorship, ethics committee approval, clinical trial registration documentation, and conflict of interest forms and statements, are properly completed, although these duties may be delegated to one or more

co-authors. The corresponding author should be available throughout the submission and peer review process to respond to editorial queries in a timely manner, and after publication, should be available to respond to critiques of the work and cooperate with any requests from the journal for data or additional information or questions about the article.

Contributors: Any researcher who does not meet all four ICMJE criteria for authorship discussed above but contribute substantively to the study in terms of idea development, manuscript writing, conducting research, data analysis, and financial support should have their contributions listed in the Acknowledgments section of the article.

Changes to Authorship: Any changes to authorship (the addition, deletion or rearrangement of author names in the authorship of accepted manuscript) needs to be approved by the Editor-in-Chief after a written confirmation by a corresponding author including the reason the name should be rearranged and all the signature of co-authors.

For more information, please refer to the Research and Publication Ethics page on the journal website.

Copyrights, Open Access, Data Sharing, and Archiving

Copyright: Copyright in all published material is owned by the Korean Academy of Conservative Dentistry. Authors must agree to transfer copyright (https://rde.ac/src/author_form.pdf) during the submission process. The corresponding author is responsible for submitting the copyright transfer agreement to the publisher.

Open Access Policy: *RDE* is an open-access journal. Articles are distributed under the terms of the Creative Commons Attribution License (https://creativecommons.org/licenses/by-nc/4.0/), which permits unrestricted non-commercial use, distribution, and reproduction in any medium, provided the original work is properly cited. Author(s) do not need permission to use tables or figures published in *RDE* in other journals, books, or media for scholarly and educational purposes.

Data Sharing: *RDE* encourages data sharing wherever possible unless this is prevented by ethical, privacy, or confidentiality matters. Authors may deposit their data in a publicly accessible repository and include a link to the DOI within the text of the manuscript.

Clinical Trials: *RDE* accepts the ICMJE Recommendations for data sharing statement policy. Authors may refer to the editorial, "Data Sharing Statements for Clinical Trials: A Requirement of the International Committee of Medical Journal Editors," in the Journal of Korean Medical Science (https://doi.org/10.3346/jkms.2017.32.7.1051).

Archiving Policy: It is accessible without barrier from PubMed Central (https://www.ncbi.nlm.nih.gov/pmc/journals/2010/), Korea Citation Index (https://kci.go.kr), or National Library of Korea (https://nl.go.kr) in the event a journal is no longer published.

For more information, please refer to the Editorial Policy page on the journal website.

Article Processing Charge

Authors of accepted articles must pay the following fees:
An Article Processing Charge (APC) of USD 300 shall be levied on Review Articles, Research Articles, and Case Reports submitted on or after May 1, 2026.
Editorials, Letters to the Editor, Open Lectures, and Readers' Forum articles are exempt from the APC.
A transaction fee of 3% may be applied, as applicable, depending on the payment method.

Submission of Manuscripts

Copyright Assignment: Authors submitting a paper do so on the understanding that the work and its essential substance have not been published before and are not being considered for publication elsewhere. The submission of the manuscript by the authors means that the authors automatically agree to assign exclusive copyright to *RDE* if and when the manuscript is accept-

ed for publication.

Submission: *RDE* requires electronic submission of all manuscripts. All manuscripts must be submitted to *RDE* through the website (https://www.editorialmanager.com/rde/) with a cover letter to the editor. Manuscripts may be submitted at any time. Authors may send queries concerning the submission process, manuscript status, or journal procedures to the Editor. Please contact the Editor by E-mail at editor@rde.ac.

Blinded Peer Review Process: Manuscripts that do not conform to the general aims and scope of the journal will be returned immediately without review. All other manuscripts will be reviewed by experts in the corresponding field (at least two referees). The Editorial Board may request authors to revise the manuscripts according to the reviewer's opinion. The revised manuscript may go through a second review by referees. A final decision on approval of publication of the submitted manuscripts is made by the Editorial Board.

Manuscript Preparation

General Requirements

- **Publication types:** Articles falling into the following categories are invited for submission: Research Articles, Case Reports, Review Articles, Editorials, Open Lectures, and Comments for the Reader's Forum.
- **Language:** The language of publication is English. It is recommended that international authors who are not native speakers of English seek help during manuscript preparation. The authors must have the article reviewed by a professional English editorial service before submission and submit the certificate of English proofreading as a supplement. The terminology used should follow the most recent edition of Dorland's Illustrated Medical Dictionary.
- **General text style:** Use Times New Roman 10-point font. Scientific units should be followed by the International System of Units. When non-standard terms appearing 3 or more times in the manuscript are to be abbreviated, they should be written out completely in the text when first used with the abbreviation in parenthesis. For medicine, use generic names. If a brand name should be used, insert it in parentheses after the generic name.
- **Statistical analysis:** Authors are strongly encouraged to consult a statistician for statistical analysis. Manuscripts with inappropriate statistical analysis methods will be returned to the authors without being reviewed.
- **Ethical approval:** All studies using human and animal subjects or specimens obtained from such subjects (such as extracted teeth) should include an explicit statement in the Methods section identifying the review and approval by the ethics committee for each study and provide an approval number. Manuscripts must be accompanied by a statement in the cover letter that the experiments were undertaken with the understanding and written consent of each subject and according to the above-mentioned principles.
- **Permissions:** If all or parts of previously published quotations, tables, or illustrations are used, permission must be obtained from the copyright holder concerned. The authors will be held responsible for failing to acquire proper permission before submission.
- **Reporting guideline:** For specific study designs, such as randomized controlled trials, studies of diagnostic accuracy, meta-analyses, observational studies, and non-randomized studies, we strongly recommend that authors follow and adhere to the reporting guidelines relevant to their specific research design. Randomized controlled trials should be presented according to the CONSORT guidelines (http://www.consort-statement.org). For case reports, authors should follow the CARE guidelines (https://www.care-statement.org). Authors should upload a completed checklist for the appropriate reporting guidelines during initial submission. Some reliable sources of reporting guidelines are EQUATOR Network (https://www.equator-network.org/) and NLM (https://www.nlm.nih.gov/services/research_report_guide.html).
- **Data statement:** Authors should state the availability of data in submission. If you have made your research data available in a data repository, you can link your article directly to the dataset. If the data is unavailable to access or unsuitable to post, authors must indicate why during the submission process, for example by stating that the research data is confidential. The statement will appear with your published article.

Manuscript Structure and Format

Key features and limits of articles are summarized below. However, the limits are negotiable with the editor.

Type	Abstract	Reference (max)	Table/Fig (max)
Review Article	· Unstructured · Max 200 words	70	NL
Research Article	· Structured : Objectives / Methods / Results / Conclusions · Max 250 words	40	Total 8
Case Report	· Unstructured · Max 200 words	30	Total 6
Editorial	No abstract	10	Total 2
Open Lectures	No abstract	NL	NL
Comments for the Reader's Forum	No abstract	NL	NL

NL, no limit.

Units, symbols, figures, tables, and references used must conform to the current issue or the linked article on our website.

- **Title page:** The title page of the manuscript should include the title of the article, the full name of the author(s), academic degrees, institutional affiliations, a running title (of seven or fewer words), correspondence, and declarations.
  - Title: The title should be concise and precise. It should be of 20 or less words, or it should fit within two lines. Only the first letter of the first word of the title should be capitalized.
  - Authors: Listed authors should include only those individuals who have made a significant creative contribution. *RDE* allows multiple authors to be specified as having equally contributed to the article as co-first authors or co-corresponding authors. While the contact information of all the corresponding authors is published in the article, only one corresponding author (the submitting author) is solely responsible for communicating with the journal.
  - Correspondence: The affiliation, address, telephone number, and e-mail address should be given.
  - Declarations: The declarations include conflicts of interest, funding, authors' contributions, ORCID, data availability statement, and acknowledgments.

Conflicts of interest	If there are any conflicts of interest, authors should disclose them in the manuscript. Disclosures allow editors, reviewers, and readers to approach the manuscript with an understanding of the situation and background of the completed research. If there are no conflicts of interest, authors should include the following sentence: "No potential conflict of interest relevant to this article was reported."
Funding	All sources of funding applicable to the study should be stated here explicitly.
Authors' contributions	The contributions of all authors must be described using the CRediT (https://casrai.org/credit/) taxonomy of author roles.
	Author Contributions Conceptualization: name; Data curation: name; Formal analysis: name; Funding acquisition: name; Investigation: name; Methodology: name; Project administration: name; Resources: name; Software: name; Supervision: name; Validation: name; Visualization: name; Writing - original draft: name; Writing - review & editing: name. (name: the last name and initials; eg, Cho BH)
ORCID	All authors are required to provide ORCID identification numbers. Please list the names of all authors and include the corresponding ORCID iD next to each name.
	ORCID Byeong-Hoon Cho https://orcid.org/0000-0001-9641-5507 Kyung-San Min https://orcid.org/0000-0002-1928-3384
Data availability statement	**Data are available in a public, open-access repository:** Please state the repository name, the persistent URL, and any conditions of reuse. All data that are publicly available and used in the writing of an article should be cited in the text and the reference list, whether they are data generated by the author(s) or by other researchers. **Data are available upon reasonable request:** Please describe the data (eg, de-identified participant data), who has access to the data, their publishable contact information, and the conditions under which reuse is permitted. **All study-related data is included in the publication or provided as supplementary information:** Please ensure this does not include patient identifiable data. **Data sharing is not relevant because no datasets were created and/or analyzed for this study:** Please state 'Not applicable' in this section. **No data are available:** Please state 'Not applicable' in this section.

Acknowledgments	All persons who have made substantial contributions, but who have not met the criteria for authorship, are acknowledged here.

- **Abstract:** The abstract should consist of a single paragraph with no more than 250 words for research articles and 200 words for case reports or review articles and should give details of what was done. The structured abstracts of research articles are to contain the following major headings: **Objective, Methods, Results, Conclusion**; and Keywords of no more than six words in alphabetical order. The abstracts of review articles or case reports don't need a structured format, but keywords should be listed. The keywords should be from Medical Subject Headings (MeSH) when possible (https://meshb.nlm.nih.gov/search) but non-MeSH subject headings may be used if deemed appropriate by the authors. Keywords should be written in small alphabetic letters with the first letter in capital. Separate each word by a semicolon.
- **Main text**
  - Introduction: The introduction should briefly review the pertinent literature in order to identify the gap in knowledge that the study is intended to address. The purpose of the study, the tested hypothesis, and its scope should be described.
  - Methods: The explanation of the experimental methods should be concise and sufficient for repetition by other qualified investigators. Procedures that have been published previously should not be described in detail. However, new or significant modifications of previously published procedures need full descriptions. Clinical studies or experiments using laboratory animals or pathogens should mention approval of the studies by relevant committees in this section. The sources of special chemicals or preparations should be given along with their location (name of company, city and state, and country). If the study utilized a commercial product, the generic term should be used and the product name, manufacturer, city, and country should be stated in parentheses. The methods of statistical analysis and the criteria for determining significance levels should be described.

An **ethics statement** should be placed here when the studies are performed using clinical samples or data, and animals. An exemplary is shown below.

Human	The study protocol was approved by the Institutional Review Board of OOO (IRB No: OO-OO-OO). Informed consent was obtained by all participants (or the participant's legal guardian) / Informed consent was waived by the IRB.
Animal	The procedures used and the care of animals were approved by the Institutional Animal Care and Use Committee at OOO University (approval No. ******).
Clinical trial	This is a randomized clinical trial on the second phase, registered at the Clinical Research Information Service (CRIS, https://cris.nih.go.kr), No. *******. * Other international registration is also acceptable.

Description of participants: Ensure correct use of the terms sex (when reporting biological factors) and gender (identity, psychosocial or cultural factors), and, unless inappropriate, report the sex or gender of study participants, the sex of animals or cells, and describe the methods used to determine sex or gender. If the study was done involving an exclusive population, for example in only one sex, authors should justify why, except in obvious cases (eg, prostate cancer). Authors should define how they determined race or ethnicity and justify their relevance.

  - Results: This section should present only the observations with minimal reference to earlier literature or possible interpretations by the authors. Data must not be duplicated in Tables and Figures. In tables and figures, magnification rates and units should be stated. SI (Le système International d'Unités) units should be used. Tables, figures, and legends of tables and figures may be included in the text or attached as separate pages at the end of the manuscript. Files containing figures and tables must also be submitted as separate files.
  - Discussion: The discussion section should describe the major findings of the study. Both the strengths and the weaknesses of the observations should be discussed. In addition, suggestions for further research topics may be included if needed.
  - Conclusions: A brief conclusion based on the findings of the study and a comment on the potential clinical relevance of the findings should be summarized. The conclusion section should be described in a narrative manner, without numbering.
- **References:** References should be obviously related

to the document. In the text, references should be cited with Arabic numerals in brackets, numbered in the order cited. The reference list should be typed double-spaced on a separate page and numbered in the order the reference citations appear in the text. For journal citations, include surnames and initials of authors, complete title of article, name of journal (abbreviated according to the NLM Catalog; https://www.ncbi.nlm.nih.gov/nlmcatalog/journals/), volume, inclusive page numbers, and year of publication. When books are cited, either inclusive page numbers or chapter numbers should be included. Please note that theses or doctoral dissertations, which have not been published in peer-reviewed journals, should not be cited as references.

If needed, single or double authors should be acknowledged in the text, eg, Ford and Roberts. If there are more than two authors, the first author followed by *et al*. is sufficient, eg, Tobias *et al*.

We recommend the use of EndNote for reference management and formatting. For reference style and format, please refer to the following examples.

Journal article	1. Oh HK, Shin DH. Effect of adhesive application method on repair bond strength of composite. Restor Dent Endod 2021;46:e32. List all authors when six or fewer (ex. reference 1); when seven or more, list six and add *et al*. (ex. reference 2 and 4). 2. Bergamo ET, Yamaguchi S, Lopes AC, Coelho PG, de Araújo-Júnior EN, Benalcázar Jalkh EB, *et al*. Performance of crowns cemented on a fiber-reinforced composite framework 5-unit implant-supported prostheses: in silico and fatigue analyses. Dent Mater 2021;37:1783-1793. 3. Shah RA, Hsu JI, Patel RR, Mui UN, Tyring SK. Antibiotic resistance in dermatology: the scope of the problem and strategies to address it. J Am Acad Dermatol 2021 Sep 20 [Epub]. https://doi.org/10.1016/j.jaad.2021.09.024. 4. Van Meerbeek B, Vargas M, Inoue S, Yoshida Y, Peumans M, Lambrechts P, *et al*. Adhesives and cements to promote preservation dentistry. Oper Dent 2001;(Supplement 6):119-144. 5. Yoshida Y, Van Meerbeek B, Okazaki M, Shintani H, Suzuki K. Comparative study on adhesive performance of functional monomers. J Dent Res 2003;82(Special Issue B):Abstract 0051, pB-19.
Book & Book chapter	6. Seltzer S, Bender IB. The dental pulp: biologic considerations in dental procedures. 3rd ed. Lippincott; 1984. p400. 7. Fouad AF, Levin L. Pulpal reactions to caries and dental procedures. In: Hargreaves KM, Cohen S, Berman LH, eds. Cohen's pathways of the pulp. 10th ed. Mosby Elsevier; 2010. p504-528.
Website	8. International Association of Dental Traumatology (IADT). The dental trauma guide [Internet]. IADT; 2014 [cited 2021 Jun 10]. Available from: https://dentaltraumaguide.org
Corporate publication	9. ISO-Standards ISO 4287 Geometrical Product Specifications Surface texture. Profile method: terms, definitions and surface texture parameters. 1st ed. Geneve: International Organization for Standardization; 1997. p1-25.

- **Tables:** Tables should be included in the text so that they may be edited if necessary. The title of each table should be placed on the top. The first letter of the first word should be capitalized. All abbreviations should be explained in each table. Footnotes should be indicated in superscript as [a), b), c)], and so on.
- **Figures:** Illustrations must be submitted in electronic format with file sizes appropriate for publication. Figures should be submitted as .tif or .jpg files. PowerPoint files are not accepted. All images should be at least 300 dpi and 5 × 5 cm in size, with 500 dpi recommended. If the figures represent a series of related content, it is recommended to present them as panels (A, B, C...) within a single figure. Figure legends should be included as text so that they be edited if necessary. All abbreviations should be explained in each figure. Microscopic images should include the staining method and magnification (eg, hematoxylin and eosin stain, ×400). Figures may use arrows, arrowheads, asterisks, circles, or other indicators as needed for clarity, with each indicated element described in the figure legends.
- **Other types of articles**
  - Review articles: Review articles should be divided into Introduction, Review, and Conclusions. The Introduction section should focus on placing the subject matter in context and justifying the need for the review. The Review section should be divided into logical sub-sections in order to improve readability and enhance understanding. Search strategies must be described and the use of state-of-the-art evi-

dence-based systematic approaches is expected. The use of tabulated and illustrative material is encouraged. The Conclusion section should reach clear conclusions and/or recommendations on the basis of the evidence presented. If a review includes a meta-analysis as part of a systematic review, it should be submitted as a research article.

- Case reports: Case reports should be divided into Introduction, Case Report(s), Discussion, and Conclusions. They should be well illustrated with clinical images, radiographs, diagrams, and where appropriate, supporting tables and graphs. However, all illustrations must be of the highest quality.
- Comments for the Reader's forum: Reader's forum will present various questions, suggestions, and critiques on the subjects of operative dentistry, restorative dentistry, and endodontics from the readers.

Manuscript Files Accepted

- **Final version:** After a paper has been accepted for publication, the author(s) should submit the final version of the manuscript. The names and affiliations of authors should be double-checked, and if the originally submitted image files were of poor resolution, higher-resolution image files should be submitted at this time. Illustrations must be submitted in electronic format with file sizes appropriate for publication. All images should be at least 300 dpi and 5 × 5 cm in size, with 500 dpi recommended. Symbols (eg, circles, triangles, squares), letters (eg, words, abbreviations), and numbers should be large enough to be legible on reduction to the journal's column widths. All symbols must be defined in the figure caption. When submitted as separate files, name of the author, and illustration number should be stated in the file name. If references, tables, or figures are moved, added, or deleted during the revision process, renumber them to reflect such changes so that all tables, references, and figures are cited in numeric order.
- **Errata and Corrigenda:** To correct errors in published articles, the corresponding author should contact the journal's Editorial Office with a detailed description of the proposed correction. Corrections that profoundly affect the interpretation or conclusions of the article will be reviewed by the editors. Corrections will be published as corrigenda (corrections of author's errors) or errata (corrections of publisher's errors) in a later issue of the journal.

Contacting the Journal

Editorial assistant: Hye-Young Lee
RDE editorial office
The Korean Academy of Conservative Dentistry
B163, Seoul National University Dental Hospital, 101 Daehak-ro, Jongno-gu, Seoul 03080, Korea
Tel: +82-2-763-3818, Fax: +82-2-763-3819, E-mail: editor@rde.ac

History of the Recommendations

Enacted in March 2, 2012
Modified: August 4, 2023
Last modified: November 4, 2024

RDE Restorative Dentistry & Endodontics

Author's checklist

Authors have written the manuscript in compliance with Instructions to Authors and Recommendations for the Conduct, Reporting, Editing, and Publication of Scholarly Work in Medical Journals (https://www.icmje.org/icmje-recommendations.pdf) from the International Committee of Medical Journal Editors, and the Guideline of Committee on Publication Ethics (https://publicationethics.org).

Cover letter

☐ Manuscript's title
☐ Statement that your paper has not been previously published and is not currently under consideration by another journal.
☐ Brief description of the research you are reporting in your paper, why it is important, and why you think the readers of the journal would be interested in it.
☐ Contact information for you and any co-authors.
☐ Confirmation that you have no competing interests to disclose.

Title page

☐ Title page including the title of the article, the full name of the author(s), academic degrees, positions, institutional affiliations, a running title (of 7 or less words), correspondence, and declarations.

Declaration

☐ Conflicts of interest, funding, authors' contributions, ORCID, data availability statement, and acknowledgments

Abstract

☐ Original article: <250 words; structured abstract— Objective, Methods, Results, Conclusion
☐ Review article: <200 words; unstructured abstract
☐ Case report: <200 words; unstructured abstract

Keyword

☐ Keywords should be from MeSH subject headings when possible.

Main text

☐ Information regarding approval of an institutional review board and obtaining informed consent should be mentioned.
☐ Original article: Introduction/Methods/Results/Discussion/Conclusions
☐ Review article: Introduction/Review/Conclusions
☐ Case report: Introduction/Case Report(s)/Discussion/Conclusions

Reference

☐ Refer to the reference format in the author's guideline.

Table

☐ If tables are included, they should be included as text and not as illustrations so that they may be edited if necessary.

Figure

☐ Figure legends should be included as text and not as illustrations so that they may be edited if necessary.

Author's form

☐ All authors have completed the Copyright Transfer Agreement and Ethics Concerning Human Subjects.

Conflict of interest form

☐ All authors have completed the COI Statement.

Permission

☐ The authors are responsible for obtaining permission from the copyright holder to reprint any previously published material in RDE.

RDE Restorative Dentistry & Endodontics

Copyright transfer agreement

Manuscript title _____

_____

Corresponding author name _____

Fax _____ E-mail _____

The authors of the article hereby agree that the Korean Academy of Conservative Dentistry holds the copyright on all submitted materials and the right to publish, transmit, sell, and distribute them in the journal or othermedia.

Corresponding author

Print name _____

Signed _____ **Date** _____

Co-authors

Print name _____ **Print name** _____

Signature/Date _____ **Signature/Date** _____

Print name _____ **Print name** _____

Signature/Date _____ **Signature/Date** _____

Print name _____ **Print name** _____

Signature/Date _____ **Signature/Date** _____

Print name _____ **Print name** _____

Signature/Date _____ **Signature/Date** _____

RDE Restorative Dentistry & Endodontics

Conflict of interest form

Manuscript title _____

_____

As the corresponding author, I declare the following information regarding the specific conflicts of interest of authors of our aforementioned manuscript.

Examples of conflicts of interest include the following: source of funding, paid consultant to sponsor, study investigator funded by sponsor, employee of sponsor, board membership with sponsor, stockholder for mentioned product, any financial relationship to competitors of mentioned product, and others (please specify).

Author	No conflict involved	Conflict (specify)

I accept the responsibility for the completion of this document and attest to its validity on behalf of all co-authors.

Corresponding author (name/signature) _____ _____

Date _____